Modelling Rainforest Canopy Photosynthesis across the Amazon Basin

Mercado Montoya, L.M.

2007

Modelling Rainforest Canopy Photosynthesis across the Amazon Basin

Lina María Mercado Montoya

VRIJE UNIVERSITEIT

Modelling Rainforest Canopy Photosynthesis across the Amazon Basin

ACADEMISCH PROEFSCHRIFT

ter verkrijging van de graad Doctor aan
de Vrije Universiteit Amsterdam,
op gezag van de rector magnificus
prof.dr. L.M Bouter,
in het openbaar te verdedigen
ten overstaan van de promotiecommissie
van de faculteit der Aard- en Levenswetenschappen
op maandag 11 juni 2007 om 13.45 uur
in de aula van de universiteit,
De Boelelaan 1105

door
Lina María Mercado Montoya
geboren te Medellín, Colombia

promotor	:	prof.dr. A.J. Dolman
copromotor	:	prof.dr. J.J. Lloyd

CONTENTS

Symbols and abbreviations

A	μmol m^2 s^{-1}	CO_2 assimilation rate or gross primary productivity
a	‰	Fractionation due to diffusion of CO_2 from the leaf surface to the substomatal cavity
A_v	μmol m^2 s^{-1}	CO_2 assimilation rate controlled by the rate of carboxylation when rubisco activity is limiting
A_J	μmol m^2 s^{-1}	CO_2 assimilation rate limited by the rate of electron transport
AGB	Mg C ha^{-1}	Above ground biomass
ANPP	Mg C $ha^{-1}year^{-1}$	Above ground primary productivity
b	‰	Fractionation of the enzyme catalyzed fixation of CO_2
C_a	mol	CO_2 concentration within the canopy or CO_2 ambient partial pressure
C_c	Pa	Partial pressure of CO_2 in the chloroplast
C_i	mol	Intercellular CO_2 concentration
C_i/C_a	mol mol^{-1}	Ratio of intercellular to outside leaf [CO_2]
C_p	J mol $^{-1}k^{-1}$	Specific heat capacity of the air
$\overline{C_i / C_a}$	mol mol^{-1}	Average C_i/C_a
D	m	Zero plane displacement of the vegetation
$\overline{D}$	mol mol^{-1}	Long-term vapour pressure deficit
D_C	mol mol^{-1}	Vapour pressure deficit
D_0	dimensionless	Empirical parameter in stomatal conductance model (Leuning 1995)
E_v	J mol^{-1}	Activation energy for the temperature dependency of Rubisco capacity
E_J	J mol^{-1}	Activation energy for the temperature dependency of the potential rate of electron transport
f	dimenssionless	Spectral correction factor of light
F_c	μmol m^2 s^{-1}	Flux of CO_2 measured by the eddy correlation system
F_d		Fraction of diffuse irradiance
g_o	mol m^{-2} s^{-1}	Minimum stomatal conductance to water vapour when A=0 in the stomatal conductance model of Leuning (1990)
g_1	dimensionless	Empirical coefficient in the stomatal conductance model of Leuning (1990)
G	W m^{-2}	Flux of sensible heat loss from the soil
G_a	mol m^{-2} s^{-1}	Aerodynamical conductance
G_r	mol m^{-2} s^{-1}	Radiative conductance of the canopy
G_s	μmol m^2 s^{-1}	Stomatal conductance to water vapour
G_P	μmol m^2 s^{-1}	Net carbon assimilation or net carbon uptake
G_{s_eddy}	mol m^{-2} s^{-1}	Stomatal conductance derived from the latent heat fluxes measured by eddy correlation and estimated by inversion of the Penman Monteith equation
G_{PP}	Mg C $ha^{-1}year^{-1}$	Simulated gross primary productivity or gross canopy assimilation rate (i.e. total photosynthesis, includes daytime leaf respiration)
$G_{P(N)}$	Mg C $ha^{-1}year^{-1}$	Simulated net carbon uptake from parametersiations based on leaf

		N
$G_{P(P)}$	Mg C $ha^{-1}year^{-1}$	Simulated net carbon uptake from parametersiations based on leaf P
GPP	Mg C $ha^{-1}year^{-1}$ or μmol m^2 s^{-1}	Gross primary productivity or gross canopy assimilation rate
h	%	Humidity at the leaf surface
h_t	m	Eddy covariance measurement height
H	W m^{-2}	Flux of sensible heat loss from the canopy
H_J	J mol^{-1}	Parameter that controls maximum optimum temperature of J_{max}
I_2	μmol quanta m^2 s^{-1}	Absorbed irradiance that reaches photosystem II
I_0	μmol quanta m^2 s^{-1}	PAR reaching the leaf or canopy surface
J	μmol m^2 s^{-1}	Potential rate of electron transport
J_{max}	μmol m^2 s^{-1}	Light saturated potential rate of electron transport capacity at canopy temperature
$J_{max,25}$	μmol m^2 s^{-1}	Light saturated potential rate of electron transport capacity at 25 °C
J_{max}/V_{max}	μmol m^2 s^{-1} / μmol m^2 s^{-1}	Ratio of potential rate of electron transport capacity to maximum carboxylation capacity of Rubisco
J_s	μmol m^2 s^{-1}	CO_2 assimilation rate limited by the rate of triose phosphate utilisation
k	dimensionless	von Karman's constant
k_n	dimensionless	N allocation coefficient
$k_{n\_control}$	dimensionless	N allocation coefficient for control simulations
K_c	Pa	Michaelis-Menten constant for carboxilation by Rubisco
K_o	Pa	Michaelis-Menten constant for oxygenation by Rubisco
L	m	Monin-Obukhov length
LAI	m^2 m^{-2}	Leaf area index
LAVPD	mol mol^{-2}	Leaf to air vapour pressure deficit
M	W m^{-2}	Net heat stored in the canopy from biochemical reactions
N_E	μmol m^2 s^{-1}	Net ecosystem exchange measured by eddy correlation
N_{Enight}	μmol m^2 s^{-1}	Night time net ecosystem exchange measured by eddy correlation
NEE	μmol m^2 s^{-1}	Net ecostyem exchange
NPP	Mg C $ha^{-1}year^{-1}$	Net primary productivity
P	Pa	Atmospheric pressure
P_i	mg	Inorganic phosphate
r	%	Leaf reflectance in the visible band
r_a	s m^{-1}	Aerodynamical resistance
R	J mol^{-1} K^{-1}	Universal gas constant
R_n	W m^{-2}	Net radiation flux (short and long wave)
R_{ni}	W m^{-2}	Isotermal net radiation flux
R_C	μmol m^2 s^{-1}	Leaf dark respiration rate during the day
$R_{C,25}$	μmol m^2 s^{-1}	Rate of canopy respiration at 25 °C
R_{CS}	μmol m^2 s^{-1}	CO_2 efflux from decomposition of coarse litter
R_D	μmol m^2 s^{-1}	Rate of canopy dark respiration at canopy temperature
$R_{D,25}$	μmol m^2 s^{-1}	Rate of canopy dark respiration at 25 °C

R_E	μmol m^2 s^{-1}	Total ecosystem respiration rate
R_{ED}	μmol m^2 s^{-1}	day time total ecosystem respiration
R_S	μmol m^2 s^{-1}	CO_2 efflux from the soil, which includes root respiration and decomposition from roots, fine and coarse litter
R_{E_NL}	μmol m^2 s^{-1}	non-leaf ecosystem respiration rate
R_W	μmol m^2 s^{-1}	Respiration rate from live stems and branches
s	Pa K^{-1}	Slope of the relationship between vapour pressure and temperature
S_J	J $mol^{-1}K^{-1}$	Parmeter that controls minimum optimum temperature dependencies of J_{max}.
St	W m^{-2}	Energy stored in the biomass and in air within the canopy
S_T	mol m^2 s^{-1}	Canopy CO_2 storage flux
Solar D	W m^{-2}	Solar diffuse radiation
t	%	Leaf transmittance in the visible band
T_a	K	Absolute air temperature
T_C	K	Absolute temperature of the leaf or canopy
T_{opt}	K	Absolute temperature optimum of J_{max}
u	m s^{-1}	Horizontal windspeed
u^*	m s^{-1}	Friction velocity
V_{max}	μmol m^2 s^{-1}	Maximum carboxylation activity of Rubisco
V_{max} top	μmol m^2 s^{-1}	Top of the canopy V_{max}
$V_{max,25}$	μmol m^2 s^{-1}	V_{max} at 25 °C
V_{maxN}	μmol m^2 s^{-1}	Top of the canopy V_{max} parameterised with leaf N
V_{maxP}	μmol m^2 s^{-1}	Top of the canopy V_{max} parameterised with leaf P
V_{max_canopy}	μmol m^2 s^{-1}	Total canopy level V_{max}
V_{max_leaf}	μmol m^2 s^{-1}	Maximum carboxylation capacity by Rubicsoat the leaf level
VPD	mol mol^{-2}	Above canopy vapour pressure deficit
wd	g cm^3	Above ground stem wood density
z	m	Reference height above the ground
α	mol CO_2 mol $^{-1}$PAR	Quantum efficiency for CO_2 fixation or quantum yield
β	W m^{-2}/ W m^{-2}	Bowen ratio
δ	kg m^{-3}	Density of the air
δ^{13}C	‰	Carbon isotope composition
δ_{atm}	‰	Carbon isotope composition of air
$\overline{(\delta^{13}C)}$	‰	Simulated average integral of photosynthetic discrimination during the different seasons analyzed
ΔT	K	Term that accounts for temperature difference between the canopy and the air surrounding it.
ε	Pa K^{-1}/ Pa K^{-1}	Ratio of slope of the relationship between vapour pressure and temperature, and the psichrometer constant
ε_f	%	Leaf emissivity
Φ	mol electrons mol^{-1} photons	Quantum efficiency for CO_2 fixation or quantum yield
γ		Psichrometer constant
Γ^*	Pa	CO_2 compensation point in the absence of mitochondrial respiration

λ	mol mol^{-1}	Parameter from the 'Lambda model' for stomatal conductance.
λE	W m^{-2}	Flux and latent heat loss from the canopy
θ	dimensionless	Curvature factor of light response of electron transport rate function
σ	W m^{-2} K^{-4}	Stefan Boltzman constant.
ξ	m m^{-1}	Used to calculate stability correction factors
Ω	Pa K^{-1} /Pa K^{-1}	Decoupling coefficient
ψ_M	m m^{-1}	Diabatic correction factor for momentum
ψ_H	m m^{-1}	Diabatic correction factor for heat

Abbreviations

ATP	Adenosine triphosphate
DW	Dry weight
ECMWF	European Center for medium range weather forecast
ENSO	El Niño Southern oscinaltion
GIMMS	Global Inventories Monitoring and Modelling Studies
GEM-SA	Gaussian Emulation Machine for Sensitivity Analysis
INPA	Instituto Nacional de Pesquisas da Amazônia
LBA	Large-Scale Biosphere - Atmosphere Experiment in Amazonia
NADPH	Nicotinamide adenine dinucleotide phosphate
NIR	Near infra red radiation
PAR	Photosynthetic active radiation
RAINFOR	Amazon Forest Inventory Network
RMSE	Root Mean Square Error
Rubisco	Ribulose-1,5 –bisphosphate carboxylase-oxygenase
RuBP	Ribulose biphospate
TPU	Triose Phopshpate Utilization

Abstract

The Amazon forest, the largest example of tropical rainforest in the world (Laurance 2000), is an important component of the global carbon cycle. This is due to its capacity to assimilate and store large amounts of carbon (Dixon et al. 1994), and the potential for this ecosystem to release carbon and become a significant future source of atmospheric CO_2, and thus contribute to climate change (Cox et al. 2000; Malhi et al. 1998; Saleska et al. 2003). Understanding ecosystem functioning in the Amazon forest and its response to changing atmospheric composition and climate is of major importance for modelling the contemporary and future global carbon balance. This study provides information that helps to advance our knowledge in modelling tropical forest carbon and water fluxes. Here a model is developed to simulate rain forest Gross Primary Productivity, GPP, across an East-West transect in the Amazon basin. The model is built using existing literature and validated against eddy correlation data at five flux sites in the Amazon rain forest. Scaling functions are derived between Rubisco capacity, a proxy for photosynthetic capacity, and foliar nutrients (i.e. V_{max} versus foliar N, and also relationships between V_{max} and foliar P), to provide estimates of canopy photosynthetic parameters for a diverse range of forests across the Amazon region. A simple mechanism of phosphorous limitation to photosynthesis is implemented in the model. With such model, a sensitivity analysis is used to explore the possibility of photosynthesis being limited by either leaf nitrogen or leaf phosphorous in the Amazon rainforest.

During this model evaluation and exercise of scaling up GPP from stand to regional level, issues relating to uncertainty in data used for model validation and parameterisation are addressed. Also the sensitivity of the model to parameter uncertainty, alternative process representations and uncertainties associated with scaling up parameters from site to regional level are investigated.

Results from the model evaluation suggest that i) With adequate parameterisation, photosynthesis models that take into account the separation of diffuse and direct irradiance and the dynamics of sunlit and shaded leaves accurately represent photosynthesis in this forest, ii) Stomatal conductance formulations that only take into account atmospheric demand are unable to correctly simulate moisture and CO_2 fluxes in forests with a pronounced dry season, particularly during the afternoon conditions, (iii) The most crucial uncertainties are associated with the eddy correlation data, and in particular, estimates of ecosystem respiration, but also in the data used for model parameterisation, iv) To accurately simulate GPP and energy partition the most critical parameters and model processes are the quantum yield of photosynthetic uptake, the maximum carboxylation capacity of Rubisco (an enzyme of crucial importance in photosynthesis), and simulation of stomatal conductance. Additionally, validation of simulated diffuse irradiance is needed.

The sensitivity exercise of scaling up model parameters from stand to regional level, based on the assumption of N or P limiting forest productivity, suggests that if phosphorus limits photosynthesis in these forests, there should be a gradient in GPP across the Amazon basin, with higher GPP at sites where foliar P is highest (i.e. many of the western sites in Amazonia) and lowest where foliar P is lowest (mostly sites in central and eastern Amazonia). Under these conditions, our results indicate the contribution of spatial variability in GPP, soil properties and plant hydraulic traits to observed patterns in plant growth across the

Amazon basin. If P limits photosynthesis in this forest, or at least in the areas where foliar P is lowest, the forest may fail to respond to increasing atmospheric CO_2. Global carbon cycle models do not account for this effect, and assume enhanced photosynthesis under elevated atmospheric CO_2. Therefore such a result would have major implications for the future global carbon budget, i.e. Amazon rainforests would contribute more to atmospheric CO_2 than hitherto anticipated, with important ramifications for the rate of global warming. On the other hand, our results suggest that if nitrogen limits photosynthesis in these forests, photosynthesis will not vary across the study transect. This favours the homogeneous parameterisations used in global carbon cycle models. Uncertainties associated with this scaling up exercise include 1) the use of data from only 4 and 5 sites from the Brazilian rainforest to derive the P and N scaling functions, respectively, which are subsequently used to extrapolate over the whole region, 2) the gradient in GPP under P limitation is governed by a single point (out of 4) responsible for the slope and the regression fit in the P scaling function, and 3) the implementation of P limitation in the model presented here is very simplistic. It assumes that even though there is a large amount of leaf N in rubisco, a key enzyme in photosynthesis, leaf P could still be a proxy for photosynthetic capacity. Therefore leaf P is related to the V_{max} parameter. However, it is worth mentioning that the mechanism by which P constrains photosynthesis in vegetation under limited P availability is not well understood (Campbell and Sage 2006).

Results from this study question the assumption of N limiting of photosynthesis in global and regional models for this ecosystem, showing the need for more field studies looking at the nature of nutrient limitation in forests across the Amazon basin and its link to photosynthesis in contrasting P environments.

Introduction

One of the most well known changes in Earth's atmosphere during the 20th century has been the increase in concentration and growth rate of CO_2 in the atmosphere, as measured at Mauna Loa since the mid-1950s (Keeling and Whorf 2002). This is a consequence of carbon emitted to the atmosphere from fossil fuel burning and cement production powered by economic activities, as well as deforestation, especially in the tropics (Prentice et al. 2001). Further increases in atmospheric CO_2 concentrations are expected throughout the 21st Century. As CO_2 is a greenhouse gas, its rapid increase is likely to be a major factor responsible for global warming (Prentice et al. 2001).

Atmospheric CO_2 concentrations are shaped by uptake and emissions of CO_2 from the land, oceans and through human activities. Throughout the Holocene, the land and oceans were almost in equilibrium with the atmosphere, resulting in almost constant atmospheric CO_2 concentrations (Prentice et al. 2001). Powered by industrial activities, this equilibrium was disrupted by the onset of the industrial revolution, starting in the 18th Century, and the injection of CO_2 into the atmosphere from fossil fuel burning and land use change (Prentice et al. 2001). At the present-day approximately one third of the carbon emissions from human activities stay in the atmosphere, with the remainder sequestered by the oceans and land ecosystems (Prentice et al. 2001). This rise of CO_2 in the atmosphere has the potential to affect terrestrial and marine ecosystems. Increasing ocean CO_2 uptake leads to higher ocean acidity, which is accompanied by changes in seawater chemistry which has the potential to affect marine life (Orr et al. 2005). In terrestrial ecosystems, elevated CO_2 concentrations in the air can stimulate plant photosynthesis (Lloyd and Farquhar 1996), the CO_2 fertilisation effect. This alters the amount of carbon stored in plant biomass, litter and in the soils, giving rise to a carbon sequestration capacity of ecosystems. Recent research has found the sink capacity to vary among terrestrial ecosystems. For instance, temperate deciduous forests seem to take up twice as much carbon as temperate coniferous forests (Valentini et al. 2000; Baldocchi et al. 2001). The carbon balance of tropical forests in the Amazon has been a subject of great controversy. Results from studies vary in both magnitude and sign, with some investigators suggesting the possibility of a carbon sink (Araújo et al. 2002; Carswell et al. 2002; Grace et al. 1995; Malhi et al. 1998; Phillips et al. 1998) while other results suggest carbon release (Saleska et al. 2003). In addition to the atmospheric [CO_2] increase and the induced fertilization effect, associated global warming may lead to higher rates of plant and soil respiration and an associated net carbon release. Given the variation in response among ecosystems, it is important to quantify the individual contributions of ecosystems to the global carbon sink. However it is also important to consider the flows of carbon going in and out of terrestrial ecosystems, as the differential response of processes to changes in climate and atmospheric composition determine the net ecosystem response.

Tropical rain forests constitute one of the Earth's major global ecosystems due to their productivity (Field et al. 1998; Grace et al. 2001; Melillo et al. 1993), their capacity to store carbon (Dixon et al. 1994) and their effects on global climate (Silva Dias et al. 1987; Zhang et al. 1996). Due to their environmentally privileged location, tropical forests assimilate and store large amounts of carbon which also has the potential to be released and become a significant source of atmospheric CO_2 (Cox et al. 2000; Malhi et al. 1998; Saleska et al. 2003). Understanding their functioning and responses to a changing atmosphere and climate is of a major

importance.

The Amazon rainforest is the largest example of tropical rainforest in the world, covering an area of 5×10^6 km^2 (Laurance 2000). It is estimated to be among the most productive ecosystem in the world (Grace et al. 2001). Of all tropical ecosystems, the Amazon forest has recently received a lot of attention due to its potential capacity to act as a source or sink of carbon dioxide (Grace et al. 1995; Lloyd and Farquhar 1996: Phillips et al. 1998; Prentice and Lloyd 1998; Tian et al. 1998). Results from global carbon cycle models have shown the significant effect of Amazonian forests being either source or sink on estimates of the global carbon budget (Prentice and Lloyd 1998; Tian et al. 1998; Cox et al. 2000). Indeed Cox et al. (2000), projects large-scale forest dieback across Amazonia in the 21st Century, with associated emissions contributing to an amplification of human-induced climate change. This type of result from climate-carbon cycle models needs to be refined by using calibrated models that are constrained by data from the Amazon region. Parameterised and validated ecosystem gas exchange and vegetation models for the Amazon region will likely lead to improved present and future carbon balances. This is of vital importance to improve the accuracy of climate-carbon cycle model simulations of future atmospheric carbon dioxide concentration and climate.

Land surface schemes within Global circulation models (GCMs) usually represent vegetation as a combination of plant functional types (Sitch et al. 2003) and each plant functional type is characterized by a single set of parameters. This means the entire Amazon rainforest is taken as a physiologically uniform entity. Besides the fact that across the Amazon basin there is considerable spatial variability in climatic conditions and soil types, recent research has found differences in forest structure and dynamics (Lewis et al. 2004). Results from field observations have shown major differences in above-ground net primary productivity (ANPP), above-ground biomass and tree dynamics across Amazonia; West Amazonia being more dynamic with younger trees, higher stem growth rates and lower biomass than in central and eastern Amazon (Baker et al. 2004; Malhi et al. 2004; Phillips et al. 2004). Above-ground net primary productivity (ANPP), i.e. annual biomass increment, has been estimated to vary by a factor of 3 across Amazonia (Malhi et al. 2004). Different hypotheses have been proposed to explain the observed spatial variability in ANPP: First, due to the proximity to the Andes, sites from western Amazonia tend to have richer soils than central and eastern Amazon and therefore soil fertility may be responsible for the high wood productivity found in western sites. Second, if gross primary productivity (GPP), the sum of net above- and below-ground production and plant respiration, is constant across the Basin, different patterns of carbon allocation across from western to eastern Amazonia could also explain the observed gradient in ANPP. Finally, if GPP is not constant but varies across this transect, spatial variability in GPP of the same order found for ANPP could also account for the observed gradient in ANPP. A basin wide simulation with a canopy level gas exchange model is needed to infer the likelihood of spatial variability in GPP, bearing in mind a single model parameterisation for the Amazon region might be a major simplification if aiming for a realistic result.

One of the most important components of the carbon balance in terrestrial ecosystems is the gross primary productivity which accounts for the total amount of carbon that is fixed during photosynthetic CO_2 assimilation by vegetation. The amount of carbon absorbed by plants depends not only on the physiological capability of the plant itself but also on its environment. Radiation, nutrients, and water are among the major

requirements for plant carbon assimilation. GPP tends to be highest in tropical areas where climatic and environmental conditions are least limited (Lloyd and Farquhar 1996), with plants rarely limited by low temperatures and usually privileged in terms of radiation and water availability. However in many tropical areas highly weathered soils of low nutrient status predominate and this may provide a limitation on GPP through low levels of foliar P and/or N (Lloyd et al. 2001).

At present, GPP at the stand level can be estimated from measurements and/or from model simulations. Stand level estimates of GPP based on measurements can be derived either from leaf level gas exchange, i.e. net assimilation scaled up to canopy level, or from stand level measurements of net ecosystem exchange (NEE) using the eddy correlation technique added to estimates of ecosystem respiration. At a stand level, GPP is usually modelled by scaling leaf level photosynthetic uptake to canopy level. The physiology and key controls on rates of photosynthetic carbon fixation at the leaf level are well understood (Farquhar and von Caemmerer 1982). Under the assumption of nitrogen (N) limitation, leaf photosynthesis is usually modelled based on the measured linearity between photosynthetic capacity and N content per unit leaf area (Evans 1993; Field and Mooney 1986; Hirose and Werger 1987; Pettersson and McDonald 1994). Leaf photosynthesis is scaled up to canopy level based on the hypothesis that N partitioning within canopies changes with irradiance in such a way as to maximize whole-canopy photosynthesis (Evans 1989a, 1989b, 1993; Hikosaka and Terashima 1995). This optimal approach to N partitioning is frequently used in the ecosystem/global modelling community. However, for tropical ecosystems it has been suggested that leaf phosphorous (P) rather than leaf N may be the key limiting nutrient constraining productivity of lowland rainforests, where soils are highly weathered, phosphorous availability is low and nitrogen is relatively abundant (Vitousek and Sanford 1986). Aside from the importance of many sugar-phosphates in photosynthesis and respiration, phosphorous plays an essential role in energy metabolism because of its presence in important molecules that store energy which are essential to the Calvin cycle (Salisburry and Ross 1992). Therefore, deficiencies in phosphorous can limit the rates of RuBP regeneration (RuBP is the CO_2 acceptor molecule in the Calvin cycle) and consequently carbon assimilation (Lambers et al. 1998). It is likely the low P concentrations in tropical forest leaves may constrain photosynthetic rate, at least for some tropical forests (Lloyd et al. 2001).

Field work observations and models can come together to improve, parameterise and evaluate models within the limitations imposed by the measurements. For instance concurrent measurement of fluxes from eddy correlation and meteorological variables have been of considerable use within the modelling community, allowing models that simulate plant carbon and energy exchange at the ecosystem level to be compared with corresponding ecosystem level data. This type of model calibration and evaluation can be made at different regions and ecosystems aiming to improve model estimates of regional and global carbon balance and future estimates of atmospheric CO_2 levels.

During the past ten years the use of the eddy correlation method has increased considerably and emerged as a routine tool for assessing ecosystem carbon and vapour exchange with the atmosphere on time scales of hours-to-years (Baldocchi 2003), often with a major goal of quantifying the global carbon balance (Dolman et al. 2003). In addition to measuring the carbon balance at short and long time scales at the ecosystem level, the eddy correlation method is a useful tool for understanding the magnitude and variation in responses of

vegetation to environmental variables at individual sites (Law et al. 2002).

Even though the increased availability of eddy correlation flux data has been very useful for calibrating and evaluating a model's ability to simulate measurements and ecosystem responses to different environmental variables, it is important to note some limitations of the method. A frequent failure to close the energy balance, especially problematic at forest ecosystems (Baldocchi et al. 2003; Finnigan et al. 2003 Wilson et al. 2002; Massman and Lee 2002), makes it difficult to assess the modelled partition of net radiant energy. One additional significant difficulty in using eddy correlation carbon fluxes lies in the fact the method estimates the net carbon exchange which comprises two large and opposing fluxes associated with processes that often occur simultaneously: photosynthesis by leaves, and whole–ecosystem respiration, i.e. the combination of plant and heterotrophic respiration. Separating the net into its component fluxes is not an easy task, and is usually achieved by relating respiration to the net ecosystem exchange measured during night-time. There are two drawbacks in estimating ecosystem respiration using this method: first, daytime ecosystem respiration differs from night-time due to temperature differences especially at the canopy level. Second and most importantly, there is a frequent apparent failure of the system to measure night-time respiration fluxes at low wind speed conditions (Aubinet et al. 2002; Massman and Lee 2002; Pattey et al. 2002; Saleska et al. 2003). Furthermore, the storage flux term, defined as the rate of change in CO_2 concentration within the canopy between the forest floor and the eddy correlation measurement height, is often evaluated at one location, not taking into account the heterogeneity in the source distribution and horizontal air movement such as drainage flow associated with topography (Pattey et al. 2002). Ecosystem respiration can be also determined, when there is available information of the different respiration terms from each ecosystem compartment, e.g. the leaves, bole, roots and soils.

Different models of leaf photosynthesis and stomatal conductance that scale up leaf processes to canopy level have been forced, calibrated and evaluated using meteorology measured together with fluxes from eddy correlation from single sites in tropical (Harris et al. 2004; Lloyd et al. 1995; Williams et al. 1998; Zhan et al. 2003; Aragao et al. 2004), conifer (Arneth et al. 1998) and deciduous (Baldocchi and Harley 1995) forests. If a temporal and spatial integration over a region is to be made, models should be tested against more than one site in order to see different canopy response functions to environmental variables. For example eddy correlation systems have been installed on top of several towers at different sites in the Brazilian Amazon (See Figure 1 for sites studied in this thesis) to monitor the rainforest exchange of energy and carbon with the above atmosphere. There have already been modelling studies at single sites: at Jaru (Lloyd et al. 1995), Tapajos (Aragao et al. 2004) but mostly at the Manaus site (Harris et al. 2004; Lloyd et al. 1995; Williams et al. 1998; Zhan et al. 2003), however no single modelling study has been undertaken for all tower sites.

Figure 1. Rainforest site locations used in this study. Locations with more than one site have in parenthesis the number of sites and places where there are eddy correlation systems have in parenthesis (tower).

Objective

The main goal of this thesis is to develop a model to simulate rain forest Gross Primary Productivity, GPP, along an East-West transect across the Amazon basin to specifically address the following questions:

1.- Can the observed GPP and energy fluxes derived from eddy correlation be consistently simulated at different Amazonian rainforest sites?

2.- What are the advantages and disadvantages of the modelling approach used?

3.- What constrains a model evaluation using eddy correlation flux data for Amazonian sites?

4.- What can be learnt from this up-scaling exercise about GPP in the Amazon basin?

5.- How sensitive is simulated GPP to environmental variables?

6.- What uncertainties are associated with up scaling relationships based on leaf N and leaf P?

With the motivation to estimate rainforest GPP across the Amazon basin and with the need to refine ecosystem gas exchange models that describe photosynthetic carbon uptake in this region, this study intends to give a first estimate of GPP across a transect in the Amazon basin. To achieve this, initially two ecosystem gas exchange models, the big leaf and sun/shade models, are calibrated and evaluated against eddy correlation data from a single site in the Amazon basin. The performance of both models to reproduce measurements of carbon uptake and energy balance is evaluated in Chapters 1 & 2, respectively. Then, based on better performance, a single approach is chosen (sun/shade) and in Chapter 3, the parameterised model is applied and evaluated at five rainforest sites in the Amazon Basin using available eddy correlation and meteorological data at each site. Subsequently, relationships between maximum rate of carboxylation and foliar nutrients (i.e. relationship between V_{max} and foliar N, and also possible relationships between V_{max} and foliar P) are derived as scaling functions that the model can test to scale up to the basin level. Finally in Chapter 4, these relationships of V_{max} versus foliar N and versus foliar P, are used to simulate GPP at 35 sites across the Amazon Basin (Figure 1). This employs a unique set of foliar N and P content and leaf area index (LAI) taken in situ from the RAINFOR Consortium data set (unpublished data) along with three hour meteorology provided by the European Centre for Medium-Range Weather Forecast (ECMWF) weather forecast model as forcing data to produce simulated net assimilation for the period 1982-2001. In this chapter the sensitivity of the simulated gross primary productivity based upon parameterisations of canopy photosynthetic capacity using foliar N and also on foliar P is tested. Furthermore, detection of spatial variability in GPP and any relationships to climatology, leaf area index (LAI) and stand-level above-ground net primary productivity across the 35 rainforest sites is made. Finally, in Chapter 5 a synthesis of the major results and interpretations is presented, and answers are given to the major questions of this thesis.

1 Modelling Amazonian forest eddy covariance data: A comparison of big leaf versus sun/shade models for the C14 tower at Manaus. I. Canopy photosynthesis[1]

1.1 Introduction

Tropical rain forests play an important role in the global carbon budget covering 12% of the planet's land surface and containing around 40% of the carbon in the terrestrial biosphere (Taylor and Lloyd 1992). It has been estimated that they may account for as much as 50 % to the global net primary productivity (Grace et al. 2001).

Recently, some studies have suggested the possibility that mature rainforests are currently acting as net carbon sinks. This implication comes from forest inventories (Phillips et al. 1998) eddy covariance measurements (Malhi et al. 1998) and global atmospheric inversions (Rödenbeck et al. 2003). Some terrestrial modelling studies (Tian et al. 1998) have also suggested that undisturbed Amazon forest can be a strong net sink of CO_2 particularly during wet years or can be a carbon source when precipitation in much of the Amazon Basin is severely reduced (i.e during strong *El Niño* events). The measured magnitude of the sink is still controversial due to the range of reported values and it is clear that the magnitude of the sink in Amazonia can have important implications for the global carbon cycle.

There is a need to parameterise and validate ecosystem gas exchange and vegetation models for the Amazon region in order to adequately simulate present and future carbon balances. Calibrated models for the Amazon region are also of vital importance to improve accuracy of climate models' simulations of future carbon dioxide concentration and climate.

In the absence of major disturbances such as fire, gross primary productivity together with ecosystem respiration constitute the major components of an ecosystem's carbon balance. In this study, we concentrate on modelling gross primary productivity using two simple approaches to simulate canopy photosynthesis: big leaf and sun/shade models.

Among the terrestrial ecosystem biophysical modelling community, the merit of separating the contributions from sunlit and shaded foliage to canopy photosynthesis in model simulation has been recognized for some time (de Pury and Farquhar 1997; Goudriaan 1977; Medlyn et al. 2000; Norman 1980; Thornley 2002; Wang and Leuning 1998). This is because the photosynthesis of shaded leaves should retain an essentially linear response to above canopy irradiance even though photosynthesis of sunlit leaves may be light saturated. The sun/shade approach is expected to give more accurate predictions because of its separation of the leaves into dynamically changing sunlit and shaded groups exposed to very different radiation environments.

[1] Part of this chapter has been published as Mercado et al. (2006).

A closely related issue is the importance of separating diffuse skylight and direct sunlight when considering the penetration and absorption of radiation through the canopy. This is because of their different attenuation in canopies and the temporal and spatial variation in illumination intensity (de Pury and Farquhar 1997; Goudriaan 1977). Under clear sky conditions most of the solar irradiance is direct beam radiation, whereas under overcast conditions the radiation is almost all diffuse. The partitioning of the incoming radiation into diffuse and direct portions thus creates spatial bimodality in the illumination of the canopy: sun foliage receives diffuse and direct irradiance and shade foliage receives only diffuse irradiance.

Canopy light use efficiency (ratio of amount of CO_2 fixed to amount of absorbed photosynthetically active radiation, PAR) has been reported to be higher under diffuse irradiance than under direct radiation for individual trees and forest canopies (Gu et al. 2002; Law et al. 2002; Lloyd et al. 1995). This can be explained by the following reasoning: since photosynthesis of individual leaves saturates at high irradiances, it is at low irradiances when individual leaves present their highest efficiencies. If light is mostly diffuse, the volume of shade in the canopy is minimal and the whole canopy should be more efficient under low irradiances. If light is mainly direct, there are well defined shadows that occupy larger amounts of leaves in the canopy and light use efficiencies will be lower (Roderick et al. 2001).

Avoiding the separation of leaves into sunlit and shaded is one of the main drawbacks of big leaf models because it has a potential to lead to overestimation of canopy photosynthesis (de Pury and Farquhar 1997). Theoretically then, an accurate separation of diffuse and direct irradiance together with an accurate division of sun and shade foliage should be a crucial issue in modelling canopy photosynthesis.

Our main objective here is to calibrate and test these two approaches for modelling canopy photosynthesis, namely the big leaf and sun/shade parameterisations. The big leaf model (Lloyd et al. 1995) is calibrated against eddy covariance data, and sun/shade (de Pury and Farquhar 1997) is parameterised using derived leaf level photosynthetic parameters from vertical profiles of leaf photosynthetic capacities together with data of vertical distribution of leaf area density. More specifically, we wanted to compare and evaluate the behaviour of both models for an Amazonian ecosystem.

1.2 Materials and methods

1.2.1 Site

The study site is an undisturbed mature lowland rain forest in the central Brazilian Amazon, close to Manaus, (2° 35’ S, 60° 06’ W). It is part of the Cuieiras biological reserve owned by the Instituto National de Pesquisas da Amazonia (INPA). The forest has a closed canopy of about 35-40 m height with a few emergent trees reaching up to 45m (Ranquin de Merona et al. 1992). Permanent forest inventory plots established around the study area (2^o 30’ S, 60^o 06’ W) by the Biomass and Nutrient Experiment (BIONTE) and the Biological Dynamics of Forest Fragments Project (BDFFP) measured an average of stand biomass of 324.14 Mg ha^{-1} (reported in Chambers et al. (2001)). A leaf area index of 5.7 m^2 leaves m^{-2} ground has been measured at this site (Meir et al. 2000) with values in the range [4.1-5.7] having been measured in nearby forests by S. Patiño (pers. comm.). The landscape consists of plateaus and valleys with soil type decreasing gradually from oxisols in the uplands (where the measurement tower was located) and upper parts of the

valleys to utisols and spodosols in the valley slopes. There is a gradual decrease in clay content from oxisols (80% - 90%) to spodosols (2% - 5%). This decrease in clay content is accompanied by an increase in quartz from the upper to the lower level of the toposequence (Bravard and Righi 1989).

Central Amazonia is characterized by a seasonal rainfall regime with a dry season (usually with monthly precipitation lower than 100 mm) from July to October. The annual mean temperature is 26 °C. Leopoldo et al. (1987) reported an average annual precipitation of 2101 mm for the Manaus region during the 1931-1960 period. Of the total precipitation, around 73% falls in short heavy rains (Leopoldo et al. 1987).

1.2.2 Data

1.2.2.1 Fluxes and meteorology

Models were tested against measurements of carbon dioxide, water vapour and sensible heat fluxes made by an eddy covariance system of the type described by Moncrieff et al. (1997) located 5 m above the top of a 41.5 m tower, “C14”, previously known as “ZF2”. Meteorological data (global solar radiation, wind speed, air temperature, and wet bulb temperature) used as input data to the models come from an automatic weather station located 2.5 m below the top of the same tower. A detailed description and analysis of the carbon dioxide flux data used here has been provided by Malhi et al. (1998).

The dataset used here to test the models was obtained towards the end of the dry season and the beginning of the wet season of 1995 (mid October to mid December). We have used only this period to calibrate and test the models because this was the only period within the original Malhi et al. (1998) dataset when CO_2 canopy storage estimates were obtained.

A lack of closure of the energy balance is a well-recognized problem of the eddy covariance method (Baldocchi 2003; Goulden et al. 1996; Massman and Lee 2002; Wilson et al. 2002). But recently this problem has been associated with a failure to take into account low frequency contributions to the overall ecosystem flux due to a short mean removal period (Finnigan et al. 2003; Sakai et al. 2001). For the Manaus C14 site described by Malhi et al. (1998), it was found that once turbulent transport at low frequencies (on time scales of 1 to 4 hours) was taken into account, the energy balance of the forest was much improved (Finnigan et al. 2003; Malhi et al. 2002). Including the correction for low frequency contributions to fluxes, sensible heat fluxes increased by 43.3%, latent heat fluxes by 32.1% and day time CO_2 fluxes increased by 30.7%. Fluxes from this “recalculated data set” (Malhi et al. 2002) have thus been used here for calibration (big leaf) and validation (big leaf and sun /shade) of the models.

Because the carbon dioxide fluxes determined by eddy covariance are net ecosystem exchange rates, in order to determine canopy CO_2 assimilation rate, A, it is necessary to take into account the ecosystem respiration rate, R_E.

$$A = N_E - \mathrm{R}_E \qquad (1)$$

$$N_E = \mathrm{F}_c + \int_0^{h_t} \frac{\partial \mathrm{C_a}}{\partial \mathrm{t}} \mathrm{dz} \quad (2)$$

where A is assimilation or gross primary productivity and N_E is net ecosystem exchange measured by eddy covariance, both in [μmol m^2 s^{-1}]. F_c is the flux of CO_2 measured by eddy correlation [μmol m^2 s^{-1}]. The integrand in [μmol m^2 s^{-1}], represents the rate of change in the CO_2 concentration (C_a) within the canopy between the forest floor and the eddy covariance measurement height, h_t.

1.2.2.2 Ecosystem respiration

The eddy covariance technique has become a very important and widely used tool to measure the net ecosystem exchange of CO_2 at regional levels, and theoretically, it should be possible to use the night time eddy correlation fluxes to determine the respiration of an ecosystem. But like other measuring techniques, this method has limitations and most of the limitations occur at night time when air is typically stratified which is associated to low turbulence (Aubinet et al. 2002; Baldocchi 2003; Goulden et al. 1996; Massman and Lee 2002). Massman and Lee (2002) report eddy covariance limitations being mainly of instrumental and meteorological types. Since eddy covariance is a technique that performs best when turbulent conditions predominate, the usual stable atmospheric conditions occurring during night time might make sensor limitations a significant restriction for accurate measurements. Large footprints, gravity waves, advection and low turbulence are among the most significant meteorological restrictions (Massman and Lee 2002). An analysis of the database used for this study reports underestimation of the night time fluxes especially at low wind speeds (Malhi et al. 1998). Specifically because of the undulated topography formed by valleys and plateaus in the Manaus region and because the C14 tower is located on a plateau, it might be possible that on calm nights, part of the CO_2 that is being respired is draining to the valleys without being registered by the tower sensors (Araújo et al. 2002). Because of all these uncertainties with night time eddy correlation fluxes, ecosystem respiration rates in this study were taken from direct chamber measurements of the different contributions to the ecosystem CO_2 efflux performed in sites nearby and scaled up appropriately.

We define ecosystem respiration as the summation of different contributions from live leaves (R_C), stems and branches (R_W), soil (which includes root and fine litter decomposition in the soil surface) (R_S) and coarse litter (R_{CS}) contributions. All terms are in [μmol m^2 s^{-1}].

$$R_E = R_S + R_W + R_C + R_{CS} \quad (3)$$

Leaf respiration (ground area basis basis) was modelled for this site and measurements of soil and stem respiration (Chambers et al. 2004) and that of coarse litter (Chambers et al. 2001) in an area nearby were used to parameterise the models. Coarse litter respiration was taken as a constant 0.5 μmol m^2 s^{-1} and stem respiration was taken as 1.1 μmol m^2 s^{-1} (both terms in ground area basis) with the same temperature dependence as for canopy respiration in equation (11) below. The soil respiration measurements (Chambers et al. 2004) were performed during the period (2000-2001, *La Niña* years). We used soil respiration data from October, November and December 2000. Precipitation during these months was higher in year 2000

than in 1995. In the same study, Chambers et al. (2004) found that there is a decrease in soil respiration with increasing volumetric water content of the soil. Because precipitation regimes were different during 1995 and 2000, soil volumetric water content might have been higher for 2000 than during 1995. Therefore, soil respiration during the period October-December 95 might have been slightly higher than the ones during the same months in year 2000. This implies that our estimations of gross photosynthesis used here to fit and test the models, using net ecosystem exchange measured by the eddy covariance system plus ecosystem respiration could have been slightly higher as well.

1.2.3 Theory and Models

1.2.3.1 Leaf biochemistry

The biochemistry of C_3 photosynthesis is given by Farquhar and von Caemmerer (1982) as presented by Lloyd et al. (1995). Leaf level photosynthetic capacity is described as the sum of all the chloroplast capacities in a given unit area and the chloroplast properties are assumed to scale with the internal light gradient of the leaf (Farquhar et al.1989).

The CO_2 assimilation rate (A) in [µmol m^2 s^{-1}] is controlled by the rate of carboxylation when rubisco activity is limiting (A_v) at low intercellular partial pressure of CO_2 and/or high irradiances and by the rate of electron transfer when Ribulose biphospate (RuBP) regeneration is limiting (A_J) at high intercellular partial pressure of CO_2 and/or low irradiances (Farquhar et al. 1980). The rate of CO_2 assimilation is modelled as the minimum between A_v and A_J.

The rubisco-limited rate, A_v, and electron transport-limited rate, A_J, both in [µmol m^2 s^{-1}] are defined as:

$$A_V = V_{\max}\left(\frac{C_C - \Gamma^*}{K_C\left(1 + pO_2/K_0\right) + C_C}\right) - R_C \qquad (4)$$

$$A_J = \frac{J}{4}\left(\frac{C_C - \Gamma^*}{C_C + 2\Gamma^*}\right) - R_C \qquad (5)$$

where $V_{\max}$ in [µmol m^2 s^{-1}] is the maximum rate of rubisco activity, K_o and K_c in [Pa] are the Michaelis-Menten constants for carboxilation and oxygenation by rubisco, C_c in [Pa] is the partial pressure of CO_2 in the chloroplast, Γ^* in [Pa] is the CO_2 compensation point in the absence of mitochondrial respiration and R_C in [µmol m^2 s^{-1}] ground area basis, is leaf dark respiration in the light. The rubisco Michaelis constants for CO_2 and O_2 are described to follow an Arrhenius type temperature dependency as in Lloyd et al. (1995b).

The potential rate of electron transport, J in [µmol m^2 s^{-1}], is modelled as a non-rectangular hyperbolic function of the absorbed quantum flux with I_2 in [µmol quanta m^2 s^{-1}] as the absorbed irradiance that reaches photosystem II, $J_{\max}$ in [µmol m^2 s^{-1}], as saturating value and θ as curvature factor:

$$\theta J^2 - (I_2 + J_{\max})\, J + I_2\, J_{\max} = 0 \qquad (6)$$

$$I_2 = I_0\,(1-r-t)\,(1-f)\,\Phi \qquad (7)$$

with r and t being canopy reflectance and transmittance for PAR, I_0 being the PAR reaching the leaf or canopy surface in [μmol quanta m^2 s^{-1}]. Φ is quantum yield defined as the initial slope of the relationship between assimilation rate A and irradiance. It describes the efficiency with which light is converted into fixed carbon.

The temperature sensitivities for rubisco activity and electron transport are given by Farquhar and von Caemmerer (1982) as presented by Lloyd et al. (1995):

$$V_{\max} = V_{\max,25} \exp\left(\frac{E_v}{298.2R}\left(1 - \frac{292.2}{T_C}\right)\right)$$

$$J_{\max} = J_{\max,25} \frac{\exp\left[\frac{(T_C / 298.2 - 1)E_J}{RT_C}\right]\left[1 + \exp\left(\frac{298.2S_J - H_J}{298.2R}\right)\right]}{1 + \exp\left(\frac{S_J T_C - H_J}{RT_C}\right)} \quad (8)$$

(9)

where T_C is absolute temperature [K] of the leaf or canopy, R is the universal gas constant (8.314 J mol^{-1} K^{-1}), $V_{max,25}$ and $J_{max,25}$ are rubisco activity and electron transport capacity at 25 °C in [μmol quanta m^2 s^{-1}]. E_v and E_J in [J mol^{-1}] are activation energies. H_J in [J mol^{-1}] and S_J in [J $mol^{-1}K^{-1}$] control maximum and minimum optimum temperature dependencies of the electron transport rate. The temperature optimum (T_{opt}) of J_{max} is known to acclimate in different environments, and can be estimated from Farquhar et al. (1980):

$$T_{opt} = \frac{H_J}{(S + R\ln(H_J / E_J - 1))} \quad (10)$$

The temperature dependency of leaf respiration is taken as presented by Lloyd et al. (1995):

$$R_D = R_{D,25} \exp\left(308.45\left(\frac{1}{71.02} - \frac{1}{T_C - 227.13}\right)\right) \quad (11)$$

where R_D is the rate of canopy dark respiration at T_C and $R_{D,25}$ is the rate of canopy dark respiration at 25 °C, both are given in [μmol m^2 s^{-1}].

Leaf respiration is modelled to decrease with increasing light with an empirical formula obtained based on observed leaf respiration in varying light and incoming irradiance levels for spinach leaves (Brooks and Farquhar, (1985) as implemented by Lloyd et al. (1995)).

$$R_C = R_D \qquad 0<I_o<10 \text{ μmol quanta } m^{-2} s^{-1}$$

$$R_C = [0.5 - 0.05\ln(I_o)]R_D \qquad I_o>10 \text{ μmol quanta } m^{-2} s^{-1} \quad (12)$$

where R_D is the rate of canopy respiration in the dark in [μmol m^2 s^{-1}] and I_0 the irradiance reaching the canopy in [μmol quanta m^2 s^{-1}].

Because stomatal conductance is also modelled, we prefer to use equations (1) and (2) as a function of stomatal conductance for CO_2 and ambient partial pressure of CO_2. The mathematical development of these equations is presented in appendix III of Lloyd et al. (1995b).

The equations used here neglect the effect of the mesophyll conductance as in de Pury and Farquhar (1997). Based on measurements those authors argued that avoiding mesophyll conductance would have effects of less than 1% in canopy photosynthesis.

1.2.3.2 Big leaf model

A similar argument as has been applied to the scaling of chloroplast biochemical properties to the leaf level (Farquhar et al. 1989) has sometimes been applied to plant canopies. That is, if the distribution of photosynthetic capacity among leaves in a canopy is in proportion to the profile of absorbed irradiance, then the canopy can be treated as a big leaf and the equations used for individual leaves should be applicable to the canopy as a whole (Sellers et al. 1992). The main assumption of this approach is an optimal distribution of leaf nitrogen through the canopy, which means that the vertical profile of photosynthetic capacity is distributed in proportion to the time-averaged irradiance (de Pury and Farquhar 1997). The scaling from leaf to canopy level is done at the biochemical parameters (V_{max}, J_{max}) and leaf respiration (R_C). This means that stomatal conductance to water vapour, carbon assimilation and energy fluxes are simulated with the big leaf model for the whole canopy (in total canopy area basis). Furthermore, the big leaf model makes no distinction between direct and diffuse radiation, ignoring any sun fleck penetration and also the effects of leaf angles within canopy irradiance profiles. The big leaf model used in this study is described by Lloyd et al. (1995).

1.2.3.3 Sun/shade model

The main feature of this approach is the partitioning of the canopy into sunlit and shaded components. Each component is modelled as a single layer model using the biochemistry of single leaves as given in de Pury and Farquhar (1997). The division of sun and shade foliage changes during the day with solar elevation, which means that the photosynthetic capacity and the irradiance absorption of the sunlit and shaded portions of the canopy are also dynamic. All leaves are modelled to absorb diffuse, scatter diffuse and scattered beam irradiance. Sunlit leaves also receive direct-beam irradiance. The vertical distribution of leaf nitrogen, V_{max} and J_{max} within the canopy is taken to decrease exponentially with cumulative leaf area index from the top of the canopy (See Figure 1.1c, parameterisation using leaf level data), though no implicit assumption of photosynthetic capacity varying directly with average absorbed irradiance is required (as is the case in the big-leaf model).

Photosynthetic capacity of the sunlit and shaded fractions of the canopy is calculated by integrating the leaf photosynthetic capacity and the sunlit and shaded leaf area fractions respectively. Photosynthesis of the sunlit and shaded fractions in then separately calculated by use of the big leaf model (equations 4-11) with

the absorbed irradiance and photosynthetic capacity, light saturated rate of electron transport and leaf dark respiration of each fraction used instead of the equivalent leaf level variables. Finally canopy photosynthesis is calculated by adding the single contributions from the sunlit and shaded photosynthesis (already in the respective (sunlit or shade) area basis). The sun/shade model for canopy photosynthesis used here is described in detailed in de Pury and Farquhar (1997).

1.2.3.4 Stomatal conductance: The 'Lambda' model

The "lambda model" used here is based on the assumption of optimal stomatal regulation of the rates of CO_2 assimilation and transpiration per unit leaf area in a plant at a finite interval of time with changing environmental conditions except for small changes in the amount of soil water available to the plant (Cowan and Farquhar 1977).

The lambda parameter (λ) is a Lagrangean multiplier and it represents the marginal benefit of plant carbon gain relative to the cost of water loss. Lloyd et al. (1995) showed that if λ was a constant over a day and did not vary with light or leaf temperature then the relationship:

$$G_S = A\sqrt{\frac{1.6\lambda P}{(C_a - \Gamma^*)Dc}} \qquad (13)$$

should apply. Here A is assimilation in [mol $m^{-2}s^{-1}$], λ in [mol mol^{-1}], D_C vapour pressure deficit in mol fraction, P atmospheric pressure and C_a ambient partial pressure of CO_2, and Γ^* is the CO_2 compensation partial pressure in the absence of dark respiration, all expressed in [mol mol^{-1}].

1.2.3.5 Stomatal conductance: The 'Ball-Berry' model

The empirical model of Ball et al. (1987) as modified by Leuning (1990) is also tested. Stomatal conductance is calculated as:

$$G_s = g_0 + \frac{g_1 AhP}{(C_a - \Gamma^*)} \qquad (14)$$

This approach uses relative humidity at the leaf surface (h) and includes two parameters g_0 and g_1. The first parameter (g_0) corresponds to the minimum stomatal conductance to water vapour when A=0 at the light compensation point. The second parameter (g_1) is an empirical coefficient which represents the composite sensitivity of conductance to assimilation, CO_2, humidity and temperature.

Both the 'Lambda' and 'Ball-Berry' models of stomatal conductance, represented by equations (13) and (14) respectively, are coupled to the big leaf and sun and shade models. Both stomatal conductance models are known to perform best for well-watered plants (Cowan and Farquhar 1977; Leuning 1990; Leuning et al. 1995). Because this study was conducted during the end of the rainy season, the effects of soil water stress on canopy gas exchange were considered to be unimportant.

1.2.3.6 Parameterisation of the big leaf model

From the mid October-mid December 1995 data, a selected data set was used to fit the model. Criteria of selection followed the same conditions as in Lloyd et al. (1995) and in Grace et al. (1995). Data before 0900 was rejected in order to avoid the CO_2 flush or so-called morning peak. Storage terms larger than 8 μmol m^{-2} s^{-1} and smaller than -8 μmol m^{-2} s^{-1} were also neglected as were data points collected during and after rainy hours. Measurements where radiation fluctuated as a result of a moving cloud (i.e abrupt changes in solar radiation from hour to hour) were also filtered together with aerodynamic conductances lower than 0.1 μmol m^{-2} s^{-1}.

Canopy level maximum carboxylation activity of Rubisco (V_{max}), light saturated potential rate of electron transport capacity (J_{max}), rate of canopy respiration in the dark (R_D), temperature sensitivity parameters for electron transport, S_J and H_J, the curvature factor and slope of the light response curve, θ and Φ respectively, were then estimated by minimizing the error sum of squares of the model fitted to the selected data set using a simplex procedure (Nelder and Mead 1965).

1.2.3.7 Parameterisation of the Sun/shade model

Maximum canopy level rate of carboxylation by Rubisco (V_{max}), light saturated potential rate of electron transport (J_{max}) and canopy dark respiration (R_D) were calculated by numerical integration of the profiles of the leaf level V_{max}, J_{max}, R_D, and cumulative leaf area index along the canopy height as described in de Pury and Farquhar (1997). Profiles of leaf level V_{max}, J_{max} and R_D were derived from gas exchange measurements made at the same site where the C14 tower is located. Measurements were made at five different heights within the canopy (Carswell et al. 2000) (See Figure 1.1a for the vertical profile of V_{max}). Since the gas exchange measurements of Carswell et al. (2000) were undertaken only to a height of 24 m, we fitted an exponential curve to the points in Figure 1.1a and extrapolated the correspondent V_{max}, J_{max} and R_D values for 30 and 35 m height. The vertical distribution of leaf area index was determined using a photographic method to measure leaf area density (m^2 leaf m^{-3} leaf) at different heights on the same C14 tower (Meir et al. 2000) (Figure 1.1b). Using the vertical profile of leaf area density, leaf area index was calculated for each height and then the cumulative leaf area variation with height was also determined. By plotting the vertical profile of V_{max}, J_{max}, and R_D with cumulative leaf area index we found that there was indeed an exponential decrease of each of these canopy properties with height or with cumulative leaf area index. We then fitted an exponential function that was numerically integrated along the whole leaf area index to provide canopy V_{max}, J_{max} and R_D. Figure 1.1c shows the relationship between V_{max} (ground area basis) at leaf level and cumulative leaf area index. The area under the curve is the canopy carboxylation capacity.

The rest of the required parameters, curvature factor of the light response curve, θ, slope of the light response curve, Φ, and temperature sensitivity parameters of the electron transport rate, S_J and H_J, were taken from the modelling study of Carswell et al. (2000).

The lambda parameter (λ) and the parameters from the 'Ball and Berry' model (g_o and g_1) were estimated from equations (13) and (14) using the canopy assimilation rate and stomatal conductance deduced from the eddy correlation measurements. Parameterisation of both stomatal conductance models is explained in detail

in Chapter 2. Estimated values of λ, g_o and g_1 were 970 mol mol^{-1}, 0.0246 (mol m^{-2} s^{-1}) and 8.05 (dimensionless), respectively.

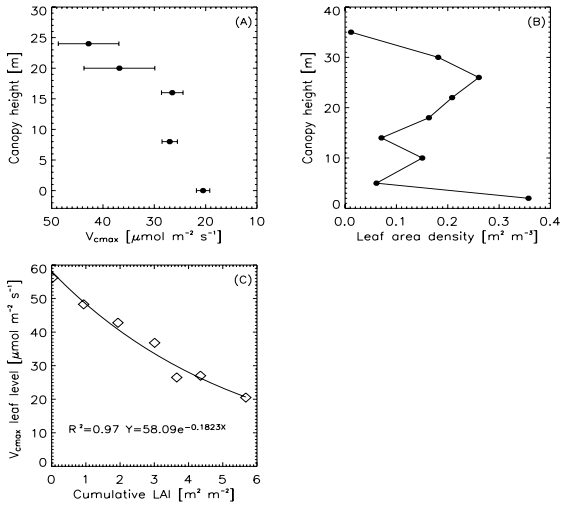

Figure 1.1. Data used for parameterisation of sun/shade model. (A) Vertical profile of leaf maximum carboxylation rate of Rubisco V_{max} (Carswell et al. 2000) (B) Vertical profile of leaf area density (Meir et al. 2000) (C) Vertical distribution of V_{max} with cumulative LAI.

1.3 Results

1.3.1 Sun/shade coupled to the 'Lambda' model

Taking the parameters of Carswell et al. (2000) gave an integrated canopy level V_{max} of 205 μmol m^{-2} s^{-1} at 25 °C with V_{max} at the top of the canopy being 58 μmol m^{-2} s^{-1} at the same temperature and with a J_{max} / V_{max} of 2.6. The rate of canopy respiration in the dark (R_D) was modelled to be 3.9 μmol m^{-2} s^{-1} at 25 ºC with canopy respiration at the top of the canopy being 1.3 μmol m^{-2} s^{-1} at the same temperature.

To run the model, the temperature sensitivity parameters of J_{max} (S_J and H_J) and the curvature factor of the non-rectangular hyperbolic function were initially taken as given by Carswell et al. (2000) from A-C_i and light response curve gas exchange measurements on individual leaves throughout the canopy (710 J K^{-1}mol^{-1}, 220000 J mol^{-1} and 0.67, respectively, with a temperature optimum of J_{max} at 32 °C).

When the sun/shade model was run with the above parameterisation, canopy daytime CO_2 assimilation rates were overestimated by on average 20 % when compared to the eddy correlation estimates (shown in Figure 1.2a-b), but when V_{max} and R_D at the top of the canopy were empirically reduced by 10% and the ratio of light saturated potential rate of electron transport to rubisco activity was reduced to 1.9, a much better fit was obtained (Figure 1.2c-d). The higher initially estimated ratio had resulted in sunlit leaves never being limited by their electron transport rate, which with shaded leaves representing about 70-85% of the canopy LAI, was the main source of the initial overestimation. The initial high ratio is also a result of the high up-scaled canopy J_{max}, related to the high nitrogen levels of the leaf level data used for up-scaling. This issue is discussed later. An even better fit was obtained when the apparent quantum yield was reduced from 0.5

(as in Carswell et al. 2000) to 0.4 (Figure 1.2e-f) with a further improvement also being obtained when one of the Carswell et al. (2000) electron transport temperature response parameters was modified slightly, increasing the temperature optimum from 32 to 39 °C (Figure 1.2g-h). The best fitted value of S_J was 693.1 J $K^{-1}mol^{-1}$ (cf. 710.0 in Carswell et al. 2000).

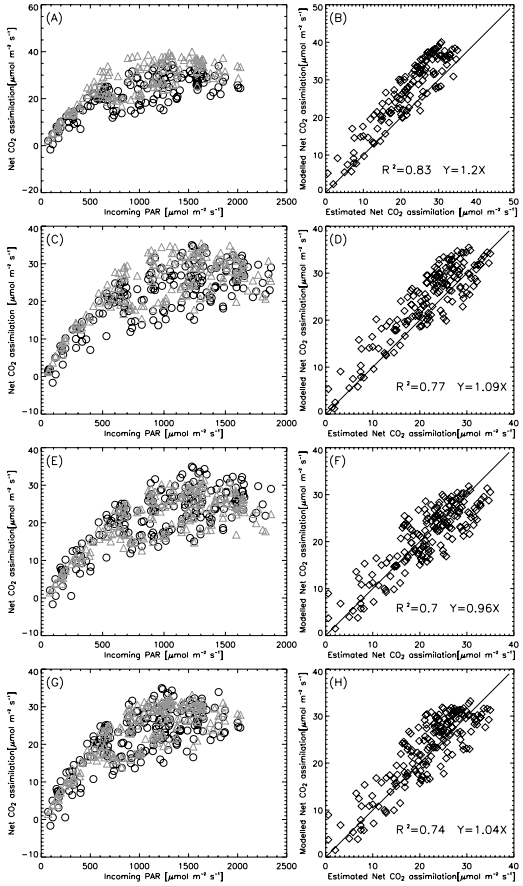

Figure 1.2. Light response (left) and goodness of fit (right) by the sun/shade model using the 'Lambda' model. Estimated (o) and modelled (∇ net CO2 assimilation. Using canopy parameters derived from up scaling leaf level V_{max}, J_{max} and R_D (A and B), top canopy V_{max} and R_D are empirically reduced by 10% and the ratio of J_{max} / V_{max} is reduced from 2.6 to 1.9 (C and D), quantum yield of light absorption reduced from 0.5 to 0.4 and changes included in (C) and (D) (E and F), all the previous changes plus the use of a fitted SJ that increased the optimum temperature of J_{max} from 32 to 39 ^oC (G and H).

1.3.2 Big leaf coupled to the 'Lambda' model

For the big leaf model the fitted values of canopy level V_{max} and J_{max} were 152 and 273 μmol m^{-2} s^{-1}, respectively at 25 °C. The fitted curvature factor for the light response curve was very low (0.17), and the best fitted quantum yield for absorbed light was 0.37. Fitted values of S_J and H_J were 687.4 J $K^{-1}mol^{-1}$ and 215.6 kJ mol^{-1}, respectively, with a temperature optimum of J_{max} of 35.2 °C. Modelled canopy dark respiration rate was 2.92 μmol m^{-2} s^{-1} at 25 ^oC.

The sun/shade model predicted higher gross photosynthetic rates than the big leaf model as a result of the higher canopy V_{max} and $J_{max,}$ but the modelled net assimilation (photosynthesis minus leaf respiration) was quantitatively similar for both models (See Figures 1.2g-h and 1.3a-b). This was because of the much higher

canopy respiration rates modelled by sun/shade, a consequence of the assumption in the initial leaf-level parameterisations of Carswell et al. (2000) that leaf respiration is not inhibited in the light. By contrast, using the parameterisation of Lloyd et al. (1995) the big-leaf model here assumes decreased respiration rates in the light (See Figure 1.4). Assuming no inhibition with light daytime foliar respiration rates have been scaled to ecosystem level for the same site in Manaus giving values between 1.8 and 7 μmol m^{-2} s^{-1} (ground area basis), averaging 4.7 μmol m^{-2} s^{-1} (Chambers J. unpublished data). Similarly, the sun/shade model predicts canopy respiration rates between 2.9 and 6.7 μmol m^{-2} s^{-1} during the day. Leaf respiration during daylight is still a parameter with a high uncertainty because it is not easy to measure due to the difficulty in separating photosynthetic and respiratory processes (Atkin et al. 2002).

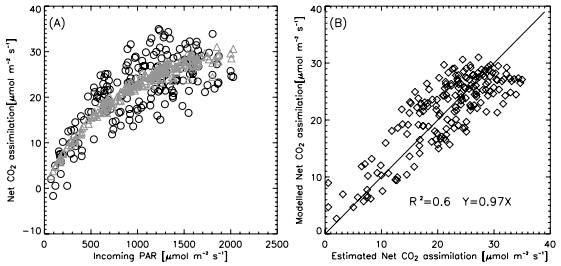

Figure 1.3. Light response curve (A) and goodness of fit as model by big leaf using the 'Lambda' model (B): Estimated (o) and modelled (∇) net CO2 assimilation**.**

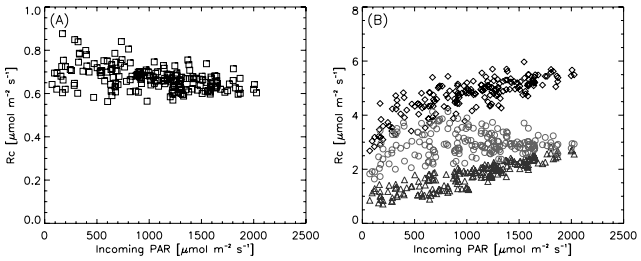

Figure 1.4. Canopy respiration rate modelled by big leaf (A) and by sun/shade (B): leaf respiration by the shaded leaf (o), leaf respiration by the sun leaf (∇), canopy respiration including sun and shade contributions (◊). Note difference in y-axis scale.

The ratio J_{max} / V_{max} for big leaf and sun and shade were very similar, 1.8 and 1.9 respectively. But, in contrast to the sun/shade model the big leaf modelled photosynthesis was limited by electron transport rate at all irradiances, despite the low θ. This can be attributed to the fact that, according to the sun/shade calculations, 70-85% of the canopy LAI is shaded, which means that the majority of the photosynthesis is indeed limited by light. In the sun/shade model, the shaded leaf fraction is limited by electron transport at all the irradiances. The rate of photosynthetic uptake in the sun leaf is light-limited at low irradiances (0-500 μmol quanta $m^{-2}s^{-1}$ PAR), and from 500 to 1000 μmol quanta m^{-2} s^{-1} PAR, it is typically close to being co-limited by rubisco and electron transport rates. At irradiances higher than 1000 μmol quanta m^{-2} s^{-1}, leaves in the sunlit fraction are light-saturated and their photosynthetic activity is then modelled to be limited by rubisco activity.

The efficiency of photosynthesis or quantum yield of absorbed light in both models was fitted and equal to

0.37 and 0.4 for big leaf and sun and shade, respectively. Even though the leaf level measurements are fitted with a value of 0.5 (Carswell et al. 2000), the theoretical optimum value (Farquhar et al. 1980), both models overestimate the data that belong to the region of slope of the light response curve when using that value. In this case, the reduction of the quantum yield of absorbed light implies a reduction in the efficiency of photosynthesis without reduction of photosynthetic capacity. This light dependent reduction is likely associated with a long term down regulation of the quantum yield of photosystem II photochemistry through a mechanism of thermal energy dissipation (Öquist et al. 1992).

The goodness of the models fit is shown in terms of r^2 and the agreement index 'd' in Figures 1.2g-h and 1.3. The index of agreement has been used in other studies (Medlyn et al. 2003); it is useful to indicate the degree which a model's predictions are error-free. The index 'd' ranges from 0 to 1 with increasing agreement between model and data. The sun/shade model had a slightly better fit (r^2 = 0.74 *vs* 0.6, d = 0.93 *vs* 0.9) but also a higher slope (1.04 *vs* 0.97) than the big leaf model. From the light response for both models, it can be seen that the sun/shade model catches some of the variability measured by the eddy covariance system, whilst the big leaf simply provides an average of the data.

Sun/shade models can clearly predict part of the variability due to the radiation treatment as the attenuation of diffuse and scattered radiation are taken into account. This is shown in Figure 1.5 where residuals of assimilation rates (modelled and estimated from eddy correlation) plotted as a function of both incoming PAR and the fraction of diffuse irradiance (F_d). Here it can be seen that at low values of F_d, the big leaf model residual plot skews markedly showing that the model tends to overestimate eddy correlation estimates of assimilation rate under these conditions (Figure 1.5a). By contrast the sun/shade has residuals relatively well distributed around the zero line (Figure 1.5b). The big leaf model is unresponsive to diffuse irradiance and the predictions are especially inaccurate at low values of F_d. At high values of PAR (also typically with low fractions of diffuse irradiance), big leaf tends to overestimation while sun shade presents a more uniform distribution of residuals along the zero line (Figures 1.5 c-d).

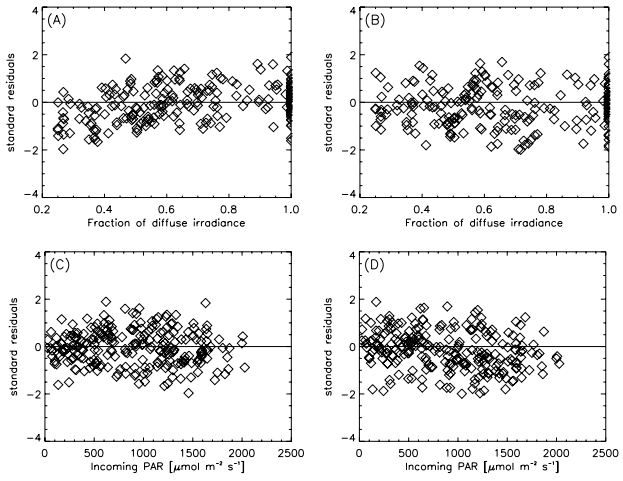

Figure 1.5. Response of incoming irradiance and fraction of diffuse irradiance to standard residuals of modelled and estimated, from eddy correlation, net assimilation rates using the 'Lambda' model. (A) and (C) are residuals by big leaf, (B) and (D) correspond to sun/shade. Positive residuals mean underestimation and negative residuals mean overestimation of simulations respect to observations.

In Figure 1.6 the standardised residuals of observed and simulated net carbon uptake against vapour pressure difference (VPD) and temperature for both models are presented. Again, this shows the generally superior performance of the sun-shade model (Figures 1.6 b,d,f,g) for which there is no bias in the model residuals when examined as a function of VPD or air and canopy temperatures. By contrast, the big leaf model (Figures 1.6 a,c,e) consistently overestimates fluxes at high VPD and temperatures. These are mainly values that also correspond to high irradiances and low fractions of diffuse irradiance.

In the case of sun/shade model, canopy photosynthesis is mainly driven by irradiance absorbed by the shaded leaves (i.e. diffuse irradiance) because 40-60% of the total photosynthesis is undertaken by the shaded part of the canopy which constitutes 70-85% of the leaf area. A plot of the light response of diffuse irradiance is presented in Figure 1.7. It can be seen that it has the same shape as the light response of photosynthesis as modelled by sun/shade (Figure 1.2).

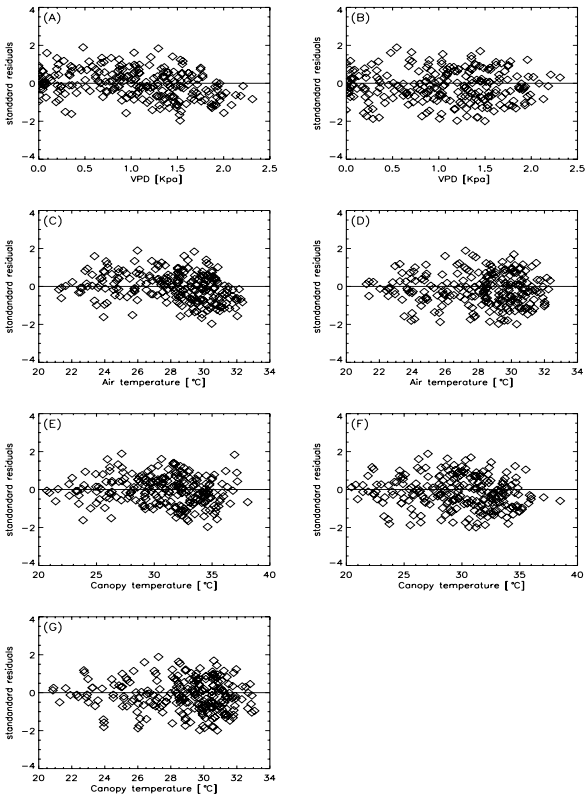

Figure 1.6. Response of VPD, air temperature and canopy temperatures to standard residuals of modelled and estimated net, from eddy correlation, assimilation rates using the 'Lambda' model. (A), (C), (E) are residuals by big leaf, (B), (D), (F) and (G) correspond to sun and shade. (F) is canopy temperature in the sun leaf, (G) is canopy temperature modelled by the shaded leaf. Positive residuals mean underestimation and negative residuals mean overestimation of simulations respect to observations.

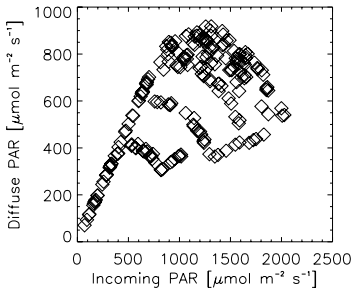

Figure 1.7. Light response of diffuse irradiance using Spitters et al. (1986) model.

If light is mostly diffuse, there are minimal shadows, and photosynthesis will be enhanced. In contrast, when there is clear sky and high PAR the shadows are well defined because most of the radiation comes from a single direction and overall photosynthesis will be lower (Roderick et al. 2001). Thus, an estimation of diffuse irradiance is a highly important variable for sun/shade models, and the accuracy of its calculation becomes very relevant. Here we lacked actual measurements, relying on simulations. This lack of measured diffuse irradiance makes it difficult to quantify the extent to which the modelled diffuse irradiance agrees with reality. Thus, four different models for calculation of global diffuse irradiance were tested (Figure 1.8): Spitters et al. (1986), Weiss and Norman (1985), Reindl et al. (1990) and Erbs et al. (1982) with the fraction for PAR being calculated in all cases using the relationships from (Alados and Alados-Arboledas 1999). Using the models from Weiss and Norman (1985), Reindl et al. (1990) and from Erbs et al. (1982), the sun/shade model predicted a strong trend of overestimation (respect to eddy correlation estimates of assimilation rates) at high diffuse irradiances and underestimation at low diffuse fractions. The best performance of sun/shade model here was obtained using formulations from Spitters et al. (1986). However, at high irradiances the modelled photosynthesis still tended to slightly overestimate. This result suggests a considerable importance for actual diffuse irradiance measurements in the Amazon region to be made in order to test and parameterise diffuse irradiance models needed for canopy photosynthesis modelling.

After accounting for variation in diffuse irradiance, canopy V_{max} for the sun and shaded leaf fractions and stomatal conductance, especially for the shaded leaf fraction, were the variables with strongest influence in modelling photosynthesis using the sun/shade model. Parameterisation of canopy V_{max} was most sensitive to the V_{max} at the top of the canopy and as already mentioned the sun/shade model could only fit the data when reducing the V_{max} and R_D at the top of the canopy by 10% and the ratio J_{max} / V_{max} from 2.6 to 1.9.

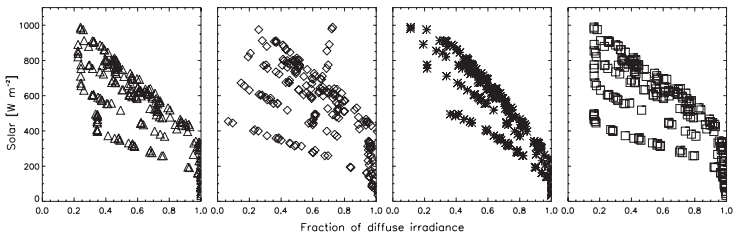

Figure 1.8. Different models for calculating the fraction of diffuse irradiance. (∇) Spitters et al. (1986), (◊) Reindl et al. (1982), (*) Weiss and Norman (1985) and (□) Erbs et al. (1982) model.

The sensitivity parameters for the temperature dependence of the light saturated potential rate of electron

transport, S_J and H_J (equation 9) were also important factors in model performance, especially S_J that controls the optimum temperature of J_{max}. Figure 1.9 shows the temperature dependence function (J_{max} / $J_{max,25}$ from equation 9) evaluated using S_J from Carswell et al. (2000), S_J fitted for big leaf, S_J fitted for sun/shade and S_J used by Lloyd et al. (1995). Besides the value of S_J used by Carswell et al. (2000), remaining S_J from other sources had similar values with optimum temperatures between 39 and 43 °C. Using S_J from Carswell et al. (2000), which has an optimum temperature of 32 °C, resulted in electron transport limited photosynthesis at canopy temperatures higher than 32 °C which implied that photosynthesis by the sunlit leaf fraction was being limited by light at high irradiances. Nevertheless, we also point out that the dataset of Carswell et al. (2000) was not parameterised at the highest canopy temperatures observed as part of this study.

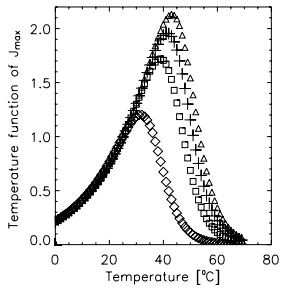

Figure 1.9. Temperature function of J_{max} (J_{max} /$J_{max,25}$ in equation 9) evaluated under different S_J with H_J of 220000 J mol^{-1}.

(◊) S_J from Carswell et al. (2000), S_J =710. J mol^{-1}K^{-1}, optimum temperature= 32 °C.

(□) S_J fitted for sun / shade, S_J = 693.124 J mol^{-1}K^{-1}, optimum temperature= 39 °C.

(+) S_J fitted for big leaf, S_J =687.392 J mol^{-1}K^{-1}, optimum temperature= 41 °C.

(∇) S_J from Lloyd et al. (1995), S_J = 683.6 J mol^{-1}K^{-1}, optimum temperature= 43 °C.

1.3.3 Sun/shade and big leaf coupled to the 'Ball and Berry' model

Using unchanged photosynthetic parameters (from last run with sun and shade in section 1.2.1 and big leaf in section 1.2.2), both the big leaf and sun/shade models were run with the 'Ball and Berry' stomatal conductance model. Replacing the 'Lamdba' model with the 'Ball and Berry' stomatal conductance model did not change to a large extent the goodness of the model to data fit for net carbon assimilation for both models of photosynthesis. Comparison of simulated net carbon assimilation by the big leaf model using the two alternative stomatal conductance approaches produced a linear relation of y=0.99x (r^2=0.99, n=238). Similar results were obtained for the sun/shade model (y=1.003x, r^2=0.99 n=238).

The standard residuals of estimated carbon uptake from eddy correlation minus modelled values, using the 'Ball and Berry' stomatal conductance formulation, are plotted against environmental variables and shown in Figure 1.10 for both the 'Big Leaf' and 'Sun/Shade' models of photosynthesis. Figures 1.10 (a and c) show a clear residual bias towards high VPD and high temperatures with the big leaf approach. The same trend was obtained using the 'Lambda' model coupled to big leaf (Figure 1.6). In contrast, coupling the 'Ball and Berry' model with the sun/shade model produces well distributed residuals (of net carbon uptake) over the zero line with VPD and air temperature. Again, similar model performance was obtained with the 'lambda'

model coupled to sun/shade. The response of PAR and fraction of diffuse irradiance to standard residuals of modelled and estimated net assimilation using the 'Ball and Berry' model for both sun/shade and big leaf was very similar to that obtained with the 'lambda' model in Figure 1.5 (results not shown for 'Ball and Berry').

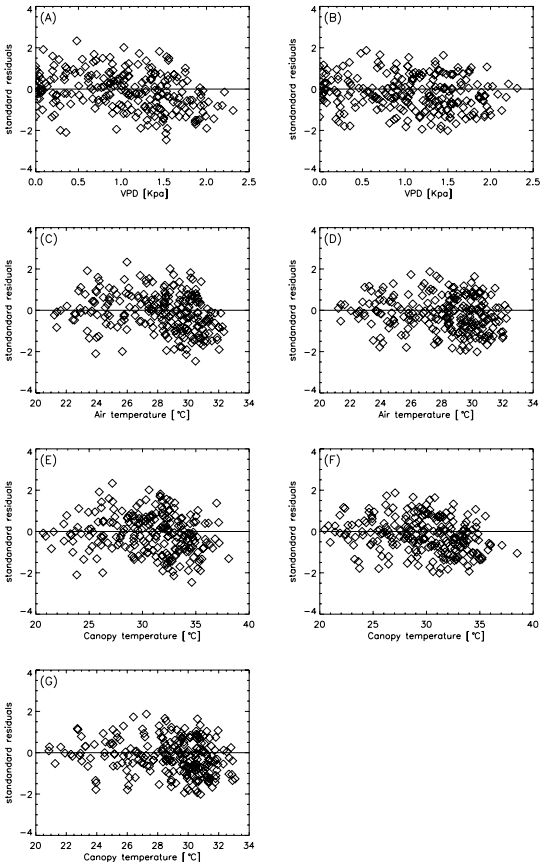

Figure 1.10. Response of VPD, air temperature and canopy temperatures to standard residuals of modelled and estimated net assimilation rates using the 'Ball and Berry' model. (A), (C), (E) are residuals by big leaf, (B), (D), (F) and (G) correspond to sun and shade. (F) is canopy temperature in the sun leaf, (G) is canopy temperature modelled by the shaded leaf. Positive residuals mean underestimation and negative residuals mean overestimation.

1.4 General discussion

The required reparameterisation of the sun/shade model shows the difficulties of scaling from leaf to canopy level and it is important to again note that a mixture of field data (V_{max}, J_{max}, $R_{D,}$ Leaf area density distribution) and fitted parameters (λ, Φ, S_J) were used for its initial parameterisation. Thus, this scaling and modelling exercise has been subject to the limitations of the goodness and representativeness of the data used to parameterise at the leaf level and the data used to test the model (eddy covariance flux data and respiration data). There are thus several explanations for the overestimation (20%) obtained when running the model with the directly scaled up canopy V_{max}, J_{max} and R_D. The leaf level gas exchange data used here comes from a study where only 9 species were measured. But (de Oliveira and Daly 1999) determined a total of 845 species by sampling 3 hectares around the Manaus area. Carswell et al. (2000) reported an average nitrogen concentration in the leaves of 2.7 %. Results from a leaf and soil sampling study (where 20 canopies were sampled for each of plateau, valley and slope topographies) 11 km away at the K34 LBA tower, obtained an average nitrogen concentration in the top leaves of 1.8% and a whole-canopy average of 1.9% (Luizao et al.

2004). When using a linear relationship between the nitrogen concentration in the leaves and V_{max} reported in Carswell et al. (2000), one can easily estimate the corresponding V_{max} and J_{max} for the top leaves with the reported leaf nitrogen at the K34 site. The V_{max} and J_{max} values obtained for the top leaves are 24.4 and 57.5 μmol m^{-2} s^{-1} respectively, with a ratio of 2.3 which are 58 and 68% lower respectively than the values estimated here (58.09 and 181.7 μmol m^{-2} s^{-1} and a ratio of 3.1) using Carswell et al. (2000) data. The correspondent V_{max} and J_{max} values at the top of the canopy using the parameterisation of sun/shade used here are 52.2 and 111.5 μmol m^{-2} s^{-1} with a fitted J_{max}/V_{max} ratio of 1.9.

This suggests that the average V_{max}, J_{max} and R_D for the C14 site could indeed be lower than implied by the more limited dataset of Carswell et al. (2000). The obtained ratio of J_{max} /V_{max} reported by Carswell et al. (2000) at leaf level for different heights ranges from 1.74 to 2.82. Our estimated value for the canopy was 1.9. Other measurements of leaf photosynthesis in the tropics have reported ratios ranging from (1.08 to 2.24) (Meir 1996) for a secondary rain forest in Cameroon, Africa and a range of 1.8-2.25 for an eastern Amazonian forest (Vale et al. 2003). Leaf respiration is one of the three parameters that is fitted to the leaf gas exchange measurements and presents the highest standard deviations (6.34 - 57.57% of the mean value, See Figure 1.11). J_{max} and V_{max} also had a range of standard deviations (of 5.5 to 13.78% and 3.15 to 23.29 % of the mean value respectively) in the Carswell et al. (2000) data set. The inclusion of these deviations adds also uncertainties to the estimations of canopy V_{max}, J_{max} and R_D.

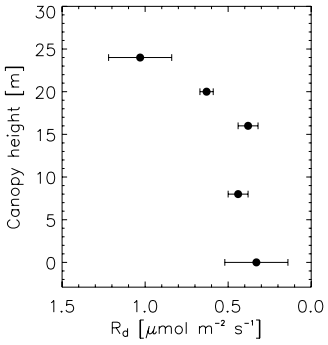

Figure 1.11. Vertical profile of leaf dark respiration (Carswell et al. 2000).

However, it is also possible that there are physiological differences between the forest at sites C14 and K34 that can explain the high difference of nitrogen concentration in the leaves. Araújo et al. (2002) compared eddy covariance measurements of CO_2 fluxes using data from the tower here used C14 and the 11 km away second tower K34. From that study, "clear differences between the towers appear in the intensities of the peak daytime sink-strength and total daily Net Ecosystem Exchange, which are higher for the C14 forest". They recognize the possibility of physiological differences in the forest sites to explain the observed difference in CO_2 uptake. This issue being possible associated to differences in topography. The plateau K34 forest has a larger area of waterlogged vegetation which could be less productive than the older and taller individual trees a the plateau C14 forest that might have better access to deep soil water (Araújo et al. 2002).

Even though the sun/shade model needed some reparametrisation to fit the eddy covariance "recalculated data set" (mainly 10% decrease in top V_{max} and R_D and J_{max} / V_{max} ratio decrease from 2.6 to 1.92), the result

obtained here with this scaling-modelling exercise supports this method of calculation of eddy covariance measurements which has yet to be widely adopted. Moreover, when comparing sun and shade to the normal data set (uncorrected for low frequency motions), a severe 50% overestimation was obtained when the leaf level parameters of Carswell et al. (2000) were employed without modification. In order to fit these "uncorrected" observations V_{max} at the top of the canopy needed to be decreased by 33% (results not shown).

A second important limitation in this study is the uncertainty involved in the data we are using to validate the models and to calibrate in the case of the big leaf model. Fitting a model to any data restricts the model results to the goodness of the data, in this case the eddy covariance and the respiration data. Eddy covariance technique works best under non-intermittent atmospheric conditions and over homogeneous vegetation located in flat terrain (Baldocchi 2003). Eddy correlation measurements over rain forests are more complicated than over flat vegetation due to the presence of uneven tall canopies. This heterogeneity results in high roughness lengths (~2m for Amazon rain forest) (Shuttleworth and Dickinson 1989) that creates large turbulent eddies that facilitate the transfer of heat and momentum between the vegetation and the atmosphere. Contributing errors in day time measurements include 2-3% for calibration of infrared gas analysers, 2% associated with time lags between velocity and scalar sensors and around 7% associated with the covariance measurement (Baldocchi 2003). Kruijt et al. (2004) reports an overall error (not accounting for night-time source error) in the CO_2 fluxes measured from eddy correlation of ± 12% for a rainforest 10 km away (Manaus K34) from the site under investigation here, and ± 32% for a rainforest site in South West Brazil (Jaru).

As mentioned in the methods section, in order to avoid the night time uncertainties with CO_2 flux measurements by eddy covariance, we used data that comes from measurements of the different contributions to ecosystem respiration. The soil respiration data used here was collected during October - November 2000, a year that had higher precipitation than in 1995. We recognize the possibility of higher respiration fluxes during the period covered here.

Using the 'Ball and Berry' or the 'Lambda' model did not make any major difference to the simulated carbon uptake or to the quality of the residuals with either photosynthesis model. Lloyd et al. (1995) obtained similar results when comparing the same two stomatal conductance models coupled to a big leaf model at a tropical rainforest site at Reserva Jaru in Rondonia. This was not unexpected because theoretically both models embody the same principles. They incorporate the well known correlations between photosynthesis and stomatal conductance and describe G_s using similar variables (i.e. VPD or relative humidity at the leaf surface, CO_2 uptake, and CO_2 concentration at the leaf surface).

1.5 Conclusion

We have shown the difficulties of scaling from the leaf up to the canopy level and the importance of having representative data to parameterise canopy gas exchange models. In order to be close to the data used to validate the sun/shade model, it was necessary to empirically reduce the estimated canopy V_{max} and R_D at the top by 10% and the ratio J_{max} / V_{max} from 2.6 to 1.9. Numerical fitting techniques also showed that parameters like S_J and apparent quantum yield could be modified within reasonable ranges in order to get a

better model performance.

When comparing the performance of both model types it is possible to conclude that numerically (in terms of goodness of fit) and qualitatively (in terms of residual response to different environmental variables), the sun/shade model was superior. Although the big leaf model provided a nice average curve of the canopy light response, compared to the sun/shade model, the overall fit was inferior and it failed to respond to variations of diffuse fraction, also showing skewed residual plots for both temperature and VPD (under both the ‘Lambda’ and the ‘Ball and Berry’ approaches for stomatal conductance). The separate treatment of sun and shade leaves in combination with the separation of the incoming light into direct beam and diffuse make sun/shade a strong modelling tool that catches part of the variability measured by eddy covariance. We have, however, also shown here the importance of good estimates of diffuse irradiance and the need of its measurement for the Amazon region for such models to provide any sort of high fidelity output. Despite some difficulties of up scaling and adequate parameterisation of the model, the sun/shade approach may provide a simple and effective tool for modelling photosynthetic carbon uptake that can be easily included in global vegetation models.

2 Modelling Amazonian forest eddy covariance data: A comparison of big leaf versus sun/shade models for the C14 tower at Manaus. II. Energy balance

2.1 Introduction

Forests play an important role in regulating regional and global climate through water, momentum and energy exchange within the atmospheric boundary layer (Miller 1997). Tropical rainforests, in particular, have a crucial role in regulating global climate processes. It has been estimated that about 50% of the total rainfall across the Amazon rainforest is locally produced (Shuttleworth 1998). Moreover, rainfall in the Amazon basin has been recognized as a modulator of convection in the Atlantic Intertropical Convergence Zone, and even over the eastern Pacific (Silva Dias et al. 1987; Werth and Avissar 2002). Zhang et al. (1996) and Werth and Avissar (2002) obtained modelling results indicating that diverse deforestation scenarios of the Amazon Basin could affect global atmospheric circulation through perturbations of both the Walker and Hadley circulation cells. In order to improve such predictions, models of energy and water vapour exchange should be calibrated and extensively validated, preferably across different tropical ecosystems.

Since the late 1980's there have only been a few short- and long-term fieldwork campaigns that have monitored meteorology and carbon and energy exchange between the rainforest and the atmosphere at individual sites across the Amazon Basin. These kinds of datasets are useful to calibrate and validate models of ecosystem gas exchange which, once validated, can be used to generate regional and long term predictions of energy and mass exchange between the atmosphere and the land surface. This study makes use of meteorology and eddy correlation fluxes measured above the forest canopy to calibrate two mechanistic models of ecosystem gas exchange. Calibration of carbon exchange has been presented in Chapter 1. This chapter focuses on net radiation energy absorbed by the canopy and its partition between sensible and latent heat. Specifically, two mechanistic approaches are evaluated, big leaf (Lloyd et al. 1995) and sun/shade models (de Pury and Farquhar 1997) using net radiation, water and sensible heat flux data measured above a rainforest in Central Amazonia.

2.2 Materials and methods

2.2.1 Site and data

The site is an undisturbed mature rainforest located 100 km north of Manaus (2°35'S, 60°06'W), around the "C14" tower previously known as "ZF2". Data used and site have already been described in the methods section of Chapter 1.

In addition to the meteorology used to force the models on an hourly time-step (solar incoming radiation, dry and wet bulb temperatures, windspeed and friction velocity), net radiation, and fluxes of sensible and latent heat, measured and estimated by the eddy correlation method (Malhi et al. 2002), were used for model comparison. Data used were collected from October 15th to December 9th during 1995 which corresponds to

the end of the dry season. See Figure 2.1.

Energy and CO_2 fluxes at this site were initially calculated using the conventional eddy correlation corrections (Malhi et al. 1998). The data set used in this study has been recalculated by Malhi et al. (2002) taking into account turbulent transport on time scales of 1 to 4 hours which led to a high percentage of energy budget closure (i.e. 94%). Due to this reason, from here on this data set is referred as the "recalculated" data set.

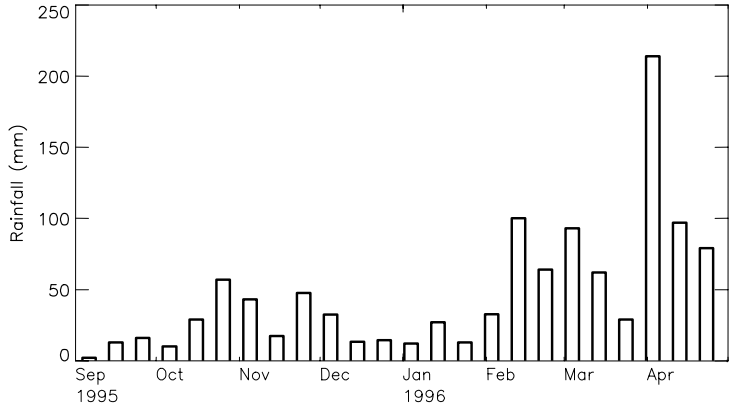

Figure 2.1. Precipitation at Manaus C14 (provided by Harris et al. (2004)).

2.2.2 Theory and models

By definition of energy balance at the stand/canopy level, the energy going into and out of the canopy should be equal to the energy stored:

$$R_n\text{-}H\text{-}\lambda E\text{-}G=M+St \quad (1)$$

where R_n is net heat gained from radiation, (short and long wave), H and λE are fluxes of sensible and latent heat losses from the canopy and G is sensible heat flux loss from the soil. M is net heat stored in biochemical reactions and St is energy stored in biomass and air within the canopy (Jones 1992). All terms expressed in [W m^{-2}].

Since leaf temperature is needed to calculate long wave radiation, net isothermal radiation, R_{ni}, was used for both model types:

$$R_{ni}=R_n+ C_pG_r\Delta T \quad (2)$$

R_n is net available energy and the term $C_pG_r\Delta T$ accounts for loss of thermal radiation from the canopy to the air under non-isothermal conditions. C_p is the specific heat of air [J mol^{-1} K^{-1}], ΔT the temperature difference between the canopy and surrounding air, and G_r is the radiative conductance of the canopy defined by Jones (1992) as:

$G_r=4\varepsilon_f\sigma T_a/C_p$ (3)

T_a is air temperature [K], ε_f leaf emissivity and σ is the Stefan Boltzman constant.
Formulations of radiative conductance and net long wave radiation absorbed by sunlit and shaded leaves were taken from Wang and Leuning (1998).

The isothermal net radiation at each leaf (for single big leaf and sun/shade approaches) is partitioned between the latent and sensible heat fluxes following the isothermal form of the Penman-Monteith equation (Jones 1992), assuming ground evaporation and soil heat flux to be negligible. This assumption is based on the observation that typically only 1% of the radiation received at the top of the canopy reaches the forest floor (Shuttleworth 1989). Since energy stored in biomass and in the canopy air and chemical energy used for CO_2 exchange are small in quantity, these terms were also neglected. At Tapajos, another rainforest site in the Brazilian Amazon, da Rocha et al. (2004) determined daytime energy storage in biomass and in the air column inside the canopy between 2 to 6 W m^{-2} and 0 to 3 W m^{-2}, respectively, with soil heat fluxes representing only 2% of the daytime net radiation.

Radiation absorption (sun/shade model)
Using formulations developed by Goudriaan (1977) as presented in Wang and Leuning (1998) and de Pury and Farquhar (1997), absorption of PAR and near infrared radiation (NIR) was estimated for the sun/shade model. The net energy available to the sunlit and shaded leaf was calculated as the sum of net absorbed PAR, net absorbed NIR and net absorbed long wave by each leaf.

Canopy stomatal conductance, G_s.
G_s derived from eddy correlation measurements
Stomatal conductance to water vapour was derived from the water vapour fluxes (i.e. through latent heat flux) measured by the eddy correlation technique (G_{s_eddy}) by inversion of the Penman Monteith equation (4) and used to evaluate simulations of G_s. Also as will be shown in the next section, G_{s_eddy} was used to infer the parameters in the stomatal conductance models.

$$G_{s\_eddy} = \frac{1}{\left[\frac{r_a \times s(R_n - \lambda E) + \delta \times C_P \times D_C}{\lambda E \times \gamma} - r_a\right]} \quad (4)$$

with s, the slope of the relationship between vapour pressure and temperature [Pa K^{-1}], γ the psychrometer constant, δ, density of the air [kg m^{-3}], C_p, specific heat capacity of dry air [J kg K^{-1}] and r_a, aerodynamical resistance [s m^{-1}]. The terms, R_n, net radiation [W m^{-2}], λE, latent heat flux [W m^{-2}], D_C, above canopy-to-air vapour pressure difference [Pa] correspond to above canopy hourly measurements.

The aerodynamic resistance r_a is calculated as in Lloyd et al. (1995):

$r_a = (u/u^*) + (1/ku^*) [ln(Z_{oM}/Z_{oH}) + \psi_M - \psi_H]$ (5)

u and u^* are horizontal windspeed and friction velocity, respectively, in [m s^{-1}], k is von Karman's constant. The stability correction variables ψ_M, ψ_H and the term $ln(Z_{oM}/Z_{oH})$ set to 1.5, were estimated following Lloyd et al. (1995).

To account for non-closure of the energy balance from eddy correlation measurements, the Bowen ratio was used to define R_n for the calculation of G_{s_eddy} in equation (4) as follows:

$$R_n = \lambda E(1+\beta) \quad (6)$$

with β defined as Bowen ratio, the ratio between the measured sensible and latent heat fluxes from eddy correlation.

The 'Lambda' and 'Ball and Berry' models

As described in Chapter 1, the 'Lambda model' and the 'Ball and Berry' models were used to simulate stomatal conductance. The lambda model is based on the assumption of optimal stomatal regulation of rates of CO_2 uptake and transpiration per unit leaf area in a plant at a finite interval of time with changing environmental conditions assuming only small changes in soil water availability to plants (Cowan and Farquhar 1977).

$$G_S = A\sqrt{\frac{1.6\lambda P}{(C_a - \Gamma^*)Dc}} \quad (7)$$

where A is assimilation [mol m^{-2} s^{-1}], D_C canopy to air vapour pressure deficit, P atmospheric pressure and C_a ambient partial pressure of CO_2. λ is a Lagrangean multiplier representing the marginal water cost of plant carbon gain (Cowan 1977; Cowan and Farquhar 1977), and is calculated as the square of the gradient between G_s and term (8) using the canopy assimilation rate and stomatal conductance (G_{s_eddy}) deduced from eddy correlation measurements.

$$A\sqrt{\frac{1.6P}{(Ca - \Gamma^*)Dc}} \quad (8)$$

The 'Ball and Berry' model (Ball et al. 1987) with slight modifications (Leuning 1990) is based on an empirical relationship that incorporates the observed correlation between A and G_s and includes the effects of leaf surface humidity (h) and ambient CO_2 concentrations on stomatal conductance:

$$G_s = g_0 + \frac{g_1 AhP}{(C_a - \Gamma^*)} \quad (9)$$

where g_0 corresponds to the minimum stomatal conductance to water vapour when A= 0 at the light compensation point, and g_1 is an empirical coefficient which represents the composite sensitivity of conductance to assimilation, CO_2, humidity and temperature. Both g_0 and g_1 are calculated as the respective intercept and slope of the linear regression between G_s and term (10) using the canopy assimilation rate and stomatal conductance deduced from the eddy correlation measurements.

$$\frac{AhP}{(C_a - \Gamma^*)} \tag{10}$$

A modified version of the 'Ball and Berry' model that includes a hyperbolic function of VPD (Leuning 1995) (equation 11) was also tested and compared to the form presented in equation (9):

$$G_s = g_0 + g_1 \left[\frac{A}{(C_a - \Gamma^*)(1 + D_C / D_0)}\right] \tag{11}$$

where D_C is the canopy to air vapour pressure deficit, and D_0 is an empirical parameter. g_1 and D_0 were fitted to G_{s_eddy} using the simplex procedure (Nelder and Mead 1965).

G_{s_eddy} is used to infer λ and g_0 and g_1 in equations (7) and (9). Stomatal conductance to water vapour, carbon assimilation and energy fluxes are simulated with the big leaf model in total canopy area basis; this is because the biochemical parameters (V_{max}, J_{max}) and day time leaf respiration (R_C) are already implicitly scaled from leaf to canopy level. Similarly for the sun/shade model, carbon assimilation and energy fluxes are modelled separately for the sunlit and shaded groups of leaves (i.e. two big leaves) and each term is simulated on a total leaf area basis of the two leaf types. Therefore canopy stomatal conductance is calculated as the sum of G_s for the sunlit and shaded groups of leaves.

Coupling to the environment

Two systems are coupled when they can exchange force, momentum, energy or mass. To determine the degree of coupling of the canopy to the environment using eddy correlation measurements or output from model simulations, the decoupling coefficient (Ω) introduced by McNaughton and Jarvis (1983) has been used. These authors partition evaporation into two terms: an equilibrium evaporation rate that only depends on the energy supply (radiation) and an imposed evaporation rate that depends on the saturation deficit of the ambient air. With the latter condition the leaf/canopy is said to be coupled to the environment. The relative importance of these terms depends on the degree of coupling of the leaf/canopy surface to the air above, varying from 0 (for fully coupled) to 1(decoupled). The decoupling coefficient (Ω) is defined as (equation 5.28 from Jones (1992)):

$$\Omega = (\varepsilon + 1)/(\varepsilon + G_a / G_s) \tag{12}$$

where $\varepsilon = s/\gamma$, and G_a is the aerodynamical conductance for water vapour ($1/r_a$). Ω is calculated for all model configurations with their respective estimates of G_a and G_s, and is also calculated using G_{s_eddy} and

corresponding values of G_a.

Model configurations

Simulations using the sun and shade and big leaf models for photosynthesis and the 'Lambda' (called hereafter the sun/shade-Lambda and big leaf-Lambda) and 'Ball and Berry' (called sun/shade-Ball and Berry and big leaf-Ball and Berry) models for stomatal conductance to water vapour are tested in this chapter and compared to measured and/or inferred fluxes from eddy correlation. All simulations were performed using data that corresponds to approximately the end of the dry season of 1995 (October 15th to December 9th).

2.3 Results

2.3.1 Canopy conductance: Lambda *vs* Ball and Berry model

As explained in the methods, λ from the 'Lambda' model was calculated (using equation 7) as the square of the gradient between G_{s_eddy} and term (8), and g_0 and g_1 from the 'Ball and Berry' model were calculated as the intercept and slope from the linear regression between G_{s_eddy} and term (10), using the canopy assimilation rate and stomatal conductance deduced from the eddy correlation measurements as shown in Figure 2.2. Because of the high variability (scatter) in canopy conductances derived from λE fluxes and in NEE from eddy correlation, the correlation coefficients of the regressions G_{s_eddy} versus term (8) and G_{s_eddy} versus term (10) were low (0.38-0.48) and depending upon the data selection criteria different values for λ, g_0 and g_1 could be obtained. Data used in Figure 2.2 (top row, n=241 data points) were filtered for time of day between 700 and 1800, VPD values higher than 0.5 kPa and G_{s_eddy} lower than 1 mol m^{-2} s^{-1}. In Figure 2.2 (bottom row, n=185) additional filters were applied. Data were also excluded when the absolute value of the CO_2 in-canopy storage term was larger than 8 μmol m^{-2} s^{-1}, the total assimilation rate estimated from eddy correlation was larger than 35 μmol m^{-2} s^{-1} and when λE was larger than 500 Wm^{-2}. It was decided to use the parameters obtained with the evaluation done with n=241 data points. This is because when implementing the 'Ball and Berry' parameters from the evaluation with n=185 data points, both big leaf and sun and shade models predicted canopy temperatures higher than 40°C at high irradiances (>1500 μmol quanta $m^{-2}s^{-1}$ PAR) which led to stomatal closure in both photosynthesis models. This situation did not occur with the 'Lambda' model but to be able to compare both model performances it was necessary to use the parameters inferred from the same data points. The simulated energy partition was very sensitive to the λ parameter and in this case, λ=980 mol mol^{-1} from the evaluation with n=241 favoured a better simulated energy partition when compared to the measurements (results not shown) than with λ=870 mol mol^{-1} (n=185). On the other hand, the simulated net carbon assimilation was insensitive to small changes in λ (not shown).

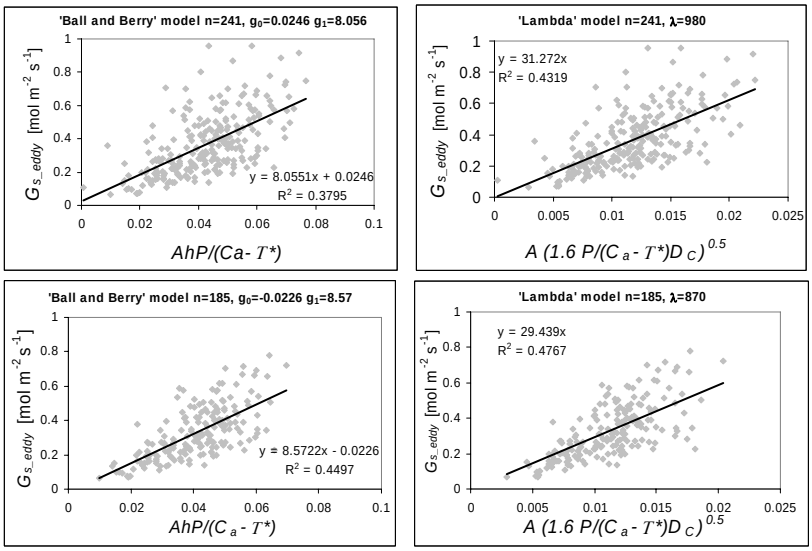

Figure 2.2. Calculation of λ and g_0 and g_1 parameters from the 'Lambda' and 'Ball and Berry' models for stomatal conductance in equations (7) and (9) respectively. Data points used for evaluation on top plots were filtered for time of day between 700 and 1800, VPD values higher than 0.5 kPa and G_{s_eddy} lower than 1 mol m^{-2} s^{-1}. Data used for evaluation on bottom plots were filtered for the same conditions described for the top plots but also excluding data where the absolute value of the CO_2 in-canopy storage term was larger than 8 μmol m^{-2} s^{-1} and data where the total assimilation rate estimated from eddy correlation was higher than 35 μmol m^{-2} s^{-1}. Data values where λE was larger than 500 Wm^{-2} were also excluded.

Lacking measurements of canopy conductance to validate simulated conductance, G_s was calculated from the λE fluxes (derived from eddy correlation) through inversion of the Penman Monteith equation (4) but also using Bowen ratio as expressed in equation (6). This calculation comprises an aggregation of the uncertainties that come with the measurements of environmental variables (i.e wind speed, wet and dry bulb air temperatures) and eddy correlation calculation of energy fluxes (H and λE) needed in the equation.

Sensitivity of the simulated G_s with both 'Ball and Berry' (from equation 9) and the 'Lambda' model to relative humidity at different temperatures is shown in Figure 2.3. G_s simulated with the 'Lambda' model (solid hyperbolic line) decreases with increasing temperature while the opposite happens with the 'Ball and Berry' simulated (solid straight line) G_s but with a lower magnitude. Both models usually agree on a G_s range of 0.4 –0.8 mol m^{-2} s^{-1} at temperatures around 30-35 °C. At lower temperatures and for all relative humidities, (i.e low VPD) simulated G_s with the 'Lambda' model tends to be higher than with the 'Ball and Berry' model. Furthermore, the modified version of the 'Ball and Berry' model that includes a hyperbolic function of VPD (Leuning 1995) (equation 11) was also tested and is shown in Figure 2.3 (dotted lines). This shows that the 'Ball and Berry' model in the form of equation (11) has the same response as the 'Lambda model below a relative humidity of about 0.8 at all temperatures tested. Parameters $g_1$and D_0 were fitted to G_{s_eddy} using the simplex procedure, giving parameter values of 13.8 and 1038.8, respectively (overall regression error=0.488 expressed as the function minimum), g_o was taken as derived in Figure 2.2 at n=241. Simulations presented from here on with the 'Ball and Berry' model were performed with the version of the model that includes direct dependency on relative humidity (equation 9).

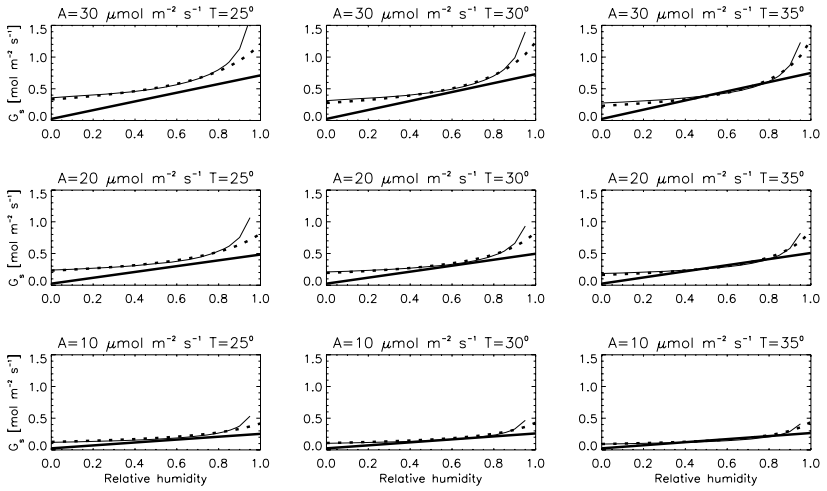

Figure 2.3. Simulated G_s responses to relative humidity under various temperatures (T) and assimilation rates (A) by the 'Lambda' model (solid hyperbolic line and the 'Ball and Berry' model with dependence on relative humidity (equation 6) (straight solid line) and the 'Ball and Berry' model with dependence on VPD (equation 12) (dotted hyperbolic line).

At an hourly resolution there is high variability in simulated G_s but also on G_{s_eddy} (not shown). In an attempt to understand the high variability in modelled and estimated G_{s_eddy} stomatal conductance, the average hourly conductances were calculated and a comparison of the diurnal cycle of both simulated and estimated conductances is presented in Figure 2.4. Using the 'Lambda' model, the mean canopy conductance simulated by the big leaf closely follows the pattern obtained for the estimated mean G_{s_eddy} with a tendency to underpredict G_{s_eddy}, especially between 0800 and 1000 am. Simulated G_s with sun/shade (coupled to the 'Lambda' model) overpredicts mean G_{s_eddy} from 0800-1200 am. Using the 'Ball and Berry' model, simulated mean diurnal cycle of G_s with the big leaf model tended to underpredict mean G_{s_eddy} with an almost flat mean diurnal cycle; only simulated mean G_s decreased after 1500. Simulated mean diurnal cycle of G_s with the sun and shade model (coupled to the 'Ball and Berry' model) followed closely the mean diurnal cycle of G_{s_eddy}. Comparison of the mean diurnal cycle of the simulated G_s with both photosynthesis models and both stomatal conductance formulations is shown in Figure 2.5. Using the sun/shade model, the mean diurnal cycle of simulated G_s tends to be lower for the 'Ball and Berry' model than the 'Lambda' model before 1200, with no great difference between both approaches later in the day. Using the big leaf model, the mean diurnal cycle of simulated G_s tends to be lower with the 'Ball and Berry' model than with the 'Lambda' model especially from 0800 to 1000. This is linked to the different responses of simulated G_s (with both models) to relative humidity at different temperatures as shown in Figure 2.3. At relative humidity values higher than 0.7 simulated G_s with the Ball and Berry model (equation 9) is usually lower than simulated with the 'Lambda model'. These conditions are the usual for the morning (see mean diurnal cycles of relative humidity and VPD in Figure 2.6).

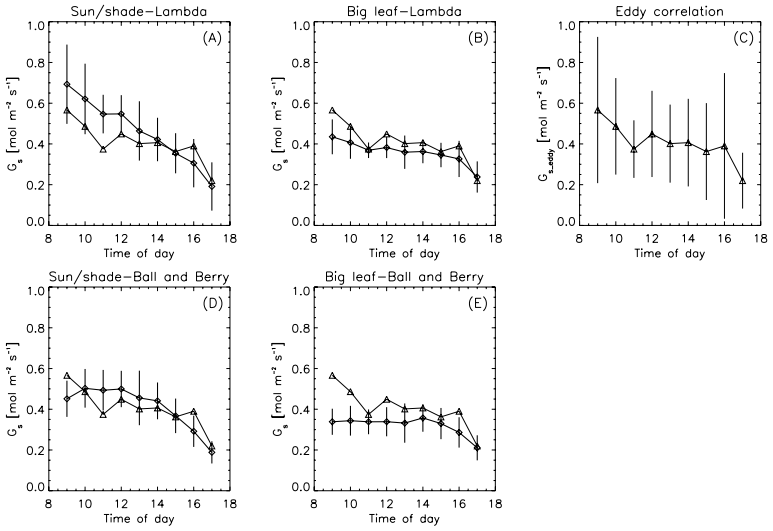

Figure 2.4. Diurnal cycle of mean hourly stomatal conductance. Simulated G_s by sun and shade (A) and by big leaf (B) coupled to the 'Lambda model. (C) G_s estimated by water fluxes from eddy correlation, G_s simulated by sun/shade (D) and by big leaf (E) coupled to the 'Ball and Berry' model. Error bars correspond to standard deviation of simulated G_s or G_{s_eddy} (only in C). In all cases, simulated G_s is represented by diamonds and G_{s_eddy} by triangles.

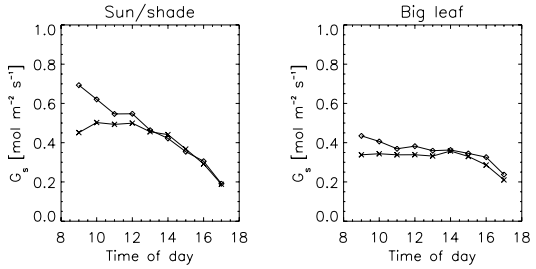

Figure 2.5. Diurnal cycle of mean hourly stomatal conductance. Simulated G_s by sun and shade and by big leaf coupled to the 'Lambda' model (diamonds) and to the 'Ball and Berry' model (crosses).

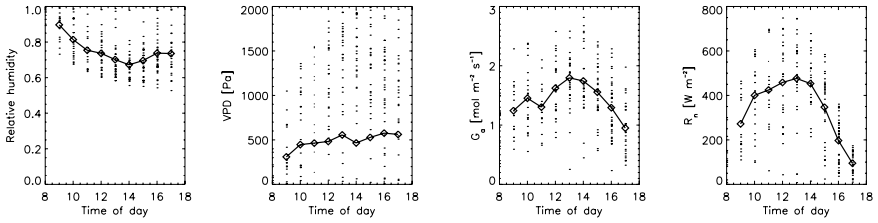

Figure 2.6. Mean diurnal cycle of measured R_n, above air VPD, relative humidity (estimated from VPD) and aerodynamical conductance G_a (estimated as $1/r_a$ with r_a defined in equation 9) using the above canopy measurements of windspeed. Dots correspond to hourly values and diamonds are mean hourly values**.**

Residuals of G_s (calculated as G_{s_eddy} minus simulated G_s) were relatively well distributed around the zero line when plotted against above canopy VPD, PAR, air temperature and time of day (Figure 2.7). All model configurations had very similar responses to the meteorological variables except from G_s simulated by sun/shade-Lambda (Figure 2.7, first column) where it is clear simulated G_s was higher (than measured) before 1400 than in the other cases. Notice a trend in simulated G_s to overpredict G_{s_eddy} at the highest VPD and at the highest air temperatures under all model configurations.

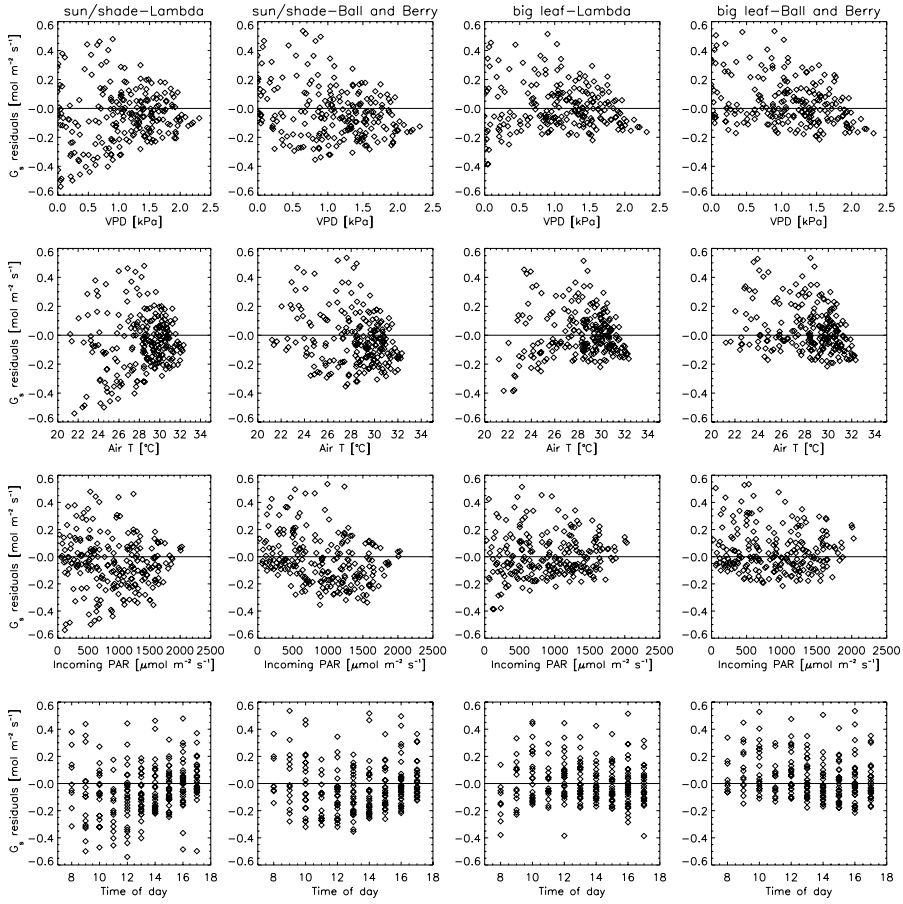

Figure 2.7. Residual (calculated as G_{s_eddy} minus simulated G_s) responses of G_s to above canopy to air VPD, incoming PAR, above canopy air temperature and time of day. A positive residual means underestimation, negative means overestimation of simulated G_s relative to G_{s_eddy}.

2.3.2 Energy balance

Simulated λE and H, and R_n under all model configurations were compared to the eddy correlation data set from Malhi et al. (2002) and to net radiation measurements above the canopy, respectively. Statistics from the model evaluation are presented in Table 2.1. According to the regression analysis, the recalculated fluxes of latent and sensible heat account for 95% of the variance in net radiation measurements with an energy balance closure of 89%. Comparing simulated R_n from all model configurations, all approaches account for a high percentage of variance in the measurements of R_n ($r^2 \geq 0.95$). The sun/shade model had a lower slope (0.95) than big leaf (0.98) when simulated and measured R_n were fitted to a straight line with zero intercept. This is because both models tended to slightly underestimate net radiation measurements below 200 W m^{-2}, with a greater underestimation for the sun/shade model (18% respect to the measurements) than big leaf (7% respect to the measurements) in this range. Probing more closely, it was found that net radiation values below 200 W m^{-2} occurred during all times of the day. Since net radiation measurements are taken at the top of eddy correlation towers and these values are associated with uncertainties on the order of 10%, this fit can be regarded as satisfactory. Moreover, overall underestimation of net radiation as simulated with the sun/shade approach is linked to the model tendency to overestimate surface albedo (i.e. underestimation of absorbed radiation in the visible and near infrared bands) as has been reported by Wang (2003). In a

comparison study of three different radiation models, Goudriaan's model (similar formulation to radiation absorption in the sun and shade model used in this study) was compared with a two stream approximation model which includes a more theoretically rigorous radiation absorption approach, and the reported result (Wang 2003) was underestimation of the fraction of visible and NIR radiation absorbed by the canopy by up to 14 % and 10% respectively by the sun/shade approach.

Table 2.1. Evaluation of model performance and data[*].

Model configuration or data	Variable	a	r^2	RMSE[**]
Big leaf-lambda	H	0.97	0.9	41.7
	λE	1.02	0.94	61.41
	R_n	0.98	0.99	20.42
Big leaf-Ball and Berry	H	1.01	0.89	46.94
	λE	0.99	0.93	62.04
	R_n	0.98	0.99	20.98
Sun/ shade-lambda	H	1	0.91	42.37
	λE	0.98	0.93	62.22
	R_n	0.95	0.99	29.88
Sun/ shade-Ball and Berry	H	0.96	0.89	44.17
	λE	1. 0	0.93	64.65
	R_n	0.95	0.99	31.16
Eddy correlation	$(H+\lambda E)$ *vs* R_n	0.89	0.96	77.39

The regression is calculated as: modelled flux= a × measured flux.
In the case of eddy correlation measured $(H+\lambda E)$ = a × measured R_n
[**] Root mean square error

From comparisons of estimated H and λE by eddy correlation versus model simulations, it can be concluded that in general there is a good agreement ($r \geq 0.89$ in all cases) between simulation and observation for all model configurations using the "recalculated" data set. Note that RMSE was usually lower for simulations with the 'Lambda' model than with the 'Ball and Berry' model. Further, when comparing simulations with the big leaf and sun and shade schemes coupled to the same stomatal conductance model (Table 2.2), there was good agreement between simulated R_n, λE and H by both photosynthesis models.

Table 2.2 Comparison of simulated energy balance between model configurations[*].

Variable	'Lambda'model			'Ball and Berry' model		
	a	r^2	RMSE[**]	a	r^2	RMSE[**]
H	1.01	0.95	13.3	0.93	0.96	25.49
λE	0.96	0.99	22.8	1.01	0.99	21.14
R_n	0.97	0.99	31.06	0.98	1	14.35

[*]The regression is calculated as: modelled flux with sun/shade= a × modelled flux with big leaf
[**] Root mean square error

A qualitative assessment of simulated H and λE is shown through their residuals (calculated as measured minus simulated flux) as functions of PAR, VPD, air temperature and time of day respectively for all model configurations (Figures 2.8 and 2.9). Simulations under all model configurations show similar responses for the variables tested. In all cases the residuals were usually well distributed around zero. However notice the response at VPD values higher than 2 kPa (only few data points) and at the highest air temperatures where measured λE was overestimated under all model configurations. The opposite response was obtained for H.

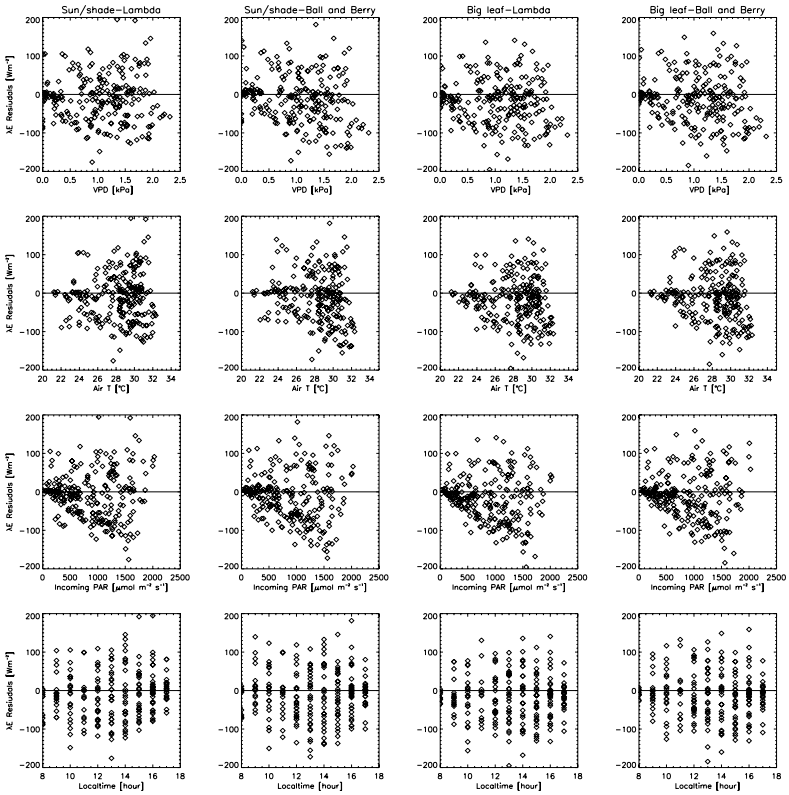

Figure 2.8. Residuals of λE (calculated as measured minus simulated flux) as function of PAR, VPD, air temperature and time of day for all model configurations.

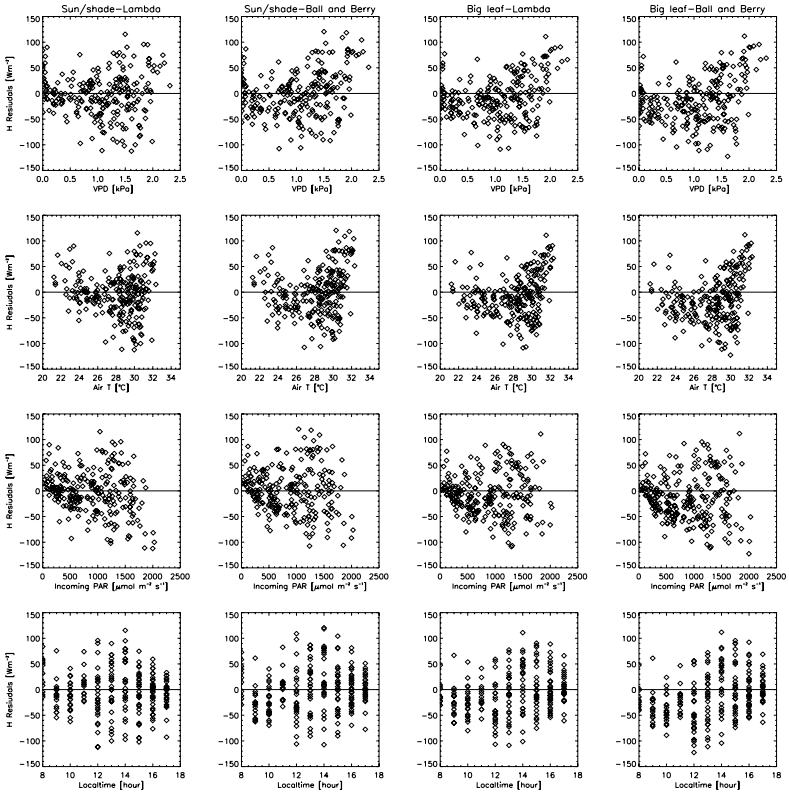

Figure 2.9. Residuals of H (calculated as measured minus simulated flux) as a function of PAR, VPD, air temperature and time of day for all model configurations.

2.3.3 Sensitivity of simulated λE to simulated G_s

From results shown in Table 2.1 and Figures 2.8 and 2.9, it can be concluded that under all model configurations, λE was satisfactorily well simulated when compared to the eddy correlation measurements, even though the simulated conductance did not always agree with G_{s_eddy}. To investigate the effect of small changes in simulated G_s on simulated latent heat fluxes, the decoupling coefficient (Ω) introduced by McNaughton and Jarvis (1983) (equation 12) was used. A comparison of the diurnal cycle of both simulated (Ω) and estimated (Ω) using G_{s_eddy} is shown in Figure 2.10 for all model configurations. Values of mean hourly (Ω) estimated from G_{s_eddy} varied between 0.52 and 0.62. Simulated (Ω) with the big leaf model (under both stomatal conductance approaches) followed closely the estimates of (Ω) inferred from G_{s_eddy}. Simulated (Ω) with the sun shade model (under both stomatal conductance approaches) tended to overpredict (Ω) calculated with G_{s_eddy} during most of the day. This is because of higher simulated G_s with the sun and shade model when compared to G_{s_eddy}. However, the simulated mean diurnal cycle of (Ω) for the separate sunlit and shaded groups of leaves ranged between 0.3 and 0.6 with a diurnal cycle pattern similar to the mean diurnal cycle of their respective simulated G_s, i.e. higher simulated (Ω) during the morning (before 1300) than during the afternoon (not shown). G_a used in all cases was calculated using windspeed measurements at the top of the canopy, omitting any existing in-canopy windspeed profiles. The simulated mean diurnal cycle of G_a is shown in Figure 2.6.

The intermediate values of (Ω) shown in Figure 2.10 suggest a forest which is not completely coupled or uncoupled to the air above, implying that intermediate degrees of stomatal control prevail and λE depends jointly on R_n, VPD and windspeed. Further, from the sensitivity of Ω to variations of G_s and G_a it is concluded that for this forest to be strongly coupled ($\Omega \leq 0.2$) to the atmosphere above, the correspondent G_a should be higher than 20 μmol m^{-2} s^{-1} (Figure 2.11).

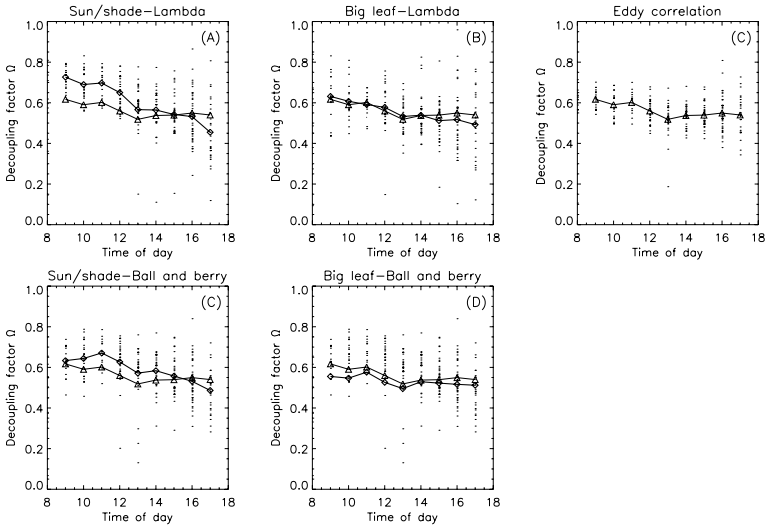

Figure 2.10. Diurnal cycle of mean hourly decoupling factor *(Ω)*. Simulated *(Ω)* by Sun and shade (A) and by big leaf (B) coupled to the 'Lambda model. (C) (Ω) estimated with G_{s_eddy}. Simulated (Ω) by sun/shade (D) and by big leaf (E) coupled to the 'Ball and Berry' model. Dots correspond to half hourly simulated (Ω) or (Ω) calculated using G_{s_eddy} (only in C). In all cases, simulated (Ω) is represented by diamonds and (Ω) inferred from G_{s_eddy} by triangles.

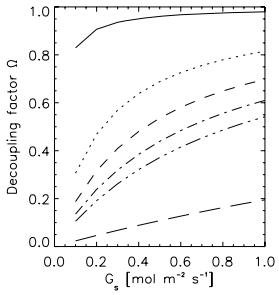

Figure 2.11. Sensitivity of (Ω) to variations in G_s and G_a. G_a =0 mol m^{-2} s^{-1}, (solid), G_a =1 mol m^{-2} s^{-1} (dotted), G_a = 2 mol m^{-2} s^{-1} (dashed), G_a =3 mol m^{-2} s^{-1} (dash dot), G_a =4 mol m^{-2} s^{-1} (dash dot dot), G_a =20 mol m^{-2} s^{-1} (long dashes).

To find out under which circumstances the simulated λE was sensitive to changes in G_s, a sensitivity test of λE calculated using the Penman Monteith equation was conducted (using the meteorological conditions for this site, see mean diurnal cycles in Figure 2.6). Results showed the sensitivity of simulated λE to small changes in G_s increased with decreasing G_s (simulated λE most sensitive below G_s of 0.4 μmol m^{-2}s^{-1} for the studied conditions) and with increasing net radiation, VPD and aerodynamical conductance (G_a) (calculated as $1/r_a$). This can be seen in Figure 2.12 where simulations of λE for a range of G_s from 0 to 1 mol m^{-2}s^{-1} assuming an error in G_s of ±0.1 (continuous lines) and 0.2 (dashed lines) mol m^{-2}s^{-1} are shown at different meteorological conditions (R_n [200 and 600 Wm^{-2}], VPD [0.5 and 2.5 kPa] and G_a [0.5, 2 and 3 mol m^{-2} s^{-1}]). Sensitivity of simulated λE to small changes in G_s is numerically shown in Table 2.3 for three cases: the first case considers the most sensitive situation, highest VPD, R_n and G_a (VPD=2.5 kPa, R_n=600 W m^{-2}, G_a=3 mol m^{-2} s^{-1}), the second and third cases consider typical morning (VPD=0.5 kPa, R_n=400 Wm^{-2}, G_a=1 mol m^{-2} s^{-1}) and afternoon (VPD=1 kPa, R_n=300 W m^{-2}, G_a=1.5 mol m^{-2} s^{-1}) conditions (see Figure 2.6 for mean diurnal cycles of meteorology). From the sensitivity presented in Table 2.3 it can be concluded that for the prevailing morning and afternoon conditions, small changes in simulated G_s do not change simulated λE by a large percentage when G_s is higher than 0.2 and this sensitivity (of simulated λE to small changes in simulated G_s) decreases with increasing G_s.

Table 2.3. Sensitivity of simulated λE to small changes in G_s. Numbers correspond to percentage of increase (+) or decrease (-) of simulated λE when changing G_s by ± 0.1 and ± 0.2 mol m^{-2} s^{-1}.

		G_s=0.2		G_s=0.4		G_s=0.6		G_s=0.8	
VPD=2.5 kPa, R_n=600 W m^{-2}, G_a=3 mol m^{-2} s^{-1}	G_s±0.1	**+34**	**-43**	+14	-17	+9	-8	+6	-5
	G_s±0.2	**+61**	**-100**	+25	-38	+20	-4	+13	-10
VPD=0.5 kPa, R_n=400 W m^{-2}, G_a=1 mol m^{-2} s^{-1}	G_s±0.1	+20	-34	+8	-11	+4	-5	+2.	-3
	G_s±0.2	+34	- 100	+13	-25	+6	-11	+4	-6
VPD=1 kPa, R_n=300 W m^{-2}, G_a=1.5 mol m^{-2} s^{-1}	G_s±0.1	+25	-38	+9	-13	+5	-6	+3	-4
	G_s±0.2	+44	- 100	+17	-30	+9	-14	+6	-8

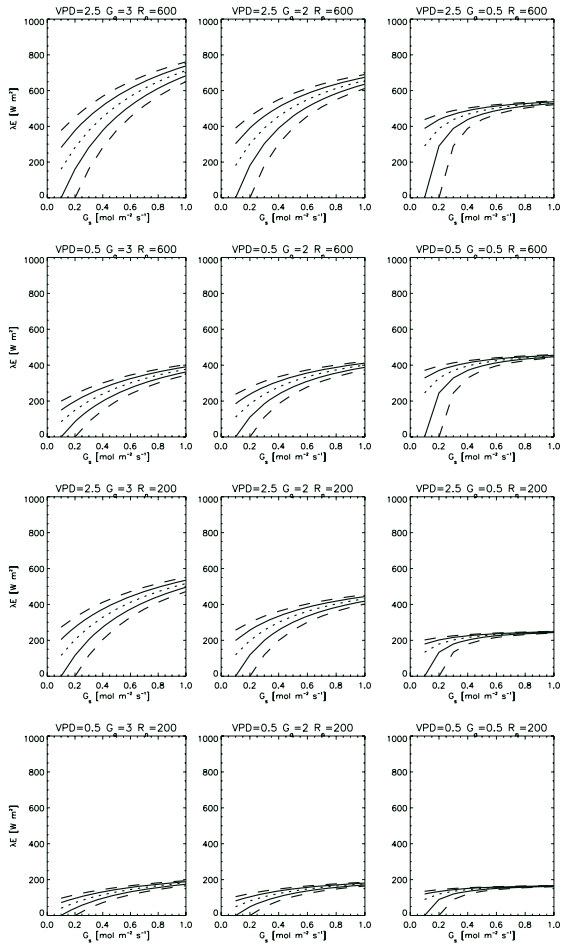

Figure 2.12. Sensitivity of simulated λE (calculated using the Penman Monteith equation) to small changes in G_s under different meteorological conditions. Simulations of λE for a range of G_s from 0 to 1mol m^{-2} s^{-1} (dotted lines) were performed assuming an error in G_s of ±0.1(continuous lines) and 0.2 (dashed lines) µmol m^{-2} s^{-1} at different meteorological conditions : R_n [200 and 600 Wm^{-2}], VPD [0.5 and 2.5 kPa] and G_a [0.5, 2 and 3 mol m^{-2} s^{-1}].

2.4 Discussion

Evaluation of the energy balance simulated by the sun and shade and big leaf models coupled to two stomatal conductance models has shown the ability of the models to reproduce some of the observed variability from eddy correlation with no major qualitative or quantitative difference between the photosynthesis models tested (Table 2.1, Table 2.2). Despite the good agreement between modelled fluxes and eddy correlation measurements, it is important to keep in mind that the energy balance closure of this data set was achieved at the cost of a 4 hour rotation averaging (Malhi et al. 2002) which is still a matter of debate among the eddy correlation researchers. This method of calculation has yet to be widely used and, when applied with different rotation period, it has not produced energy balance closure at other sites in the Amazon rainforest. For instance, von Randow et al. (2004) working with a data set from a rainforest in south western Amazon in Brazil (Jaru) increased averaging time up to 8 hours and could not achieve closure of the energy balance. Miller et al. (2004) working with eddy correlation data from Tapajos increased averaging time up to 2 hours and obtained only minor improvements in the closure of the energy budget. According to Iwata et al. (2005) extending averaging period beyond one hour did not increase the fluxes at a site in eastern Amazonia (Caxiuana, Brazil).

The radiation scheme used sets the boundaries in how well all energy fluxes are simulated. Here two different radiation descriptions were used and both still underestimate net radiation measurements below 200 W m^{-2} by 10 and 20% for the big leaf and sun/shade models, respectively. But it is important to reiterate that net radiation measurements and calculations comprise uncertainties on the order of about 10%. Even though, simulated G_s differed between the various model configurations, simulated λE and H were relatively well simulated and similar fits to the eddy correlation measurements were obtained with all models (Table 2.1 and Figures 2.7 and 2.8). Even though simulated λE appears to be controlled by both the net radiation flux and the simulated stomatal conductance (decoupling factor ~ 0.5 - 0.6), it was shown that under the prevailing diurnal conditions, simulated λE is fairly insensitive to small changes in simulated G_s when G_s is higher than 0.2 and this sensitivity decreases with increasing G_s (Table 2.3). Furthermore, evaluation of simulated G_s was done with G_{s_eddy} which was estimated via inversion of the Penman-Monteith equation (equation 4) using water fluxes estimated by eddy correlation and meteorology from the top of a tower. This calculation comprises a mixture of uncertainties associated with the instruments and from the calculation of each of the variables used to calculate conductance (See standard deviation of G_{s_eddy} as error bars in Figure 2.4c). In addition to the uncertainties involved in the calculation of stomatal conductance from the Penman-Monteith equation, there have been concerns regarding its underlying assumptions. The assumption of similarity between the source and sink vertical distributions of momentum, sensible heat, water vapour and CO_2 in layers above the top of the vegetation canopy has been the major subject of debate. Philip (1996) and Tanner (1963) showed that Monteith's assumption of similarity between the wind, vapour and temperature profiles down the canopy can not hold and therefore profile extrapolation of these entities down to the zero plane would produce errors affecting the Monteith calculation of stomatal conductance.

From the stomatal conductance formulations tested, both models predicted similar response of simulated λE to the environment (Figure 2.8). Obtained parameters with both stomatal conductance models were in good agreement with values reported in the literature. Ball and Berry (1990) found values of g_1 varying from 8.0 to 16.4 for C_3 plants for the formulation presented in equation (5). Obtained g_1 and D_0 with the formulation presented in equation (12) were in good agreement with values reported by Leuning (1995). Lloyd et al. (1995) obtained -0.02 and 12.37 for g_0 and g_1, respectively, for the 'Ball and Berry' model (equation 9) and 1950 mol mol^{-1} for λ in the 'Lambda' model for a tropical rainforest in south western Brazil in Reserva Jaru. The values obtained in this study were lower than those of Lloyd et al. (1995). Obtained values from this study were 0.025, 8.06 and 980 mol mol^{-1} for g_0 and g_1 and λ respectively. However, Lloyd and Farquhar (1994) obtained λ =750 mol mol^{-1} for a generic rainforest using laboratory gas exchange data. According to Lloyd (1995), the forest in Jaru has larger conductances that at Manaus and there are possibly differences in species composition and soil nutrition that could explain the difference in conductances. Further, as will be shown in Chapter 3, λ for the forest at Jaru was fitted to the data with a larger value than at this site in Manaus. From the sensitivity of the simulated G_s to relative humidity under different temperatures using the 'Lambda' model and two forms of the 'Ball and Berry' model (either with direct dependence on relative humidity or VPD), it was shown that both models had the same performance up to a relative humidity of 80% when considering the 'Ball and Berry' model with dependence on VPD. This implies that the same performance can be obtained either with one parameter (λ) or with three (g_0, g_1 and D_0), which gives advantage to the 'Lambda' model. The modelling study from Lloyd et al. (1995) reports similar model

performance when implementing both stomatal conductance models coupled to the big leaf model for a rainforest in south west Brazil (Jaru).

The type of empirical models for stomatal conductance evaluated in this study are well known for performing best at non-water stressed conditions with the major drawback of non inclusion of water stress (Dewar 1995; Katul et al. 2000; Leuning 1995). Model evaluation in this study used data from the end of the dry season of 1995 (see rainfall in Figure 2.1) assuming well watered conditions. However, residuals of simulated λE and H had a biased trend to over predict the few measurements at the highest VPD and highest temperatures under both formulations of stomatal conductance, which could be linked to a signal of water stress. According to Malhi et al. (2002) and Williams et al. (1998), reductions in surface conductance at this site during the dry season were driven by increases in soil hydraulic resistance. Harris et al. (2004) used the same data set to calibrate the stomatal conductance/photosynthesis module of a global land surface scheme. Their calibrated model was able to capture decreases in canopy stomatal conductance when soil moisture dependence was included, leading to satisfactory estimates of carbon uptake, but at the cost of poor long term estimates of latent and sensible heat.

2.5 Conclusion

From the model evaluation conducted in this study it is concluded that both the sun and shade and the big leaf approach can qualitatively and numerically simulate accurately the energy fluxes from the rainforest at the given meteorological conditions with any of the stomatal conductance approaches tested. It has also been shown that because at the predominant atmospheric conditions simulated latent heat was not highly sensitive to small changes in simulated stomatal conductance, variation of simulated G_s among models did not affect the overall fit to the observations with any of the models.

However in terms of simulating carbon uptake, it was shown in Chapter 1 that the sun and shade model was qualitatively superior to big leaf. Thus, for further simulations of carbon and energy fluxes in the following chapters of this thesis, the sun and shade model will be used due to its qualitative superiority with respect to the big leaf coupled to the ‘Lambda’ model that requires only one parameter and performs equally well as the 3-parameter ‘Ball and Berry’ stomatal conductance model.

3 Model evaluation at five rainforest sites in the Amazon using eddy correlation data

3.1 Introduction

The eddy correlation technique uses micrometeorological theory to interpret measurements of the covariance between vertical wind velocity and fluctuations of scalar concentrations above or within vegetated surfaces (Baldocchi and Meyers 1998; Moncrieff et al. 1997). During the past ten years the use of the eddy correlation method has increased considerably and emerged as a routine tool for assessing ecosystem carbon and water vapour exchange with the atmosphere on time scales of hours-to-years (Baldocchi 2003). In addition to measuring the carbon balance at short and long time scales at the ecosystem level, the eddy correlation method is a useful tool for understanding the response of vegetation to environmental variables at individual sites (Law et al. 2002). Fluxes from eddy correlation together with concurrent meteorological data have been of considerable use within the modelling community, allowing models that simulate plant carbon and energy exchange at the ecosystem level to be evaluated against measurements made at the same scale. This type of model calibration and evaluation can be performed in different regions and ecosystems with the overall goal to improve model estimates of regional and global carbon balance and future estimates of atmospheric CO_2 concentration. Improved representation of gross assimilation within simulations of coupled climate and carbon dynamics should lead to better estimates of long-term carbon sinks and sources (e.g., Sitch et al. (2003)).

Even though the increased availability of eddy correlation flux data has been very useful in evaluating the ability of models to simulate measurements and ecosystem responses to different environmental variables, it is important to note some limitations of the method. A frequent failure to close the energy balance, especially in forest ecosystems (Baldocchi et al. 2003, Finnigan et al. Wilson et al. 2002, Masman et al. 2002), makes it difficult to assess the modelled partition of net radiant energy into its component latent and sensible heat fluxes. Also the eddy correlation method provides an estimate of the net carbon exchange which comprises fluxes from two processes that occur simultaneously: leaf photosynthesis and ecosystem respiration. Separating the net exchange into individual contributions from these two processes is non trivial. The standard method uses the net ecosystem exchange measured during night time to derive the ecosystem respiration. There are two drawbacks with this method. First, daytime ecosystem respiration differs from night time due to temperature differences especially at the canopy level. Second, and most importantly, there is a frequent failure of the system to measure night time respiration fluxes at low wind speed conditions (Aubinet et al. 2002; Massman and Lee 2002; Pattey et al. 2002; Saleska et al. 2003). Furthermore, the storage flux term added to the CO_2 flux, is often evaluated at one location, not taking into account the heterogeneity in the source distribution and horizontal air movement such as drainage flow associated with topography (Pattey et al. 2002). Ecosystem respiration can also be determined, when sufficient information is available on the individual respiration terms, i.e. plant tissue and soil respiration. However, the main difficulty with this method is to estimate soil respiration. Due to the interannual variability of rainfall, the flux of CO_2 from the soil can vary from year to year over the same season because of the dependency of soil respiration on soil water content (Davidson et al. 2000; Chambers et al. 2004). There is an optimum for soil respiration at intermediate soil water contents with decreases in respiration at water content both above and

below the optimum (Davidson et al. 2000). In addition, some of the eddy correlation studies are not conducted at the same time as the soil respiration measurements. In summary, use of ecosystem respiration derived from any of the mentioned methods adds uncertainty to the model evaluation.

Carbon isotope ratios (δ^{13}C) of plant tissues provide important information on stomatal limitations to plant canopy photosynthetic activity (Farquhar et al. 1989). Leaf isotope ratios of C_3 plants give an indication of the average intercellular CO_2 concentration (C_i) during photosynthetic periods (Farquhar et al. 1982). Because C_i is affected by the demand (CO_2 for photosynthesis) and supply of CO_2 (regulated by stomatal conductance), environmental factors such as light, water supply and nitrogen content are recorded in the carbon isotope ratios of plant tissues. Therefore, isotopic measurements of this type place a constraint on models of isotopic discrimination during photosynthesis (Aranibar et al. 2006). This approach has been used in some modelling studies. In the study of Aranibar et al. (2006) the sensitivity of photosyntheic carbon isotope discrimination to the parameters of the stomatal conductance model was used to provide an additional constraint to the model. Aranibar et al. (2006) selected values for their stomatal conductance parameter that produced similar simulated discrimination as inferred from foliar isotope ratios measured at their study site. Similarly in the present study, foliar carbon isotopes are compared with simulated values, and are also used to help constrain the stomatal conductance parameterisation.

The physiology and key controls on rates of photosynthetic carbon fixation at the leaf level are well understood (Farquhar and von Caemmerer 1982). Under the assumption of nitrogen (N) limitation, leaf photosynthesis is usually modelled based on the measured linearity between photosynthetic capacity and N content per unit leaf area (Evans 1993; Field and Mooney 1986; Hirose and Werger 1987; Pettersson and McDonald 1994). This reflects the large investment of nitrogen in photosynthetic machinery (more than half of the total). In addition to nitrogen other nutrients like phosphorous (P) play an important regulatory role in photosynthesis. Furthermore, Nitrogen limitation is widespread in many natural ecosystems (Lambers 1998). However, for tropical ecosystems, some authors have recognized the efficient phosphorous utilization in infertile oxisol/utislols in tropical rainforests (Vitousek and Sanford 1986), and have suggested that leaf phosphorous (P) rather than leaf N may be the key limiting nutrient constraining rainforest productivity (Vitousek et al. 1986).

Furthermore, due to the low foliar P content in tropical forest leaves, it is likely that their low P concentrations may constrain their photosynthetic rate, at least for some forests (Lloyd et al. 2001). Partitioning of the products of photosynthesis is largely determined by the availability of inorganic phosphate inside the plant cells. When the rate of export of photosynthetic products is low, photosynthetic rates can become limited by feedback inhibition. Under these circumstances there is low inorganic phosphate in the chloroplasts and therefore the formation of ATP (molecule for energy storage) is reduced and the activity of the Calvin cycle declines, meaning that the carboxylation activity of Rubisco (related to the $V_{\max}$ parameter in the Farquhar and von Caemmerer (1982)) and consequently the rate of photosynthesis drop.

Different models of leaf photosynthesis and stomatal conductance that scale up leaf processes to the canopy level have been forced, calibrated and evaluated using meteorology measured together with fluxes from eddy correlation from single sites in tropical (Harris et al. 2004; Lloyd et al. 1995; Williams et al. 1998; Zhan et

al. 2003) boreal (Arneth et al. 1998) and temperate (Baldocchi and Harley 1995) forests. Before a model is applied to infer regional fluxes, it should first be evaluated at more than one site, in order to test the ability of the model to reproduce the observed differential response of canopy types to environmental variables. For example eddy correlation systems have been installed on top of various towers in the Brazilian Amazon to monitor the rainforest exchange of energy and carbon with the atmosphere. There have already been modelling studies at single sites: at Jaru (Lloyd et al. 1995), but mostly at the Manaus site (Harris et al. 2004; Williams et al. 1998; Zhan et al. 2003), but no single modelling study has undertaken all tower sites simultaneously.

The motivation behind this study is to refine ecosystem gas exchange models in order to better represent the gross carbon uptake of forests in the Amazon basin, utilising the available eddy correlation data for model evaluation and calibration. Our first objective is to assess and then improve model performance of simulated carbon uptake and energy partition at five rainforest sites in the Amazon basin. We first employ the mechanistic sun/shade model for photosynthesis coupled to a stomatal conductance model ('Lambda' model), which was calibrated at one rainforest site, as described in Chapters 1 and 2. This model is applied at all 5 sites. Model results are evaluated against fluxes of carbon and energy derived from eddy correlation data, and measurements of foliar carbon isotope fractionation available at 4 of 5 the study sites (Ometto et al. 2006). Uncertainties are explored within both model parameters and observations of eddy correlation and ecosystem respiration. Whilst taking account of these uncertainties and with the aid of foliar carbon isotope measurements, model parameters are subsequently adjusted, within acceptable bounds, to better fit the observations. The second objective of this chapter is to produce a canopy scale function to scale up to basin level. Here we relate canopy maximum carboxylation capacity of rubisco activity (V_{max}) at each site to foliar N. Additionally, given the possibility of phosphorous deficiency in tropical leaves being an important constraint on photosynthesis (Lloyd et al. 2001), relationships between V_{max} and foliar phosphorous are also explored.

The main questions to be answered in this chapter are:

1. Can the sun and shade model reproduce the observed net carbon uptake (G_P) using the parameterisation from Chapter 1at the five flux tower sites?

2. If not, how can the model agreement to the observations be improved?

3. What are the major constraints to such model-data evaluation?

4. What are the strengths and weaknesses of the sun and shade approach coupled to the Lambda model evaluated at the 5 rainforest sites?

5. How can this modelling exercise be used to extrapolate simulations to the basin level?

3.2 Materials and Methods

3.2.1 Overview

To answer these questions the following steps are undertaken in this study:
1. Initially observed net photosynthetic uptake (G_P) from the flux towers is estimated from measured Net ecosystem exchange (N_E) and inferred ecosystem respiration from various sources at the different sites.

2. The parameter for top of the canopy V_{max} is calculated using measurements of leaf nitrogen (N) from top canopy leaves and relationships of measured V_{max} and leaf N already used in Chapter 1. Using V_{max} and other parameters and meteorological variables for each site G_P is initially simulated.

3. A sensitivity analysis of simulated G_P by the sun and shade model is conducted to identify key model parameters affecting the light response of G_P. The model is subsequently recalibrated based on this analysis and findings of step 2.

4. The model is also fitted to the observations using a Simplex procedure (Nelder and Mead 1965) which minimizes the error sum of squares between the model and data at each site. The reasons for this are twofold: first, to compare these results to the manual calibration undertaken in step 3, and second to provide best fitted V_{max} for each site.

5. Make linear regressions of best fitted V_{max} against Leaf N and leaf P.

3.2.2 Data

3.2.2.1 Tower sites, fluxes and meteorology

Eddy correlation measurements made above five primary rainforest sites in the Brazilian Amazon (hourly time step) were used to compare model predictions with observations, with associated meteorological variables obtained by the same measurement groups used as forcing data. A summary of data used and site characteristics is given in Tables 3.1 and 3.2, respectively, and site locations are shown in Figure 3.1. Information on instruments used for measurements and methods for flux calculations at each site can be found in the original references for these measurements as given in Table 3.2.

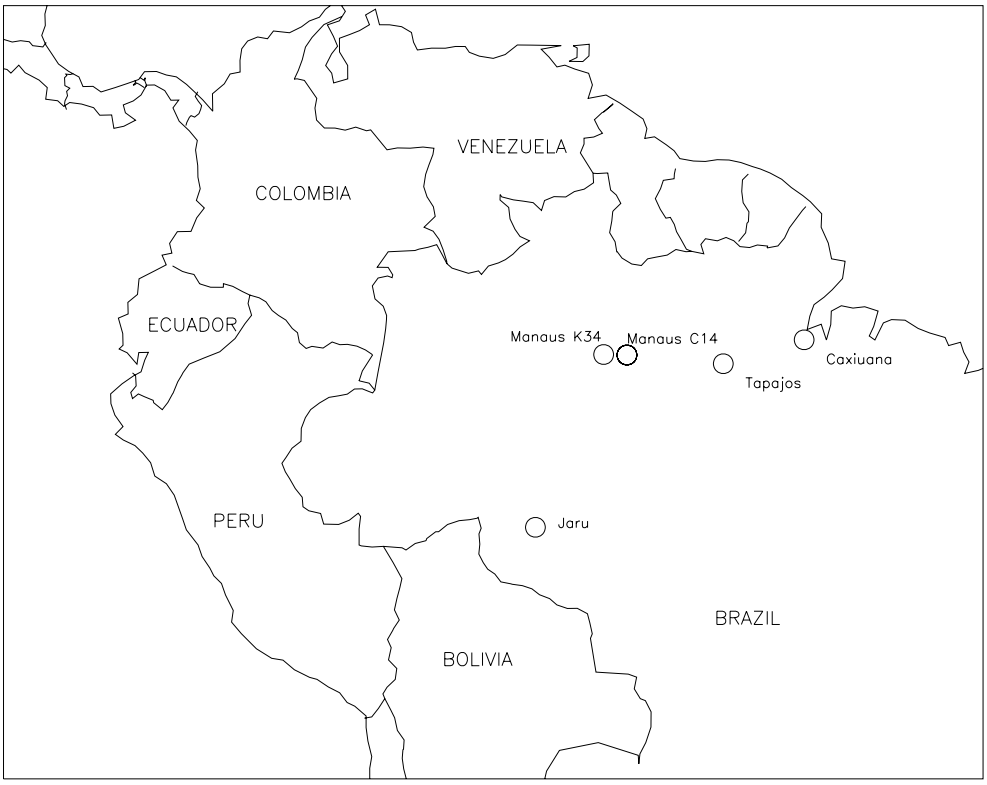

Figure 3.1. Locations of rainforest sites with eddy correlation systems used in this study.

Table 3.1. Information about eddy correlation data used from five sites in the Brazilian Amazon.

	Man C14	Man K34	Jaru	Tapajos	Caxiuana
Period used	10/1995–07/1996	10/1999–05/2000 10/2000–12/2000	All 1999 All 2000	All 2001 All 2002	1999
Storage Flux	Modelled	Measured	1999 measured 2000 modelled	measured	Measured Few small gaps modelled
Energy balance closure	94%	70%	70%	87 % including heat storage from ground and vegetation	70%
Correction applied to data used	Low frequency contributions	no corrections applied to data set used at the time simulations were performed.	no corrections applied to data set used at the time simulations were performed.	Night time u*	Low frequency contributions

Table 3.2. General characteristics of five rainforest sites in the Brazilian Amazon.

	Man C14	Man K34	Jaru	Tapajos km 67	Caxiuana
Geographical coordinates	2° 35' 21.08''S 60° 06' 53.63''W	2° 36' 32.67'' S 60° 12' 33.48''W	10° 4.706'S 61° 56.03 'W	03° 03' S 54° 56'W	01.42° S 51.32°W
Location	Cuieiras Reserve Previously known as ZF2 Manaus, Amazonas	10 km away from the C14 site Manaus, Amazonas	Reserva Jaru 100 km north of Ji –Parana, Rondonia	Tapajos National forest 70 km south of Santarem, Para	1 km north of field station floresta Nacional de Caxiuana, Para
Tower height [m]	41.5	52	62	65	51.5
Mean elevation [m]	100-150	100±50	150-200	90	15
Landscape	Undulating: Plateau and valleys	Undulating: Plateau and valleys	Gently sloping plain	Flat plateau	Flat plateau
Forest type	Terra firme	Terra firme	Terra firme	Terra firme	Terra firme
Canopy height [m]	30-35	30-35	35 up to 45[1]	40 emergent up to 55	~35
LAI [$m^2 m^{-2}$]	5.6	4.4	4	6.7	5.4
Type of soil	Oxisol-utisol	Oxisol-utisol	Red –yellow acrisol[1]	Oxisol	Older oxisol
Mean temperature[°C]	26.7	26.7	25-27	max [24-32] & min [20-25][5]	27
Mean precipitation [mm $year^{-1}$]	1900-2300	1900-2300[2]	1900	1920	2300
Dry season length (months with rainfall <100mm)	June-Sept	June-Sept	May/June-September	June-December	June-August
Mean aboveground biomass [Tonne ha^{-1}]	300-350[3]	300-350[3]	220[4]	349.1[3]	371.7[3]
Reference to site and eddy correlation data	Malhi et al. (1998) Malhi et al. (2000)	Araújo et al. (2002) Chambers et. al. (2004)	von Randow et al. (2004)	Saleska et al. (2003) From a neighbouring site (km 83): Goulden et al. (2004) Miller et al. (2004) Da Rocha et al. (2004)	Carswell et al. (2000) Iwata et al. (2005)

[1]von Randow et al. (2004), [2]Chambers et al. (2004), [3]Baker et al. (2004), [4]Meir (1996),[5]Goulden et al. (2004)

The meteorological data used for model input comes from automatic weather stations located at the top of the towers. Global solar radiation, wind speed and air temperature are available at all towers. To determine atmospheric water vapour content, methodologies differed between sites – values are derived from wet bulb temperatures at Manaus C14 and Caxiuana, from dew point temperatures at Tapajos and from relative humidity measurements at Jaru and Man K34.

Fluxes of carbon dioxide determined at the top of the measurement towers correspond to net ecosystem exchange rates (N_E). In order to determine the net canopy assimilation rate (i.e. total photosynthesis minus daytime canopy leaf respiration R_C) (G_P) or gross canopy assimilation rate (i.e. total photosynthesis, includes daytime leaf respiration) (G_{PP}), it is necessary to consider respectively the non-leaf ecosystem respiration rate R_{E_NL} or the total ecosystem respiration rate R_E and carbon dioxide accumulated inside the canopy:

$$G_P = N_E - R_{E\_NL} \quad (1)$$

$$G_{PP} = G_P + R_C = N_E - \mathrm{R}_E \quad (2)$$

$$N_E = \mathrm{F}_c + \int_0^{h_t} \frac{\partial \mathrm{C_a}}{\partial \mathrm{t}} \mathrm{dz} \quad (3)$$

where F_c is the flux of CO_2 measured by eddy correlation [μmol m^2 s^{-1}] and the integrand in [μmol m^2 s^{-1}], represents the rate of change in the CO_2 concentration (C_a) within the canopy between the forest floor and the eddy correlation measurement height, h_t and it is often referred to as 'the change in canopy storage flux'. Canopy CO_2 storage flux (S_T) is estimated from measurements of within canopy CO_2 concentrations and it is usually measured along with eddy correlation flux data.

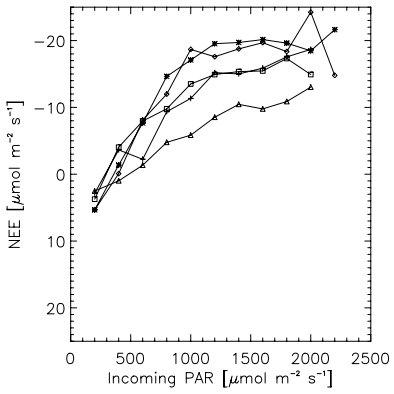

Figure 3.2. Light response of N_E measured by eddy correlation averaged over 200 μmol quanta m^{-2} s^{-1} bins at the different tower sites. Data used correspond to the period July-December. Δ Tapajos, * Man K34, ◊ Jaru, □ Caxiuana, + Man C14.

Of the five sites, the canopy storage flux was determined from measurements at Man K34, Tapajos, Jaru 1999 and Caxiuana. Data provided by collaborators from Manaus C14 only included storage measurements for the period October-November 1995. Lacking measurements at Manaus C14 for the remaining period of study and at Jaru during 2000, simulated storage fluxes (provided by collaborators) were used. Simulated and measured storage flux for all the sites are shown in 3.3.

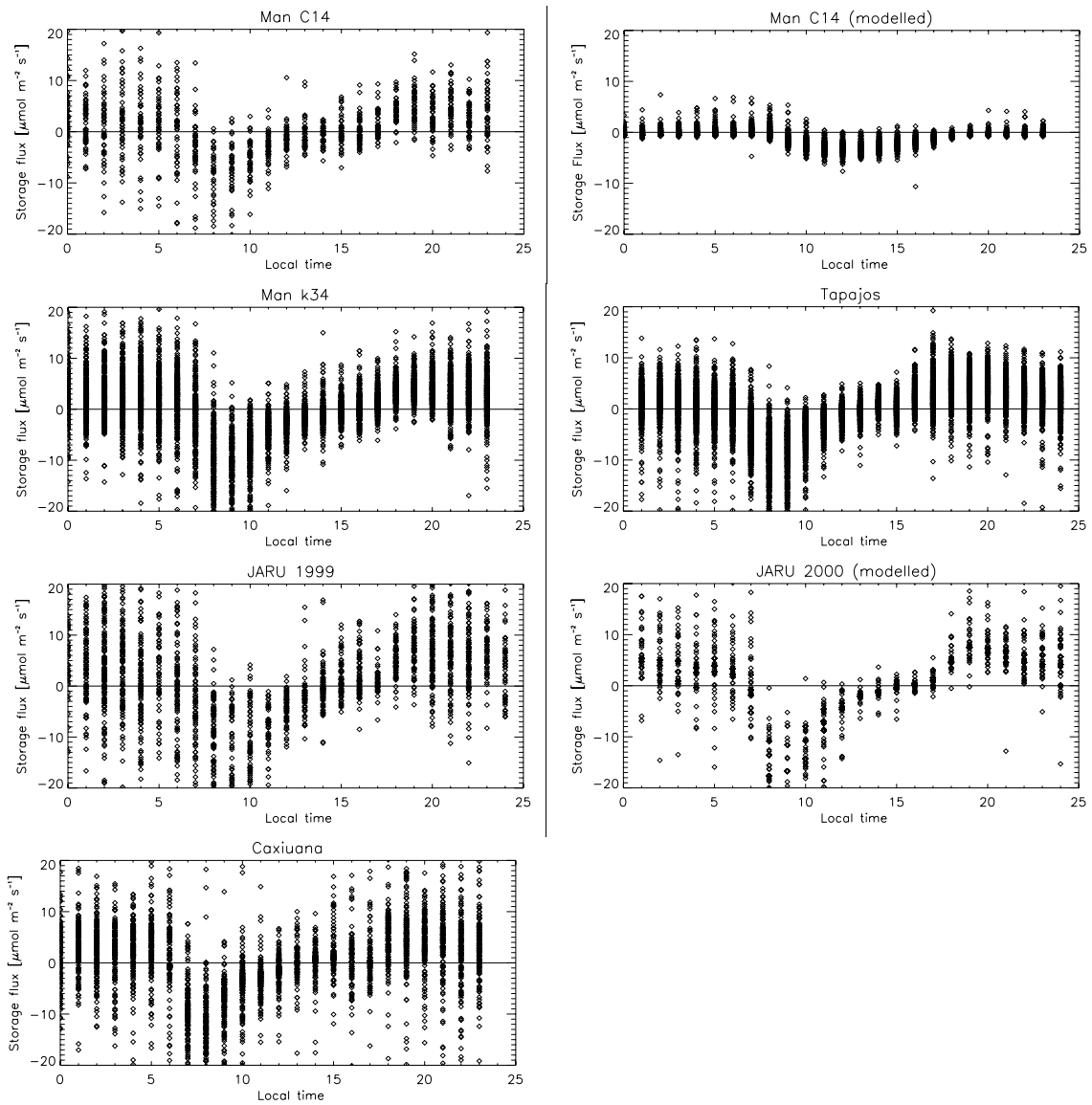

Figure 3.3. Canopy CO_2 storage flux estimated from within measured canopy concentrations of CO_2 and simulated when there were no measurements. Measurements of storage flux at Manaus C14 correspond to the period October-November 1995.

To calculate photosynthesis from measured eddy correlation N_E, it was necessary to use either G_P or G_{PP} depending upon the ecosystem respiration available at each individual site. At sites where it was possible to estimate the separate contributions to ecosystem respiration, i.e. from stems and branches, soil and coarse litter (Man K34, Jaru and Man C14), the term net assimilation or net uptake is used, and is here after referred to as G_P. This term accounts for the balance of the parallel processes of photosynthesis and leaf respiration. At Man K34, Jaru and Man C14 the 'observed' G_P was calculated as:

$$G_P = -N_E + R_{E\_NL} = -N_E + R_S + R_W + R_{CS} \quad (4)$$

R_{E_NL} is the sum of all respiratory contributions from soil (autotrophic and heterotrophic in ground area basis), coarse litter, stems and branches. R_W represents the respiration contribution from stems and branches, R_S from soil (which includes root and fine litter decomposition at the soil surface) and R_{CS} accounts for

coarse litter respiration. At sites where ecosystem respiration was given as a single flux (Caxiuana and Tapajos), the term Gross photosynthesis, G_{PP}, is used and it is defined as the total amount of carbon that is taken up by the vegetation. At Tapajos and Caxiuana, total ecosystem respiration was available and G_{PP} was calculated as:

$$G_{PP} = - N_E + R_E \quad (5)$$

where R_E is defined as R_{E_NL} plus respiratory contributions from daytime leaf canopy respiration.

To derive G_P or G_{PP} at the five tower sites, different methodologies for estimating ecosystem respiration had to be used, these again dependent upon the techniques employed by the original investigators.

3.2.2.2 Respiration calculation

For both Manaus sites, soil respiration was derived from measurements of soil respiration undertaken between June 2000 and July 2001 over all topographic areas at the Man K34 site (see Figure 3 in Chambers et al. (2004). Stem respiration (ground area basis) was taken as 1.1 μmol m^{-2} s^{-1} as measured by Chambers et al. (2004) at a site around Man K34, with the same temperature dependency as leaf canopy respiration in equation 9 in Chapter 1, using modelled canopy temperature from the shaded leaves as a surrogate for stem temperature. Similarly for coarse litter respiration, a value of 0.5 μmol m^{-2} s^{-1} was used as measured by Chambers et al. (2004) at a rainforest in the area around Man K34. Respiration from coarse litter respiration was assumed constant during the day. Any small diurnal variation was assumed to have little impact on the total ecosystem respiration.

Ecosystem respiration at Jaru was determined using a soil respiration rate of 5.22 μmol m^{-2} s^{-1}, as measured by Meir et al. (1996), and assumed constant through time. Stem respiration was taken as 0.75 μmol $m^{-2}s^{-1}$ (Meir and Grace 2002) with a canopy temperature (from shaded leaves) dependency as for canopy respiration in equation (7). Coarse litter respiration rates were assumed to be the same as at Manaus, and assumed constant throughout the day.

Daytime ecosystem respiration at Caxiuana was modelled using a Q_{10}-type temperature response function with an equivalent Q_{10}= 2. This was made using a mean night time temperature and respiration rate, given a lack of sufficient temperature variation to fit the Q_{10}-temperature function (Y. Malhi pers. comm.). Ecosystem respiration, meteorology and the eddy correlation flux data were provided by Dr. Y Malhi (University of Oxford). It should be noted that this simulated ecosystem respiration term also included an estimate of canopy respiration.

Ecosystem respiration at Tapajos was taken from Saleska et al. (2003, Figure 2B). These authors report an average seasonal cycle of whole ecosystem respiration derived from night time net ecosystem exchange measurements filtered to exclude friction velocity (u*) values lower than 0.2 m s^{-1}. Night time u* filtered N_E at Tapajos was in apparent good agreement with night time N_E inferred from Radon-222 measurements at the same site (Martens et al. 2004). Because ecosystem respiration at Tapajos (Saleska et al. 2003) was derived

from night time data, an attempt to include diurnal variability to ecosystem respiration was achieved by subtracting night time modelled canopy leaf respiration and adding daytime modelled canopy leaf respiration to the original values from Saleska et al. (2003). Inclusion of diurnal variability of coarse litter respiration was made in a similar way to leaf respiration by assuming coarse litter temperatures to be two degrees lower than air temperatures measured above the canopy. No major increase in the diurnal ecosystem respiration was obtained due to the low night time and day time air temperatures measured over the studied period especially during the wet season (See Figure 3.34).

A summary of how ecosystem respiration was calculated for each site is included in Table 3.3 and the light response of R_E is shown in Figure 3.4 for all sites during the wet season. Notice the high ecosystem respiration (simulated) obtained for Caxiuana (provided together with the eddy correlation flux measurements and meteorology by Y. Malhi).

Table 3.3. Calculation of ecosystem respiration for the different sites. All respiration terms are in μmol m^{-2} s^{-1} (ground area basis).

Site	Method of calculation	Source	R_E
Man C14	Sum of individual components of R_E R_S at soil T min-max [2.1-4.10][1] R_{CS} (at 25 °C) 0.5 R_w (at 25 °C) 1.1 $R_{C,25}$ 3.5	 Chambers et al. (2004) Chambers et al. (2000) Chambers et al. (2004) Modelled	 min-max [7.2-9.2]
Man K34	Sum of individual components of R_E R_S at soil T min-max [2.1-4.10] [1] R_{CS} (at 25 °C) 0.5 R_w (at 25 °C) 1.1 $R_{C,25}$ 2.5	 Chambers et al. (2004) Chambers et al. (2000) Chambers et al. (2004) Modelled	 min-max [6.2-8.2]
Jaru	Sum of individual components of R_E R_S (at soil temperature) 5.22 R_{CS} (at 25 °C) 0.5 R_w (at 25 °C) 0.75 $R_{C,25}$ 2.66	 Meir et al. (1996) Chambers et al. (2000) Meir et al. (1996) Modelled	 9.3
Tapajos	Inferred from night time fluxes by filtering out data below particular u* thresholds corrected for daytime respiration rates $R_E = N_{Enight}$ min-max [8-10.6] [1] $R_{C,25}$ 2.26	 Saleska et al.(2003) Modelled	Min-max [8-10.6]
Caxiuana	Inferred from night time fluxes by filtering out data below particular u* thresholds, and applying the Michaelis Menten equation with a fixed Q_{10} of 2 to soil temperature data to estimate daytime respiration rates R_E (at 25 °C) 8.6 $R_{C,25}$ 2.7	 Iwata et al. (2005) Modelled	8.6

[1]Range represents seasonal variation.

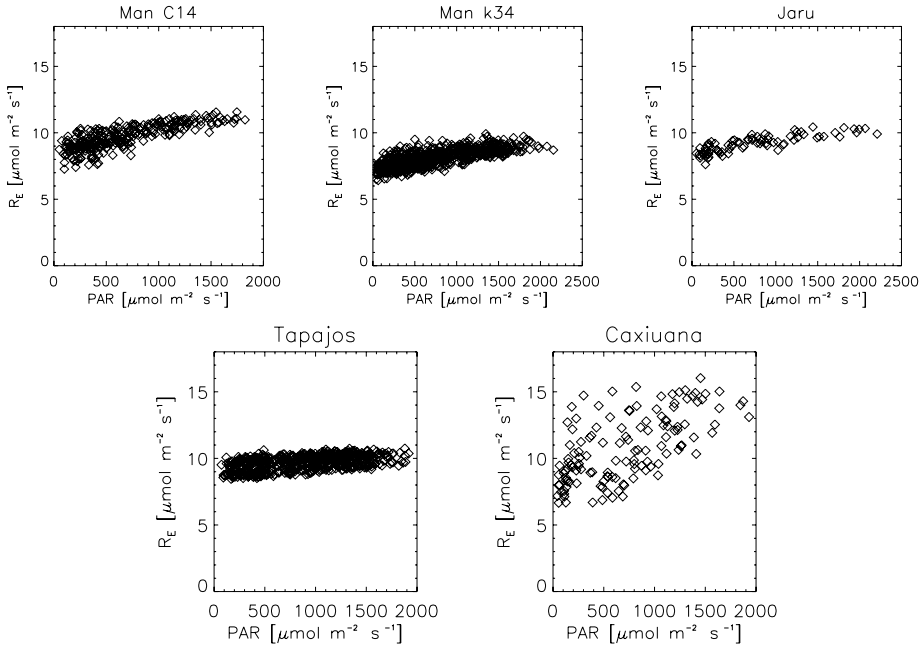

Figure 3.4. Estimated daytime ecosystem respiration (for method see Table 3.3) at all sites during the wet season. Note the larger values at Caxiuana**.**

Foliar N and P

Leaf Nitrogen for all sites except Man C14 was initially taken from the data set from the RAINFOR Consortium (unpublished data). These data were collected as part of the RAINFOR project, a network of forest plots across the Amazon basin in which forest biomass and dynamics are monitored, to understand their relationship with soil and climate (www.geog.leeds.ac.uk/projects/rainfor). The dataset includes leaf N and leaf P from top leaves at about 87 plots along a transect from west to east Amazonia, including 3 of the Brazilian flux sites used in this study. It does not include leaf N content for Man C14 or Jaru although it does have data for another very similar forest. As explained in Chapter 1 leaf N for Man C14 was taken from the Carswell et al. (2000) data set which contains vertical distribution of leaf N. Further, additional datasets are used to supplement or compare against the Carswell et al. and RAINFOR data sets. For instance, a recent study from Ometto et al. (2006), where leaf samples were collected at some of the Brazilian sites, reports much lower N values for Man C14 at the top leaves, than those reported by Carswell et al. (2000). Also they found no major differences between leaf nitrogen at Man K34 and Man C14. A summary of foliar N from these data sets and from other studies is presented in Table 3.4. Note the large range in foliar N from the different sources.

Table 3.4. Foliar N and specific leaf area (where available) from top canopy leaves (unless specified otherwise) reported by various sources and used for model parameterisation.

Source		Man C14	Man K34	Jaru	Tapajos	Caxiuana
Carswell et al. (2000) at 24 m	[mg g^{-1}]	30.5 ±0.06				
	[g m^{-2}]	3.61± 0.17				
SLA	[cm^2 g^{-1}]	87.3±3.4				
Carswell et al. (2000)						
Leaf N extrapolated to top	[g m^{-2}]	4.4				
SLA	[cm^2 g^{-1}]	65.87				
Ometo et al. (2006) from all heights	[%]	2.07 ±0.7	2.04±0.6	2.48±0.65	2.45±0.76	
RAINFOR Consortium						
(unpublished data) sun leaves	[mg g^{-1}]		23.10		23.06	19.9
	[g m^{-2}]		2.22		2.03	1.6
SLA	[cm^2 g^{-1}]		103.97		115.76	124.29
Vale et al. (2003) at 30 m	[g m^{-2}]					2.6
SLA	[cm^2 g^{-1}]					76.69
Domingues et al. (2005) top leaves	[g m^{-2}]				2 - 3.5	
Meir et al. (2001) at 30- 35 m	[g m^{-2}]			2.9		
Used for parameterisation	[g m^{-2}]	4.1*	3.2	3.7	2.03	2.6

*This value corresponds to 90% of the value extrapolated to the canopy top using Carswell et al. (2000) dataset as parameterised in Chapter 1.

Foliar carbon isotopes

Measurements of foliar isotopic fractionation from the study of Ometto et al. (2006) were used for model evaluation where available (not available for the Caxiuana site).

3.2.3 Model parameterisation

The sun and shade model for photosynthesis (de Pury and Farquhar 1997) coupled to the stomatal conductance 'Lambda' model (Cowan 1977; Cowan and Farquhar 1977) as described in Chapter 1 and 2 were used for simulations at the five rainforest sites.

Parameterisation of canopy photosynthetic capacity for the sun and shade model has already been explained in detail in Chapter 1 for the Manaus C14 site. A brief description on parameterisation of the other four sites follows. Canopy level maximum carboxylation activity of Rubisco (V_{max}) was calculated from leaf nitrogen concentrations (on a leaf area basis) from top canopy leaves and the estimated leaf area index (LAI) from the RAINFOR Consortium (unpublished data). V_{max} at the top of the canopy was calculated assuming a linear relationship between leaf N content per unit leaf area and V_{max} derived using leaf level data taken at Manaus C14 (Carswell et al. 2000) and Caxiuana (Vale et al. 2003) for samples taken at different heights within the canopy. An exponential decrease of V_{max} with height (or more precisely with cumulative leaf area) was then assumed for all five canopies as was observed for the profile of V_{max} derived from gas exchange measurements at the Manaus C14 site (Carswell et al. 2000). This is shown in Figure 3.5. With this parameterisation V_{max} for the top and bottom 50% of canopy leaves averages 65% and 35% of the V_{max} of the uppermost leaves, respectively. Having defined this distribution of V_{max} with cumulative leaf area, total canopy V_{max} was then calculated at each site as the integral of leaf level V_{max} over cumulative leaf area index, as described in de Pury and Farquhar (1997):

$$V_{\max} = \int_0^{LAI} V_{\max\_leaf}\, dl \qquad (6)$$

where V_{max_leaf} is the maximum carboxylation activity of Rubisco at the leaf level in area basis, l is the cumulative leaf area index from the top of the canopy down to any level in the canopy and LAI is the total canopy leaf area index. The canopy level V_{max} is equivalent to the area under the exponential curve shown in Figure 3.5 for the Manaus C14 site. The same method was used for all five tower sites using the correspondent leaf N content per unit leaf area and LAI at each forest. Model sensitivity to other V_{max} (i.e. foliar N) vertical distributions through the canopy is evaluated in Chapter 4.

Initial parameterisation of V_{max} was undertaken using foliar N from the RAINFOR Consortium (unpublished data) for all sites except at Man C14 which was parameterised using Carswell et al. (2000) dataset as described in Chapter 1. The model is calibrated to better fit the Eddy covariance measurements by adjusting foliar N (and thus canopy V_{max}) within the bounds of uncertainty. Implications of the recalibration are discussed.

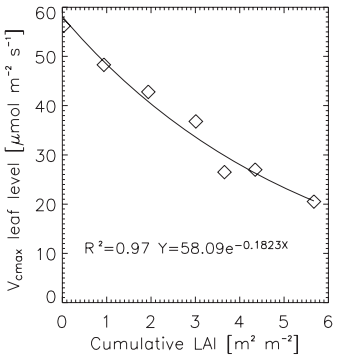

Figure 3.5. Vertical profile of leaf level V_{max} with height (i.e. increasing cumulative leaf area) at the Manaus C14 site.

Canopy respiration (in ground area basis) was simulated for all sites using the parameterisation for the sun and shade model in Chapter 1, and assumed to decrease exponentially with cumulative leaf area index. Top of the canopy respiration at all sites was taken as a constant fraction of V_{max} from top leaves as derived in Chapter 1 from the Carswell et al. (2000) data set (i.e. $0.022 \times V_{max}$). Total canopy respiration R_C was subsequently calculated using the same nitrogen allocation coefficient obtained for the exponential regression of V_{max} against cumulative leaf area index, with a temperature dependence of canopy respiration given by Lloyd and Taylor (1994).

$$R_C = R_{D,25} \exp\left(308.45\left(\frac{1}{71.02} - \frac{1}{T_C - 227.13}\right)\right) \qquad (7)$$

where R_C is the rate of canopy dark respiration during the day at canopy temperature T_C and $R_{D,25}$ is the rate of canopy dark respiration at 25 °C, with both respiration terms given in [μmol m^2 s^{-1}].

The light saturated potential rate of electron transport capacity (J_{max}) was taken as a constant fraction of V_{max} as derived in Chapter 1 in the parameterisation of the sun/shade model for the Manaus C14 site. Thus a ratio J_{max} / V_{max} of 1.92 was obtained and assumed for all five model calibration sites. The initial slope of the light response curve, Φ, was first taken as parameterised for the Manaus C14 site in Chapter 1. Where necessary this parameter was adjusted, within the range of measurements provided, at individual sites to better reproduce the light response of G_P.

The remaining parameters for the sun/shade model, *viz*. the curvature factor of light response curve, θ, and the temperature sensitivity parameters of the electron transport rate S_J and H_J and rubisco and leaf respiration temperature sensitivities were taken from Chapter 1 (i.e. θ and H_J were taken as parameterised in the study of Carswell et al. (2000) at the leaf level and S_J was taken as fitted for the sun/shade model).

Leaf reflectance and transmittance were assumed identical at all sites. Values were taken from the study of Poorter et al. (1995) where measurements were made along a vertical gradient in canopies in a tropical rainforest in Costa Rica.

In Chapter 2, the lambda (λ) parameter for stomatal conductance was calculated using stomatal conductance derived from eddy correlation measurements of latent heat flux, net carbon assimilation and VPD measured above the rainforest. Due to the high variability in estimates of stomatal conductance and net carbon assimilation from eddy correlation, the obtained regressions used to estimate λ were poor (not shown). Instead, following other studies (Katul et al. 2000; Aranibar et al. 2006) it was decided to use foliar carbon isotopes measurements from the different sites to help constrain the parameterisation of lambda (λ). Initial values of λ were calculated using the Farquhar et al. (1993) version of the model that allows λ to be estimated from $\overline{C_i / C_a}$, the derived from the δ^{13}C measurements and the long-term VPD ($\overline{D}$):

$$\lambda \approx \frac{1.6\overline{D}(C_a - \Gamma^*)}{C_c^2\left[1 - \frac{\overline{C_i}}{C_a}\right]^2} \qquad (8)$$

Subsequently, following Aranibar et al. (2006), values of λ were chosen that produced similar simulated discrimination as foliar isotope ratios measured at the different sites.

3.2.4 Simulation of δ^{13}C

Simulated isotopic composition of leaves δ^{13}C (‰) was calculated for the canopy following Farquhar et al. (1982) as:

$$\delta^{13}C = \delta_{atm} - a - (b - a)C_i / C_a \qquad (9)$$

where *a* corresponds to maximum fractionation due to diffusion of CO_2 in air (4.4 ‰) and *b* is the maximum fractionation in the carboxylation reaction (30 ‰) (Farquhar et al. 1982). δ_{atm} is δ^{13}C of the air, taken as -8.0 (‰), the late twentieth century mean atmospheric background value (Ehleringer et al. 1987). The ratio C_i/C_a corresponds to simulated daytime hourly values from the whole canopy. The simulated average integral of photosynthetic discrimination during the different seasons analyzed ($\overline{\delta^{13}C}$) is calculated with equation (9) using the photosynthetic flux weighted average C_i/C_a :

$$\overline{\delta^{13}C} = -12.4 - 25.6\frac{\sum_{i=1}^{n} G_{Pi} * (C_i / C_a)}{\sum_{i=1}^{n} G_{Pi}} \qquad (10)$$

3.2.5 Model evaluation

Simulated net carbon uptake and energy partition were evaluated using eddy correlation data for all sites. Simulations for the Manaus C14 site were evaluated during three seasons (end of dry season of 1995, wet season and dry seasons of 1996) while evaluation from Chapter 1 and 2 correspond only to the period during the end of the dry season of 1995 and data used corresponded to a period of time when storage fluxes were measured. As mentioned in Table 3.1 storage fluxes used for the Manaus C14 site were simulated (Malhi et al. 1998).

Further, eddy correlation measurements above forest ecosystems often fail energy balance closure tests (Baldocchi 2003; Finnigan et al. 2003; Massman and Lee 2002; Wilson et al. 2002). For this reason it is more practical to test model performance of energy partition using the evaporative fraction (defined as the ratio between the latent heat flux and the sum of the latent and sensible heat fluxes). There is considerable variability in the hourly calculated evaporative fraction, therefore model performance is evaluated using the mean diurnal cycles of measured and simulated evaporative fraction. In addition, simulated δ^{13}C values are compared to measurements of foliar isotopic fractionation from the study of Ometto et al. (2006) where measurements are available (not available for the Caxiuana site).

Having an accurate simulated δ^{13}C helps to substantiate the results for simulated photosynthetic uptake and at the same time δ^{13}C fixes the range within which the lambda parameter can vary. By increasing or decreasing lambda (therefore simulated stomatal conductance increases or decreases respectively), the partition of energy into sensible and latent heat fluxes is changed and the model can easily fit the measured energy balance, but at the same time the lambda parameter affects the photosynthetic rate through C_i/C_a and thus the simulated δ^{13}C. Therefore a realistically simulated δ^{13}C is a valuable diagnostic for testing the validity of the lambda parameter applied in a fully linked carbon/water/energy exchange model as is used here.

Model parameters were adjusted in order to obtain better agreement between model and observations at all sites. To verify the obtained parameters, the model was also numerically fitted to the observations.

3.2.6 Scaling up to basin level

An attempt to produce a canopy scale function to scale up simulations to basin level is presented at the end of this chapter. Such scaling up is made based on the model evaluation and calibration for the five tower sites. The scaling function can be used to parameterise the model at other sites, using the linear regression obtained from relating the best V_{max} obtained from parameterisations at each of the 5 sites to its correspondent foliar N. Further, given that phosphorous (P) plays a regulatory role in the partition of the products of photosynthesis directly affecting the activity of the Calvin cycle and therefore affecting the activity of Rubisco carboxylation, relationships between V_{max} and foliar P were explored as well.

3.3 Data-Model Evaluation

Parameters used for simulations at all sites are found in Table 3.5.

Table 3.5. Parameters for sun/shade simulations at each site.

	Man C14	Man K34	Jaru	Tapajos	Caxiuana
Top Leaf N [g m^{-2}] Used for parameterisation	4.1	3.2	3.7	2.03	2.6
LAI [m^2 m^{-2}]	5.63*	4.4$^{\nabla}$	4.0*	6.5$^{\nabla\Diamond}$	5.43$^{\nabla}$
V_{max} top canopy [µmol m^2 s^{-1}]	52.3	40.5	47.1	24.5	32.1
Canopy V_{max} [µmol m^2 s^{-1}]	185.1	127.8	118.5	100.2	109.7
Quantum yield, Φ	0.4	0.35	0.35	0.30	0.5
Teta, $\theta^{\times}$ curvature factor S_J^+ [J $mol^{-1}K^{-1}$] H_J^+ [J mol^{-1}] J_{max} / V_{max}	0.7 693.124 220000. 1.92	0.7 693.124 220000. 1.92	0.7 693.124 220000. 1.92	0.7 693.124 220000. 1.92	0.7 693.124 220000. 1.92
Year **Lambda, λ** [mol mol^{-1}]	1995 **1200** 1996 **1200**	1999 **2000** 2000 **2000**	1999 **2000** 2000 **2000**	2001 **2000** 2002 **2000**	1999 **1800**

* Meir et al. (2000); $^{\nabla}$RAINFOR Consortium (unpublished data): $^{\Diamond}$Nepstad et al. (2002) $^{\times}$curvature factor, equation 5 in Chaper 1. $^{+}$ Parameters that control maximum and minimum optimum temperature dependencies of J_{max}.

3.3.1 Man C14

Parameters used for this site were derived in Chapter 1. However the λ parameter of the stomatal conductance model (obtained value in Chapter 2 was λ=970 mol mol^{-1}) for this site was λ=1200 mol mol^{-1}. Using a λ=1200 mol mol^{-1} not only produced similar results for carbon uptake as with λ=970 mol mol^{-1} during all seasons, but also produced a better simulated energy partition during the wet and dry seasons, i.e. evaporative fraction (compared to the measurements) and simulated δ^{13}C values that were closer to the measurements.

The light response of hourly observations and simulations of G_P for the Manaus C14 site during three seasons is presented in Figure 3.6. Plots of standardised residuals of observed minus modelled G_P are shown in Figures 3A-1-3 and statistics of the model data comparison in Table 3.6. This shows that at end of both the dry and rainy seasons the model was able to fit the data relatively well. Moreover, residuals of measured and modelled G_P versus PAR, VPD, and air temperature were uniformly dispersed over the zero line (Figures 3A-1-3), although with a slight tendency towards overestimation during the wet season

(Figure 3A-2). During the dry season (July-August 96), the model tended to overestimate the data.

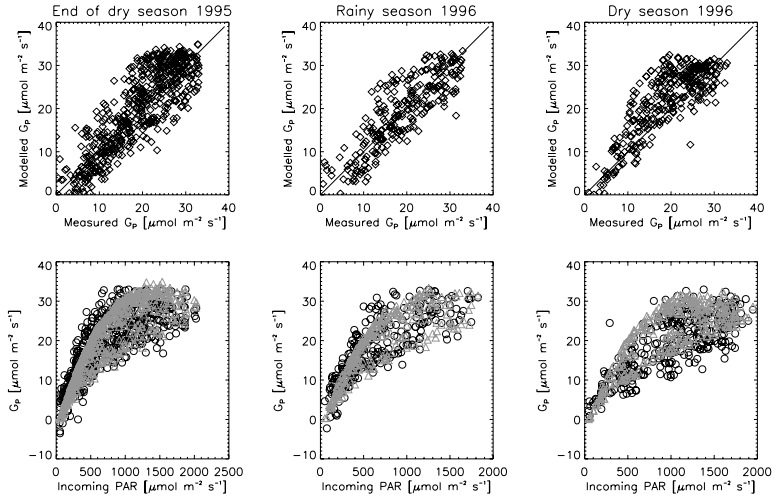

Figure 3.6. Man C14. Light response of modelled (Δ) and measured (o) net carbon uptake and 1:1 line of modelled *vs* observed net uptake.

Table 3.6. Statistics of model-data comparison for G_P* during the seasons tested

Season	a	r^2	RMSE**
End of dry 1995	1.04	0.95	4.89
Wet 1996	1.09	0.95	4.47
Dry 1996	1.11	0.96	4.89

* The regression model, modelled flux= a × measured (or estimated from eddy correlation) flux
** Root Mean Square Error (RMSE)

An examination of residuals versus time of the day during all three seasons (See Figures 3A-1-3) shows a general tendency for the model to overestimate early morning fluxes (0900-1000) (these correspond to high C_a values) and underestimate fluxes in the late afternoon, this problem being greatest during the dry season. This model tendency to over- and under-predict the early morning and late afternoon measured G_P is associated with low modelled storage flux values. As explained in the methods, canopy CO_2 storage flux values used for this site were simulated, as provided by the original investigators for this tower site (Malhi et al. 2002). From Figure 3.3 it can be seen that in general, the absolute value of modelled storage tends to be lower than measured. Residuals of measured minus modelled storage fluxes were calculated and are shown in Figure 3.7 against time of day for the period when measurements were available, October-November 1995. Figure 3.7 shows that during the day, between 0900 -1000, modelled storage tends to be lower than that measured (implying a lower total measured N_E and G_P, see equation 3), and in the late afternoon, i.e. 1700-1800, modelled storage tends to be over predicted (implying a higher measured N_E and G_P). Storage fluxes during hours 1100-1600 were better predicted. Therefore this trend of the simulated storage to under and over predict the measurements in the morning and afternoon, respectively, is linked to the model tendency to overestimate early morning net carbon uptake fluxes and underestimate net carbon uptake fluxes in the late afternoon.

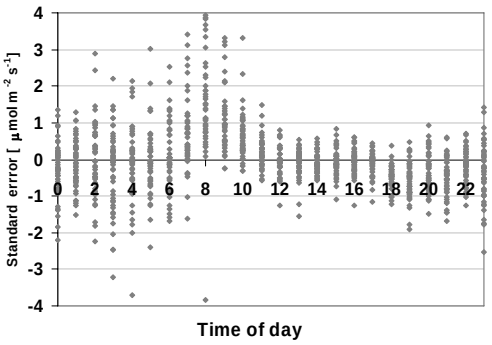

Figure 3.7. Standardised residuals of measured versus modelled storage flux at Man C14 during the period October-November 95.

As the model was initially calibrated on data from the end of the dry season only for this site (Chapter 1) the tendency to overestimate the net carbon uptake fluxes during the dry season was not totally unexpected and could be explained as follows by a variety of phenomena, perhaps acting in concert: 1) decreases in canopy conductance due to low soil water availability, 2) reductions of canopy LAI due to leaf fall and 3) underestimation of the prescribed soil respiration used to calculate G_P from eddy correlation. Hereafter, each possibility is explored.

1) Decreases in canopy conductance due to low soil water availability

Reduced precipitation during the dry season and associated decreases in soil water content have been measured in the area of Manaus (Hodnett et al. 1995; Hodnett et al. 1996). Such low soil water contents could potentially limit canopy gas exchange. However, evidence of water uptake from deep roots below 3.6 m has been found in forests in the same region during the dry season (Hodnett et al. 1995; Hodnett et al. 1996a; Hodnett et al.1996b). Nevertheless, Malhi et al. (1998) and Harris et al. (2004) worked with the same data set used here and suggested stomatal conductance may have been limited by low soil moisture during the period September - November 1995. Results from the energy balance modelling are useful in this respect and are shown in Figure 3.8 and statistics of the comparison are given in Table 3.7. Simulated energy partition is also evaluated using the mean diurnal cycle of evaporative fraction as shown in Figure 3.9 which seems to be relatively well simulated with a slight underestimation (with respect to the observations) during the wet season. Bearing in mind the energy balance closure from the data (Malhi et al. 2002) (See Table 3.7 for closure at each season), latent and sensible heat were indeed generally satisfactory modelled. However, during the dry season there is a clear tendency for the model to underestimate the latent heat flux measurements, λE, at values higher than 400 W m^{-2} (Figure 3.8) and overestimate λE below 400 W m^{-2}. This means that adjusting the model to reduce canopy conductances and hence lower rates of canopy photosynthetic would increase the under prediction of latent heat fluxes above *ca.* 400 W m^{-2}.

Further, using a smaller value of lambda, λ, during the dry season decreases the simulated stomatal conductance, therefore decreasing the simulated C_i/C_a ratio and latent heat fluxes, implying lower simulated evaporative fraction which results in underestimation of the simulated evaporative fraction with respect to the observations. This is shown in Figure 3.10 where the diurnal cycle of evaporative fraction is shown as simulated with λ equal to 970 mol mol^{-1} (as obtained in Chapter 1 and 2 during the end of the dry season),

and an underestimation of the mean evaporative fraction is obtained during the wet and dry seasons. Furthermore, comparison of simulated and measured $\delta^{13}C$ (Table 3.8) shows that the model over predicts the measured values and the over prediction was larger with the simulations performed with λ equal to 970 mol mol^{-1} than with λ equal to 1200 mol mol^{-1}.

In summary, using a lower simulated stomatal conductance did not improve the simulated energy partition during the dry season. However, simulated $\delta^{13}C$ was more overestimated (less negative) with λ equal to 970 mol mol^{-1} than 1200 mol mol^{-1}. Model evaluation of $\delta^{13}C$ suggests that overestimation of simulated net carbon uptake (with respect of the observations) during the dry season was not caused by overestimation of canopy conductance. Furthermore, simulated values of $\delta^{13}C$ were larger (i.e less negative) than the values reported by Ometto et al. (2006) at this site (Table 3.8). The observations suggest a larger C_i/C_a ratio than obtained with the simulations. If the sun/shade model was to predict values of simulated $\delta^{13}C$ of the same order as reported by Ometto et al. (2006), the λ parameter needed to be on the order of 2000 mol mol^{-1} (results not shown). However, simulations with such a λ result in overestimation of evaporative fraction (results not shown) with minor increases in simulated net carbon uptake.

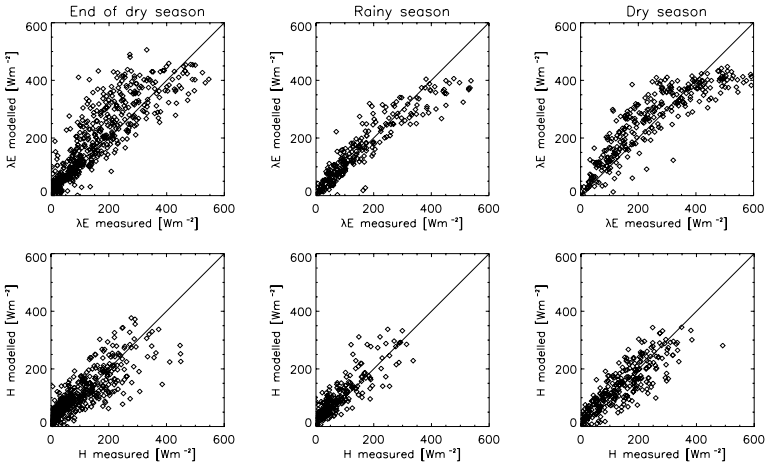

Figure 3.8. Modelled and measured latent and sensible heat fluxes at Manaus C14.

Table 3.7. Statistics of model-data comparison for energy fluxes during the seasons tested and energy balance closure of the measurements.

Season	λE^*			H*			R_n *vs* $(\lambda E$ + H$)^{**}$		
	a	r^2	RMSE	a	r^2	RMSE	a	r^2	RMSE
End of dry 1995	1.08	0.89	75.5	0.9	0.83	52.5	0.89	0.91	94.09
Rain 1996	0.91	0.95	46.5	1.06	0.87	44.8	0.93	0.96	67.3
Dry 1996	0.95	0.94	71.16	0.93	0.9	47.8	1.04	0.95	95.93

* The regression model is modelled flux= a × measured flux

** The regression model is measured $(\lambda E + H)$ = a × measured R_n

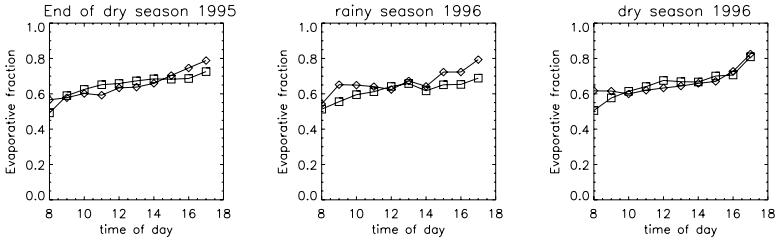

Figure 3.9. Man C14 Mean diurnal cycle of measured (◊) and simulated (□) evaporative fraction simulated with λ=1200 mol mol^{-1}.

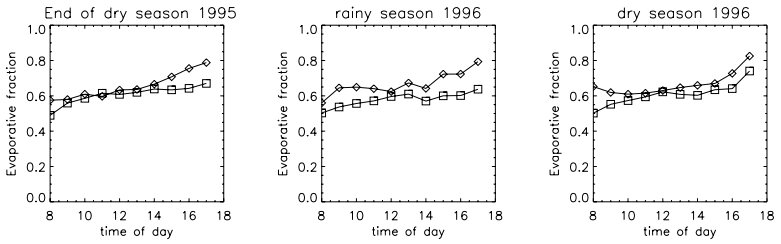

Figure 3.10. Man C14 Mean diurnal cycle of measured (◊) and simulated (□) evaporative fraction simulated with λ=970 mol mol^{-1}.

Table 3.8. Simulated and measured carbon isotopic ratios at Man C14**.**

	δ^{13}C (‰)
Measured (Ometto et al. 2006)	-32 ± 3.0
Simulated with λ=1200 mol mol^{-1}	
End of dry season 1995	-26.95
Rainy season 1996	-25.49
Dry season 1996	-24.56
Simulated with λ=970 mol mol^{-1}	
End of dry season 1995	-24.9
Rainy season 1996	-23.3
Dry season 1996	-22.5

2) Possible reductions of canopy LAI due to leaf fall

A large increase in litterfall at the onset of the dry season has been well documented for the Manaus region (Klinge 1968; Luizao and Schubart 1987). If this increase in litterfall is caused by a decrease in LAI, forest photosynthetic carbon uptake during the dry season may decrease. To test this possibility, a model run for the dry season was undertaken assuming a 20% decrease in total LAI i.e. 20% of leaves from all over the canopy were lost (Nepstad et al. 2002; Asner et al. 2004). Even in this case, modelled G_P still overestimates the data (results not shown).

3) Low values of prescribed soil respiration rate used to calculate GP from eddy correlation

There might be a data mismatch because the soil respiration data of Chambers et al. (2004) used to derive G_P from N_E came from a study undertaken at a different time period to the eddy correlation flux measurements. The soil respiration measurements were taken during a strong *La Niña* period (June 2000-June 2001) during which the Central Amazon received some of its highest precipitation of the 20th century (Chambers et al. 2004). Comparison of soil respiration reported in the study of Chambers et al. (2004) to other studies recently performed near Manaus reveal the Chambers et al. (2004) values of 3.2 μmol m^2 s^{-1} were the lowest

in the reported range. Soil respiration measurements from Sotta et al. (2004) around the Man C14 site during the end of wet and beginning of dry season in 1997 averaged 6.4 μmol m^2 s^{-1}. Araújo A. (pers. comm.) recently measured soil respiration in a plateau forest around the K34 site (rainy season of 2005) with an average value of 5.1 μmol m^{-2} s^{-1}, and Carmo et al. (2006) measured CO_2 fluxes from the soil at the C14 site during 2004 and obtained 5.4 ± 1.4 and 5.5 ± 1.1 μmol m^{-2} s^{-1} during the wet and dry seasons respectively. On the other hand, Chambers et al. (2004) reported only an average of 2.6 μmol m^2 s^{-1} for soil respiration during the dry season months of his measurements at the Man K34 site in plateau area. However, this comparison is undertaken using different precipitation patterns each year and this shows the important dependency of soil respiration on soil moisture. For instance, Sotta et al. (2004) has shown that soil water plays an important role in regulating the CO_2 efflux from the soil especially in dry periods during and soon after precipitation events. Davidson (2000) reports optimum conditions for soil respiration at intermediate water contents with decreases in respiration at water content both above and below the optimum. Furthermore, different techniques of measurements could also explain some of the differences in measured soil respiration rates (Sotta et al. 2004). Other studies that measured soil respiration at different sites in the Amazon are reported in Table 3.9. Values reported by Chambers et al. (2004) clearly fall in the lower range of the reported measurements in Table 3.9.

Table 3.9. Mean value of soil CO_2 flux and methodologies used in other studies done in the Amazon region (Modified from Sotta et al. (2004)).

Source	Place	Mean μmol CO_2 m^{-2} s^{-1}	Methodology
Coutinho and Lamberti (1971)	Barcelos, AM, Brasil	2.8	KOH 0,5 N Solution
Martins an Matthes (1978)	Manaus, AM, Brasil	1.4±0.5	KOH 0,5 N Solution
Medina (1980)	San Carlos, Venezuela	3.1±0.5	KOH 0,5 N Solution
Wofsy et al. (1988)	Reserva Ducke, Manaus	4.5	
Fan et al. (1990)	Reserva Ducke, Manaus	5.9	IRGA-dynamic[1]
Trumbore et al. (1995)	Paragominas, PA, Brasil	6.1	IRGA- dynamic chamber[1]
Meir (1996)	Reserva Jarú, RO, Brasil	5.5±1.6	IRGA- dynamic chamber[1]
Sotta et al. (2004)	Manaus, AM, Brasil	6.4±0.25	IRGA- dynamic chamber[2]
Chambers et al. (2004)	Manaus, AM, Brasil	3.2	IRGA- dynamic chamber[1]
Silva de Souza (2004)	Manaus, AM, Brasil	5,76	IRGA- dynamic chamber[1]
Carmo et al. (2006)	Manaus, AM, Brasil	5.4±1.4 wet 5.5±1.1dry	IRGA- dynamic chamber[2]
Salimon (2004)	Rio Branco,Acre	3.9	IRGA- dynamic chamber[1]
Davidson et al. (2004)	Tapajos, Santarem	2.64	Dynamic chamber
Davidson et al. (2000)	Paragominas, Para	5.3	IRGA, dynamic[1]
Sotta et al. (2006)	Caxiuana	3.9±0.1 (dry and wet)	Closed dynamic system
Carmo et al. (2006)	Caxiuana	6.1±1.4 wet 5.1±1.5dry	IRGA- dynamic chamber[2]
Keller et al. (2004)	km 67 Tapajos	3.2± 0.4 wet 2.3± dry	Autochamber

[1] closed system; [2] open system

In summary, because of the dependency of soil respiration on soil water content and given the interannual variability of rainfall and the fact the Chambers et al. (2004) reported values for soil respiration are much lower than what has been recently found for the Manaus area, it is likely that the described soil respiration term is low. This contributes to a low estimate for the observed G_P which can explain the apparent overestimation of G_P by the sun and shade model. Values of soil respiration used in this study are shown in Figure 3A-7. Notice that soil respiration values are especially low during the dry season months and highest during the end of the dry season which is the season for which best results were obtained in terms of carbon uptake (presented in Chapter 1 and in this chapter).

In conclusion, underestimation of the prescribed soil respiration term is the most likely explanation for the model to overestimate the observed G_P during the dry season.

In order to help resolve the issue, measured CO_2 fluxes i.e. F_c in equation 3, measured N_E and G_P (estimated from eddy correlation as $G_P = -N_E + R_S + R_W + R_{CS}$) were grouped and averaged over 200 μmol quanta m^{-2} s^{-1} bins for the three different seasons (Figure 3.11). From the light response of measured mean values of F_c, N_E and G_P at the different seasons, it was found that the light response of the measured G_P did not follow the same seasonal pattern as the light response of the measured F_c (CO_2 flux) and N_E. From the light response of both F_c and N_E, it can be observed that the initial slope was almost the same for the three seasons, although it was slightly higher during the wet season. In contrast, from the light response of the measured G_P, taking the period near the end of dry season as reference (season with best results), it can be seen that the initial slope during the dry season is slightly lower than the slope during the end of the dry season. Also the initial slope during the wet season almost matches the end of dry season data. The observed seasonal variation in slopes of the light response measured between N_E and G_P is due to differences in ecosystem respiration, most likely due to the soil respiration term. If the estimated G_P (from eddy correlation N_E and ecosystem respiration) was to have the same seasonal pattern as observed in F_c and N_E fluxes, the ecosystem respiration term would need to be adjusted. Given the above reasons and taking into account the reported soil respiration values at the Manaus area, the soil respiration term was adjusted (increased) within the reported range of variation of soil respiration measurements (Table 3.9) to obtain for G_P the same seasonal patterns as observed for F_c and N_E fluxes (See Figure 3.11 for corrected G_P). Figure 3A-7 includes the Chambers et al. (2004) estimates and the respiration values used. Comparison of modelled versus observations was repeated with the new higher soil respiration (See Figure 3.12 for light response of corrected G_P and Figures 3A-5-6 for residuals). Using this higher soil respiration rate parameterisation, residuals and goodness of fit did not change during the wet season but improved for the dry season (the slope of the 1:1 line, modelled G_P versus observations, reduced from 1.11 to 1.06 with r^2 unchanged and with a p-value equal zero in both cases). Residuals during the dry season improved but still showed a bias towards an overestimation of simulated net carbon uptake with respect to observations. A sensitivity run assuming a 20% decrease in LAI, consistent with the observed increase in leaf fall, was performed but had little effect on results (obtained slope of the linear regression of modelled G_P versus observations, equal to 1.04 with r^2 remaining unchanged as reported in Table 3.6 and p-value equal to zero). Unless soil respiration or total ecosystem respiration would have been even higher than considered for this site or LAI even lower that considered (20% lower) there was no other obvious explanation for the dry season overestimation of net carbon uptake fluxes relative to the observations.

Summary

Using the parameterisation given in Table 3.5 the sun/shade model could reasonably well simulate the end of dry season net carbon uptake. Simulated net carbon uptake during the wet and the dry season of 1996 was overestimated, with respect to the measurements, especially during the dry season. It is concluded that the low value of prescribed soil respiration could account for model-data discrepancies. Soil respiration was adjusted (increased within the range of reported measured values) under the assumption that measurements of F_c, N_E and G_P should follow the same seasonal pattern as explained in Figure 3.11. Further, residuals of net carbon uptake had a biased trend with time of day at all seasons tested. This was associated with the storage fluxes used for calculation of N_E. Simulated storage fluxes had a tendency to under- and over-predict the measurements in the morning and afternoon respectively, implying low and high estimates of measured N_E (equation 3), respectively. This resulted in a model tendency to overestimate early morning, and underestimate afternoon, net carbon uptake fluxes. Measured values of $\delta^{13}C$ could only be explained by the model using a higher λ than 1200 mol mol^{-1}. However, using a higher λ, simulated λE increases, consequently increasing the simulated evaporative fraction, which would lead to an over prediction of energy partition (not shown).

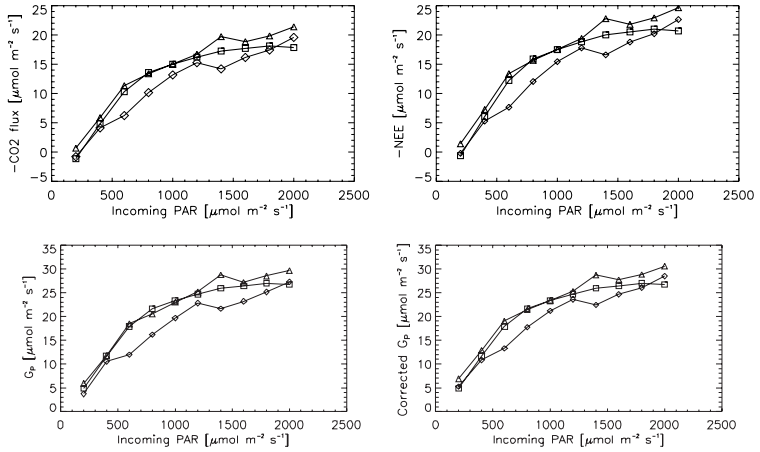

Figure 3.11. Man C14. Light responses of measured CO_2, $-N_E$ and G_P ($-N_E + R_{E\_NL}$) during dry, wet and end of dry season for the Man C14 site. ∇ Wet, ◊ Dry, □ End of dry. Corrected G_P was corrected for soil respiration.

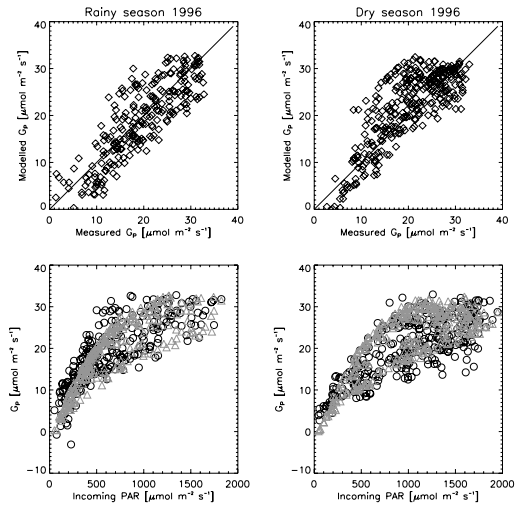

Figure 3.12. Comparison of modelled (Δ) net uptake versus data (o) using with higher soil respiration at Man C14.

3.3.2 Man K34

The initial model evaluation was made using leaf N from the RAINFOR Consortium (unpublished data) to calculate top of the canopy V_{max} (equal to 28.9 μmol m^{-2} s^{-1}) and the rest of parameters were taken as for Man C14 from Chapter 1. Qualitative evaluation of this simulated net carbon uptake was initially undertaken by comparing the light response of simulated and data derived estimates of G_P as shown in Figure 3.13. There were two major differences between simulated and estimated G_P from eddy correlation: first, maximum measured assimilation is underestimated by the model and second, the initial linear increase in measured G_P with PAR is overestimated by the model.

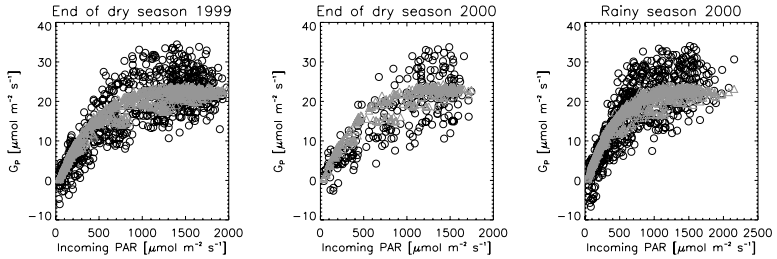

Figure 3.13. Man K34. Light response of modelled (Δ) and measured (o) G_P (i.e. net photosynthetic uptake) using soil respiration measurements from Chambers et al (2004). Initial model parameterisation using V_{max} at the top of the canopy was 28.9 μmol m^{-2} s^{-1} and Φ =0.4.

A sensitivity study was conducted for a single season to find out under which parameterisation the simulated carbon uptake would best fit the observations. The sensitivity study was carried out on V_{max}, the curvature factor θ and the quantum yield, Φ, (Equation 6 in Chapter 1). These parameters were chosen because of their role in the shape of the light response curve of photosynthesis. This was undertaken under the assumption that the parameters for temperature sensitivity of J_{max}, the J_{max} / V_{max} ratio and leaf respiration had adequate parameterisation.

Firstly, sensitivity tests were undertaken varying θ, keeping Φ equal to 0.5 as Carswell et al. (2000) and Vale et al. (2003) used for their leaf level parameterisations. A set of simulations were performed using the following parameterisations:

Top of the canopy V_{max} calculated with leaf N from the RAINFOR Consortium (unpublished data) (V_{max}= 28.9 μmol m^{-2} s^{-1}) with θ varying from 0.1 to 1 (Figure 3.14).

Top of the canopy V_{max} parameterised using leaf N plus one standard deviation (of leaf N) from the RAINFOR Consortium (unpublished data) (V_{max}= 40.5 μmol m^{-2} s^{-1}) with θ varying from 0.1 to 1 (Figure 3.15). According to the V_{max} - leaf N relationship used in this study, this value of V_{max} is equivalent to a foliar N content of 3.2 g m^{-2} which is 30% higher than the mean leaf N value (2.2 g m^{-2} from 19 trees) from the RAINFOR Consortium (unpublished data) for Man K34 plateau.

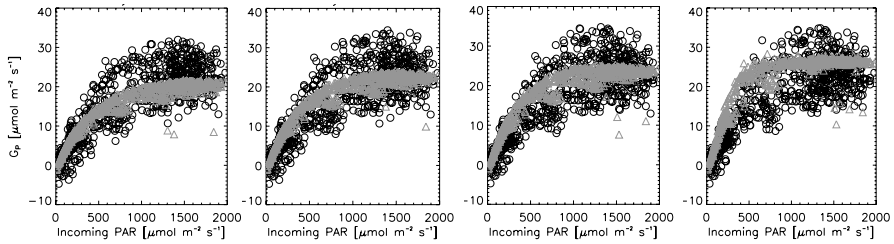

Figure 3.14. Sensitivity of simulated G_P (Δ) (observed (o)) to different curvature factors θ of the electron transport function (θ from left to right is 0.1, 0.5, 0.7 and 1.) with $\Phi = 0.5$ and top of the canopy V_{max}= 28.9 μmol m^{-2} s^{-1}) at Man K34 during the end of the dry season 1999.

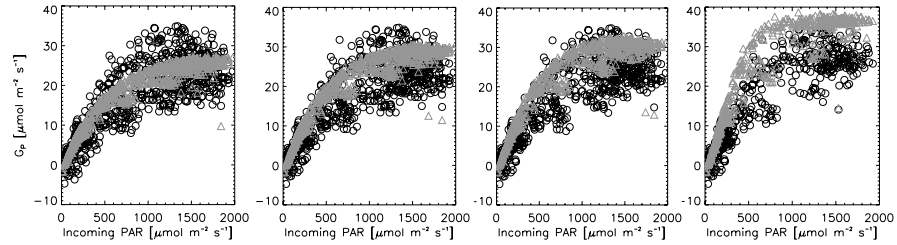

Figure 3.15. Sensitivity of simulated G_P to G_P (Δ) (observed (o)) to different curvature factors θ of the electron transport function (from left to right 0.1, 0.5, 0.7 and 1.) with $\Phi = 0.5$ and top of the canopy V_{max}= 40.5 μmol m^{-2} s^{-1}) at Man K34 during the end of the dry season 1999.

From the sensitivity analysis presented in Figure 3.14 it is concluded that by varying the curvature factor θ of the light response of photosynthesis to any value within its range, the simulated G_P cannot explain the variability found in the observations. With values of θ = 0.1 (first column) the model can simulate relatively well G_P in the range [0-500] μmol m^{-2} s^{-1} quanta PAR with G_P underestimated by the model at higher irradiance. With θ greater than 0.1, the model tends to overestimate the observations in the region of linear increase of G_P with light. Furthermore, using a higher V_{max} (Figure 3.15) and $\theta = 0.1$ results in better agreement with the observations. Again, using values of θ greater than 0.1 and a higher V_{max} (Figure 3.15), simulated G_P overestimated the observations at all irradiances. In conclusion, the sensitivity analysis presented in Figures 3.14 and 3.15 shows that using a very low value of θ (approximately 0.1 or lower) could fit the observations at PAR values between 0-500 μmol m^{-2} s^{-1} quanta PAR. Also using a higher V_{max} than initially parameterised, which was based on leaf N from the RAINFOR Consortium (unpublished data), the model was also in better agreement with the observations at higher irradiance values [500-2000 μmol m^{-2} s^{-1} quanta PAR]. However this value of θ is very low, compared with θ values reported in the literature (0.7-0.95), when fitting leaf gas exchange measurements to the Farquhar and von Caemmerer (Farquhar et al. 1980; 1982) C_3 photosynthesis model (Carswell et al. 2000; Collatz et al. 1990a; Leuning 1990).

Secondly, sensitivity tests were carried out varying Φ keeping θ fixed at 0.7 as Carswell et al. (2000) and Vale et al. (2003) used in their leaf level parameterisations. The following simulations were undertaken.
Top of the canopy V_{max} calculated with leaf N from the RAINFOR Consortium (unpublished data) (V_{max}= 28.9 μmol m^{-2} s^{-1}) with Φ varying from 0.5 to 0.2 (Figure 3.16).
Top of the canopy V_{max} parameterised in this study (i.e. with leaf N plus one standard deviation from the RAINFOR Consortium (unpublished data), V_{max}= 40.5 μmol m^{-2} s^{-1}) with Φ varying from 0.5 to 0.2 (Figure 3.17).

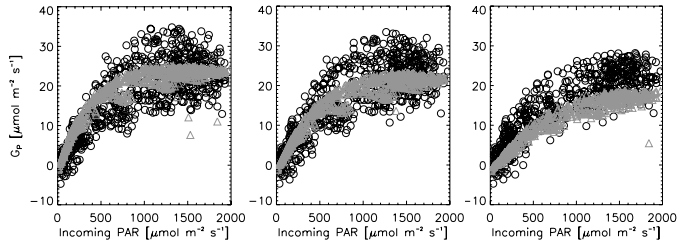

Figure 3.16. Sensitivity of simulated G_P to G_P (Δ) (observed (o)) to various quantum yield Φ (from left to right 0.5, 0.35 and 0.2) with θ=0.7 and top of the canopy V_{max}= 28.9 μmol m^{-2} s^{-1}) at Man K34 during the end of the dry season 1999.

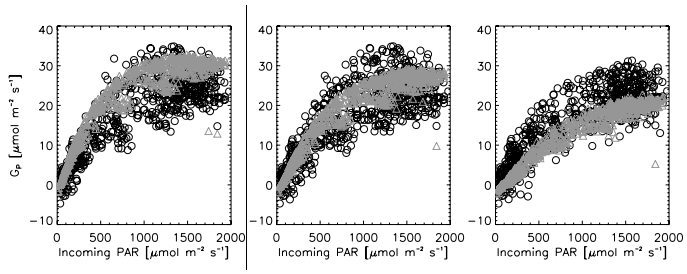

Figure 3.17. Sensitivity of simulated G_P to G_P (Δ) (observed (o)) to various quantum yields Φ (from left to right 0.5, 0.35and 0.2) with θ=0.7 and top of the canopy V_{max}= 40.5 μmol m^{-2} s^{-1}) at Man K34 during the end of the dry season 1999.

From the sensitivity analysis presented in Figure 3.16 it is concluded that simulated G_P can not explain the variability found in the observations when only the quantum yield parameter, Φ, is varied. With values of Φ=0.5 (first column) the model overestimates observations in the region of linear increase in G_P with light. Also maximum G_P values are underestimated by the model. With $\Phi = 0.35$, the model-data comparison improves in the region of the linear increase of G_P with light. However, at the same time the model-data comparison in the region of light saturation of photosynthesis is poor with simulated G_P values underestimated with respect to the observations. With $\Phi = 0.2$, the model underestimates the observations of G_P in all cases. Furthermore, using a higher V_{max} (Figure 3.17), maximum simulated G_P is higher than in simulations presented in Figure 3.16. Simulated G_P over and underestimates the data in runs with quantum yield values of 0.5 and 0.2, respectively (Figure 3.17, plots on the right and on the left). The model is close to observations when a quantum yield of 0.35 is chosen.

From this exercise it is concluded that in order to fit better the observations it is necessary to vary two parameters. V_{max} needs to be larger than initially parameterised based on leaf N from the RAINFOR Consortium (unpublished data), using a V_{max} versus leaf N relationship inferred from the Carswell et al. (2000) and Vale et al. (2003) data sets. Also it is necessary to vary either θ (using a very low value compared that reported in the literature) or to use a lower value of Φ than adopted by Carswell et al. (2000). Furthermore, other studies using leaf level gas exchange measurements used different values for Φ and θ to those used in this study and in Carswell et al. (2000) and Vale et al. (2003), when fitting to the C_3 photosynthesis model of Farquhar and von Caemmerer (1982). The study of Leuning (1990) fitted Φ, J_{max} and V_{max} and two parameters from their stomatal conductance model using a fixed curvature factor θ of 0.95 (cf. 0.7 in Carswell et al. 2000 and in this study), obtaining fitted leaf level Φ varying from 0.14 to 0.16. According to Leuning (1990), variation in Φ has little physiological meaning due to the interaction between

Φ and θ that occurs during the non-linear curve fitting procedure. According to Collatz et al. (1990a), the curvature parameter θ has no mechanistic basis and must be chosen empirically with θ estimated from experimental responses, yielding values of θ in the range 0.8 - 0.99. Additionally, θ can be viewed as an indicator of the extent to which sequential steps co-limit photosynthesis with θ close to 1 indicating the extent to which co-limitation is minimized. From the two options given above and given that other modelling and measuring studies use quantum yield values on the order of 0.14 to 0.29 (Domingues et al. 2005; Ehleringer and Bjorkman 1977; Leuning 1990; Long et al. 1993), we decided to parameterise the model using a V_{max} = 40.5 μmol m^{-2} s^{-1} and Φ= 0.35 (the Man C14 site was simulated with a Φ of 0.4) leaving θ constant and equal to 0.7. This approach of adjusting V_{max} and Φ to better fit the observations is adopted at the other sites where necessary.

Light responses and 1:1 lines of modelled G_P versus observations for the Man K34 site are shown in Figure 3.18. Statistics of the model-data comparison are given in Table 3.10. According to the comparison shown in Figure 3.18, the sun/shade model slightly overestimated the data (by ~10%) during the end of the dry (2000) period, but provided a good fit for the end of dry season period of 1999 and rainy season of 2000. The corresponding residual of estimated G_P ($-N_E + R_E$) minus simulated G_P against different variables are shown in Figures 3A-8-10. Residual responses of net carbon uptake to the fraction of diffuse irradiance (F_d), PAR, C_a and time of day showed no model bias during the three periods. Responses to VPD and air temperature showed a strong tendency for the sun/shade model to overestimate fluxes at the highest VPD and temperatures and again to overestimate the net carbon uptake observations during the end of the dry period of 2000.

Table 3.10. Statistics of model-data comparison for G_P* during the seasons tested at Man K34.

Season	A	r^2	RMSE**
End of dry 1999	1.05	0.96	4.36
End of dry 2000	1.09	0.96	4.47
Rain 2000	0.98	0.95	4.36

* The regression model is modelled flux= a × measured (or estimated from eddy correlation) flux
** Root mean square error

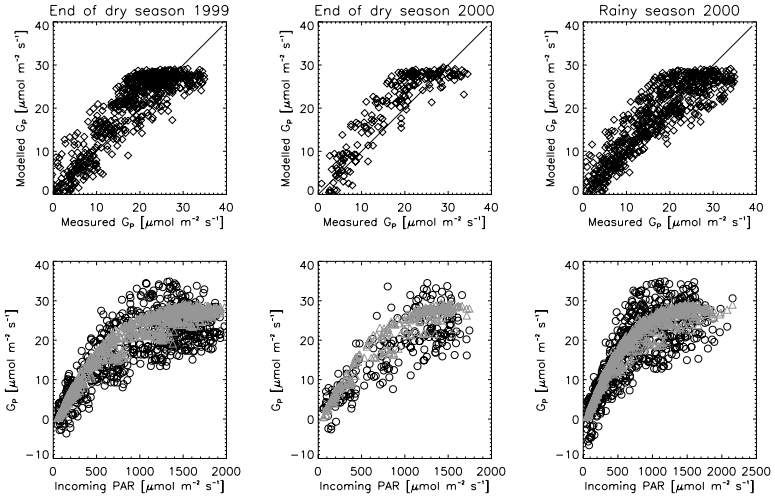

Figure 3.18. Man K34. Light response of modelled (Δ) and measured (o) G_P (i.e. net photosynthetic uptake) and 1:1 line of modelled against observed G_P using soil respiration measurements from Chambers et al. (2004). Model was re-parameterised using V_{max} at the top of the canopy of 40.5 μmol m^{-2} s^{-1} and Φ=0.35.

To investigate the reasons for the strong model bias towards overestimation at high VPD and high air temperatures, residuals of latent heat flux and residuals of net radiation were examined as a function of air temperature, VPD and time of day (Figures 3A-11-12). There is indeed a very strong tendency to overestimate estimated latent heat and measured net radiation at high VPD and high air temperatures, and this seems to be linked to time of day (i.e. late afternoon). On the contrary, underestimation tends to occur during the early morning under low VPD and lower air temperatures.

The model bias towards overestimating carbon, net radiation and latent heat fluxes at high VPD and air temperatures may be linked to a low sensitivity of the stomatal conductance model to high VPD. Sensitivity of the model was tested using different lambda values (results not shown). Nevertheless, the bias towards high VPD and high temperatures persisted.

Comparison of simulated and measured mean diurnal cycle of evaporative fraction (Figure 3.19), shows that the sun/shade model tends to overestimate latent heat during the late afternoon (1500, 1600, 1700) but slightly underestimates latent heat fluxes during the early morning (0900-1000) during the end of the dry season of 1999 and 2000, with these trends being more pronounced during the rainy season of 2000. This result was already shown in Figures 3A-11-12 and it is probably linked to a model tendency to over predict carbon and latent heat fluxes at high VPD. Furthermore, during the rainy season of 2000 the model tends to underestimate latent and overestimate sensible heat fluxes at all times of day. At the same time, from the model data comparison to G_P (Figure 3.18 and Table 3.10), it seems that the sun/shade model performed satisfactorily during all seasons with a 9% overestimation at the end of the dry season of 2000. In order to understand where the problem lies, the carbon isotopic ratio $\delta^{13}C$ was calculated for each season (Table 3.11) and compared to $\delta^{13}C$ values recently published for this site (Ometto et al. 2006).

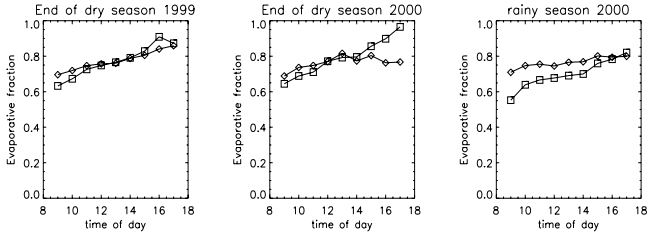

Figure 3.19. Man K34 Mean diurnal cycle of measured (◊) and simulated (□) evaporative fraction.

Table 3.11. Simulated and measured carbon isotopic ratio at Man K34**.**

	$\delta^{13}C$ (‰)
Measured (Ometto et al. 2006)	-32.6 ±2 .7
Simulated with λ=2000 mol mol^{-1}	
End of dry season 1999	-29.1
End of dry season 2000	-28.63
Rainy season 2000	-30.39

According to Ometto et al. (2006) $\delta^{13}C$ at the top of the canopy varies within a range of [-30 and -35 ‰] with a mean value of -32.6 ± 2.7 (‰) from leaves collected at all heights, implying the sun and shade

simulations are probably satisfactory in terms of modelled carbon exchange during all seasons.

A sensitivity test showed that the model fit to evaporative fraction during the rainy season of 2000 can improve by artificially increasing the λ parameter from 2000 to 3000 mol mol^{-1}. However, increasing λ to 3000 mol mol^{-1} changes the partition between latent and sensible heat (increasing λE), improving the model comparison to evaporative fraction but at the cost of a decrease in the simulated δ^{13}C (more negative) which leads to model underestimation of δ^{13}C with respect to the measurements (results not shown).

Summary

For this site, two parameters were adjusted in order to better fit the observations: V_{max} at the top of the canopy (which consequently increased the total canopy V_{max}) and the canopy level quantum yield. Net carbon uptake was reasonable well simulated for all sites, a finding supported by the simulated δ^{13}C. Energy partition was reasonably well simulated in all seasons with the exception of the rainy season of 2000 where the model under predicted measured evaporative fraction. The model has a bias towards overestimation of carbon, net radiation and latent heat fluxes at high VPD and air temperatures. This problem could be linked to the stomatal conductance model used not being sufficiently sensitive to high VPD.

Soil respiration for this site was parameterised using Chambers et al. (2004) reported values from the wet and end of wet season periods. These values are lower than reported by other studies undertaken around the same area, and hence it is possible that soil respiration and therefore ecosystem respiration could have been higher than considered here. This would imply higher estimated G_P from the observations, which would favour the model-data comparison.

3.3.3 Jaru

Initial parameterisation of V_{max} for the top canopy leaves was undertaken using leaf N from top canopy leaves as reported by Meir et al. (2001) (calculated value of V_{max} equal to 36.2 μmol m^{-2} s^{-1}) with canopy level quantum yield, Φ of 0.4. The light response of simulated and observed G_P under this parameterisation is shown in Figure 3.20 for 1999 and 2000. From this qualitative evaluation it is concluded that the maximum rate of carbon assimilation is underestimated by the model but also the initial slope of the linear increase in photosynthesis with light seems to be overestimated by the model. As with Man K34, to improve the model-data comparison, two parameters were adjusted. V_{max} from top of the canopy and the canopy level quantum yield, Φ were empirically adjusted to provide a better fit to the observations. V_{max} for the top leaves was taken as 47 μmol m^{-2} s^{-1} (Table 3.4), corresponding to a leaf N content of 3.7 g m^{-2}, which is 30% higher than initially parameterised, as reported by Meir et al. (2001) for leaves located between 30-35 m and quantum yield was taken as 0.35. The remaining parameters were the same as for Man C14 in Chapter 1.

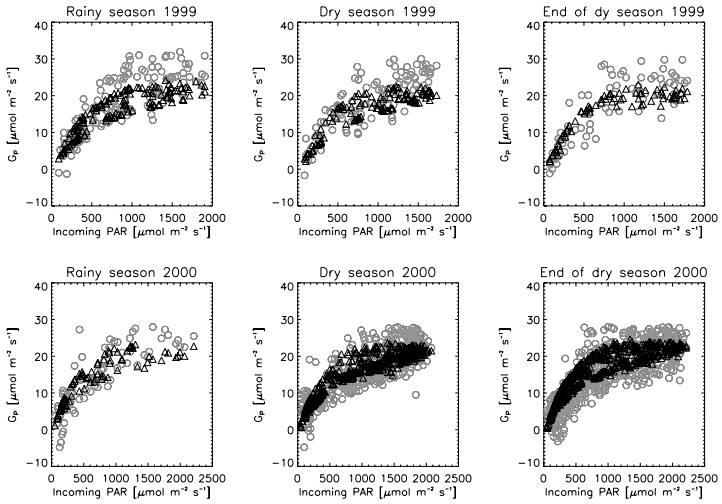

Figure 3.20. Jaru. Light response of modelled (Δ) and measured (o) G_P (i.e. net photosynthetic uptake). Initial model parameterisation using V_{max} at the top of the canopy was 36.2 μmol m^{-2} s^{-1} and Φ=0.4.

Observed and simulated G_P are shown in Figure 3.21 and Figure 3.22 for 1999 and 2000, respectively and statistics of the model data comparison are found in Table 3.12. There is less data for 1999 but it is clear the sun/shade model fits relatively well the data for 1999 up to values of 28-30 μmol m^{-2} s^{-1} after which the maximum modelled uptake tended to be lower than observed. Using the same parameterisations for 1999 and 2000 simulated G_P tended to be higher (Table 3.12) than observed during the dry and end of dry seasons of 2000. However, estimated G_P from eddy correlation measurements of N_E and estimated ecosystem respiration were lower during 2000 than during 1999.

Table 3.12. Statistics of model-data comparison to G_P evaluated at Jaru during 1999 and 2000.

Season	a	r^2	RMSE**
Rain 1999 (all data)	0.91	0.98	2.82
Dry 1999 (all data)	0.92	0.97	3.31
End of dry 1999 (all data)	0.91	0.96	2.87
Rain 1999 (only observed G_P <28 μmol m^{-2} s^{-1})	**0.95**	**0.98**	**2.83**
Dry 1999 (only observed G_P <28 μmol m^{-2} s^{-1})	**0.95**	**0.97**	**3.16**
End of dry 1999 (only observed G_P <28 μmol m^{-2} s^{-1})	**0.95**	**0.97**	**3.16**
Rain 2000 (all data)	0.91	0.95	4.35
Dry 2000 (all data)	1.04	0.95	3.87
End of dry 2000 (all data)	1.01	0.95	4.35
Rain 2000 (only observed G_P <28 μmol m^{-2} s^{-1})	**0.98**	**0.95**	**3.6**
Dry 2000 (only observed G_P <28 μmol m^{-2} s^{-1})	**1.08**	**0.96**	**3.6**
End of dry 2000 (only observed G_P <28 μmol m^{-2} s^{-1})	**1.09**	**0.96**	**3.9**

* The regression model is modelled flux= a × measured (or estimated from eddy correlation) flux
** Root mean square error

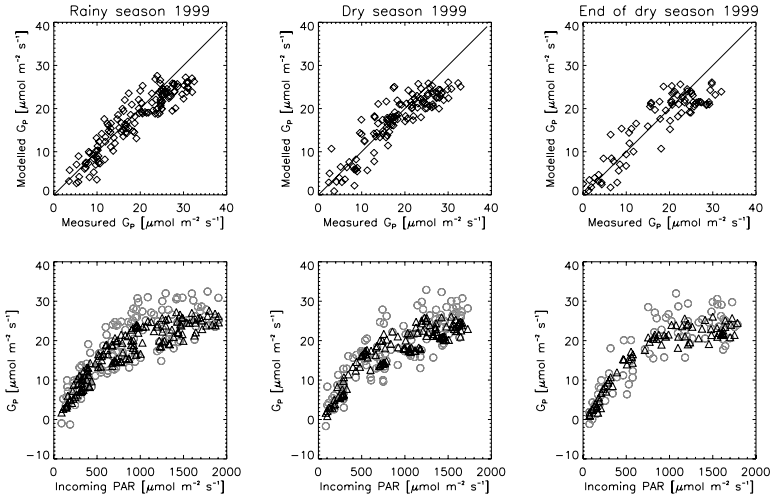

Figure 3.21. Jaru 1999. Light response of modelled (Δ) and measured (o) G_P (based on observations and estimations of ecosystem respiration and net carbon uptake) and 1:1 line of simulated versus observed G_P.

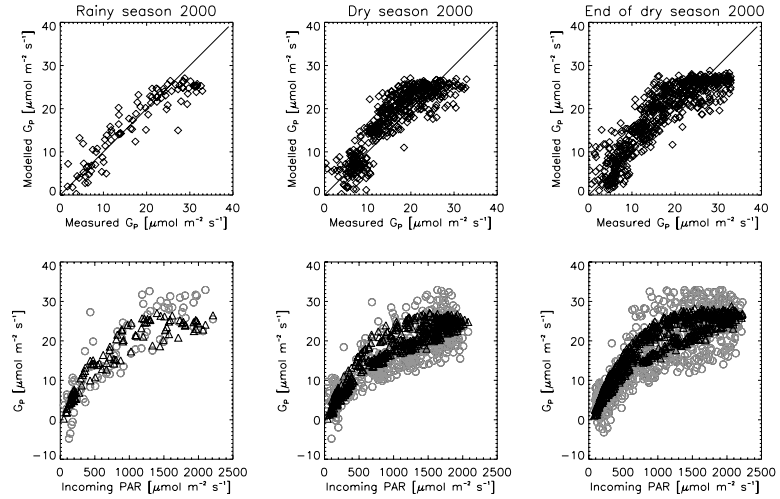

Figure 3.22. Jaru 2000. Light response of modelled (Δ) and measured (o) G_P from ($-N_E + R_E$) and 1:1 line of simulated versus observed G_P.

Nevertheless canopy CO_2 storage flux data during 2000 is from a model (von Randow et al. 2004), and when compared to storage measured at Jaru during 1999 (See Figure 3.3), it can be seen that the absolute value of modelled storage during 2000 tended to be lower than the measurements. In addition to the lower storage flux used during year 2000 there are few other explanations for the lower 'observed' G_P during this year. Figure 3.23 gives a summary of meteorology (VPD and air temperature), observed (CO_2, N_E, G_P, and R_E) and simulated fluxes (G_P) averaged over 200 μmol quanta m^{-2} s^{-1} bins for each season in both years. Estimated G_P during the dry and end of dry season in year 2000 was lower than in 1999. This is because the CO_2 and N_E fluxes during these seasons appear to be lower than during 1999, likely due to the higher VPD during 2000. Even though CO_2 and N_E appear to have been smaller during 2000, which already reduced estimated G_P, ecosystem respiration during 2000 may be underestimated. Ecosystem respiration at this site was estimated using soil respiration that was assumed diurnally and seasonally invariant, as there is little indication of seasonal differences in efflux rates from rainforest soil at Jaru and near constant soil temperatures following Meir (1996) and Lloyd et al. (1995). According to results presented for 1999 a constant soil respiration

seemed adequate in this respect. But rainfall during 2000 was generally greater than during 1999 (see Figure 3A-15) and the profile of soil water content in top soil layers was slightly lower during 1999 than during 2000 (Figure 5 in von Randow et al. (2004)). One can speculate that soil respiration may have been slightly higher during 2000. Also, trunk respiration was taken as 0.75 μmol m^2 s^{-1} (Meir and Grace 2002) with canopy temperatures (from shaded leaves) driving canopy respiration. Since air temperatures were slightly lower in 2000 at PAR values below 1000 μmol m^2 s^{-1} (See Figure 3.23 for temperature versus irradiance), modelled ecosystem respiration was slightly lower at these irradiances during year 2000.

Since precipitation was higher in 2000 than 1999 (see Figure 3A-15) and no effects of soil moisture deficit on canopy gas-exchange were readily apparent in either year (von Randow et al. 2004), it seems unlikely that modelled fluxes overestimate data during 2000 due to an overestimation of canopy conductance due to soil moisture stress. In another modelling approach, Lloyd et al. (1995) used eddy correlation flux data for the same site during dry and wet seasons of 1992 and 1993 and also found no indication of soil moisture deficits on canopy carbon uptake once the VPD effects had been taken into account. von Randow et al. (2004) measured the soil moisture profile down to 3.4 m for the period February 1999 – September 2002 and found indications of water extraction from deep layers, especially during the dry season due to root uptake (to supply transpiration) and lateral drainage.

JARU 1999

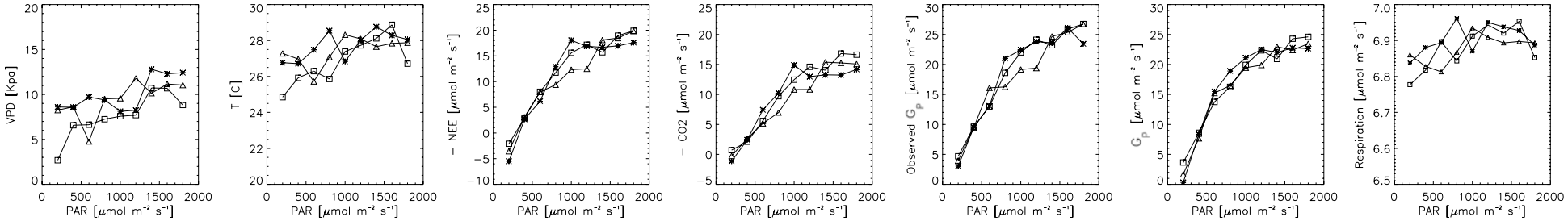

JARU 2000

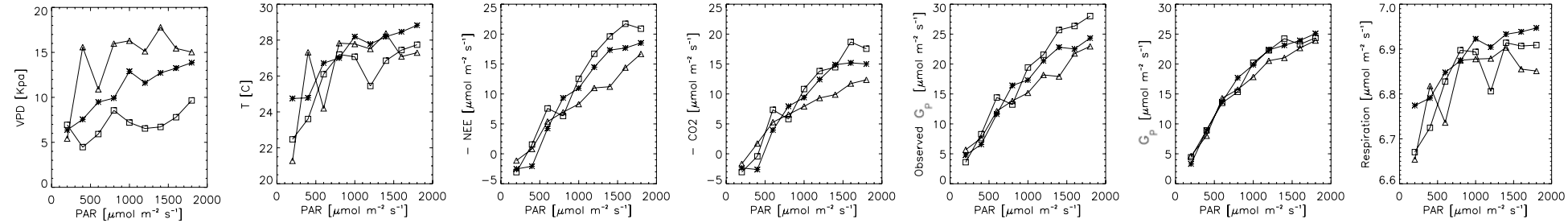

Figure 3.23. Average VPD, air temperature, $-N_E$, CO_2, observed and simulated G_P and ecosystem respiration (R_E) at different irradiance classes during 1999 and 2000. Dry season (▽), End of dry (∗), and rainy season (□).

There are minor differences in simulated G_P between 1999 and 2000 despite a higher VPD in both dry and end of dry season of 2000. This again shows low sensitivity of simulated G_P to changes in VPD.

Residual plots of measured minus simulated G_P to meteorology and time of day for 1999 and 2000 are shown in Figures 3A-16-18 for the rainy, dry and end of dry seasons for 1999 and Figures 3A-19-21 for 2000. As is the case for Man K34, residual responses to VPD and air temperature during dry and end of dry season of 2000 showed a bias, tending to overestimate at high VPD (usually higher than 20 kPa) and associated higher air temperatures. This effect was neither apparent in 1999 nor during the rainy season of 2000. However, the amount of data available for these periods was relatively small. Residuals of simulated and 'observed' latent heat (λE calculated as the difference between measured net radiation and sensible heat flux) and also residuals of net radiation (measured minus observed) showed a VPD bias as well. Again this probably represents a low sensitivity of the stomatal conductance model to high VPD (See Figures 3A-22-25).

Bearing in mind the energy balance closure at this site was only 63 and 65 % for data from 1999 and 2000 respectively, the simulated energy partitioning into sensible and latent heat was evaluated comparing model with measured evaporative fraction (Figures 3.24 and 3.25). It can be concluded that for the whole data series latent heat fluxes are underestimated by the model and sensible heat fluxes are overestimated especially during the rainy season of 2000. On the other hand simulated δ^{13}C (‰) was in reasonable agreement with values reported by Ometto et al. (2006) for leaves measured at 26 m at the Jaru site (i.e -32.3 ±2.0, See Table 3.13).

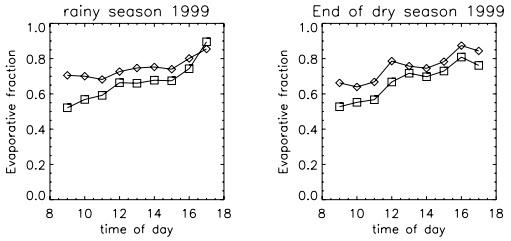

Figure 3.24 Jaru 1999. Mean diurnal cycle of measured (◊) and simulated (□) evaporative fraction. There were not enough data for the mean diurnal cycle during the dry season 1999.

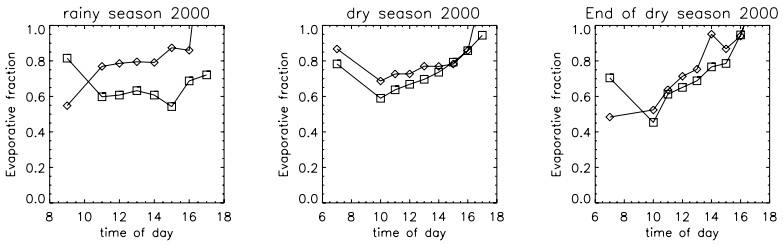

Figure 3.25. Jaru 2000. Mean diurnal cycle of measured (◊) and simulated (□) evaporative fraction.

Table 3.13. Simulated and measured carbon isotopic ratios at Jaru.

	$\delta^{13}C$ (‰)
Measured (Ometto et al. 2006)	-32.3 ± 2.0
Simulated with λ=2000 mol mol^{-1}	
Rainy season 1999	-30.40
Dry season 1999	-30.21
End of dry season 1999	-29.96
Simulated with λ=2000 mol mol^{-1}	
Rainy season 2000	-29.46
Dry season 2000	-30.32
End of dry season 2000	-28.79

Summary

As for Man K34 two parameters (V_{max} from top of the canopy and canopy quantum yield) were adjusted to improve model-data fit. Under this reparameterisation, the model fitted reasonably well the observations of net carbon uptake during both years with a tendency to overestimate by only 9% at the end of dry and dry seasons of 2000. However, comparison of simulated and measured storage fluxes at Jaru showed that the supplied modelled storage fluxes during 2000 could have been underestimated. Due to different precipitation regimes during 1999 and 2000 the prescribed soil respiration for 2000 could have been underestimated. Further, the carbon uptake result is reinforced by a good model-data comparison to leaf carbon isotopes. The main model drawbacks are 1) underestimation of latent heat fluxes (evaporative fraction) during all seasons tested and 2) low sensitivity to VPD (simulated G_P varied little from 1999 to 2000 even though there were differences in VPD over seasons and residuals of measured and simulated carbon uptake showed VPD biased towards overestimation of carbon uptake).

3.3.4 Caxiuana

A leaf N content of 2.6 g m^{-2} was used to parameterise canopy V_{max}. This is 60% larger than the N content of mean sunlit leaves from the RAINFOR Consortium data set (unpublished data) (1.6 g m^{-2}), and equivalent to a V_{max} at the canopy top of 18.7 μmol m^{-2} s^{-1}. A leaf N content of 2.6 g m^{-2} is, however, the same as the nitrogen content from another data set (Vale et al. 2003) taken from top leaves collected at 30 m height (equivalent to V_{max}= 32.1 μmol m^{-2} s^{-1}). Thus as for the Jaru and Man K34 sites, a higher V_{max} than initially parameterised using leaf N content from Meir et al. (2001) and from the RAINFOR Consortium (unpublished data) favoured a higher modelled maximum assimilation that coincided better with the data used for model comparison (See Figure 3.26 for simulations using initial parameterisation, i.e. with V_{max}=18.7 μmol m^{-2} s^{-1}).

Caxiuana was the only site where the model parameter quantum yield of absorbed light (Φ), was 0.5 (See Table 3.4), the same as fitted when leaf level gas exchange measurements were made for different seasons at this site (Vale et al. 2003). As previously mentioned, from comparison of the light response of measured N_E for all tower sites (Figure 3.2), we found that Caxiuana together with Manaus C14 are the sites with the greatest slope.

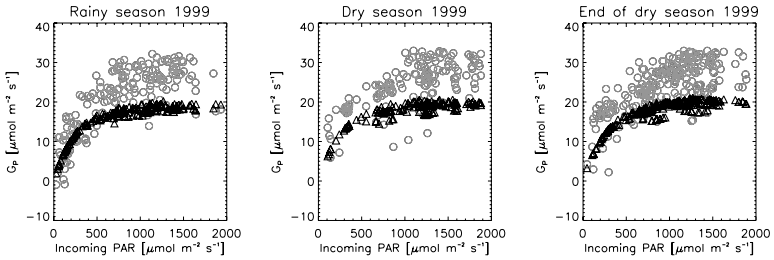

Figure 3.26. Caxiuana 1999. Light response of modelled (Δ) and measured (o) G_{PP}. Initial parameterisation with V_{max}=18.7 μmol m^{-2} s^{-1}.

Observed and modelled light response of gross uptake, G_{PP} (i.e. net uptake G_P + R_E) and 1:1 line of modelled versus observed G_{PP} for Caxiuana (i.e. $-N_E$ from eddy correlation + simulated day time ecosystem respiration provided together with eddy correlation and meteorology data) are presented in Figure 3.27. Statistics are shown in 3. 14. The model fits the data relatively well during all three seasons.

Seasonal patterns of climatology, measured N_E, and G_{PP} and simulated G_{PP} are hereafter briefly discussed:
-Seasonality in climatology, diurnal and night time fluxes at Caxiuana during these periods have already been discussed by Carswell et al. (2002) and are shown here again in Figure 3A-26. From Figure 3A-26, the wet season of 1999 had much lower irradiance, air temperature and VPD than during the rest of the year.

-Day time N_E fluxes during the dry season were lower than fluxes during the end of the dry season and wet season. Also nocturnal respiration was significantly higher in the dry season compared with the wet season. This was most likely due to changes in temperature (See Figure 3.28 and 3A-26).

-On the other hand, G_{PP} from the observations, calculated as $-N_E$ plus daytime ecosystem respiration, had little seasonality as showed in Figure 3.28. The simulated mean diurnal cycle of G_{PP} (Figure 3.29) is similar to that derived from the eddy correlation measurements. G_{PP} was lowest during the wet season of 1999. This means that according to the sun/shade model, the effect of lower solar radiation and lower temperatures on photosynthetic uptake during the wet season was larger than the effect of larger VPD on photosynthetic uptake during the dry and end of dry seasons.

Table 3.14. Statistics of model-data comparison for G_P * during the seasons tested at Caxiuana.

Season	a	r^2	RMSE**
Rain 1999 (all data)	0.91	0.98	2.82
Dry 1999 (all data)	0.91	0.97	3.31
End of dry 1999 (all data)	0.91	0.96	3.74
Rain 1999 (only observed G_P <28 μmol m^{-2} s^{-1})	1.09	0.96	4.24
Dry 1999 (only observed G_P <28 μmol m^{-2} s^{-1})	1.07	0.97	3.87
End of dry 1999 (only observed G_P <28 μmol m^{-2} s^{-1})	1.06	0.97	4.35

* The regression model is modelled flux= a × measured (or estimated from eddy correlation) flux
** Root mean square error

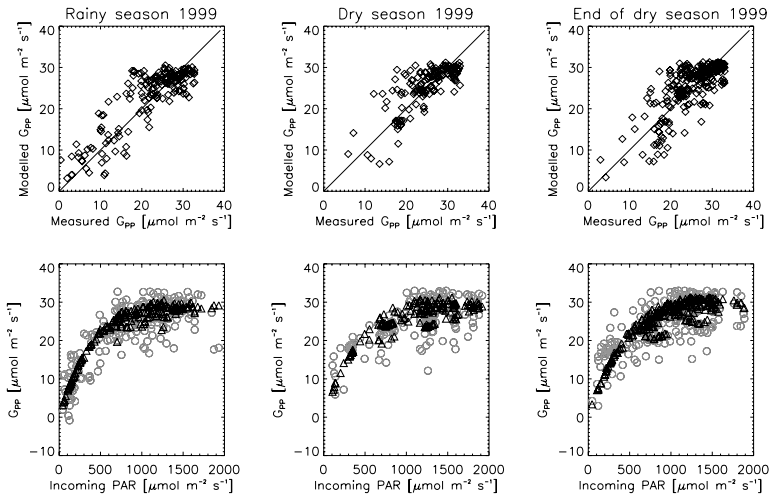

Figure 3.27. Caxiuana 1999. Light response of modelled (Δ) and measured (o) G_{PP} and one to one line of modelled versus observed G_{PP}.

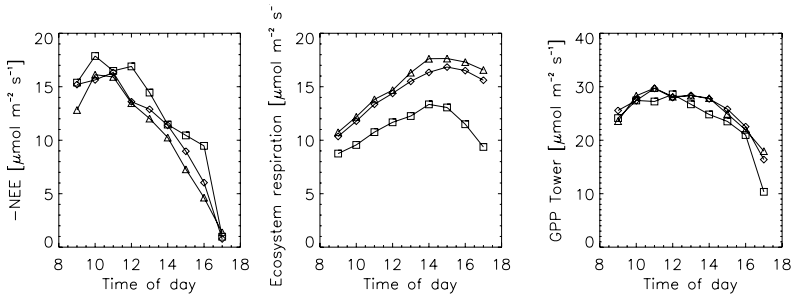

Figure 3.28. Caxiuana 1999. Mean diurnal cycle of N_E measured by eddy correlation. Simulated daytime Ecosystem respiration (simulated as a function of air temperature using Q_{10} of 2) and G_{PP} estimated from eddy correlation. (Δ) dry season 1999, (◊) end of dry season 1999 and (□) rainy season 1999.

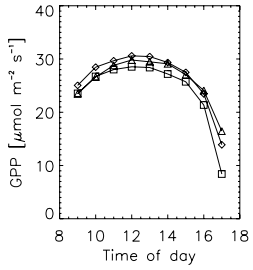

Figure 3.29. Caxiuana 1999. Mean diurnal cycle of simulated G_{PP} (calculated as net photosynthetic uptake plus canopy respiration) during 1999. (Δ) dry season (◊) end of dry season (□) rainy season.

Response of residuals of net carbon uptake to different environmental and non environmental variables for Caxiuana during year 1999 are given in Figures 3A-27-29 during rainy, dry and end of dry season. Since residuals are well distributed over the zero line in Figures 3A-27-29, it can be concluded that there is no model bias response to PAR, air temperature, VPD, fraction of diffuse irradiance, C_a or time of day. However, it is important to mention that there are less data points available at this site.

The energy balance was evaluated by comparing simulated against measured evaporative fraction (Figure 3.30). In general the model tends to underestimate latent and overestimate sensible heat fluxes during

end of dry and rainy seasons, but performed slightly better during the dry season.

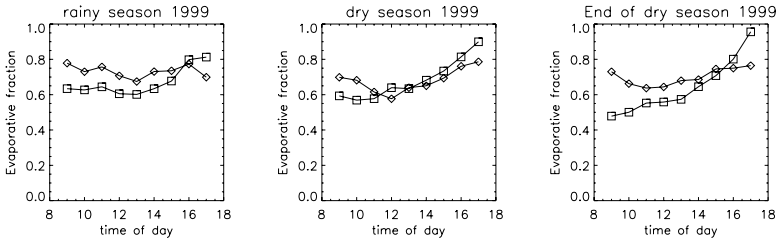

Figure 3.30. Caxiuana 1999. Mean diurnal cycle of measured (◊) and simulated (□) evaporative fraction.

Although the goodness of fit for the comparison of gross photosynthetic carbon uptake was good, the partitioning of energy into latent and sensible heat fluxes seemed quite poor. Thus, in order to corroborate the carbon uptake result, model predicted δ^{13}C was calculated as shown in Table 3.15.

Table 3.15. Simulated carbon isotopic ratio at Caxiuana.

	δ^{13}C (‰)
Simulated with λ=1800 mol mol^{-1}	
Rainy season 1999	-29.97
Dry season 1999	-29.15
End of dry season 1999	-29.47

Model sensitivity to higher values of lambda, λ, was tested in order to improve the partition of energy (results not shown). Higher lambda implies increased latent heat fluxes, improving the evaporative fraction comparison, with a modest change in gross carbon uptake and a decrease (more negative) in simulated δ^{13}C. Reported δ^{13}C values for leaves measured at other sites than at Caxiuana, i.e. Manaus, Jaru and Tapajos are on the order of -32.3 ± 2.5 ‰. In the absence of a measured value at Caxiuana, lambda was set to 1800 mol mol^{-1} which provided simulated δ^{13}C values close to reported values for other sites.

Summary

The model was parameterised for this site based on leaf N values from Vale et al. (2003) that provided a good fit to the observations. However N from Vale et al. (2003) is higher than reported from the RAINFOR Consortium data set (unpublished data). For this site, no VPD bias to carbon uptake was obtained. However, there were fewer data points available here than for other sites where the simulated carbon uptake bias towards high VPD was observed (Man K34 and Jaru). Again, using the adjusted V_{max}, a good fit to carbon uptake was obtained for all seasons at the cost of a poor energy partition. Note, this was the only site parameterised with a quantum yield of 0.5, and at the same time this site had the highest ecosystem respiration (Figure 3.4). The high ecosystem respiration at this site favours a steep slope in the light response of measured $N_{E,}$ and G_{PP}, and also to high corresponding maximum values, which contributes to the good model agreement with the observations using Φ=0.5.

3.3.5 Tapajos

Top of the canopy V_{max} was initially derived from leaf N content from the RAINFOR Consortium data set (unpublished data), obtaining a V_{max} = 24 μmol m^{-2} s^{-1}. An initial quantum yield of 0.4 was used. Modelled

G_{PP} against PAR is shown in Figure 3.31. Using this parameterisation simulated maximum assimilation values were inside the range of the corresponding observations. Note the range in variation of the observations (~15 to ~30 μmol m^{-2} s^{-1}) in the region where photosynthesis saturates with light (i.e. where maximum assimilation rates occur). Therefore the model was parameterised with V_{max} = 24 μmol m^{-2} s^{-1} unlike other sites where it was always necessary to increase canopy V_{max} to fit better the observations. Furthermore, simulated G_{PP} in the region of the linear increase in photosynthesis with light was always larger than observed. Due to this reason, the quantum yield parameter was adjusted and reduced to 0.30. Other parameters used for simulations are shown in Table 3.5. Note that V_{max} at this site was the lowest among the 5 sites, and this also corresponds to the lowest simulated G_P.

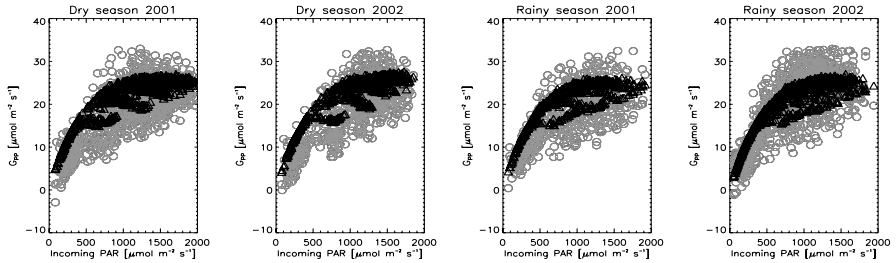

Figure 3.31. Tapajos 2001-2002. Light response of simulated (Δ) and observed (o) gross uptake (calculated as $-N_E$ from eddy correlation + total ecosystem respiration corrected for daytime canopy respiration). Initial parameterisation top of the canopy V_{max} = 24 μmol m^{-2} s^{-1} and canopy Φ=0.4.

Comparison of simulated gross uptake using the recalibrated parameters (V_{max} = 24 μmol m^{-2} s^{-1} and Φ= 0.30) against observations (estimated as $-N_E + R_E$ corrected daytime canopy respiration, as explained in the methods) is shown in Figure 3.32 and Table 3.16**.** The sun/shade model tends to overestimate the data up to an estimated G_{PP} of 28 μmol m^{-2} s^{-1} during the whole data series, dry and wet seasons from 2001 and 2002.

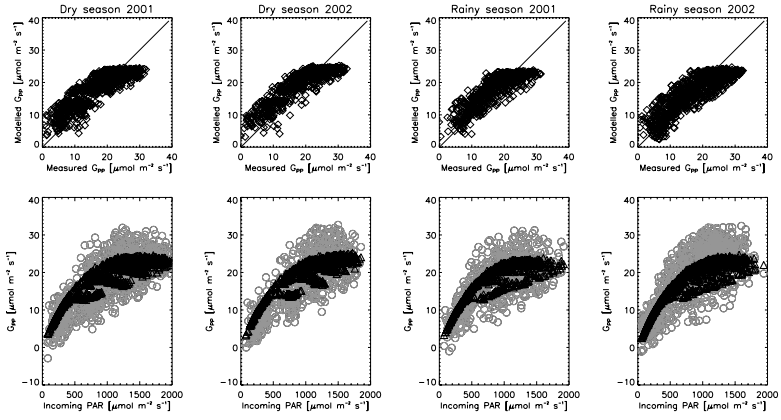

Figure 3.32. Tapajos 2001-2002. Light response and 1:1 line of simulated and observed gross uptake (calculated as $-N_E$ from eddy correlation + total ecosystem respiration corrected for daytime canopy respiration) parameterised with V_{max} = 24 μmol m^{-2} s^{-1} and Φ=0.30.

Table 3.16. Statistics of model-data comparison for G_{PP}* during the seasons tested at Tapajos.

Season	A	r^2	RMSE**
Rain 2001 (all data)	0.98	0.96	3.6
Dry 2001 (all data)	0.99	0.96	3.6
Rain 2002 (all data)	0.90	0.96	3.6
Dry 2002 (all data)	0.99	0.96	3.74
Rain 2001 (only observed G_{PP}<26 μmol m^{-2} s^{-1})	1.02	0.98	3.16
Dry 2001 (only observed G_{PP}<26 μmol m^{-2} s^{-1})	1.04	0.97	3.16
Rain 2002 (only observed G_{PP}<26 μmol m^{-2} s^{-1})	0.97	0.96	3.46
Dry 2002 (only observed G_{PP}<26 μmol m^{-2} s^{-1})	1.06	0.97	3.31

* The regression model is modelled flux= a × measured (or estimated from eddy correlation) flux
** Root mean square error

Residuals of observed and simulated G_{PP} responses to incoming irradiance, air temperature, atmospheric CO_2, fraction of diffuse irradiance, canopy to air vapour pressure difference and time of day are shown in Figures 3A-30-33. According to the residual responses there is a slight tendency to overestimate G_{PP} data at high air temperatures and high VPD values. This bias towards overestimating observed G_{PP} at high VPD and air temperatures might be time of day related with the model tending to over predict observations during early mornings (0700-0800) and afternoons (1400-1700). This issue is analysed by plotting the measured and observed light response of G_{PP} at different times of day for various values of VPD (plots in Appendix 3A); an explanation follows:

1) In Figure 3A-34 (third row**)** it is shown that many of the points that are in the region of linear increase of net carbon uptake with light correspond to hours 0700 and 0800 a.m. and to hours between 1400 and 1700.
2) In Figure 3A-35, it is shown that the model tends to overestimate data between 0700 - 0800 and 1400 - 1700, but between 900 and 1300 hours the model fits the observations slightly better.
3) Data between hours 0900 and 1300 belong to the region where photosynthesis saturates (see first row in Figure 3A-34). In this region residuals of observed and simulated net carbon uptake are better distributed over the zero line but there is still a tendency to overestimate data points with high VPD and air temperature which are time of day related (Figure 3A-36).
4) Between 1200 and 1300 hours, VPD is usually higher than earlier in the morning and some of these data points are located in the lowest part of the cloud of data points (see second row in Figure 3A34) and are overestimated by the model (see fourth row for all times of day in Figure 3A-34).

The tendency for the model to over predict fluxes in the afternoons might indicate a decrease in uptake or an increase in respiration. Here, as described in the methods, we used the same prescribed ecosystem respiration for 2001 and 2002, which included seasonal variations. However, because 2002 had a wetter rainy season, soil respiration may have been lower if water storage exceeded the level up to the point where inhibition of respiratory activity occurs due to inadequate oxygen supply (Schuur 2001). In an analysis of the carbon fluxes inferred from eddy correlation at a nearby site (km 83 site) during the period July 2000 to July 2001, Goulden et al. (2004) concluded that the decline in afternoon CO_2 uptake resulted from a change in photosynthesis rather than a change in respiration. Goulden et al. (2004) attributed the afternoon decline in photosynthesis to either a stomatal response to VPD, or to a change in biochemistry of photosynthesis due to elevated temperature or a circadian rhythm or a combination of mechanisms. From an analysis of soil water

content measurements, Goulden et al. (2004) also suggested that leaf desiccation was not responsible for the afternoon decline in photosynthesis. In general, no moisture stress has been reported at Tapajos which is explained as a consequence of deep rooting that allows extraction of soil moisture stored deep in the soil (Nepstad et al. 1994); Nepstad et al. 2002, da Rocha et al. 2004). However, da Rocha et al. (2004) do not exclude the possibility of plant water stress during a strong *El Niño* event. Furthermore, Goulden et al. (2004) in their analysis fitted measured N_E to a simple hyperbolic curve and found the same residual trend as in this study with the sun/shade model, i.e. overestimation of uptake in the afternoon was linked to air temperature and VPD.

Seasonality of N_E and ecosystem respiration has been measured at Tapajos and contrary to other sites like at Manaus (Malhi et al. 1998) or Caxiuana (Carswell et al. 2002), Tapajos has higher N_E during the dry season than during the wet season (Saleska et al. 2003). According to Saleska et al. (2003) and Goulden et al. (2004), ecosystem respiration has a strong seasonal behaviour at this site, having its maximum during the wet season and minimum during the dry season. Reduction of ecosystem respiration during the dry season is mainly driven by reduced forest floor (soil, litter and coarse woody debris) decomposition. Furthermore, part of the reason for the high ecosystem respiration is related to the stock of above-ground dead wood which is notably large in comparison with other sites (Keller et al. 2004). According to Keller et al. (2004) the coarse woody debris at km 67 in Tapajos (site used here) is two to four times larger than the standing stock of coarse woody debris measured close to Manaus (Chambers et al. 2000; Kirschbaum et al. 2003; Nascimento and Laurance 2002). Rice et al. (2004) and Saleska et al. (2003) hypothesized that the Tapajos forest is recovering from recent episode(s) of disturbance which caused sharply elevated mortality, preceding the onset of the eddy correlation measurements used in this study, which caused a large increase in the dead wood pool.

Contrary to N_E and ecosystem respiration, the response of gross ecosystem production to the seasonality in precipitation is weak (Saleska et al. 2003; Goulden et al. 2004). Figure 3.33 shows the mean diurnal cycle of PAR, VPD, air temperature, N_E and G_{PP} (estimated from eddy correlation measurements and simulated) for the dry and wet seasons of 2001 and 2002, which illustrates differences in air temperature and VPD. Measured N_E and G_{PP} were lowest during the wet season of year 2001. The wet season of 2002 produced similar fluxes to the dry season of 2001 and 2002. Even though there is a notable difference in meteorology from dry to wet seasons, the sun/shade model predicted a modest seasonality in gross uptake with maximum assimilation rates varying little from season to season. This is because, during the wet season the effect of lower VPD on modelled uptake is counteracted by the effect of lower irradiance and much lower temperatures during this season. To this end, the sensitivity of J_{max} and V_{max} to temperature is shown in Figure 3.34. At high irradiance, photosynthesis by sunlit leaves is mostly rubisco limited and the temperature effect on V_{max} affects photosynthesis undertaken by sunlit leaves. On the other hand, photosynthesis of shaded leaves is always limited by the rate of electron transport (J in equation 5, Chapter 1). The rate of electron transport is expressed in terms of quantum yield, a curvature factor (θ) and J_{max} which is the maximum rate of photosynthetic electron transport at saturating irradiance. This means the temperature effect on J_{max} mostly affects shaded leaves.

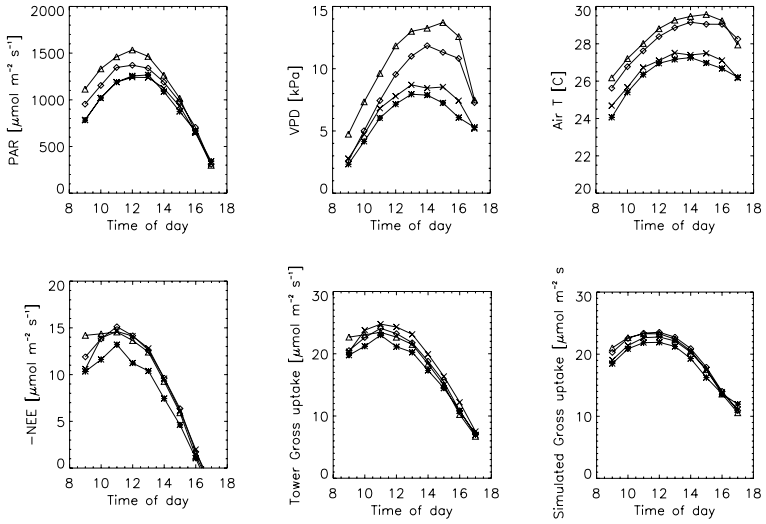

Figure 3.33. Tapajos 2001-2002. Mean diurnal cycle of PAR, air temperature, VPD, -N_E and Gross uptake (i.e. $-N_E$ + ecosystem respiration (estimated by Saleska et al. (2003) from mean annual of u* night time eddy correlation data and corrected for daytime canopy respiration). (Δ) Dry season 2001, (◊) Dry season 2002, (*) Rainy season 2001, and (×) Rainy season 2002.

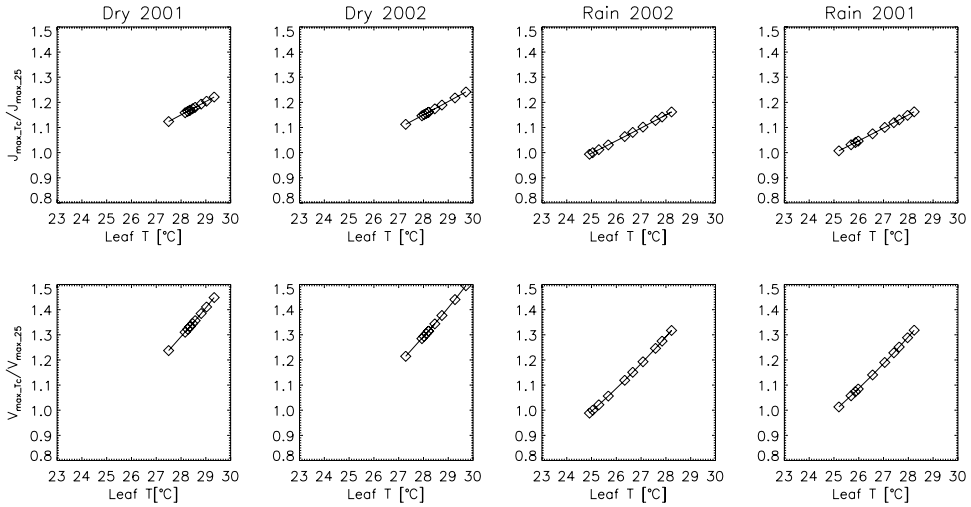

Figure 3.34. Temperature functions of V_{max} and J_{max} evaluated at mean temperatures for each season.

An increase in litterfall has been measured at Tapajos at the end of the wet and beginning of dry season which is probably partly linked to a decrease in LAI (Goulden et al. 2004; Nepstad et al. 2002; Rice et al. 2004) and associated variations in canopy photosynthesis (Goulden et al. 2004). Since there was no data available on LAI seasonality at Tapajos at the time simulations were undertaken, for the modelling purposes here, seasonality in LAI was not considered in the main model run. Model G_{PP} sensitivity to LAI values above and below (10 and 30 %) the value assumed for this site (LAI= 6.5 m^2 m^{-2} taken from the RAINFOR Consortium, unpublished data) was tested obtaining corresponding increases in G_{PP} of 3 and 7 % and decreases in G_{PP} of 4 and 14% (these percentages were calculated with respect to the simulated G_{PP} obtained with LAI= 6.5 m^2 m^{-2}).

In order to assess the energy partition into sensible and latent heat fluxes, the mean diurnal cycle of measured

and simulated evaporative fraction were compared (See Figure 3.35). Underestimation of λE and overestimation of H is simulated with a lambda of 2000 mol mol^{-1} which, nevertheless produces values of simulated δ^{13}C (See Table 3.17) which agree with those reported by Ometto et al. (2006) at this site.

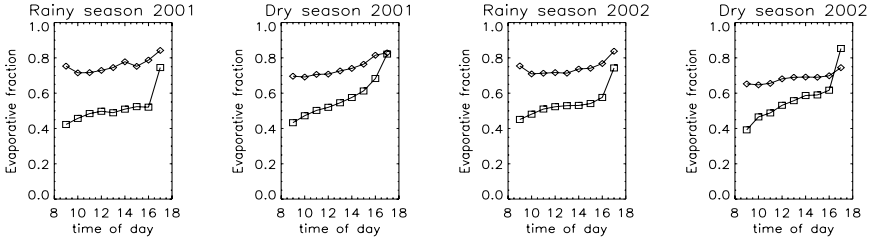

Figure 3.35. Tapajos 2001-2002. Mean diurnal cycle of measured (◊) and simulated (□) evaporative fraction.

Table 3.17. Simulated and measured carbon isotopic ratio at Tapajos.

Season	δ^{13}C (‰)
Measured (Ometto et al. 2006)	-32.9 ± 2.1
Simulated Rain 2001	-30.29
Simulated Dry 2001	-30.69
Simulated Rain 2002	-31.54
Simulated Dry 2002	-31.42

To improve the model fit for evaporative fraction, different values of the lambda parameter were used. Higher values of lambda (λ=2000 mol mol^{-1} used for current simulations) were tested and a lambda of 5000 mol mol^{-1} agreed closely with the measured evaporative fraction, with an average simulated δ^{13}C of - 33.8 ‰, which is on the low end of range reported by Ometto et al. (2006) for Tapajos. However, to preserve the isotope ratios, the initial value of lambda of 2000 mol mol^{-1} was kept. Next, different values of LAI or V_{max} from the top of the canopy were assigned. A sensitivity test was conducted using a higher LAI than used here but improvements in evaporative fraction were minor (not shown). A higher V_{max} (than used in the current parameterisation) increases uptake and latent heat fluxes at the cost of over predicting the measured gross uptake at the tower (not shown).

Summary

Parameterisation of V_{max} for top of the canopy was based on leaf N data from the RAINFOR Consortium (unpublished data). Tapajos was the only site that did not need any increase in this parameter to fit the observations. The canopy quantum yield used for simulations was the lowest among sites (canopy Φ= 0.30). Gross carbon uptake was relatively well simulated up to a value of 26 μmol m^{-2} s^{-1} after which the model underestimated the observations. However, similar to Man K34 and Jaru, residuals of the G_{PP} model against observations showed a model bias at highest values of VPD and air temperature which seems to be linked with time of day. Furthermore, a lambda of 2000 mol mol^{-1} was used for parameterisation of the stomatal conductance model which provided reasonable values of simulated δ^{13}C but a poor comparison to evaporative fraction.

3.3.6 Model calibration

As has been shown for all sites, two model parameters (top of the canopy V_{max} and Φ) were usually adjusted to produce a better fit with the observations. To verify these results, the model was calibrated using a simplex procedure to minimize the error sum of squares of the modelled photosynthesis minus the sum of net ecosystem exchange as measured by eddy correlation plus the estimated ecosystem respiration from a selected data set (Nelder et al 1965). The following parameters were estimated from the fitting procedure: top of the canopy V_{max}, the ratio J_{max} / V_{max} and the canopy level quantum yield, leaving λ equal to the values already parameterised. The remaining parameters, the curvature or shape factor (θ) of the non-rectangular hyperbolic function for electron transport and the temperature sensitivity parameters of J_{max} (S_J and H_J) were not fitted and taken as constant (Table 3.5). The curvature factor θ and H_J from Table 3.5 were taken from Carswell et al. (2000) and S_J was fitted in Chapter 1, increasing the temperature optimum from 32 to 39 °C. The best fitted value (in Chapter 1) of S_J was 693.1 J $K^{-1}mol^{-1}$ (cf. 710.0 in Carswell et al. 2000). Table 3.18 includes the fitted V_{max}, J_{max} / V_{max} ratio and Φ at each site and also the corresponding values from the recalibration at each site. Manaus C14 was already fitted in Chapter 1.

Table 3.18. Fitted V_{max} from top canopy leaves, J_{max} / V_{max} and quantum yield (Φ) at each site.

Site	V_{max} top fitted	J_{max}/V_{max} fitted	Φ fitted	V_{max} top recalibrated	Φ Recalibrated
Manaus- K34	40	1.9	0.35	40.5	0.35
Jaru	51.89	1.82	0.4	47.1	0.35
Caxiuana	32.11	1.9	0.5	32.5	0.5
Tapajos	47.49	2.96	0.16	24.5	0.3

Note that for a fixed curvature factor equal to 0.7, top of the canopy V_{max} and canopy level Φ were similar to the recalibration values. However, at Tapajos the fitted Φ was much lower and fitted top of the canopy was almost double that initially parameterised, and the fitted J_{max} / V_{max} value is too high. Further, the sun/shade model was run using the parameters presented in Table 3.18. Results from Man K34, Jaru and Caxiuana were similar to results presented in this chapter for the same sites with the parameterisation presented in Table 3.5. This is because the fitted parameters did not differ greatly when compared to the values individually parameterised at each site. However, for Tapajos, similar results to those already shown (using parameterisation from Table 3.5) were also obtained with less overestimation of net photosynthesis due to the very low quantum yield used (0.16) in Table 3.18.

In conclusion, the model calibration presented in this section shows similar results to those previously obtained in this chapter when each site was analysed individually. This confirms the parameter adjusting undertaken at each site which was based on the sensitivity analysis presented. Finally it is worth mentioning that due to the high variability of the measurements of net ecosystem exchange from the eddy correlation system, numerical fitting exercises are difficult to carry out, leading in many cases to no convergence to any solution. The sensitivity analysis followed by parameter adjusting undertaken in this study served to provide the fitting routine with initial model parameters.

3.3.7 Scaling up to basin level

Two methods were used to scale up to the basin level, one based on leaf N and the other based on leaf P. Phosphate limitation to photosynthesis is linked to a failure in the capacity of starch and sucrose synthesis to match the capacity of the production of triose phosphates in the Calvin cycle, usually when both C_i and light are high. The result is an inadequate rate of release of inorganic phosphate in the chloroplast to recycle the P sequestered in the production of triose phosphates. In this case inorganic phosphorous can limit photosynthesis (Harley et al 1991). This has been included in the biochemistry of C_3 photosynthesis initially postulated by Farquhar et al. (1980) and later expanded (Farquhar and von Caemmerer 1982) by some authors (e.g. Collatz et al. 1991; Harely and Sharkey 1991; Harley et al.1992). For example, Collatz et al. (1991) suggest that the capacity of export or utilization of the products of photosynthesis is approximately equal to the maximum value of photosynthetic uptake at saturating irradiance, defining the triose phosphate utilization (TPU) limitation as:

$$J_s = V_{max}/2 \qquad (11)$$

where J_s is the export capacity or utilization of the photosynthetic products (most likely sucrose synthesis). Since the Collatz et al. (1991) definition of the TPU limited rate of assimilation is a function of V_{max}, we decided to relate V_{max} to leaf P for the 5 study sites.

Linear relationships between mean leaf N (and leaf P) content per weight and per leaf area, using the RAINFOR Consortium data set (unpublished data), and best fitted V_{max}, obtained in the previous section from recalibrated parameterisation at each site were initially used. However, because Φ affects to some extent the efficiency of V_{max}, to be able to relate V_{max} to leaf N and leaf P under the same conditions, V_{max} and J_{max} / V_{max} were fitted again but with a fixed quantum yield of 0.4, with results shown in Table 3.19. Using this parameterisation for the sun/shade model similar results are obtained at all sites except at Tapajos. At Tapajos, the model overestimated gross photosynthesis considerably. The reason for this high overestimation is the high V_{max} and high quantum yield from Table 3.19.

Table 3.19. Fitted V_{max}, J_{max} / V_{max} with (Φ=0.4) at each site.

Site	V_{max} top fitted [μmol $m^{-2}s^{-1}$]	original V_{max} [μmol $m^{-2}s^{-1}$]	J_{max}/V_{max}	Φ
Manaus K34	37.8	40.5	1.9	0.4
Jaru	51.89	47.1	1.82	0.4
Caxiuana	39.44	32.5	1.83	0.4
Tapajos	40	24.5	1.88	0.4

For all sites V_{max} in dry weight (DW) and on an area basis from Table 3.19 were then related to foliar N and P (DW basis) taken from the RAINFOR Consortium (unpublished data), as shown in Figure 3.36 and Table 3.20. V_{max} on an area basis was converted to (DW) using specific leaf area (mass of leaves per unit area) from the RAINFOR Consortium (unpublished data). The highest correlations are for leaf P with V_{max} on both a DW and area basis. Correlations with leaf N were significant only when using V_{max} on an area basis. Obtained correlation coefficients from the relationships between V_{max} with leaf P and leaf N on an area

basis (See Figure 3A-37) were lower than those obtained for V_{max} with leaf P and N on a DW basis. All correlations with leaf P were still significant and higher than with leaf N. Table 3.20 includes two regressions calculated with an extra data point using mean foliar P (all heights) reported for the Man C14 by Meir et al. (2001). Using this extra point [0.7 mg mg^{-1}], the correlation between V_{max} and leaf P (both in DW) is still significant.

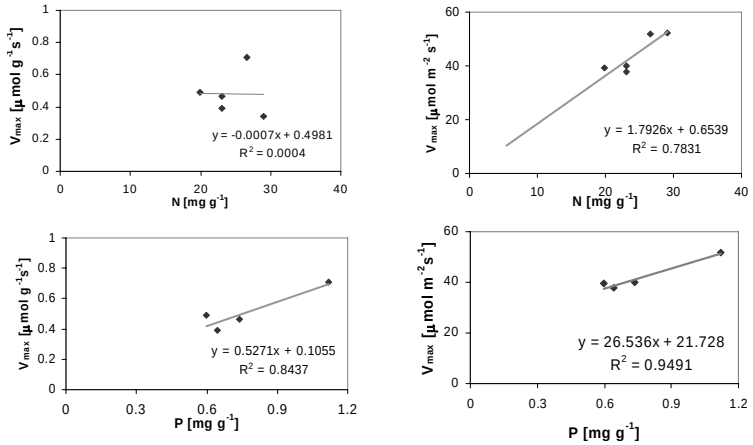

Figure 3.36. Linear regressions obtained from best fitted V_{max} in DW and in area basis (with Φ= 0.4 against foliar N and foliar P in DW.

Table 3.20. Statistics of regressions of V_{max} in area and DW basis against foliar N and foliar P.

	a	b	r^2	p-value
V_{max} [μmol g^{-1} s^{-1}] *vs* N[mg g^{-1}]	0.49	-0.0008	0.0	0.976
V_{max} [μmol m^{-2} s^{-1}] *vs* N[mg g^{-1}]	1.0	1.78	0.779	0.047
V_{max} [μmol g^{-1} s^{-1}] *vs* P[mg g^{-1}]	0.106	0.527	0.844	0.081
V_{max} [μmol m^{-2} s^{-1}] *vs* P[mg g^{-1}]	21.7	26.5	0.949	0.026
V_{max} [μmol g^{-1} s^{-1}] *vs* P[mg g^{-1}] **	0.094	0.54	0.844	0.027
V_{max} [μmol m^{-2} s^{-1}] *vs* P[mg g^{-1}]**	27.25	22.42	0.4242	0.234

** Regressions calculated with an extra data point corresponding to leaf P from Manaus C14 reported by Meir et al. (2001) as mean leaf P for this site.

3.4 Discussion

3.4.1 Model parameterisation

Initial evaluation of all sites using the parameterisation from Chapters 1 and 2 showed that maximum assimilation was underestimated (at Man K34, Jaru and Caxiuana) by the sun and shade model and simulated G_P was higher than the observations at low light levels (at Man K34, Jaru and Tapajos). Results from a sensitivity analysis showed that in order to better fit the observations it was necessary to adjust two parameters: V_{max} (increase from initial value) and either Φ (decreasing from initial value) or θ (decreasing to very low values). Based on reported values of Φ and θ from other measuring and modelling studies it was decided to decrease Φ.

Increasing the initial value of V_{max} implied a higher leaf N than the mean reported value, but still within one standard deviation. One explanation for the need of a higher leaf N to increase the apparent V_{max} might lie in the original leaf N - V_{max} relationship used to determine V_{max} at the top of the canopy at all sites. This was derived using leaf N and V_{max} data from leaf gas exchange measurements at Man C14 at different heights

from Carswell et al. (2000) and at Caxiuana from Vale et al. (2003), the only leaf level data available at the time simulations were undertaken. If the leaf N - V_{max} relationship was to be taken using only the Caxiuana values or from a subsequent data set from Domingues et al. (2005) at Tapajos, then V_{max} associated with a given leaf N is higher. See Table 3.21 for all regressions and Table 3.22 for calculated V_{max} using the mentioned regressions and reported values from top canopy leaves from those studies. From Table 3.21 and 3.22 it is clear that the regression based on the Carswell et al. (2002) data set predicts the lowest V_{max}. This is because leaf N from this data set are the highest from all data sets considered in Table 3.21. Moreover, leaf N reported from Carswell et al. (2000) for Man C14 are also higher than leaf N reported at Man K34 (RAINFOR Consortium, unpublished data), sites which are only 10 km apart. Furthermore, a recent study (Ometto et al. 2006) that collected leaf N at both of Manaus sites (i.e. C14 and K34) found no significant difference between leaf N content at Man K34 and Man C14. However, using the high leaf N at the top of the canopy from Man C14 i.e. high V_{max}, the sun/shade model predicts reasonably well the carbon and energy measured by the recalculated data set of Malhi et al. (2000) as shown in Chapters 1, 2 and in this chapter. Moreover, from the comparison of eddy correlation flux data from both Man C14 and Man K34 site, Araújo et al. (2002) found clear differences between total daily N_E and the peak daytime sink-strength being highest for the Man C14 forest. Araújo et al. (2002) suggest the observed differences could be linked to the fact that the plateau forest at C14 has older and taller individual trees than the plateau forest at K34, which covers a larger area of waterlogged vegetation which could be less productive.

Additionally, the reported values of V_{max} from top of the canopy at Tapajos (Domingues et al. 2005) and at Caxiuana (Vale et al. 2003) (Table 3.22) are close to the range of V_{max} parameterised but also fitted in section 3.3.6 in this chapter. Furthermore, from the V_{max} values reported in Table 3.22 it is concluded that when regressions of V_{max} *vs* leaf N from Domingues et al. (2005) and Vale et al. (2003) are used, predicted values of V_{max} were close to those for the individual site parameterisation and also to those from the numerical fitting exercise presented in section 3.3.6.

Table 3.21. Regresions of canopy V_{max} against foliar N in area basis from different sources.

Source	Regression V_{max} [μmol $m^{-2}s^{-1}$] *vs* leaf N [g m^{-2}]	r^2	Site
Carswell et al. (2000) and Vale et al. (2003)	V_{max} = 13.46 N - 2.81	0.8	Manaus C14 and Caxiuana
Carswell et al. (2000)	V_{max} = 12.99 N - 3.84	0.97	Manaus C14
Vale et al. (2003)	V_{max} = 23 N - 17.2	0.98	Caxiuana
Domingues et al. (2005)	V_{max} = 23 N - 7.02	0.51	Tapajos

Table 3.22. Calculated top of the canopy V_{max} in [μmol $m^{-2}s^{-1}$] using regressions of V_{max} against foliar N from different sources and reported values of V_{max} from top canopy leaves.

	Jaru	Caxiuana	Caxiuana	Tapajos	Man K34	Man C14
Leaf N [g m^{-2}]	2.9[+]	1.6[*]	2.6[◊]	2.03[*]	2.2[*]	4.4[Δ]
V_{max} calculated with Carswell et al. (2000) and Vale et al. (2003) regression	36.2	18.7	32.2	24.5	27.1	56.5
V_{max} calculated with Vale et al. (2003) regression	49.5	19.5	42.6	29.5	33.9	84.2
V_{max} calculated with Domingues et al. (2005) regression	59.7	29.7	52.8	39.7	44.1	94.4
V_{max} parameterised in this study	**47.1**	**32.1**	**32.1**	**24.5**	**40.5**	**52.3**
V_{max} fitted in this study	51.9	39.4	39.4	40.0	37.8	
V_{max} reported for single sites at top of the canopy			42.61[◊]	[28-75][**]		42.8°

[*]Values taken from the RAINFOR Consortium (unpublished data), [+] Meir et al. (2001) at 30- 35 m, [◊] Mean vaule at 30 m reported by Vale et al. (2003), [Δ] extrapolated value to the top of the canopy from Carswell et al. (2000) data set, ° Carswell et al. (2000) at 24 m, [**]reported by Domingues et al. (2005) for top canopy leaves

The quantum efficiency for CO_2 fixation or so called quantum yield was used in equation (12) to estimate the irradiance absorbed by photosystem II. In equation (12) the parameters r and t are leaf reflectance and transmittance and f is the fraction of light lost as absorption by other than chloroplast lamellae, which increases with leaf thickness (Farquhar et al. 1980). According to Farquhar et al. (1980), there is a limitation to electron transport if insufficient quanta are absorbed. Therefore one quantum must be absorbed by each of the two photosystems to move an electron to the level of water and to the level of $NADP^+$, and therefore Φ in equation (12) must be 0.5. Equation 13 can be rewritten using α, which intrinsically includes f and Φ also defined as intrinsic quantum efficiency for CO_2 uptake. The form of equation (13) is the most commonly used in modelling studies and α is the parameter value usually reported. Farquhar et al. (1980) defined a theoretical upper limit to quantum yield α (when f=0) in the absence of oxygenation set by NADPH or by ATP requirement whose values are 0.5 and 0.4, respectively.

$$I_2 = I_0\,(1-r-t)\,(1-f)\,\Phi \qquad (12)$$

$$I_2 = I_0 \times (1-r-t)\,\alpha \qquad (13)$$

A list of reported α used or determined in modelling and experimental studies is shown in Table 3.23. Values obtained in this study are indeed within the published range of variation with α for Caxiuana within the range of the reported theoretical upper limit for quantum yield. According to Leuning (1990), when fitting α and θ to gas exchange measurements, the obtained variation in α has little physiological meaning due to the interaction between α and θ that occurs during the non-linear curve fitting procedure. The curvature parameter θ has no mechanistic basis (Collatz et al. 1990b), however it can be viewed as an indicator of the extent to which co-limitation (of light and rubisco limitations) of photosynthesis is present with θ approaching 1 meaning that co-limitation is minimized. But a certain level of co-limitation is always present (Woodrow and Berry 1988). Values of θ in some of the modelling studies (listed in Table 3.23), include variations from 0.7 - 0.95. Moreover, a recent modelling study using data for Jaru and Cuieiras

optimized parameters of the C_3 photosynthesis model obtained an α of 0.15 and 0.2 and θ equal to 0.8 and 0.9 (Simon et al. 2005). Domingues et al. (2005) measured leaf photosynthesis at the same Tapajos forest site as used in this study. They adopted a fixed α of 0.19 following Ehleringer and Bjorkman (1977) fitting light response measurements of photosynthesis to a non-rectangular hyperbolic model. The curvature factors derived from such a fitting exercise ranged between 0.45 and 0.9 for most of the cases. However, for 3 out of 19 cases, the derived curvatures factors were as low as 0.31 and 0.19 (Domingues et al. 2005).

Variation in the parameterised value of α for the different sites of this study could simply be a result of interaction between α and θ (fixed to 0.7). On the other hand, as it was shown in Figure 3.2, there were differences in the slope of the light response of measured N_E among sites which could have physiological meaning, i.e. differences in efficiency of photosynthetic uptake due to plant stress which so far do not appear to be water stress. Detailed measurements would be required to examine variation of α across sites.

Table 3.23. Comparison of α as reported in various studies and obtained in this study. Unit conversion is done assuming that to produce 1 mol of CO_2, 4 electrons are needed.

Study	Use	α [mol CO_2 mol $^{-1}$PAR]	α [mol electrons mol^{-1} photons]	θ
Ehleringer and Bjorkman (1977)	Measured	0.073	0.29	
Ehleringer and Pearcy (1983)	Measured	0.052	0.22	
Long et al. (1993)	Measured	0.093	0.372	
Farquhar et al. (1980)	theoretical upper limit of α	0.125 0.11	0.5 0.44	
Thornley (2002)	used for model parameterisation	0.05	0.2	
Wand and Leuning (1998)	used for model parameterisation	0.096	0.385*	
Harley et al. (1992)	used for model parameterisation	0.06	0.24	
Collatz et al. (1991)	used for model parameterisation	0.08	0.32	0.95
Leuning 1990	fitted to leaf gas exchange measurements	[0.032-0.066]*	0.128-0.264	0.95
Leuning (1995) Leuning (1995b)	used for model parameterisation	0.05*	0.2*	0.95 0.9
Medlyn elt al. (2002)	used for model parameterisation	0.093 0.074$^{\Delta}$	0.372 0.29	0.9
de pury and Farquhar (1997)	used for model parameterisation	0.106	0.425	0.7
This study Man C14 (Φ=0.40) Man K34 (Φ=0.35) Jaru (Φ=0.35) Tapajos (Φ=0.30) Caxiuana (Φ=0.50)	used for model parameterisation	 0.085 0.074 0.074 0.063 0.106	 0.34 0.3 0.3 0.25 0.425	 0.7 0.7 0.7 0.7 0.7

*value including absorbed photon irradiance $^{\Delta}$ including leaf absorptance of 0.8

3.4.2 Data

The two major limitations to this data-model evaluation are the difficulties to estimate ecosystem respiration and the lack of energy balance closure from the eddy correlation data. Due to the spatial and seasonal

variability of soil respiration (Chambers et al. 2004; Silva de Souza 2004), but also due to different meteorological conditions (mainly precipitation regimes) during the measurement period and the period used here for model comparison, it is highly probable that there were differences between the measured respiration and that assumed for model comparison. Another source of uncertainty in the ecosystem respiration is associated to the leaf respiration term. There is increasing evidence to show that leaf respiration rates are lower when plants are photosynthetically active (Atkin et al. 2000; Atkin et al. 1998; Brooks and Farquhar 1985; Hoefnagel et al. 1998). Unfortunately, biochemical models of gas exchange do not include these effects yet and neither did the leaf level parameterisations used in this study. A recent study (Wohlfahrt et al. 2005) assessing daytime ecosystem respiration in a mountain meadow found that a failure to include light inhibition of canopy respiration resulted in an overestimation of daily estimates of ecosystem respiration and hence gross primary productivity from eddy correlation measurements. Their results suggest a reduction in estimated GPP from eddy correlation measurements on the order of 11-13% and 13-17% for a low and high estimate of the simulated maximum leaf-level reduction of dark respiration. Another study using eddy correlation data from various sites within Europe (Janssens et al. 2001) reports a 15% (as an upper limit) reduction in estimated total ecosystem respiration when considering daytime inhibition of leaf respiration.

Furthermore, there are considerable uncertainties in eddy correlation systems in the Amazon rainforest. For instance, there is a large sensitivity (10-25 % annually) to: the treatment of low frequencies and non-horizontal flow, being lower (<3 % annually) for the treatment of high frequency loss; delay corrections and data spikes (Kruijt et al. 2004). The total uncertainly in daytime measurements estimated for the Manaus K34 and Jaru site are ±12 and 32 % respectively (Kruijt et al. 2004). In addition to the uncertainties in the measured N_E at all sites, the estimates of total ecosystem respiration and use of modelled storage flux imposed another uncertainty to the comparison presented. Further, non-closure of the energy balance in the eddy covariance data (Aubinet et al. 2002; Massman and Lee 2002) forced the evaluation of energy partition in terms of evaporative fraction, but due to the high variability in the measurements we decided to test the model against mean diurnal cycles only.

In order to close the energy balance, fluxes of carbon and energy have been subject to different modes of data processing and post processing correction at each site, i.e., linear detrending and low frequency contributions to total fluxes (Finnigan et al. 2003; Malhi et al. 2002), angle of attack dependent calibration (Gash and Dolman 2003; van der Molen et al. 2004). With respect to linear detrending, and accounting for low frequency contributions and angle of attack dependent calibrations, in 2 out of 5 cases the energy balance improved and the CO_2 fluxes increased as well (Malhi et al. 2002; von Randow et al. 2004). In general, the non-closure of the energy balance at four of the five sites used could imply a possible missing CO_2 signal not being sensed by the measuring instruments and causing some of the model/data mismatch, but the extent to which this has occurred is unknown. After recalibration of fluxes for angle of attack and low frequency contributions, the energy and carbon fluxes increased (compared to data without this calibration) (Gash and Dolman 2003; van der Molen et al. 2004). However, the increase in percentage closure of energy fluxes was not always the same as the increase in percentage of carbon fluxes (See Table 3.23). Furthermore, Araújo A. (pers. comm.) obtained an increase of 8% on average for sensible, latent and CO_2 fluxes after recalculating the fluxes including the angle of attack correction for the Man K34 site.

Table 3.23. Increases of CO_2 and energy fluxes (in %) as measured by eddy correlation after corrections.

	Man C14	Jaru
Correction	Low frequency contribution[1]	Angle of attack[2]
Sensible heat	43.3	7.1
Latent heat	32.1	8.2
Day time CO_2	30.	11.3

[1] Malhi et al. (2002), [2] von Randow et al. (2004).

Increases in litterfall at the end of the wet season/onset of dry season are well documented for some sites in the Amazon region (Goulden et al. 2004; Klinge 1968; Luizao and Schubart 1987; Nepstad et al. 2002) but the expected decrease in LAI that accompanies this has not been measured and the phenology behind this phenomenon still needs to be better understood. Besides satellite derived LAI, in situ measurements of seasonality in LAI are very scarce for the Amazon region. Lacking this type of information/data, LAI seasonality was not included in any of the sites unless there were available LAI data (used only at Caxiuana). Seasonality of LAI is supposed to play a major role in driving seasonality of gross uptake at Caxiuana and Tapajos (Carswell et al. 2002; Goulden et al. 2004).

3.4.3 Model evaluation

The fact that the model had a bias towards overestimation of measured carbon uptake at high VPD (not fount at Man C14 and Caxiuana where residuals of carbon uptake did not show any trend with VPD), and temperature usually linked to afternoon values, shows the insensitivity of the model to close the stomata under these conditions. However, the observed decrease in CO_2 uptake at high VPD and air temperatures may not be caused by plant water stress because at least for the period studied, the original investigators have argued that there were no indications of water stress at Tapajos (da Rocha et al. 2004; Goulden et al. 2004; Saleska et al. 2003) nor at Jaru (von Randow et al. 2004). Manaus K34 was studied here only during the wet and end of dry periods. Furthermore, Tuzet et al. (2003) suggest that such model insensitivity to afternoon conditions (high VPD and air temperatures) may result from inadequate/ or in this case no coupling of stomatal conductance to the dynamics of water transport from soil to the roots and leaves. This suggests the need for a stomatal conductance formulation that includes stomatal regulation taking into account both the external environment (demand) but also the dynamics of water movement from the soil/root to the leaf (supply) (Fisher et al. 2006; Tyree 2003).

The underestimation of simulated latent heat fluxes at 4 of 5 sites could mean the model needs larger simulated G_s to fit the observations. For instance, the best simulated energy partition was at Man C14 which is the site with the highest V_{max} at the top of the canopy and a relatively high fitted quantum yield (0.4). At the same time, it was also the only site where the measurements managed to nearly close the energy balance. On the other hand, the worst simulated partition of energy balance was at Tapajos where not only the V_{max} at the top was lowest but also the fitted quantum yield (0.3). Furthermore, a larger simulated G_s could be obtained either by increasing the λ parameter from the stomatal conductance model or by increasing the simulated assimilation rate. Sensitivity analysis showed that by increasing λ, the C_i/C_a ratio increased and

therefore the simulated $\delta^{13}C$ decreased (becoming more negative), and usually this led to model underestimation with respect to the observations of $\delta^{13}C$. The second option would be to increase simulated G_P which automatically would lead to model overestimation with respect to the observations. However, if it would be possible to accept the fact that associated with a failure to close the energy balance there is an associated non-measured CO_2 flux signal, then the measured and simulated G_P should have been higher, which consequently would then increase the simulated latent heat and therefore improve the model comparison to evaporative fraction measurements.

Generally, besides the VPD bias towards overestimation (found at 3 of 5 sites) the sun and shade model performed well in simulating the carbon uptake of all tower sites, a finding supported by the reasonably well simulated $\delta^{13}C$. At the same time, the model failed to simulate the energy partition (overestimation of latent heat fluxes) at 4 out of 5 sites. Further, Morales et al. (2005) in a recent study evaluated 4 process–based models against eddy correlation flux data at 15 European sites and found that no single model performed well on both carbon and water fluxes, the two variables evaluated. According to Morales et al. (2005), two of the models better at simulating carbon fluxes and the remaining two models performed better in simulating water fluxes. Another modelling study using the land surface scheme of the Hadley Centre GCM carried out an evaluation with the same data set as used here for the Man K34 site, and obtained better results for carbon uptake than for energy partition (Mercado et al. 2007).

3.4.4 Scaling up to basin level

From the relationships between V_{max} and leaf N and leaf P, unfortunately there are only four data points and the high correlation coefficient obtained from the correlations between V_{max} with leaf P is due to a single point, which has the highest leaf P in the data set. Bearing in mind the limited data (4 points), these results could suggest the possibility of foliar P as a good predictor of photosynthetic capacity for Amazonian forests. This needs to be verified by field observations and unfortunately, the eddy correlation systems have never been installed at sites where leaf phosphorous concentrations are higher than at the 5 Brazilian sites used here. This is important, because Patiño et al. (in prep) found higher average foliar P for western sites such as in South Peru and Ecuador than the current Brazilian sites used in this study.

3.5 Summary

The sun and shade model was initially unable to accurately reproduce the observed net carbon uptake (G_P) and energy exchange using the parameterisation from Chapter 1 and 2 at the four remaining flux tower sites. There are two main reasons that can explain the model data discrepancy. First, discrepancies of maximum assimilation rates are linked to the V_{max} model parameter which was obtained from a relationship (V_{max} *vs* leaf N) that was found to predict much lower values of V_{max} than recently published regressions for other sites. The second reason is linked to model data discrepancies of G_P at low levels of irradiances. In this study we found that there are variations in the light response of the measured N_E and possibly of G_P (assuming a reasonable estimate of ecosystem respiration) across sites and therefore a single parameterisation (e.g. in this case adopted from Chapter 1) could not account for the observations at all sites. Therefore, reparameterisation (within measured uncertainty bounds) was needed. Even though there is still room for improvement, after reparameterisation, the sun and shade model could relatively well reproduce the

carbon uptake at all sites tested. This result is supported by the ability of model to reproduce values of $\delta^{13}C$ discrimination, although this was obtained with a poor partition of energy at 4 from 5 sites. Additionally, the sun and shade model coupled to the lambda model for stomatal conductance showed an inability to accurately capture carbon and energy fluxes at high VPD, over predicting fluxes due to poor performance of the stomatal conductance model under these conditions, suggesting the need for a better stomatal conductance formulation that includes both stomatal control from the outside environment (hydraulic demand) and also the dynamics of water transport from the roots to the leaf (hydraulic supply).

The major constraints to such model-data evaluation are imposed by the uncertainty in the estimates of ecosystem respiration, mainly due to the seasonality of soil respiration, but also CO_2 storage fluxes and uncertainties associated with measurements from the eddy correlation N_E and non-closure of the energy balance.

This modelling exercise can be used to extrapolate simulations to the basin level. We developed empirical relations between best fits of V_{max} and foliar N and P concentrations that can be tested to scale up to the basin level. Furthermore, the relationship between of V_{max} and P suggests the possibility of foliar P being a better predictor for canopy photosynthetic capacity than foliar N in these forests. This result highlights the need for field studies to further investigate the relationship between photosynthesis and leaf phosphorous in Amazonian forests. Bearing in mind that these relationships were derived from only four data points, one of which drives the regression (V_{max} *vs* leaf P), a step forward is taken in the next chapter by simulating the sensitivity of GPP to V_{max} parameterised using leaf P and leaf N at 35 sites across the Amazon Basin.

4 Predicting Gross Primary Productivity of rainforest across 35 sites in the Amazon basin

4.1 Introduction

Gross primary productivity (GPP) can be defined as the total amount of carbon fixed during photosynthetic CO_2 assimilation by vegetation. GPP is one of the two most important components of the carbon balance in terrestrial ecosystems, the other being the rate of ecosystem respiratory carbon losses. The amount of carbon absorbed by plants depends not only on the physiological capability of the plant but also on its environment. Radiation, nutrients, and water are among the major requirements for plant carbon assimilation. Constraints on plant physiological activity differ among ecosystems and geographic location. Water availability, temperature and radiation have been estimated to limit carbon uptake by plants over 40%, 33% and 27% of the Earth's vegetated surface, respectively (Nemani et al. 2003), with nitrogen (N) availability the main limiting nutrient for photosynthesis of higher plants (Field and Mooney 1986). GPP is highest in moist tropical areas where climatic and environmental conditions are most favourable (Lloyd and Farquhar 1996) with plants rarely limited by low temperatures and usually privileged in terms of radiation and water availability. Nevertheless in many tropical areas, highly weathered soils of low nutrient status predominate and this may provide a limitation on GPP through low levels of foliar phosphorous (P) and/or N (Lloyd et al. 2001).

Tropical rain forests constitute one of the major global ecosystems due to their productivity (Field et al. 1998; Grace et al. 2001; Melillo et al. 1993), their capacity to store carbon (Dixon et al. 1994) and their effects on global climate (Silva Dias et al. 1987; Zhang et al. 1996). Due to their environmentally privileged location, tropical forests assimilate and store large amounts of carbon, and are potentially a significant source of carbon to the atmosphere (Cox et al. 2000; Malhi et al. 1998; Saleska et al. 2003). Among all tropical ecosystems, the Amazon forest has recently received a great deal of attention due to its capacity to act as a source or sink of atmospheric carbon dioxide (Grace et al. 1995; Lloyd and Farquhar 1996; Phillips et al. 1998; Prentice and Lloyd 1998; Tian et al. 1998).

Recent research has also found major differences in above-ground net primary productivity (ANPP), above-ground biomass and tree dynamics across Amazonia. West Amazonia is more dynamic, with younger trees, higher stem growth rates and lower biomass than central and eastern Amazon (Baker et al. 2004; Malhi et al. 2004; Phillips et al. 2004). A factor of three variation in above-ground net primary productivity has been estimated across Amazonia by Malhi et al. (2004). Different hypotheses have been proposed to explain the observed spatial variability in ANPP (Malhi et al. 2004). First, due to the proximity of the Andes, sites from western Amazonia tend to have richer soils than central and eastern Amazon and therefore soil fertility could possibly be highly related to the high wood productivity found in western sites. Second, if GPP does not vary across the Amazon basin then different patterns of carbon allocation to respiration and above- and below-ground production could also explain the observed ANPP gradient. However since plant growth depends on the interaction between photosynthesis, transport of assimilates, plant respiration, water relations and mineral nutrition, variations in plant gross photosynthesis (GPP) could also explain the observed variations in ANPP. A basin wide application of the canopy level gas exchange model is therefore needed to

investigate spatial variability in GPP. Such a study differs from one using a global vegetation model (Cox et al. 1998; Sitch et al. 2003) where single plant functional type parameter values are assigned and assumed invariant with environmental condition. Instead, a more specific description of photosynthetic capacity across the basin is required. A study of this kind can inform the global vegetation/climate community as to the need for variability in key model parameters in order to accurately simulate carbon fluxes across the Amazon basin.

Under the assumption of nitrogen (N) limitation, leaf photosynthesis is usually modelled based on the measured linearity between photosynthetic capacity and N content per unit leaf area (Evans 1993; Field and Mooney 1986; Hirose and Werger 1987; Pettersson and McDonald 1994), and is scaled up to canopy level based on the hypothesis that N partitioning within canopies changes with growth irradiance in such a way as to maximize photosynthesis (Evans 1989a, 1989b, 1993; Hikosaka and Terashima 1995). This type of approach has also been used by the ecosystem/global modelling community. However, for tropical ecosystems it has been suggested that leaf phosphorous (P) rather than leaf N constrains rainforest productivity (Vitousek 1984; Vitousek and Sanford 1986). For instance, using foliar δ^{15}N Martinelli et al. (1999) found nitrogen to be relatively abundant in tropical rainforest in comparison to temperate forests. Additionally, Vitousek (1984) found low phosphorous concentrations (<0.04 %) in litterfall. Phosphorous concentrations were correlated with the amount of litterfall, suggesting that phosphorous is the major controller of litterfall production. It is likely that low foliar P content in tropical forest leaves limits leaf photosynthetic rate, at least for some forests (Lloyd et al. 2001).

The biochemistry of photosynthesis has been explained through the behaviour of a single enzyme, ribulose-1,5 –bisphosphate carboxylase-oxygenase (Rubisco), with its rate of carboxylation being limited by one of three processes (Farquhar et al. 1980) which independently respond to variations in intercellular CO_2 content (C_i), nutrient levels and radiation. At low C_i and high radiation, carboxylation is limited by the capacity of Rubisco to consume the CO_2 acceptor molecule, i.e. ribulose biphospate (RuBP); as C_i increases, carboxylation is limited by the rate at which (RuBP) is regenerated in the Calvin cycle through limited photosynthetic electron transport; and when both C_i and light are high, the RuBP generation can be limited by the rate of release of inorganic phosphorous (Pi) via starch and sucrose synthesis which may become insufficient to recycle the Pi sequestered in the production of triose phosphates. The latter limitation is also called triose phosphate utilization (TPU). Furthermore, at very high atmospheric [CO_2], photosynthetic rates are limited by TPU, thus phosphorous is a primary factor constraining the response of photosynthesis to increasing CO_2 (Harley and Sharkey 1991; Harley et al. 1992; Lewis et al. 1994).

Phosphorous is a key element in photosynthesis. It is needed to form the major product of photosynthesis, triose–phosphate, exported from the chloroplast to the cytosol in exchange for inorganic phosphate (P_i) (Lambers et al. 1998; Salisburry and Ross 1992). Additionally, phosphorous is contained in Calvin cycle enzymes, and in many sugar phosphates involved in respiration and other metabolic processes. Therefore, P plays a key role in energy metabolism due to its presence in important molecules that store energy which are essential to the Calvin cycle (Salisburry and Ross 1992). Several studies have shown yP deficiency to reduce photosynthesis (Brooks 1986; Campbell and Sage 2006; Jacob and Lawlor 1992; Sharkey 1985; Terry and Ulrich 1973). However, the mechanisms by which P deficiency affects photosynthesis are not well

understood (Campbell and Sage 2006). Triose phosphate utilization (TPU) is known to be a phosphate limitation mechanism to photosynthesis. This limitation is usually detected as a loss of O_2 sensitivity in photosynthesis (Sharkey 1985). However, several studies have found no TPU limitation in plants grown under P deficiency (Brooks 1986; Brooks et al. 1988; Campbell and Sage 2006). Other possible mechanisms by which P deficiency affects photosynthesis are via reductions in Rubisco activity (Brooks 1986; Brooks et al. 1988), reductions in the rate of RuBP regeneration, reduction of quantum yield due to photoinhibition caused by reduced efficiency of RuBP regeneration at low irradiances, and reductions in the Calvin cycle activity due to reductions in key regulatory enzymes of the cycle (Brooks 1986; Campbell and Sage 2006). Only the TPU mechanism of P limitation on photosynthesis has been incorporated into biochemical models of C_3 photosynthesis (Collatz et al. 1991; Harley and Sharkey 1991; Harley et al. 1992; Sage 1990). Implementation of the TPU limitation to photosynthesis in the Collatz et al. (1991) model suggests that the capacity of export or utilization of the products of photosynthesis is approximately equal to the maximum photosynthetic uptake at saturating irradiance, defining the TPU limitation as

$$J_s = V_{max}/2 \quad (1)$$

where J_s is the capacity of the export or utilization of the products of photosynthesis (most likely sucrose synthesis). However, many of the models that include TPU limitation predict photosynthesis to be insensitive to O_2 and CO_2 and thus can not explain the observations which indicate that under P deficiency increasing O_2 stimulates carbon uptake and increasing CO_2 inhibits carbon uptake (Harley and Sharkey, 1990).

Photosynthesis is usually modelled based on the measured linearity between photosynthetic capacity and N content per unit leaf area (Evans 1993; Field and Mooney 1986; Hirose and Werger 1987; Pettersson and McDonald 1994). This reflects the large investment of nitrogen in photosynthetic machinery (more than half of the total). Nitrogen limitation is widespread in natural ecosystems (Lambers 1998). However for tropical ecosystems, a few studies have shown a close correlation between photosynthesis and foliar P concentrations (Cromer et al. 1993; Lovelock et al. 1997; Raaimakers et al. 1995) (See Figure 2 in Lloyd et al. 2001). Likewise in Chapter 3 a close correlation between fitted top of the canopy V_{max} and measured leaf P was obtained. Note, the analysis was based on only four points, with a single point driving the regression. Nevertheless, existing data, albeit limited, suggests a close relationship between foliar phosphorous and photosynthesis in Amazon rainforest, and given the evidence of P deficiency reducing photosynthetic uptake, the possibility of P limiting photosynthesis across Amazonia warrants further investigation. In this chapter we test the sensitivity of simulated photosynthesis to the parameterizations of V_{max} based on leaf N and leaf P derived in Chapter 3. Taking into account the limitations of the model and data used to derive these relationships, rainforest GPP is simulated at 35 sites across the Amazon Basin. A unique data set of foliar N and P content and leaf area index taken in situ by the RAINFOR Consortium (www.geog.leeds.ac.uk/projects/rainfor) were used along with three hourly meteorology provided by the European Centre for medium range weather forecast (ECMWF) model as forcing data to simulate net assimilation for the period 1982-2001.

More specifically the main objectives of this chapter are:

First, following on from the findings of Chapter 3, in this chapter we test the sensitivity of simulated GPP at 35 sites to variations in specific model parameterisations and forcing: i) to variations in key model parameters (V_{max}, quantum yield and J_{max} / V_{max}), ii) to variations in the vertical distribution of N within the canopy, iii) to variations in leaf area index (LAI) and iv) the response of simulated GPP to a strong dry event.

Second, to test the sensitivity of simulated GPP at 35 sites across the Amazon Basin for the period 1982-2001 to the different parameterisations of rubisco capacity, i.e. V_{max} paramaterised based on leaf N and V_{max} parameterised based on leaf P.

Third, to identify the major factors influencing simulated photosynthesis at the 35 sites

Fourth, to detect spatial variability in simulated GPP and to ascertain the associated underlying causes by exploring relationships between this variability and climatology, LAI, and aboveground net primary productivity (ANPP).

Fifth, to evaluate simulated carbon uptake across the 35 sites using measured foliar isotopic fractionation ($\delta^{13}C$). These data are the only observations available to evaluate the simulations across the 35 rainforest sites in the Amazon Basin.

4.2 Material and Methods

4.2.1 Terminology

$G_{P(N)}$ and $G_{P(P)}$ represent the net carbon assimilation, i.e. gross uptake minus daytime canopy respiration, based on leaf N and leaf P parameterisations of canopy V_{max}, respectively. V_{maxN} and V_{maxP} are top of the canopy V_{max} parameterised with leaf N and leaf P, respectively.

4.2.2 Overview

To achieve the objectives, the following steps are undertaken:

For the first objective, a set of sensitivity experiments are carried out as explained in detail in section 4.2.3. A “control” canopy N distribution and a control LAI run for both $G_{P(N)}$ and $G_{P(P)}$ is chosen for subsequent simulations.

For the second objective, based on the results from Chapter 3, net canopy assimilation G_P is simulated at 35 sites across the Amazon basin using leaf N ($G_{P(N)}$) and leaf P ($G_{P(P)}$), respectively, as proxies for canopy photosynthesis in the parameterisation of the sun/shade model. G_P is simulated for the period 1982-2001, forced with modelled meteorology using LAI derived from satellite images and results from both simulations are compared. For the P based model, additional tests are conducted to investigate the conditions under which photosynthesis of sunlit leaves are not light limited at high irradiances. The transition from limitation

due to carboxylation capacity to limitation due to regeneration capacity mainly depends on the ratio of potential electron transport rate (Caemmerer and Farquhar 1981). Therefore simulations of $G_{P(P)}$ to variations in the J_{max} / V_{max} ratio and variations in quantum yield are tested.

To complete the third objective, an analysis of simulated monthly $G_{P(N)}$ and $G_{P(P)}$ and monthly forcing variables is presented in terms of possible linear relationships between simulated G_P and the forcing variables and variance decomposition of simulated monthly $G_{P(N)}$ and $G_{P(P)}$.

For the fourth objective, we relate simulated annual GPP (under the N and P simulations) averaged over the study period (1982-1991) at each site to the respective meteorology, LAI, measured aboveground net primary productivity (ANPP), above ground biomass, soil type, mean residence time canopy V_{max}, leaf N, leaf P and fraction of diffuse irradiance (F_d).

Finally, a comparison of modelled canopy δ^{13}C to measured δ^{13}C from top canopy leaves is presented at four sites where measurements are available.

4.2.3 Sensitivity tests

To achieve the first objective, the following sensitivity experiments for the N based simulation, i.e. $G_{P(N)}$, are undertaken:

1) To find out how variations in V_{max} affected variations in $G_{P(N)}$ across the transect, in this sensitivity test i) top of the canopy V_{max} is estimated using the different regressions of V_{max} against foliar N from Table 4.1 followed by ii) simulations of $G_{P(N)}$ using V_{max} parameterised using 3 regressions based on data from Manaus C14 and Caxiuana, Caxiuana only and Tapajos only (Table 4.1).

Table 4.1. Regressions of canopy V_{max} against foliar N on an area basis from different sources.

Source	Regression	r^2	Site
Carswell et al. (2000) and Vale et al. (2003)	V_{max} = 13.46 N - 2.8	0.8	Manaus C14 and Caxiuana
Vale et al. (2003)	V_{max} = 23 N - 17.2	0.98	Caxiuana
Domingues et al. (2005)	V_{max} = 23 N - 7.02	0.51	Tapajos
Obtained in Chapter 3	V_{max} = 4.32 N + 34	0.4	All 5 sites

2) Since all simulations presented in Chapter 3 were parameterised using the vertical distribution of leaf N measured at the Manaus C14 site (Carswell et al. 2000), in this test we examine the sensitivity of simulated $G_{P(N)}$ to various assumptions of vertical distribution of leaf N within the canopy.

3) Sensitivity of simulated $G_{P(N)}$ to LAI is tested by running the sun/shade model using the different scenarios of LAI. (See scenarios 1-4 in section 4.2.10).

From 2) and 3) a “control” N distribution and a control LAI run for both $G_{P(N)}$ and $G_{P(P)}$ is chosen for subsequent simulations in the rest of the study.

4) Since together with top of the canopy V_{max}, the canopy quantum yield parameter, Φ (equation 6 in Chapter 1) was one of the parameters adjusted in Chapter 3 to improve model comparison to observations, sensitivity of simulated $G_{P(N)}$ to variations in Φ (0.3, 0.4, and 0.5) is tested for all sites.

5) To test the effects of strong dry season events on simulated GPP, a $G_{P(N)}$ run is carried out assuming an extreme dry season event, i.e. a 30% decrease in relative humidity at all sites during all years.

4.2.4 Sites

The 35 sites used for model simulations were all primary rainforests in Amazonia located in Ecuador, Peru, Bolivia and Brazil (See Figure 4.1). For all sites foliar nutrients and leaf area index (LAI) data were collected as part of the RAINFOR Consortium (a network of forest plots across the Amazon basin that monitors forest biomass and dynamics aiming to understand their relationship to soil and climate (www.geog.leeds.ac.uk/projects/rainfor)). A description of these sites, based on Malhi et al. (2004), is presented in Table 4.2. In Table 4.2, dry season length is calculated by Malhi et al. (2004) as the average number of months per year with a rainfall less than 100 mm.

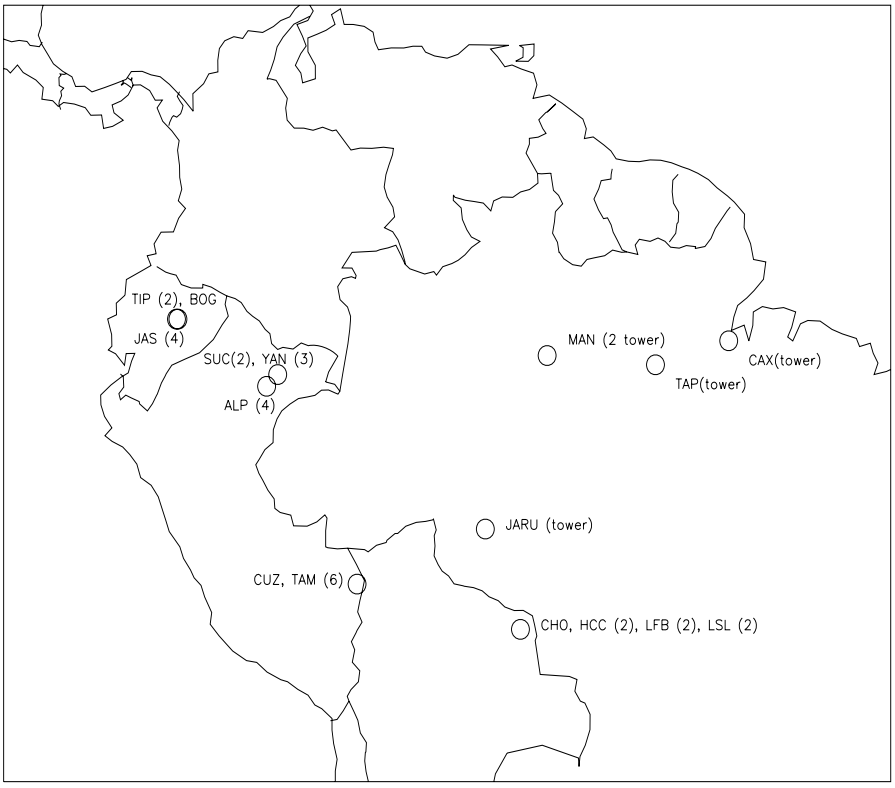

Figure 4.1. Rainforest site locations used in this study. The number of sites is given in parenthesis at locations with more than one site**.**

4.2.5 Soils

A brief description of the soil classification (with eight soil classes, taken from Malhi et al. (2004)) follows: class -1, corresponds to heavily leached white sandy soils, class-2 corresponds to heavily weathered, ancient oxisols that predominate in eastern Amazon, class -3 corresponds to younger soils and less ancient oxisols,

class -4 corresponds to less infertile lowland soils that predominate in lowlands from western Amazonia (ultisols and entisols), class -5 are soils containing alluvial deposits from the Holocene (less than 11500 years old), class -6 are young submontane soils perhaps fertilized by volcano-aeolian deposition (particularly sites in Ecuador), class -7 are seasonally flooded riverine soils, still in active deposition, and class -8 are poorly drained swamp sites, corresponding probably to histosols.

4.2.6 Leaf nutrient data: N and P

Leaf N and P contents of top canopy leaves (used to derive canopy V_{max}) are taken from the RAINFOR Consortium data set (data collected by S. Patiño at non- Brazilian sites and R. Paiva at Brazilian sites and analyzed at the Max Planck Institute for Biogeochemistry, Jena, Germany and at INPA, Manaus, respectively). The sampling protocol from the RAINFOR Consortium (unpublished data) includes an average of 20 trees sampled per plot. Leaf P and leaf N in [mg g^{-1}] were calculated as the mean value at each site. Leaf N in [g m^{-2}] is calculated using the mean of N content in [mg g^{-1}] and the mean specific leaf area, at each site (also measured as part of RAINFOR).

Table 4.2. Description of sites, locations, characteristics and type of forest modified from Malhi et al. (2004).

Plot Name and Description	Plot Code	Country	Longitude [°]	Latitude [°]	Elevation [m]	Forest Type	Annual Precipitation [mm]	Dry season Length [months]	Mean T corrected [°C]	Soil type	Soil class
Chore 1	CHO-01	Bolivia	-61.16	-14.35	170	liana forest	1357	6.23	26.17	younger oxisol (xanthic eutrustox)	3
Huanchaca Dos, plot 1	HCC-21	Bolivia	-60.75	-14.56	615	gallery forest	1332	6.44	23.53	inceptisol	6
Huanchaca Dos, plot 2	HCC-22	Bolivia	-60.74	-14.57	615	gallery forest	1332	6.44	23.53	inceptisol	5
Los Fierros Bosque I	LFB-01	Bolivia	-60.87	-14.61	225	terra firme	1313	6.46	25.96	younger oxisol	3
Los Fierros Bosque II	LFB-02	Bolivia	-60.85	-14.60	225	terra firme	1313	6.46	25.96	younger oxisol	3
Las Londras, plot 1	LSL-01	Bolivia	-61.13	-14.40	170	seasonally flooded	1424	6.00	25.70	ultisol (oxyaquic kandiudult)	7
Las Londras, plot 2	LSL-02	Bolivia	-61.13	-14.40	170	terra firme	1424	6.00	25.70	ultisol (oxyaquic kandiudult)	7
Cuzco Amazonico	CUZ-03	Peru	-69.11	-12.49	200	terra firme	2417	3.46	25.56	Holocene alluvial (inceptisol)	5
Tambopata plot zero	TAM-01	Peru	-69.28	-12.85	239	terra firme	2417	3.46	25.04	Holocene alluvial (typic dystrudept)	5
Tambopata plot one	TAM-02	Peru	-69.28	-12.83	207	terra firme	2417	3.46	25.20	Holocene alluvial (oxaquic dystrudept)	5
Tambopata plot two swamp edge clay	TAM-04	Peru	-69.28	-12.83	207	terra firme	2417	3.46	25.20	Holocene alluvial (oxaquic dystrudept)	5
Tambopata plot three	TAM-05	Peru	-69.28	-12.83	207	terra firme	2417	3.46	25.20	Pleistocene alluvial (kandiustult)	4
Tambopata plot four	TAM-06	Peru	-69.30	-12.83	214	terra firme	2417	3.46	25.16	Holocene alluvial (aquic durudept)	5
Tambopata plot six	TAM-07	Peru	-69.27	-12.83	209	terra firme	2417	3.46	25.19	Pleistocene alluvial (xanthic hapludox)	4
Allpahuayo A, poorly drained	ALP-11	Peru	-73.43	-3.95	114	terra firme	2763	0.77	26.34	entisol (typic endoaquent)	4
Allpahuayo A, well drained	ALP-12	Peru	-73.43	-3.95	114	terra firme	2763	0.77	26.34	ultisol (typic paleudult)	1
Allpahuayo B, sandy	ALP-21	Peru	-73.43	-3.95	114	terra firme	2763	0.77	26.34	ultisol (spodic udipsamment)	4
Allpahuayo B, clayed	ALP-22	Peru	-73.43	-3.95	114	terra firme	2763	0.77	26.34	ultisol (typic hapludult)	4

Table 4.2. cont.

Plot Name and Description	Plot Code	Country	Longitude [°]	Latitude [°]	Elevation [m]	Forest Type	Annual Precipitation [mm]	Dry season Length [months]	Mean T corrected [C]	Soil type	Soil class
Sucusari A	SUC-01	Peru	-72.90	-3.23	107	terra firme	2671	0.54	26.29	ultisol	4
Sucusari B	SUC-02	Peru	-72.90	-3.23	107	terra firme	2671	0.54	26.29	ultisol	4
Yanamono 01-02-03	YAN-01/02 /03	Peru	-72.85	-3.43	104	terra firme	2671	0.54	26.31	ultisol	4
Bogi 2	BOG-02	Ecuador	-76.47	-0.70	270	terra firme	3252	0.31	25.67	inceptisol	6
Jatun Sacha 2	JAS-02	Ecuador	-77.60	-1.07	450	terra firme	4013	0.18	23.38	inceptisol/oxisol	6
Jatun Sacha 3	JAS-03	Ecuador	-77.67	-1.07	450	terra firme	4013	0.18	23.38	ultisol/inceptisol	6
Jatun Sacha 4	JAS-04	Ecuador	-77.67	-1.07	450	terra firme	4013	0.18	23.38	inceptisol	6
Jatun Sacha 5	JAS-05	Ecuador	-77.67	-1.07	450	terra firme	4013	0.18	23.38	Holocene alluvial	5
Tiputini 3	TIP-03	Ecuador	-76.15	-0.64	248	seasonally flooded	3252	0.31	25.78	Holocene alluvial	7
Tiputini 5	TIP-05	Ecuador	-76.15	-0.64	258	terra firme	3252	0.31	25.78	Holocene alluvial	5
Manaus C14	Man-C14	Brazil	-60.11	-2.59	100	terra firme	2167	3	26.7	Older oxisol	2
Manaus K34	Man-K34	Brazil	-60.2	-2.6	100	terra firme	2272	3	26.7	Older oxisol	2
Caxiuana	Cax	Brazil	-51.53	-1.7	15	terra firme	2272	4	27	Older oxisol	2
Tapajos	Tap	Brazil	-54.96	-2.85	90	terra firme	1968	6	26.13	Older oxisol	2
Jara	Jaru	Brazil	-62.94	-10.08	150	terra firme	1600	5	26	Older oxisol	2

4.2.7 Foliar carbon isotopes

Measurements of foliar isotopic fractionation ($\delta^{13}C$) from top canopy leaves (Brazilian sites from Ometto et al. (2006) and non- Brazilian sites from the RAINFOR data set, not published) are used for model evaluation where available (not available for the Caxiuana site).

4.2.8 Meteorology

Besides recent (as part of the LBA project) meteorological measurements at the top of towers in different locations of the Brazilian Amazon, there is a lack of longer-term measurements of meteorological variables in the Amazon region at the time-scale required by the type of mechanistic model used in this study. For this reason this study used the meteorology produced as part of the ERA-40 project at the European Centre for medium range weather forecast, ECMWF (Betts and Viterbo 2005; Kallberg et al. 2004; Uppala et al. 2005). This provided modelled short-wave incoming radiation, air temperature and pressure, wind speed and specific humidity at three hourly time steps for the period 1982 –2001 with a resolution of 1.125 degree by 1.125 degree. Model output from the lowest atmospheric layer (model layer 60 which is 10 m above the surface) was used as forcing data for the sun/shade model at all sites. The sun/shade model was run at the same 3-hourly temporal resolution as the ECMWF data. Simulated photosynthesis was summed over the 5 daytime 3-hourly time steps to provide daily net photosynthetic uptake.
Because of the relatively large grid size and the clustered distribution of sites, the 35 sites occupied only 12 grids cells of the modelled meteorology. Description and assessment of the meteorology used are given in Appendix 4A in terms of spatial distribution of mean annual values of meteorological variables, mean annual and mean diurnal cycles and a short assessment of simulated annual climatic trends is also presented.

From the assessment of the ECMWF meteorology in Appendix 4A, a general consistency in the ECMWF meteorology from year-to-year is found, but assessment in terms of interannual variability due to ENSO events was poor and in general difficult to evaluate due to the lack of available precipitation data at each of the sites. Therefore, no analysis of potential effects of interannual variability caused by ENSO events was undertaken as part of this study. Due to differences between the reported climatic patterns from the literature and the patterns in the ECMWF meteorology (See Appendix 4A), this analysis does not focus on inter-annual variations in gross primary productivity. Rather, the focus is to detect spatial variation in simulated G_P across the sites and to ascertain the associated underlying causes.

4.2.9 Atmospheric carbon dioxide concentration

Six monthly atmospheric CO_2 concentration from 1982-2001 (340 to 373 ppm) were used as input data. Data corresponds to atmospheric CO_2 concentrations derived from in situ air samples collected at Mauna Loa Observatory, Hawaii (Keeling and Whorf 2002). Diurnal variation in atmospheric CO_2 above and within the forest canopy were measured at the rainforest in Jaru (Lloyd et al. 1996),

changing from about 410 μmol mol^{-1} in the early morning to 350 μmol mol^{-1} in the afternoon at the top of the canopy, with atmospheric CO_2 being substantially higher one meter above the forest floor. Instead of looking at diurnal variations in CO_2 uptake, the major interest in this chapter is to simulate monthly and annual G_P. Therefore above and within canopy CO_2 concentrations are taken as constant model inputs (at the mean six monthly value) assuming that neglecting its diurnal variability would not have a major impact on the overall result.

4.2.10 LAI data

A description of the two LAI data sources and how the data were used in simulations of G_P is included in Appendix 4A. From the two LAI data sets, the following four scenarios of LAI were developed to investigate the sensitivity of modelled G_P to LAI:

1) Satellite derived LAI from Global Inventories Monitoring and Modelling Studies, GIMMS, project (Nemani et al. 2003) corrected for LAI values higher than 7.0 and lower than 3.5. This correction was undertaken due to unrealistic values of satellite-derived LAI at these rainforest sites. Measured values range between 4 and 7 m^{-2} leaves m^{-2} ground (RAINFOR Consortium, unpublished data, Asner et al. 2004).
2) In an attempt to smooth the monthly changes in LAI, a 7 month running mean was applied to the satellite LAI.
3) LAI derived from hemispherical photographs (RAINFOR Consortium, unpublished data) within each forest, taken as constant throughout the simulation and
4) LAI derived from hemispherical photographs (RAINFOR Consortium, unpublished data), with a 20% reduction applied during the dry season months (monthly rainfall <100 mm). This reflects possible reductions in LAI during the dry season months (Asner et al. 2004), and aims to detect the sensitivity of the mean annual simulated G_P to seasonal LAI fluctuations. Lacking data on the exact dry season LAI reduction (Goulden et al., 2004), an arbitrary value of 20 % value was chosen. This corresponds to approximately the upper bound of the observed seasonal variation in LAI in response to seasonal dry periods as observed in Amazon forests (Asner et al. 2004, Nepstad et al. 2002).

4.2.11 Model Parameterisation

At high (Harley and Sharkey 1991; Harley et al. 1992) and moderate atmospheric CO_2 concentrations (Sharkey et al. 1986), RuBP regeneration has been found to be limited by Triose phosphate utilization (TPU) usually in plants grown with sufficient P. Conversely, under P limited conditions, some studies have found no TPU limitation, but instead decreases in rubisco levels and rubisco activity, although most often, reductions in RuBP regeneration capacity have been reported (Brooks 1986; Brooks et al. 1988; Campbell and Sage 2006; Sharkey 1985). Taking this into account, an attempt to include the effect of foliar P contents on photosynthesis simulated by the sun and shade model is carried out in a simple way, by directly relating leaf P to V_{max}. Based on the definition of TPU limitation by Collatz et al. (1991) in which TPU is a function of V_{max} (equation 1), it was decided to use the V_{max} *vs* leaf P relationship obtained in Chapter 3 for parameterisation of top of the canopy V_{max} across the study transect. In this way, leaf P is not directly included in the TPU limitation but indirectly leaf P affects

both the Rubisco or CO_2 limited rate of photosynthesis (through V_{max}) and also the RuBP regeneration or light limited rate (through J_{max}).

Bearing in mind the conditions (only 4 points with one point driving the regression coefficient) at which the regression between V_{max} and leaf P was obtained in Chapter 3 (Figure 4.2), parameterisation of canopy top V_{max} was derived from measured top of the canopy leaf P at each site.

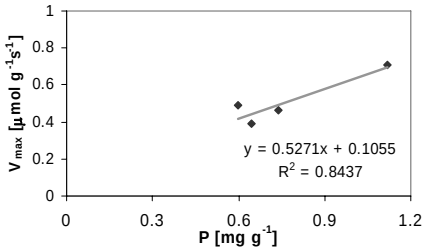

Figure 4.2. Regression of top canopy V_{max} *vs* Leaf P [mg g^{-1}] obtained in Chapter 3 from fitted V_{max} at Man K34, Jaru, Caxiuana and Tapajos when quantum yield was 0.4.

A similar approach to parameterise canopy V_{max} and J_{max} is adopted as for the five tower sites in Chapter 3, i.e. using foliar N and P data from leaves sampled at the top of the canopy and LAI from the RAINFOR Consortium data set data set (unpublished data) to calculate canopy V_{max}. As foliar nitrogen is party responsible for foliar maintenance energy cost (Lambers et al. 1998), canopy respiration R_C was parameterised for both $G_{P(N)}$ and $G_{P(P)}$ simulations using foliar N as indicated in Chapter 1 and Chapter 3. Parameterisation of quantum yield of photosynthesis, Φ, was taken as 0.4 for control simulations at all sites and other quantum yields were tested for sensitivity analysis purposes. λ, the lambda parameter used in the stomatal conductance model was taken as 1200 mol mol^{-1} for non Brazilian sites and for Brazilian sites it was taken as parameterised in Chapter 3. The same values of λ and quantum yield were taken as in simulations for the Manaus C14 site (for non Brazilian sites) because in terms of energy balance closure, this site had the most reliable data set that allowed best comparisons of carbon and energy fluxes. The J_{max} / V_{max} ratio was set at 1.92, as originally parameterised for all tower sites. Finally, the remaining parameters from the Farquhar et al. (1980) photosynthesis model *viz*. the curvature factor of the light response curve, θ, and the temperature sensitivity parameters of the electron transport rate S_J and H_J and the parameters for temperature sensitivity of Rubisco and leaf respiration, were taken as in Chapter 1.

4.2.12 Vertical distribution of N within the canopy

When considering an exponential distribution of leaf N with increasing cumulative leaf area within the canopy, the rate of decline in leaf N is defined by the N allocation coefficient (k_n), the exponent of the exponential curve (Equation 2). The exponential and its correspondent N allocation coefficient for control simulations are defined from the following distribution of V_{max} with cumulative leaf area (distribution obtained using data of vertical distribution of V_{max} and cumulative leaf area for the Manaus C14 site in Chapter 3): Average V_{max} for the top and bottom half of canopy leaves is 65% and 35% of the V_{max} at the top of the canopy, respectively. The total canopy V_{max} is calculated as:

$$V_{\max\_canopy} = \frac{V_{\max}\left(1 - e^{-k_n * LAI}\right)}{k_n} \quad (2)$$

where V_{max} and V_{max_canopy} are the top and total canopy V_{max} values, respectively.

Once the N allocation coefficient was determined at each site, a sensitivity test was performed for other possible values of N allocation coefficients (See Appendix 4B) whilst keeping LAI and total canopy leaf N constant.

4.2.13 Simulation of δ^{13}C

Simulated isotopic composition of the canopy δ^{13}C (‰) was calculated over the period (1992-2001) following Farquhar et al. (1982):

$$\delta^{13}C = \delta_{atm} - a - (b - a)C_i / C_a \quad (3)$$

where a corresponds to maximum fractionation due to diffusion of CO_2 in air (4.4 ‰) and b is the maximum fractionation in the carboxylation reaction (30 ‰) (Farquhar et al. 1982). δ_{atm} is δ^{13}C of air and it is taken as -8.0 (‰), the late twentieth century mean atmospheric background value (Ehleringer et al. 1987). The ratio C_i/C_a corresponds to simulated daytime hourly values for the whole canopy. The simulated average integral of photosynthetic discrimination during each year ($\overline{\delta^{13}C}$) was calculated with equation (3) using the photosynthetic flux weighted average C_i/C_a :

$$\overline{\delta^{13}C} = -12.4 - 25.6\frac{\sum_{i=1}^{n} G_{Pi} * (C_i / C_a)}{\sum_{i=1}^{n} G_{Pi}} \quad (4)$$

4.3 Results

4.3.1 Sensitivity tests

The major findings of the sensitivity runs 1-6 are given below, with further information found in Appendix 4B.

1) Sensitivity of top of canopy V_{max} and its variation across the study transect to the relationship of V_{max} *vs* leaf N adopted

As expected, V_{max} at the top of the canopy and its variation across sites was very sensitive to the V_{max} against foliar N regression used in its estimation. V_{max} was lowest using the regression derived from the Manaus and Caxiuana data sets (Table 4.1). Additionally, V_{max} varied least (a factor of 1.3 variation) using the regression obtained from the fitted V_{max} at the tower sites from Chapter 3

(See Figure 4B-1). Given the large variation in top of the canopy V_{max} across sites for the different relationships between V_{max} and leaf N from Table 4.1 (a factor of 3.5, 3.8 and 6 variation using regressions from Manaus and Caxiuana, only Caxiuana and only Tapajos, respectively), the sensitivity of the simulated $G_{P(N)}$ to such relationships was therefore examined.

2) Sensitivity of simulated $G_{P(N)}$ across the study transect to variations in top of the canopy V_{max}
Simulations of $G_{P(N)}$ were undertaken with V_{max} parameterised using three of the relationships from Table 4.1. For V_{max} against foliar N regressions obtained from Tapajos data and from Manaus and Caxiuana data, simulated $G_{P(N)}$ (mean annual averaged over 1982-2001) varied by a factor of 1.6 and 2.8, respectively across the 35 sites. Using the regression derived from Tapajos data, mean annual simulated $G_{P(N)}$ was similar to the $G_{P(N)}$ simulated using the regression obtained in Chapter 3, but the variation in $G_{P(N)}$ across sites using the Tapajos regression was larger. Hence simulated G_P was very sensitive to the regression used to determine the V_{max} at the top of the canopy. Table 4.3 includes a summary of the main differences in the $G_{P(N)}$ simulation over the study period for the different regressions. As expected, $G_{P(N)}$ simulated using the regression from Manaus and Caxiuana data was lowest, due to the low V_{max} from top canopy leaves.

Table 4.3. Maximum, minimum and mean annual $G_{P(N)}$ in [Mg C $ha^{-1}yr^{-1}$] from all 35 sites simulated over the period 1982-2001 using different parameterisations of V_{maxN} at the top of the canopy.

Regression	$G_{P(N)}$	Max $G_{P(N)}$	Min $G_{P(N)}$	Max $G_{P(N)}$/ Min $G_{P(N)}$
Obtained in Chapter 3,	32	36	29	1.2
From Tapajos data	31	39	24	1.6
From Manaus and Caxiuana data	21	36	13	2.8

3) Sensitivity of simulated $G_{P(N)}$ across the study transect to variations in the vertical distribution of leaf N within the canopy
Sensitivity tests of $G_{P(N)}$ to the vertical distribution of N within the canopy include steeper or less uniform N distributions than that measured at Manaus C14. This results in reduced assimilation compared to the control run (on average reductions of 4 and 2 %, See Table 4B-1) when the nitrogen allocation coefficient, k_n, was taken as 0.5 and 0.8 but slightly higher assimilation, on average 0.3% and 7%, when k_n was taken equal to 1 and 0, respectively. The low sensitivity of simulated $G_{P(N)}$ to variations in N distribution is explained in Appendix 4B by comparing the vertical profiles of V_{max} for the different N distributions to the control N distribution (See Figure 4B-2 for vertical profiles of V_{max}).

From these results, it can be concluded that under the same total canopy nitrogen and LAI as considered in the control run (N distribution inferred from measurements at Manaus C14), the simulated mean annual $G_{P(N)}$ averaged over the 1982-2001 period (Table 4B-1) was insensitive to the use of different nitrogen allocation coefficients.

4) Sensitivity of simulated $G_{P(N)}$ across the study transect to variations in LAI
Using various scenarios of LAI, results show that at the stand scale mean annual $G_{P(N)}$ for the period

1983-2001 was relatively insensitive to the method by which LAI was derived (See Figure 4B-3 and section 7.2.3 in Appendix 4 B).

For subsequent analyses, control scenarios are run using the V_{max} *vs* leaf N relationship obtained in Chapter 3, canopy N allocation inferred from measurements at Manaus C14, and LAI derived (Nemani et al. 2003) corrected for values higher than 3.5 and lower than 7.0.

5) Sensitivity of simulated $G_{P(N)}$ across the study transect to variations in quantum yield of light absorption

Comparison of simulated mean annual $G_{P(N)}$ averaged over the period 1982-2001 and over all 35 sites, parameterised with Φ equal to 0.5, 0.4 and 0.3 showed that simulated $G_{P(N)}$ with Φ =0.4 and 0.3 are on average 10 % and 25 % lower than simulated $G_{P(N)}$ with Φ= 0.5. Simulated G_P with Φ= 0.3 is on average 83 % of simulated G_P with Φ= 0.4. Quantum yield affects photosynthesis simulated under light limited conditions, which affects both sunlit and shaded leaves. Due to canopy structure and LAI of these rainforests, a high percentage of the leaves are located in the shade. See Figure 4.3 for the percentage of leaves under shade estimated according to the sun and shade model for various values of LAI at different solar angles. Furthermore, since shaded leaves receive only diffuse light and are always light limited their efficiency of carbon uptake depends on quantum yield. This means that photosynthesis undertaken by shaded leaves is totally dependent on the quantum yield parameter used for their simulations.

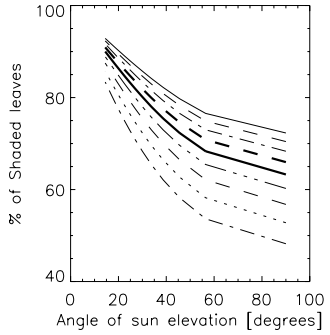

Figure 4.3. Percentage of shaded leaves as estimated by sun /shade for various values of LAI as a function of the angle of elevation of the sun. Lines represent LAI ranging from 3 to 7 in increments of 0.5 m^2 m^{-2} (from bottom to top).

6) Sensitivity of simulated $G_{P(N)}$ across the study transect to drought

As a result of assuming a 30% decrease in relative humidity at all sites during all years, $G_{P(N)}$ was reduced by 6% on average (ranging from 8.4 -3.8 %) for all sites when compared to control simulations. A larger reduction in $G_{P(N)}$ due to the imposed 30% reduction in relative humidity was expected. However the minor reduction in $G_{P(N)}$ is linked to the insensitivity of the stomatal conductance model at high VPD conditions as has been shown in Chapter 3

4.3.2 Simulated $G_{P(P)}$ *vs* $G_{P(N)}$ across the transect

Simulated mean annual G_P, averaged over the period 1982-2001 for both $G_{P(P)}$ and $G_{P(N)}$ is presented in Figure 4.4-A. Simulated $G_{P(N)}$ was largest in Brazil at Man-C14 and lowest in south Peru at

TAM-07. On the other hand, under the P based simulation, $G_{P(P)}$ was lowest in Brazil at Cax and highest in North Peru at ALP-21. Simulated $G_{P(P)}$ varied between 29 and 51 Mg C ha^{-1} yr^{-1} across the transect with a mean value of 36 Mg C ha^{-1} yr^{-1} and the corresponding values for $G_{P(N)}$ were [29-36] and 32 Mg C ha^{-1} yr^{-1}. This shows a larger variation for the $G_{P(P)}$ simulation (a factor of 1.8 variation) than under the $G_{P(N)}$ simulation (factor of 1.2 variation).

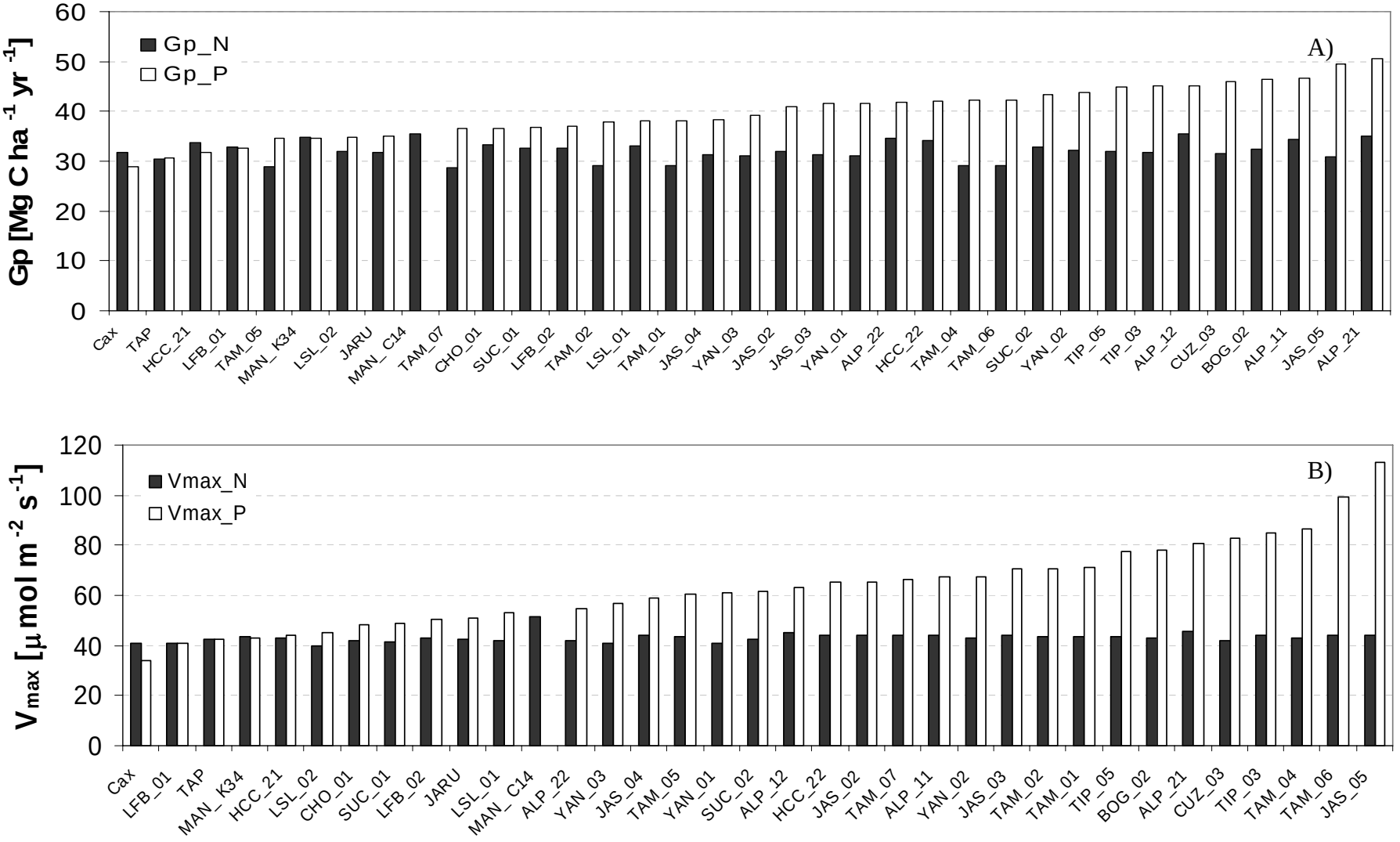

Figure 4.4. A) Mean annual $G_{P(P)}$ and $G_{P(N)}$ averaged over the period 1982-2001 organized from lowest to highest $G_{P(P)}$. B) Top canopy V_{max} calculated using leaf P (V_{maxP}) and leaf N (V_{maxN}) organized from lowest to highest V_{maxP}.

In general for non-Brazilian sites, simulated $G_{P(P)}$ was higher than $G_{P(N)}$ (at 28 out of 30 sites), due to the higher V_{maxP} from top canopy leaves used for the $G_{P(P)}$ simulations (See Figure 4.4B). V_{max} used for the simulations based on leaf P content, V_{maxP}, was higher than V_{maxN} for many sites in western Amazonia. This is because on the older oxisol soils of central and eastern Amazonia, foliar P are typically much lower than for the younger soils of western Amazonia. In contrast foliar N does not have a large variation across the basin. Figure 4.5 shows foliar P against foliar N for all sites on a dry weight basis. Foliar N varies by a factor of 2 while foliar P varies by a factor of 4. Also, variation in V_{maxP} across sites (variation by a factor of 3.3) was larger than in V_{maxN} (variation by a factor of 1.2).

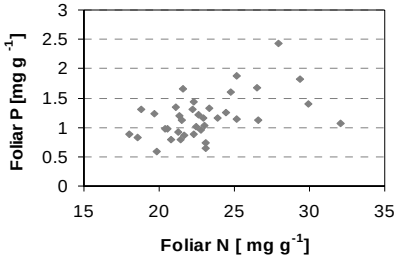

Figure 4.5. Foliar P against foliar N from top canopy leaves at 34 sites. There was no available data of foliar P from top canopy leaves from the Man-C14 site.

Main differences between the $G_{P(N)}$ and $G_{P(P)}$ simulations

The larger estimated V_{maxP} compared to V_{maxN} for the non-Brazilian sites created various differences between the simulated $G_{P(N)}$ and $G_{P(P)}$:

-According to simulations carried out using V_{maxN}, photosynthesis of sun leaves was usually Rubisco limited above about 500-800 μmol $m^{-2}s^{-1}$ quanta PAR. But using V_{maxP}, photosynthesis of the sun leaves was rubisco limited only at PAR values above 1000-1500 μmol $m^{-2}s^{-1}$ quanta PAR at sites with intermediate values of V_{maxP}. At sites where V_{maxP} was highest, photosynthesis by sunlit leaves was always modelled to be light limited. South Peruvian sites at Tambopata (TAM) illustrate this well. V_{maxP} at the TAM sites (6 sites) varies between 60.5 and 99.4 μmol $m^{-2}s^{-1}$ with the TAM sites having the lowest incoming solar radiation of the sites in the data set (Figure 4A-2). The combination of these two factors (high V_{maxP}, low irradiance), mainly the first, produced light limitation of simulated photosynthesis by the sunlit leaves at all irradiances (maximum irradiance only about 1500 μmol $m^{-2}s^{-1}$ PAR). Whether or not this actually occurs for these forests it is difficult to assess without direct measurement. To find under which conditions photosynthesis of sunlit leaves would not be light limited at high irradiances using the paramaterised V_{maxP}, a test was undertaken. The transition from limitation due to carboxylation capacity to limitation due to regeneration capacity mainly depends on the ratio of potential electron transport rate (Caemmerer and Farquhar 1981). Therefore sensitivity of simulated $G_{P(P)}$ to variations in the J_{max} / V_{max} ratio and variations in quantum yield were tested

Sensitivity of simulated $G_{P(P)}$ to variation in the J_{max} / V_{max} ratio and quantum yield

This sensitivity test was carried out using a quantum yield of 0.5 (0.4 was the parameterised value for control run) and J_{max} / V_{max} ratio of 2.0 and 2.5 for two sites (1.92 was the parameterised value for the

control run), JAS-03 (Ecuador) and TAM-01 (south Peru). Both sites have similar top of the canopy values of V_{maxP} (70.5 and 71.2 μmol $m^{-2}s^{-1}$ respectively) but belong to different grids of climatology (lower irradiance at TAM-01, Figure 4.A2). Compared to the control simulation, with a quantum yield of 0.5 the simulated electron transport limited velocity increased, producing more frequent limitation by Rubisco at high light levels. However, as a result of increasing the J_{max} / V_{max} ratio, Rubisco limitation was more frequently observed at high irradiances (See Figures 4.6 and 4.7) and had a larger effect than the increase in quantum yield. In summary in order to have non light-limited photosynthesis of sunlit leaves under the parameterised V_{maxP} (70.5 and 71.2 μmol $m^{-2}s^{-1}$ respectively) it is necessary to use a larger J_{max} / V_{max} ratio than parameterised under control simulations.

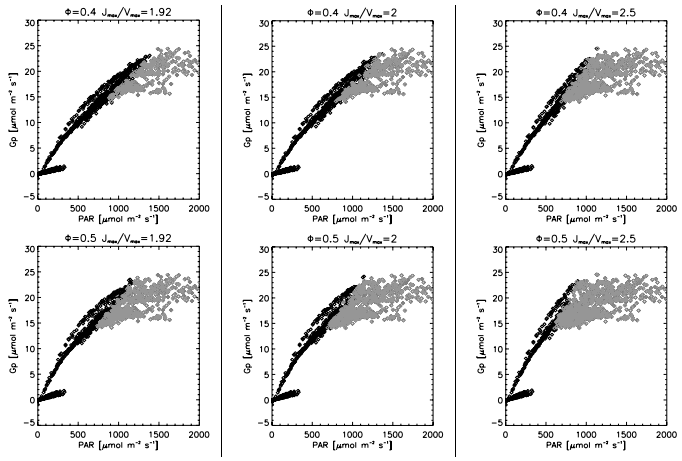

Figure 4.6. Sensitivity analysis of simulated $G_{P(P)}$ by the sunlit leaves at Jas-03 (V_{maxP} =70.5 μmol $m^{-2}s^{-1}$) to variations in quantum yield and ratio of J_{max} / V_{maxP}. Grey points correspond to rubisco limited and black points correspond to light limited conditions.

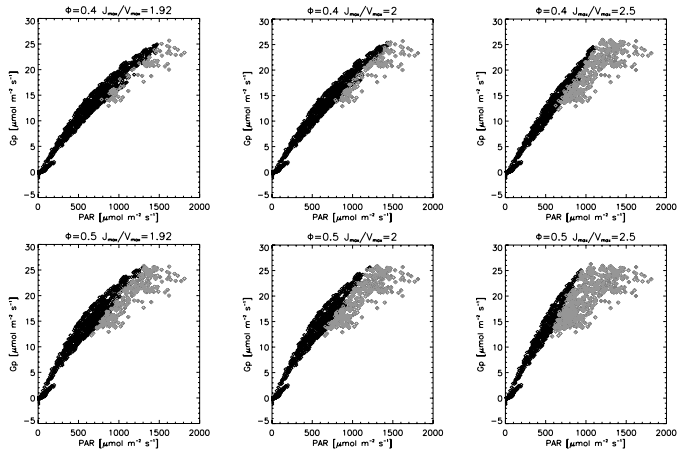

Figure 4.7. Sensitivity analysis of simulated $G_{P(P)}$ by the sunlit leaves at Tam-01 (V_{maxP} =71.2 μmol $m^{-2}s^{-1}$) to variations in quantum yield and ratio of J_{max} / V_{maxP}. Grey points correspond to rubisco limited and black points correspond to light limited conditions

4.3.3 Main variables affecting the simulated monthly $G_{P(N)}$ and $G_{P(P)}$ photosynthesis

To find out about the main variables affecting the simulated $G_{P(N)}$ and $G_{P(P)}$, scatter plots of monthly values of $G_{P(N)}$ and $G_{P(P)}$ against the various climatological and non climatological variables (air temperature, incoming short wave direct and diffuse irradiance, diffuse fraction (F_d), precipitation, atmospheric [CO_2], and LAI) are shown in Figures 4.8 and 4.9 for 5 sites for the $G_{P(N)}$ and $G_{P(P)}$, respectively. Each site in Figures 4.8 and 4.9 represents one geographical region and also each site belongs to a different grid from the ERA 40 meteorology. From the scatter plots a strong linear relationship between the simulated photosynthesis and solar diffuse irradiance is found for the $G_{P(N)}$ simulation in all regions. For $G_{P(P)}$, a strong linear relationship with diffuse irradiance was found at sites in Brazil and Bolivia with $G_{P(P)}$ in South and North Peru and Ecuador having a strong relationship with total solar radiation. The strong linear relationships suggest that a high percentage (50-90 %) of the variance in the simulated photosynthesis can be explained by variations in solar diffuse irradiance (for $G_{P(N)}$ in all regions and $G_{P(P)}$ in two regions) or by solar radiation ($G_{P(P)}$ in three regions).

Regression coefficients from the relationships with monthly solar radiation were higher under the $G_{P(P)}$ simulation than those obtained under the $G_{P(N)}$ simulation at sites in north and south Peru and Ecuador. This can probably be explained by the fact that sun leaves were generally more frequently light limited than rubisco limited in the $G_{P(P)}$ simulations, and visa versa for the $G_{P(N)}$ simulation. Sun leaves receive both direct and diffuse radiation and light limitation of photosynthesis is dependent on the rate of electron transport which can be limited by the amount of incoming radiation and the quantum yield of absorbed light (Farquhar et al. 1980).

Of the remaining variables presented in Figures 4.8 and 4.9, no strong relationships with $G_{P(N)}$ or $G_{P(P)}$ were found across all sites. Only in some cases a single variable had a strong relationship with $G_{P(N)}$ or $G_{P(P)}$ in individual regions, for instance diffuse fraction and temperature with $G_{P(N)}$ or $G_{P(P)}$ at Caxiuana. As explained in the methods, the total canopy level V_{max} was calculated as the integral of leaf level V_{max} over the total canopy LAI (equation 3). Therefore the total canopy level V_{max} is proportional to the LAI at each site. For this reason, scatter plots and correlations of $G_{P(N)}$ and $G_{P(P)}$ with total canopy V_{max} were similar to scatter plots between $G_{P(N)}$ and $G_{P(P)}$ and LAI at each site and therefore are not shown.

Variance decomposition of the simulated monthly $G_{P(N)}$ and $G_{P(P)}$ was undertaken for the same sites as in Figures 4.8 and 4.9. This calculation was carried out using a software for Bayesian analysis of Computer models (The Gaussian Emulation Machine for Sensitivity Analysis, GEM-SA, Centre for Terrestrial Carbon dynamics, University of Sheffield). Variance decomposition provides for each input (meteorology and LAI), its expected proportional contribution to the output ($G_{P(N)}$ or $G_{P(P)}$) variance and in this way it is possible to rank the inputs. Generally, the total will not sum to 100% because sometimes there are contributions from interaction (between variables) effects. Results from this analysis for the 5 selected sites (Tables 4.3 and 4.4 for $G_{P(N)}$ and $G_{P(P)}$, respectively) show solar diffuse irradiance to contribute most to the variance in $G_{P(N)}$ but also to $G_{P(P)}$, thus showing the

important contribution of this variable to the total output ($G_{P(N)}$ or $G_{P(P)}$) uncertainty.

Table 4.4. The percentage variance contribution of each input (Meteorology, [CO2] and LAI) on simulated $G_{P(N)}$.

	CAX Brazil	HCC-21 Bolivia	TAM-05 South Peru	ALP-21 North Peru	JAS-02 Ecuador
Solar	34.91	0.71	1.98	21.60	1.84
Solar diffuse	56.23	80.05	70.59	48.83	63.73
F_d	1.33	11.47	21.27	9.06	13.60
Air T	1.02	2.60	1.80	3.29	7.50
Precipitation	0.26	0.21	0.09	0.17	2.91
LAI	3.37	2.34	1.40	7.60	5.86
$[CO_2]$	1.56	1.68	1.64	7.76	2.42
Total	98.68	99.061	98.97	97.90	97.86

Table 4.5. The percentage variance contribution of each input (Meteorology, $[CO_2]$ and LAI) on simulated $G_{P(P)}$.

	CAX Brazil	HCC-21 Bolivia	TAM-05 South Peru	ALP-21 North Peru	JAS-02 Ecuador
Solar	7.03	0.56	0.57	30.92	5.59
Solar diffuse	78.40	78.98	64.48	34.86	59.16
F_d	5.41	11.66	30.67	24.84	17.16
Air T	0.43	4.58	21.8	3.45	8.43
Precipitation	0.41	0.36	0.02	0.1	1.58
LAI	5.78	1.28	0.84	2.81	4.23
$[CO_2]$	2.04	1.73	1.23	3.02	1.87
Total	99.5	99.4	100	100	98.016

.

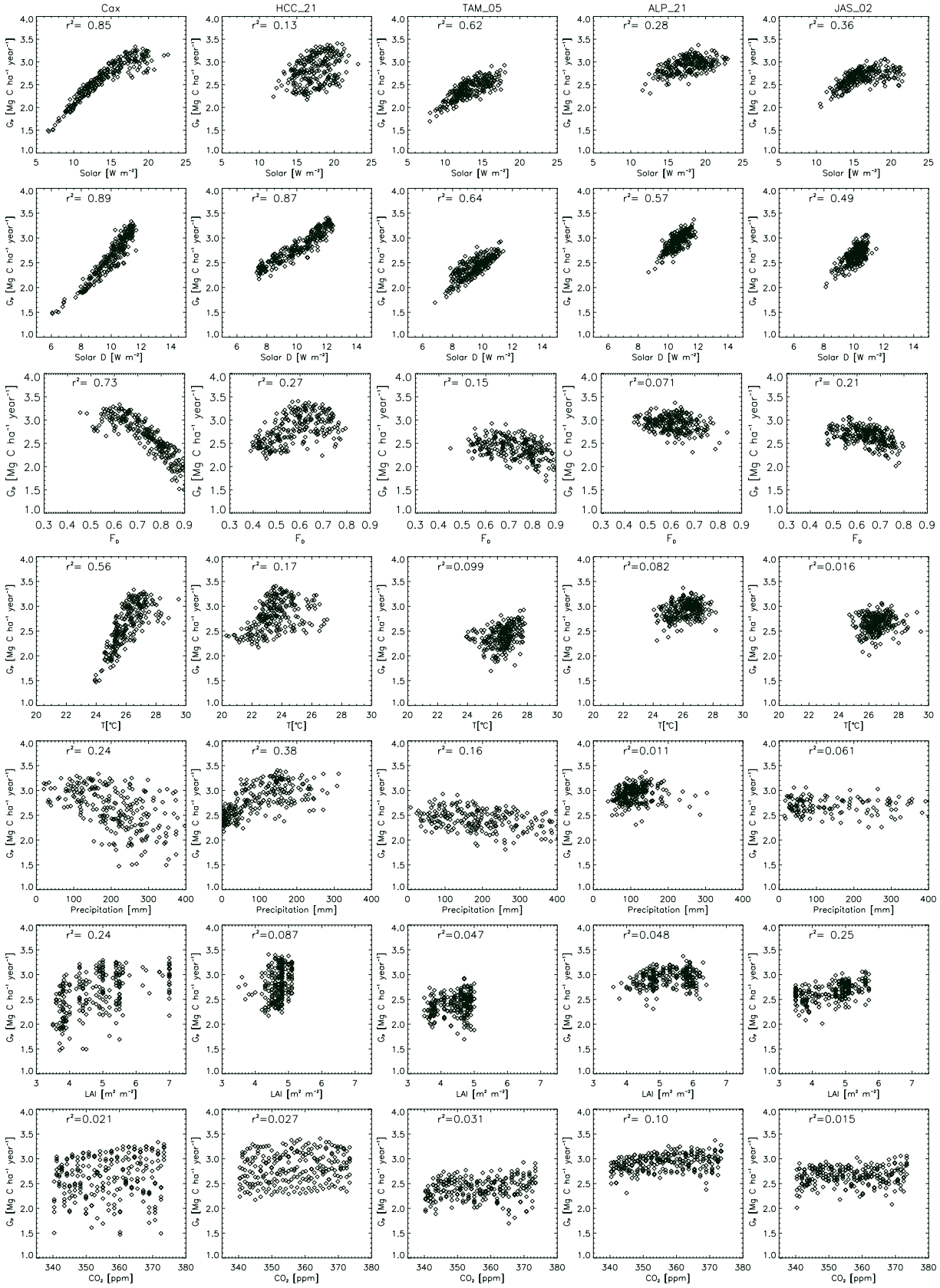

Figure 4.8. Scatter plots of monthly simulated $G_{P(N)}$ and monthly values of solar and solar diffuse radiation (Solar D), diffuse fraction (F_d), air temperature, precipitation, LAI and atmospheric [CO_2] for 5 selected sites located from left to right in Brazil, Bolivia, southern Peru, northern Peru and Ecuador.

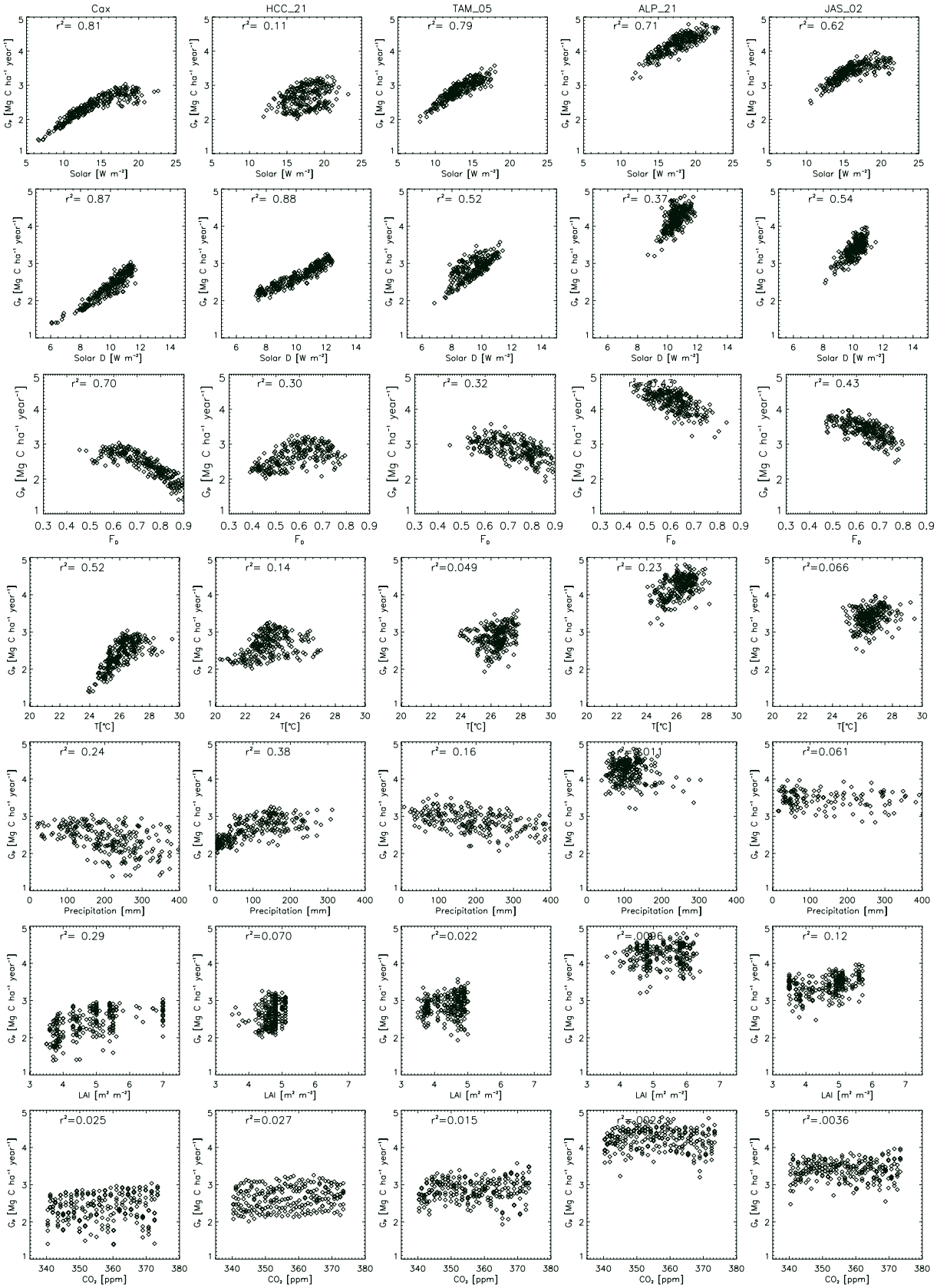

Figure 4.9. Scatter plots of monthly simulated $G_{P(P)}$ and monthly values of solar and solar diffuse radiation (Solar D), diffuse fraction (F_d), air temperature, precipitation, LAI and atmospheric [CO_2] for 5 selected sites located from left to right in Brazil, Bolivia, southern Peru, northern Peru and Ecuador.

4.3.4 Relationship of mean annual $G_{P(P)}$ and $G_{P(N)}$ averaged over the period 1982-2001 with environmental and non environmental variables.

In an attempt to find predictors of G_P and/or spatial patterns of the simulated G_P with environmental (solar and solar diffuse radiation, air temperature, diffuse fraction, precipitation and CO_2) or non environmental variables (foliar nutrients (N, P), V_{maxN} and V_{maxP}, LAI, above ground net primary productivity (ANPP), mean residence time, soil type taken from Malhi et al. (2004) and above ground biomass (AGB) from Baker et al. (2004)), linear regressions between the mean annual simulated G_P averaged over 1982-2001 and these variables were made. See Figures 4.10A and B for $G_{P(N)}$ and $G_{P(P)}$, respectively.

Relationships of simulated mean annual $G_{P(N)}$ with solar, solar diffuse, fraction of diffuse radiation and LAI have r^2 greater than 0.2 and are significant. This is because under control simulations, the lowest $G_{P(N)}$ were obtained at some of the TAM sites which receive the lowest mean annual incoming solar and solar diffuse irradiance, and highest calculated mean annual diffuse fraction. The opposite occurs at some of the northern Peruvian sites like the ALP sites; there, the simulated $G_{P(N)}$ were among the highest values simulated across the transect and mean annual solar and solar diffuse radiation were highest as well. Diffuse fraction at these sites was similar to the average value of diffuse fraction computed for all sites.

As mentioned in the overview section of the methods, linear regressions between the mean annual G_P from the non-control model simulations and variables from Figure 4.10 were made. The $G_{P(N)}$ used were already presented in sensitivity test 1, i.e. parameterised with top of the canopy V_{maxN} obtained with V_{maxN} versus Leaf N relationships from Table 4.1. Values of r^2 obrained from linear regressions of $G_{P(N)}$ with solar, solar diffuse, diffuse fraction and LAI (results shown in Appendix 4C, Figures 4C-1 and 4C-2) were less than 0.1 and not significant. This is because the lowest $G_{P(N)}$ did not coincide with sites with the lowest solar incoming irradiance. However, for non-control simulations, the linear relationship between the simulated $G_{P(N)}$ with foliar N and V_{max} at the top of the canopy was better (r^2 of 0.89 and 0.6 and p-value < 0.005 for the two V_{max} *v*s leaf N regressions tested) than under control simulations. This means that under non-control simulations, lowest $G_{P(N)}$ corresponded to sites with the lowest foliar N in area basis. The reason behind the better (compared to control run) correlations of simulated $G_{P(N)}$ with foliar N and V_{max} at the top of the canopy with the regressions tested in Figures 4C-1 and 4C-2 (Appendix 4C), may lie in the fact that the latter regressions (from Table 4.2) had originally higher r^2 than the regression used for control simulations (obtained in Chapter 3). See Table 4.1.

Relationships from the control simulations of $G_{P(N)}$ with measured above ground net primary productivity (ANPP), residence time, soil type, measured above ground biomass (AGB) (Baker et al. 2004), temperature and precipitation (from the ERA-40 meteorology), were relatively poor in terms of their regression coefficients (Figure 4.10A). This shows that according to the sun and shade model mean annual $G_{P(N)}$ averaged over the 20 year study period is not directly varying with any of the mentioned variables. Additionally, relationships between these variables and $G_{P(N)}$ from the non-

control simulations of could not explain the observed variability in ANPP (See Figures 4C-1-i and 4C-2-i).

For relationships between $G_{P(P)}$ and the variables in Figure 4.10B, r^2 from the linear regressions between mean annual $G_{P(P)}$ and foliar P, V_{maxP} and ANPP were higher than 0.1 and significant. V_{maxP} was well correlated with simulated $G_{P(P)}$ (it was not the case for V_{maxN} and $G_{P(N)}$ under control conditions). Additionally, highest V_{maxP} did not coincide with sites where $G_{P(P)}$ was highest. Moreover, even though the range of simulated $G_{P(P)}$ was larger [29 - 51 Mg C ha^{-1} yr^{-1}] than the range of $G_{P(N)}$ [29 - 36 Mg C $ha^{-1}yr^{-1}$], there was no significant relationship of $G_{P(P)}$ with any of the meteorological variables nor with diffuse fraction, LAI, soil type , residence time or AGB.

Can simulated GPP explain variations in ANPP?

According to the relationship shown in Figure 4.10B, simulated $G_{P(P)}$ can explain 20% (p-value=0.016 n=30 data points) of the observed variability in measured above ground net primary productivity (ANPP). However, when the seasonally flooded forest (TIP-03 and LS-01) and also gallery forest sites (HCC-21 and HCC-22) were excluded from the analysis, $G_{P(P)}$ could explain 39 % of the variability of ANPP (n=26 , p-value=0.0007). If soil texture (% silt or % sand) or soil type (according to Table 4.2) were included in the analysis, a higher percentage (48-63%) of the variability in ANPP could be explained (See Table 4.6). When taking into account wood density (*wd*), $G_{P(P)}$ and % of silt (data used reduced to 25 points because there was no *wd* for Man-K34), 68% of variations in ANPP could be explained with all three independent variables being significant. Taking into account only *wd* and % silt, the obtained regression was not as good as when $G_{P(P)}$ was included (considering *wd* and % silt, r^2 = 0.5, p=0.0065, 0.003, significance of F=0.0005). Table 4.6 summarises these analyses. A similar analysis was done using leaf P instead of $G_{P(P)}$ as the independent variable and soil texture (% silt or % sand), soil type (according to Table 4.2) and *wd* were taken into account as well. Surprisingly, regressions using $G_{P(P)}$ were better (higher r^2 and lower p-values) than those using leaf P as the independent variable. This shows the added value of the $G_{P(P)}$ being able to explain a greater percentage of the variability in ANPP (See Table 4.6).

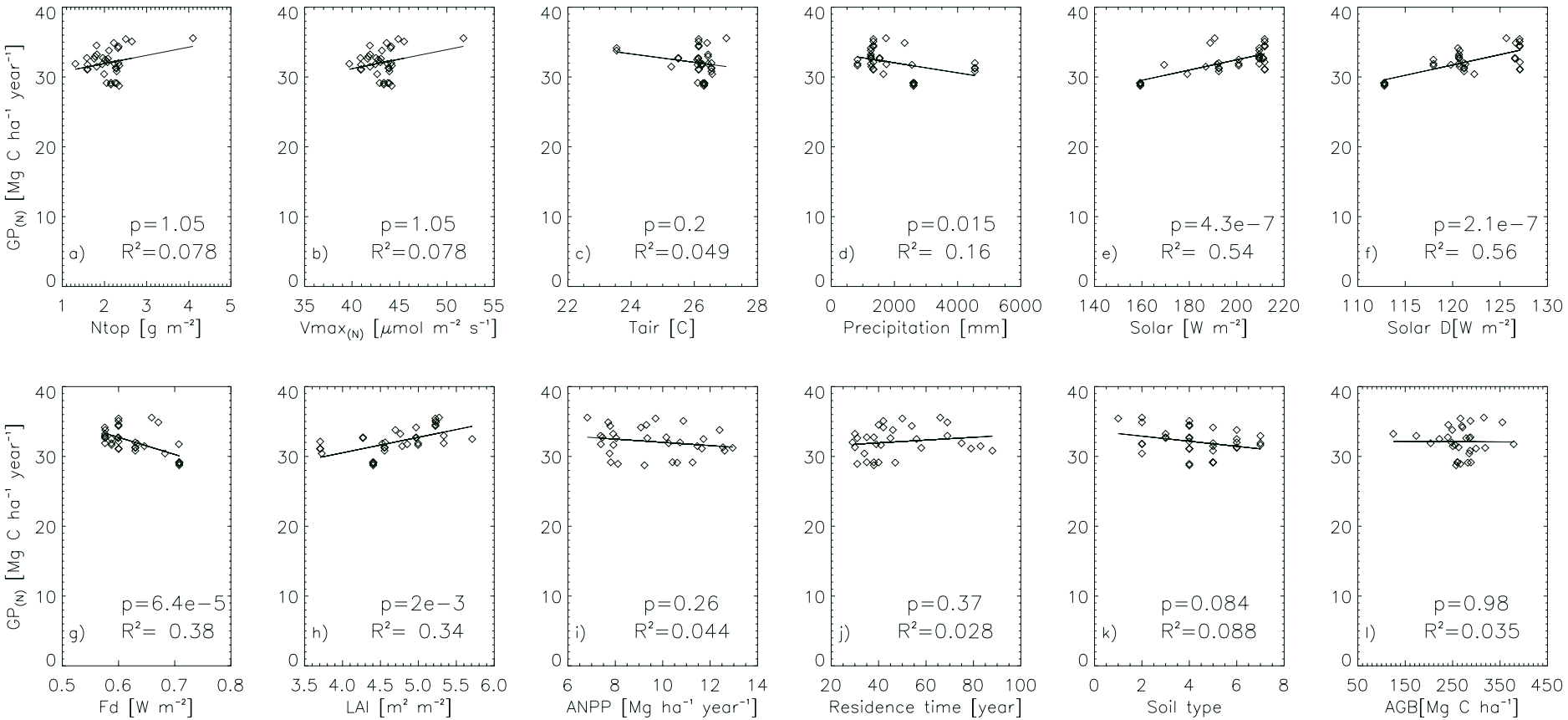

Figure 4.10A. Relationships between simulated mean annual $G_{P(N)}$ averaged over the period 1982-2001 with a) N content from top canopy leaves, b) $V_{max(N)}$ at the top of the canopy, c) mean annual air temperature, d) mean annual precipitation, e) mean annual solar incoming radiation, f) mean annual solar incoming diffuse radiation, g) fraction of diffuse irradiance h) mean annual LAI, i) above ground NPP, j) mean residence time, k) soil type, l) above ground biomass. Items i), j) and k), are taken from Malhi et al. (2004) and l) is taken from Baker et al. (2004).

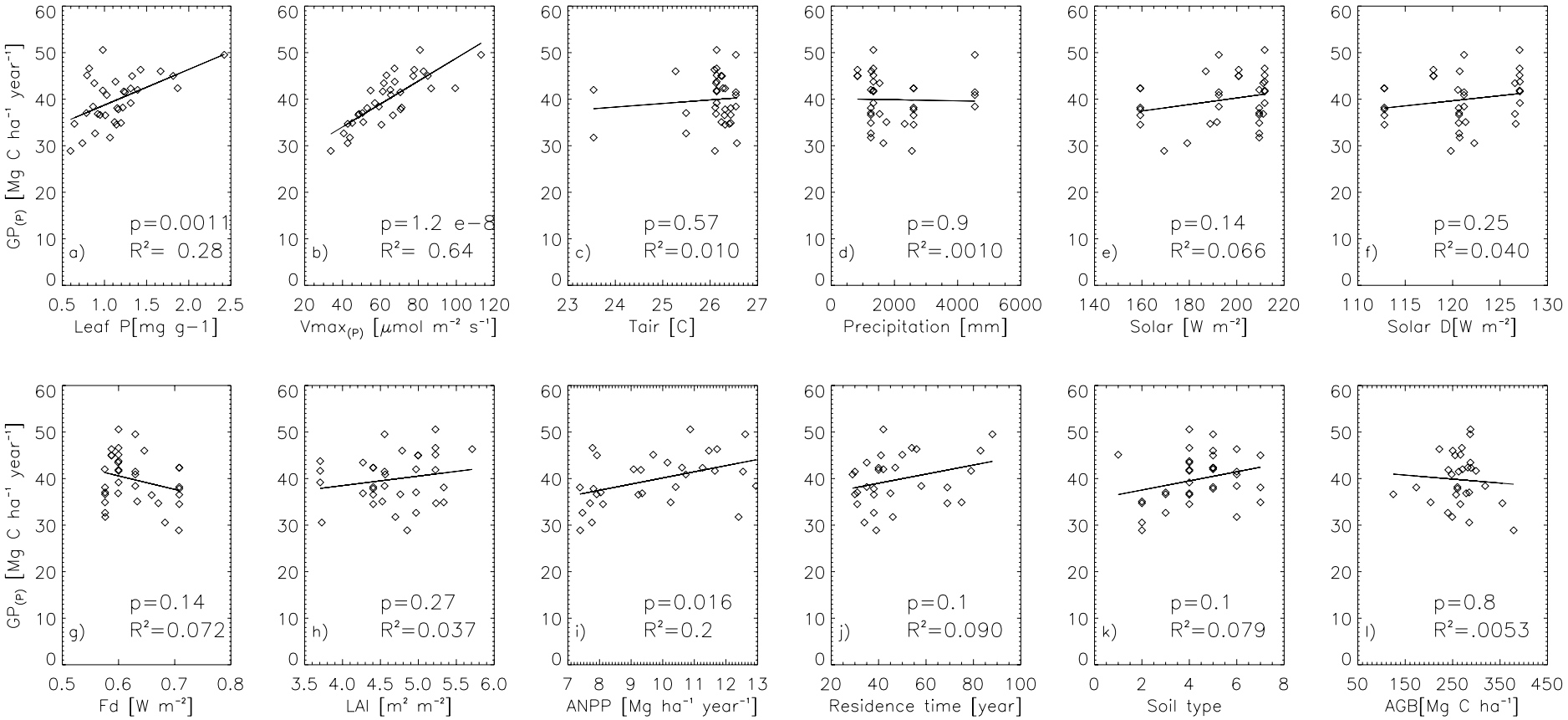

Figure 4.10B. Relationships between simulated mean annual $G_{P(P)}$ averaged over the period 1982-2001 with a) P content from top canopy leaves, b) $V_{max(P)}$ at the top of the canopy, c) mean annual air temperature, d) mean annual precipitation, e) mean annual solar incoming radiation, f) mean annual solar incoming diffuse radiation, g) fraction of diffuse irradiance h) mean annual LAI, i) above ground NPP, j) mean residence time, k) soil type, l) above ground biomass. Items i), j) and k) are taken from Malhi et al. (2004) and l) is taken from Baker et al. (2004).

Table 4.6. Regression analysis of above ground net primary productivity (ANPP) as dependent variable. n is the number of values available /used for regression.

n	Independent variable	r^2 $G_{P(P)}$	r^2 leaf P	r^2 adjusted $G_{P(P)}$	r^2 adjusted leaf P	p-value $G_{P(P)}$	p-value leaf P	Significance F $G_{P(P)}$	Significance F leaf P
30	$G_{P(P)}$ or Leaf P	**0.19**	0.19	**0.16**	0.16	**0.016**	0.015		
26	$G_{P(P)}$ or Leaf P	**0.39**	0.37	**0.36**	0.34	**0.0007**	0.001		
26	$G_{P(P)}$ or Leaf P % silt	**0.53**	0.44	**0.49**	0.39	**0.003** **0.013**	0.02 0.1	**0.00016**	0.12
26	$G_{P(P)}$ or Leaf P % sand	**0.48**	0.38	**0.44**	0.33	**0.0005** **0.048**	0.0042 0.1	**0.0005**	0.12
25	$G_{P(P)}$ or Leaf P % silt	**0.50**	0.41	**0.46**	0.36	**0.005** **0.02**	0.04 0.12	**0.0004**	0.003
26	$G_{P(P)}$ or Leaf P soil type	**0.63**	0.53	**0.60**	0.49	**0.003** **0.0007**	0.009 0.05	**1.06 e-5**	0.00016
25	$G_{P(P)}$ or Leaf P soil type	**0.61**	0.50	**0.57**	0.46	**0.003** **0.001**	0.056 0.01	**3.4 e-5**	0.0004
25	$G_{P(P)}$ or Leaf P wood density soil type	**0.65**	0.50	**0.6**	0.44	**0.002** **0.13** **0.023**	0.11 0.03 0.69	**5.3 e-5**	0.0016
25	$G_{P(P)}$ wood density % silt	**0.68**	0.50	**0.63**	0.43	**0.002** **0.008** **0.003**	0.59 0.03 0.03	**2.2 3-e5**	0.0018

4.3.5 Comparing measured and simulated mean $\delta^{13}C$

Simulated mean $\delta^{13}C$ averaged over the last 10 years of the study (1992-2001) are compared against measured $\delta^{13}C$ from top canopy leaves. (Ometto et al. 2006; RAINFOR Consortium, unpublished data) for sites where measurements were available (Figure 4.11). Sites in Figure 4.11 are organized by longitude from east to west. In Figure 4.11, i) there is no clear pattern with longitude, as found in the measurements by Martinelli et al. (1991) and Martinelli et al. (1996). These authors found that measured $\delta^{13}C$ of plant tissues increased towards the east (from about -35 to -31 ‰) in a transect across the Amazon river from 67 to 55 degrees longitude, ii) simulated $\delta^{13}C$ was most negative at Caxiuana, Man-K34 and Jaru which are the sites where λ was highest as parameterised in Chapter 3. Non-Brazilian sites were all parameterised with a lambda of 1200 mol mol^{-1} and the least negative simulated $\delta^{13}C$ was obtained under both simulations (with leaf N and leaf P) at the sites that had lowest precipitation and lowest relative humidity, i.e. LFB-01 and TIP-03 in Bolivia and Ecuador (See Figures 4A-3 and 4A-6). Agreement between simulated $\delta^{13}C$ and measurements is best at most sites in Brazil, South Peru and North Peru, with simulated values tending to be less negative than the measurements in Ecuador and Bolivia.

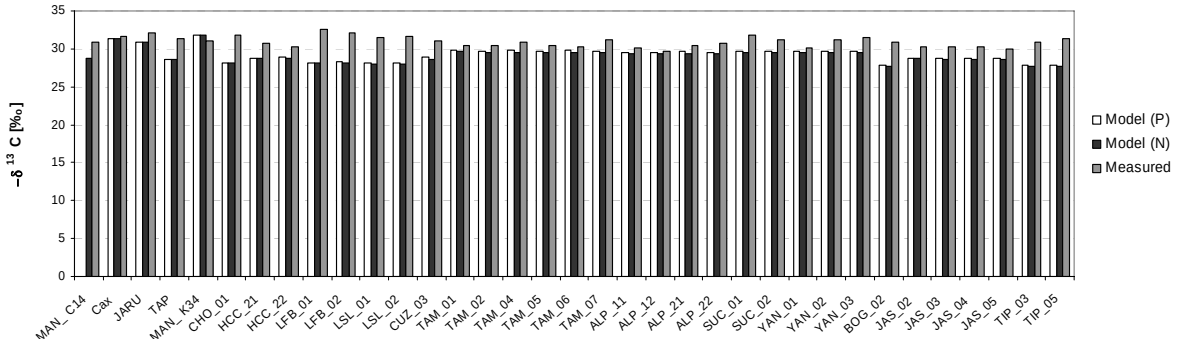

Figure 4.11. Measured and simulated isotopic composition, -$\delta^{13}C$ [‰]. Measured vales at the Brazilian sites are taken from Ometto et al. (2006). Measured $\delta^{13}C$ of the remaining sites were taken from the RAINFOR Consortium data set (unpublished data).

4.4 Discussion

4.4.1 Assessment of use of model derived meteorology on simulated G_P

It is important to recognize that the ERA 40 simulated climatology is one of the few data sets at high temporal resolution available at the current time. Even though this modelled meteorology still needs to improve in order to be more realistic, it has value as the meteorological variables are consistent with one another (e.g. solar radiation and precipitation, precipitation and relative humidity, solar radiation and air temperature are consistent modelled) and also its high, 3-hour temporal resolution enable the simulations for this study.

The use of modelled meteorology constrains to some extent the fidelity of the results presented. Due to the lack of data (records of meteorology) for the Amazon region, validation of this type of input data is difficult.

This study has shown how both solar radiation and/or and diffuse solar (for $G_{P(P)}$ and $G_{P(N)}$) are the variables that most influence simulated photosynthesis at monthly time scales (Figures 4.8 and 4.9 and Tables 4.4 and 4.5). Thus, good time series of solar radiation (used to estimate solar diffuse in this study) become very relevant for simulations of G_P. For example at the northern Peruvian sites and at 3 of the Ecuadorian sites, solar radiation from the ECMWF simulations decreased considerably between 1982 and 2001 (30 - 40 W m^{-2}), therefore affecting the simulated G_P over these sites. Another good example is at the TAM sites in South Peru. According to the ECMWF meteorology, mean annual solar radiation over the study period is 35% lower than the neighbouring Bolivian sites. Even though cloud cover might be higher at TAM, due to greater precipitation (almost double), solar radiation at TAM could still be unreasonably low (See Figure 4A-4). But again, there is no data available to evaluate the validity of these estimates. The effect of the low solar radiation at the TAM sites is clear especially in the simulation using leaf P. Since these sites have high leaf P content, i.e. high canopy V_{maxP}, simulated $G_{P(P)}$ could have been higher but the model simulations were for areas of relatively low solar radiation.

Since modelled precipitation and relative humidity are closely related, accuracy of precipitation becomes very important as well. Using available rainfall data for one JAS site in Ecuador, comparison to the ERA-40 mean annual cycle of precipitation showed a large model-data underestimation during the period June-August (not shown). According to the ERA-40, there is a pronounced dry season over during these months (along with a decrease in relative humidity). However according to precipitation records (Neil D., data not published) there is not such a pronounced dry season (defined as months with less than 100 mm rainfall) in this area with minimum monthly precipitation values of 245 mm on average (for the period 1992-2001). Furthermore, when compared to the data from Malhi et al. (2004), sites where precipitation was underestimated (all sites in northern Peru and three sites in Ecuador, Figure 4A-2-III) may also have underestimated relative humidities. With lower relative humidity in the ERA-40 forcing data than observed, a lower simulated photosynthesis than under high relative humidity conditions are expected. However, it has been shown that the stomatal conductance formulation used is insensitive to low relative humidity (high VPD). Therefore for the simulations performed in this chapter, even though the forcing relative humidity should have been higher at some sites (where precipitation was underestimated) there is probably a very small effect on the simulated photosynthesis.

4.4.2 Implications of the use of parameterisations derived from Chapter 3

This study is essentially a sensitivity analysis of scaling up (using information from parameterisation at five eddy correlation sites) to the basin level based on correlations of V_{max} *vs* leaf N and V_{max} *vs* leaf P derived from Chapter 3. Under these circumstances, the major findings are: a) simulated $G_{P(N)}$ did not have much spatial variation (1.2), while $G_{P(P)}$ varied by a factor of 1.8 across sites, and b) due to the higher leaf P in western Amazon (i.e V_{maxP}) $G_{P(P)}$ was generally highest there.

In general, simulated G_P and its spatial variability were very sensitive to the value used to parameterise top of the canopy V_{max} (shown in sensitivity test 2), which is directly related to the V_{max} *vs* leaf N or V_{max} *vs* leaf P relationship used for parameterisation (shown in sensitivity test 1).

For the parameterisations based on leaf N, the regression used was formed by 5 values from top of the

canopy V_{max} at the Brazilian tower sites (Chapter 3) and this relationship was meant to be used as the scaling up function to the Basin level. But because both the leaf N and V_{max} values were numerically relatively similar, the obtained regression had a low slope and a low regression coefficient, which did not predict a large range of V_{max} (variation by a factor of 1.2) with the observed range in leaf N (a factor of 1.3 variation) across the 35 studied sites. On the other hand, the remaining relationships reported in Table 4.2 predicted a range of variation in V_{max} (3.5, 3.8 and 6) as these relationships were created with data from different canopy heights which implied variations in both leaf N and V_{max}.

Similarly for simulations parameterized based on leaf P, the leaf P and V_{max} relationship was derived in Chapter 3 also from top of the canopy V_{max} at 4 of the Brazilian tower sites. From the 4 points used, the point or site with the highest simulated G_P coincided with highest P (Figure 4.2), with remaining 3 sites having numerically similar leaf P and similar V_{max}. Therefore the obtained linear regression was biased towards high foliar P. Consequently when using this relationship to parameterise 35 sites along the transect, sites with high leaf P will have high V_{maxP} and therefore high simulated $G_{P(P)}$ (Figure 4.10). Derived V_{maxP} ranged from 40 to 87 μmol m^{-2} s^{-1} with a mean value at 60.8 ±13.9 μmol m^{-2} s^{-1} with two outliers at JAS-05 and TAM-06 having very high values of V_{maxP} at 99 and 113 μmol m^{-2} s^{-1}, respectively. We are aware that such V_{maxP} values are high, however, Domingues et al. (2005) estimated V_{max} from top canopy leaves from leaf gas exchange measurements in a rainforest around the Tapajos area and obtained values for some species on the order of 56.3, 68.3 and 75 μmol m^{-2} s^{-1} with a mean value for all species from top canopy leaves of 45.42 μmol m^{-2} s^{-1}.

The V_{max} parameterization influenced J_{max} through the J_{max} / V_{max} ratio. The J_{max} / V_{max} ratio used for all simulations was 1.92 which is inside the published range reported in the studies of Carswell et al. (20002), Vale et al. (2003), Meir (1996) (1.08 - 2.240, 1.75 - 2.8, and 1.6 - 2.5, respectively). Sensitivity of simulated G_P to variations in this ratio showed that increasing the J_{max} / V_{max} brought forward (with respect to radiation) the transition of light limited to rubisco limited conditions, preserving colimitation between light-saturated and rubisco limited photosynthesis. Moreover, according to Long et al. (2006), to preserve colimitation, increases in the rate of carboxylation by Rubisco are accompanied by increases in J_{max} / V_{max}.

Furthermore, according to parameterisations from Chapter 3, it was decided to use a quantum yield of 0.4 at all sites, but sensitivity of G_P to variations in Φ (sensitivity test 5) showed that G_P was indeed very sensitive to this parameter. However, the comparison of simulations here are against those using Φ= 0.5, i.e. compared with those using the theoretical upper bound of quantum yield, while measurements of quantum yield reported for C_3 leaves ranges between 0.22 and 0.37 (Ehleringer and Bjorkman 1977; Ehleringer and Pearcy 1983; Long et al. 1993). Detailed measurements of quantum yield would be required to examine whether or not there is any variation of quantum yield across the 35 sites.

We are aware that the leaf P limitation was implemented in a rather crude manner in this study. For instance the N invested in Rubisco accounts for 15 to 35% of total leaf N in C_3 species (Evans 1989b) and in this study V_{maxP} was only related to leaf P. Also, P limitation has been linked to the regeneration of inorganic phosphate (Pi) and called TPU limitation to photosynthesis (Sharkey 1985; Sharkey et al. 1986) but under low P conditions, some studies have reported no TPU limitation. Such studies have found reductions in: the

activity of Rubisco (Brooks 1986; Brooks et al. 1988); the rate of RuBP regeneration; the quantum yield of photosynthesis and reductions in the Calvin cycle activity (Brooks et al. 1996; Campbell and Sage 2006). Besides the TPU limitations, none of these mechanisms are yet included in biochemical models of photosynthesis. Hence, the introduction of leaf P in this study should be regarded as an exploratory exercise to investigate the potential effect of P on photosynthesis under the assumption that Rubisco (activity and or content) is directly affected by leaf P content under abundant N conditions. Whether it is foliar N or foliar P that is limiting in tropical Amazonian forests still needs to be tested in the field but an insight into the possible implications of such limitations are investigated in this chapter.

In an increasing [CO_2] atmosphere, P plays a major role in controlling the CO_2 response of photosynthesis (Lewis et al. 1994). Under P limited conditions, increasing CO_2 has little or no impact on photosynthesis, while plants grown in P sufficient conditions have shown the expected increases in photosynthesis in response to increasing [CO_2] (Campbell and Sage 2002; Campbell and Sage 2006). According to Campbell and Sage (2006), P already restricts the response to increasing CO_2 from pre-industrial to present day concentrations in agricultural fields, which require large additions of P (Vance 2001). If it is true that tropical ecosystems such as the Amazon rainforest are P limited, the possible low responsiveness to rising atmospheric CO_2 could have major implications for the predicted global carbon budget. Smaller carbon sinks would be expected, than currently predicted by global models which include the CO_2 fertilization effect, and thus the associated higher CO_2 levels would lead to a further climate warming. This shows the need for research in the area of nutrient limitation in the Amazon rainforest and its relationship to photosynthetic carbon uptake.

In Chapter 1 it was shown that simulated diffuse irradiance had a major effect on simulated photosynthesis. A similar result was obtained in this chapter for most sites, where a high percentage of the variance of simulated monthly photosynthesis could be explained by solar diffuse radiation in most cases or by total solar radiation in few cases (Figures 4.7 and 4.8 and Tables 4.4 and 4.5). This is because according to sun/shade simulations a high percentage of the total canopy photosynthesis is undertaken by the shaded leaves and in the model shaded leaves only get diffuse irradiance. A recent observational study showed the effect of diffuse irradiance on photosynthetic uptake at a rainforest in the Brazilian Amazon. Measurements of aerosol optical depth and PAR at Jaru, showed that increasing diffuse radiation and diffuse fraction enhances transmission of radiation inside the canopy, thereby enhancing photosynthetic activity up to a threshold level at which CO_2 flux decreases probably due to a decrease in availability of PAR (Yamasoe et al. 2006). Furthermore, the study from Niyogi et al. (2004) showed an increased CO_2 sink due to an increase in aerosols loading (i.e. increase in diffuse radiation) and attributed such an increase to canopy structure. These results suggest the need for more measurements of diffuse irradiance (in parallel to eddy correlation measurements of carbon uptake) for model validation in the Amazon basin which are currently scarce.

Results from the sensitivity test using several vertical N distributions within the canopy suggested low sensitivity of GPP to N distribution. Therefore it is concluded that using the vertical distribution measured at Manaus is a reasonable assumption for our simulations across the study transect. Simulated GPP was insensitive to various LAI scenarios (Appendix 4B, Figure 4B3) indicating that assumptions of the LAI control scenario are reasonable.

The insensitivity of simulated GPP to a 30% decrease in relative humidity shows that the lambda model is not a good formulation for these forests.

4.4.3 Evaluation of simulated $\delta^{13}C$

The isotopic composition of leaves was the only data source available to evaluate the basin wide simulations presented in this study. With the parameterisation used for the lambda model of stomatal conductance, as shown Figure 4.11, the model tended to agree with the observations at sites where precipitation was highest (i.e. Brazil, North and South Peru and JAS sites in Ecuador). On the other hand, there were model data discrepancies at sites where the precipitation used to force the model was lowest and at the same sites, dry season was long and severe (i.e. Bolivian sites and some sites in Ecuador). However, as mentioned before, precipitation and the strong seasonality from the ERA-40 meteorology for most sites in Ecuador are unrealistic. Furthermore, from this evaluation it is concluded that the model predicts more negative $\delta^{13}C$ than observed under dry conditions (i.e. such at Bolivian sites which are the sites with the longest dry season and lowest precipitation). This could be linked to the already stated problem of the stomatal conductance formulation and its insensitivity to high VPD.

4.4.4 Comparison of simulated GPP to estimated GPP from eddy correlation

Comparison of simulated gross primary productivity GPP for both the N and P simulations, (calculated as net carbon uptake, $G_{P(P)}$ or $G_{P(N),}$ plus simulated day time canopy respiration) with GPP estimated from eddy correlation or from other sources of measurement where available at the five sites in the Brazilian Amazon, is summarised in Table 4.7. In general, the simulated values are usually higher than the reported measurement derived values. However, none of the reported measurements (except at Man-K34) takes into account variations in diurnal canopy respiration in response to temperature or in response to light. If one was to consider only the temperature response to leaf respiration, then the expected diurnal canopy respiration should be higher than considered during the night due to the usual higher daytime temperatures. Therefore this effect should increase the estimates of GPP from eddy correlation. However, if one was to consider both the temperature and light response of canopy respiration, i.e. inhibition by light (Atkin et al. 1998; Atkin et al. 2000), canopy respiration should be lower during the day than during the night. Failing to include light inhibition of canopy respiration implies an overestimation of daily estimates of ecosystem respiration and hence gross primary productivity from eddy correlation measurements (Janssens et al. 2001; Wohlfahrt et al. 2005). Furthermore, as explained in Chapter 3, the effect of light on leaf respiration was not considered in the simulations or in the estimates of GPP from eddy correlation.

Table 4.7. Comparison of GPP estimated by Eddy correlation and simulated $G_{P(P)}$ and $G_{P(N)}$) in Mg $ha^{-1}yr^{-1}$.

Site	$G_{PP(P)}$	$G_{PP(N)}$	GPP from Eddy correlation	Source
Manaus C14		46		Not available
Caxiuana	36	39	38.07 and 39.08*	Malhi Y. (pers. comm.)
Jaru	42	39	36 and 41*	Kruijt B. (pers. comm.)
Tapajos	37	37	24 -39 *	Saleska et al. (2003)
Manaus K34	42	42	38.8	Chambers et al. (2004)

* Not corrected for low values of $u*$

4.4.5 Relationship of simulated mean annual GPP (averaged over the study period) with measured mean annual ANPP

If photosynthesis is P limited in these rainforests, as many studies have shown under low P conditions, low P corresponds to low photosynthesis, as shown in this sensitivity study based on measured leaf P values. It might be possible that the simulated GPP values obtained with the P simulation are quantitatively unrealistic, however, the obtained spatial gradient across the basin could still be realistic. Under this assumption one can speculate that these results indicate the importance of factors other than GPP (indirectly foliar P) like soil (and it's physical properties) and plant hydraulics (related to wood density) in determining variations in plant growth across the Amazon rainforest. The chemistry of the soil and its physical properties determine the conditions for the nutrient and water access to the roots. For instance, some soils have the capacity to absorb P, i.e. P is complexed in minerals, meaning that although there may be sufficient P in the soil it is not available to the roots. The ability of plants to produce root exudates or the presence of mycorrhizae associations help to increase absorption of P. Furthermore, P tends to be more available in sands than in clays because P content in clays is usually strongly complexed in Al and F_e oxides (Lambers et al. 1998). Additionally, soil texture affects the ability of plants to extract water to sustain it's vascular system (Sperry et al. 1998). The obtained correlation of ANPP with wood density is not unexpected. Several studies have confirmed the correlation between wood density and growth (King et al. 2006; Wright et al. 2003). This is based on a gradient in wood density across the study transect, with some western Amazonian sites having lower density than central and eastern sites, (Patiño et al. in prep), which is opposite to the observed ANPP gradient (Malhi et al. 2004). According to Roderick (2000) low wood density should provide high growth rates because in low density wood there is more volume available for water transport or storage than in high density wood.

4.5 Conclusion

Results obtained in this study suggest that if photosynthesis in the Amazon rainforest is limited by N, GPP across the basin does not have a large spatial variability. This favours the homogeneous parameterisations used in global land surface schemes, in which parameters such as V_{max} are considered constant across plant functional types. However, our results suggest that if P constrains photosynthesis in these forests, there could be a gradient in GPP across the basin with many sites in western Amazonia having higher GPP than those in the east due to the observed gradient in leaf P. Under these conditions, our results indicate not only a spatial variability of photosynthesis, but also point to a spatial variability in soil properties and plant hydraulic traits affecting plant growth across the Amazon basin. Even though our parameterisations were based on a few points (4) with a single point favouring high GPP at high foliar P, the measured gradient of leaf P across the Amazon basin suggest the same result under P limited conditions. Furthermore, if these rainforests are limited by P, the inclusion of P limitations to photosynthesis into models would be needed for realistic simulations. But in order to do this there is a need for more field studies looking into the nature of nutrient limitation in the forests across the Basin and into photosynthesis in contrasting P conditions (i.e. for forest with high and low foliar P). The consequences of Amazon rainforest, or at least those parts where foliar P is lowest, being P limited in a high CO_2 atmosphere include no plant response to increasing CO_2, opposite to what is currently predicted by global models, which may lead to higher global atmospheric CO_2 concentrations and greater climate warming than hitherto expected.

Results from this study suggest that to simulate GPP in this forest a very precise prescription of LAI or vertical distribution of leaf N across the canopy is not crucial. Instead the most important factors are the parameterisation of top of the canopy V_{max}, canopy quantum yield, simulation of diffuse irradiance and representation of stomatal conductance. Such information can help inform the measurement community. To our knowledge quantum yield of photosynthetic uptake has not been measured in (or across) the Amazon rainforest. Due to the high sensitivity of the simulated GPP to this parameter, it is crucial to know if the values that are currently used for parameterisations of leaf level, canopy level and regional and global level are adequate for these forests. This study showed the importance of diffuse irradiance on modelling photosynthesis and the few experimental studies to date have found similar results. Therefore more field studies measuring diffuse irradiance and photosynthesis are needed for better understanding of this relationship and for model calibration and evaluation. This a crucial issue when models are intended to be used as tools to extrapolate to large regions like this study but also as tools to predict possible future behaviour of the forest under changing environmental conditions. It is concluded that stomatal formulations that base their predictions only on atmospheric demand like the one used in this study are not adequate for simulation of rainforest photosynthesis. Therefore a formulation which includes both the atmospheric demand and supply of water from the roots is recommended. This is important for modelling carbon and energy exchange of the rainforest especially for dry events such as the 2005 drought or for cases of increasing the frequency and/ or duration of El Niño events.

5 Summary

The aim of this thesis was to develop a model to simulate rain forest Gross Primary Productivity, GPP, along an East-West transect across the Amazon basin. Results from this study can help inform both the measurement and regional and global modelling communities on the main outstanding issues to enable accurate regional assessments of carbon uptake in these rainforests. Since the Amazon rainforest is an important component of the global carbon cycle, this study is highly relevant and more specifically can help advance our knowledge of modelling tropical forest carbon and water fluxes, because:

-GPP across the Amazon basin is poorly quantified. Currently it has been derived from measurements at only a few specific sites in the Brazilian part of the Amazon with the aid of eddy correlation data.

-Most global and regional models simulate GPP for the Amazon assuming the same photosynthetic parameters for the whole region.

-There is contemporary evidence of the effects of changes in atmospheric CO_2 concentration and climate on tropical rainforest (Lewis et al. 2004; Malhi et al. 2004; Malhi and Phillips 2004). Better models of canopy gas exchange, as developed here, can help improve the ability of models to predict the future response of the Amazon rainforest to future environmental change.

To model GPP across the Amazon the following steps were undertaken: Initially two approaches to simulate canopy photosynthesis were tested and evaluated for a single rainforest site. The big leaf and sun/shade models were calibrated and evaluated using eddy correlation fluxes and associated meteorological measurements (Chapter 1 and Chapter 2). The sun/shade model emerged as the better of the two approaches in terms of simulating the observed fluxes, therefore it was further evaluated at five rainforest sites where eddy correlation fluxes were also available. Scaling functions were derived between maximum carboxylation capacity of Rubisco, a proxy for photosynthetic capacity, and foliar nutrients (i.e. V_{max} versus foliar N and relationships between V_{max} and foliar P). These were subsequently used to provide estimates of canopy photosynthetic parameters for a range of diverse forests across the Amazon region (Chapter 3). Initially, GPP was simulated at 35 sites using the derived V_{max} versus foliar N and foliar P relationships. Corresponding GPP estimates were assessed both in terms of their sensitivity to climate and their skill in accounting for variations in above-ground Net Primary Production (ANPP) across the Basin.

Specifically this thesis addressed the following questions under two main themes:

Modelling photosynthesis and energy exchange at single sites using eddy correlation data

Can the observed GPP and energy fluxes derived from eddy correlation be consistently simulated at different Amazonian rainforest sites?

To answer this question one should bear in mind the uncertainties associated with the data used for both

model evaluation (see question on uncertainties) and relationships used for model parameterisation. After recalibration, the model was able to accurately simulate Gross Primary Productivity (GPP) at the 5 evaluated sites. This result is supported by the ability of the model to reproduce observations of leaf $\delta^{13}C$. However, there is still room for improvement. For instance, at most sites the model tended to over predict observed GPP in the late afternoon. Additionally, the energy balance was not well simulated in 4 out of 5 sites, with a model tendency to overestimate the observed evaporative fraction.

What are the advantages and disadvantages of the modelling approach used?

From the two approaches for photosynthesis evaluated (sun and shade and the big leaf), the sun and shade model is qualitatively and quantitatively superior, in terms of model fit, for modelling carbon uptake (Chapter 1). This is linked to the ability of the model to account for variations in diffuse radiation and variations in sunlit and shaded leaves. Similar results for carbon uptake and energy partition were obtained using either of the two approaches to model stomatal conductance (Lambda and Ball Berry), with each individually coupled to the two photosynthesis schemes (Chapter 1 and 2).

The model of choice, the sun and shade approach linked to the lambda formulation for stomatal conductance, tended to overpredict the observed gross primary productivity during afternoon conditions at 3 of 5 sites, i.e. high vapour pressure deficit (VPD) and high air temperatures, in both wet and dry seasons. This result is linked to the simple formulation for stomatal conductance which only considers the atmospheric demand to regulate stomata opening. Additionally, the model tended to over predict the observed evaporative fraction at 4 of 5 sites during both wet and dry seasons. This is partly due to the simple stomatal conductance formulation used. However, this problem is common to biosphere models which are either able to reproduce the observed carbon uptake or the energy balance, seldom both simultaneously (Morales et al. 2005).

In summary, we suggest the sun and shade model for photosynthesis is an appropriate tool to simulate the carbon fluxes of the Amazon rainforest with adequate parameterisation. However we suggest that this model should be linked to a stomatal conductance formulation that not only includes the atmospheric demand but also the supply of water from the soil (Fisher et al. 2006).

What constrains a model evaluation using eddy correlation flux data for Amazonian sites?

The main constraints on this type of model evaluation are uncertainties associated with the evaluation data, the net ecosystem exchange (NEE), ecosystem respiration, energy fluxes from eddy correlation and relationships between leaf N and V_{max} (based on measurements) used for model parameterisation. A brief summary of these constraints follows:

Estimates of net ecosystem exchange (NEE) from eddy correlation and estimates of ecosystem respiration rates determine the maximum rate of assimilation used to evaluate model predictions. However for two Amazonian sites the overall uncertainties associated with the eddy correlation measurements are on the order of 12 and 32% (Kruijt et al. 2004).

There are major difficulties in estimating the ecosystem respiration term in these forests. When this term is estimated using the night time NEE measurements from eddy correlation, the uncertainties are linked to poor mixing and lateral flux drainage (Aubinet et al. 2002; Massman and Lee 2002; Pattey et al. 2002; Saleska et al. 2003). When ecosystem respiration is estimated from its individual respiration components, there are also issues, mainly in determining the soil respiration term, which varies both seasonally and spatially. For most sites used in this study no parallel measurements of NEE and soil respiration were available. Therefore we used soil respiration from different years to the measurement period of eddy correlation data, and due to year to year variations in precipitation, it is likely that there are errors in our estimations of the soil respiration term. Furthermore, there are also uncertainties in the estimate of coarse litter respiration as the amount of coarse litter varies with location. For instance, the Tapajos site has at least double the coarse litter as the Manaus sites which could lead to higher coarse litter respiration at Tapajos (Keller et al. 2004). However we have no information for Caxiuana and Jaru, the other sites evaluated in this study. Furthermore, another important contributor to ecosystem respiration is leaf respiration. In this study we did not consider the inhibition of leaf respiration by light in simulations with the sun and shade model (only with the big leaf approach in Chapter 1). However, there is growing evidence of this effect, although the extent to which leaf respiration is inhibited by light is uncertain (Atkin et al. 2000; Atkin et al.2002; Brooks and Farquhar 1985; Hoefnagel et al. 1998. Non-closure of the energy balance from eddy correlation flux measurements (Araújo et al. 2002; Kruijt et al. 2004; von Randow et al. 2004) makes model evaluation difficult, and also could possibly imply a missing CO_2 signal in the measurements.

Another major constraint on this model evaluation is the reliability of the relationships used to parameterise V_{max}, a key model parameter in determining the maximum assimilation rate. Relationships of V_{max} *vs* leaf N estimated from measurements, and used here for model parameterisation, provided very low values of V_{max} compared to obtained with recent relationships obtained from measurements in the Amazon (Domingues et al. 2005; Vale et al. 2003).

Scaling from stand to region

What can be learnt from this up-scaling exercise about GPP in the Amazon basin?

Simulations assuming P limitations to photosynthetic uptake

-Spatial variation of GPP

Results from this sensitivity study suggest that if leaf P constrains photosynthesis in the Amazon region, GPP of the western sites, which have higher leaf P, would be higher than GPP in central and eastern sites, which have lower leaf P, implying a spatial variation in GPP (by a factor of 1.8) across Amazonia. Under these circumstances, a homogeneous parameterisation of photosynthetic parameters like the type used in global land surface schemes would not be appropriate.

-Relationship of GPP and above ground net primary productivity (ANPP)

Furthermore, under the assumption that P constrains photosynthesis in these forests, results suggest the contribution of not only spatial variability in GPP but also point to spatial variability in soil and plant hydraulic traits in explaining patterns of plant growth across the Amazon basin. Even though these

parameterisations are based on only 4 points, with a single point favouring high GPP at high foliar P, the measured gradient in leaf P across the Amazon basin suggest the same result in P limited conditions.

The consequences of Amazon rainforest, or at least those parts where leaf P is lowest (i.e. central and eastern Amazon regions), being P limited in a high CO_2 atmosphere include a lack plant response to the increasing CO_2, which is opposite to the assumed response built into many global models. This would imply a reduction in the expected future land carbon uptake across Amazonia, and therefore higher global atmospheric CO_2 concentrations and stronger climate change than hitherto anticipated.

Simulations assuming N limitations to photosynthetic uptake

On the other hand, results from this sensitivity study suggest that if photosynthesis in the Amazon rainforest is limited by N, GPP is likely not to vary greatly across the basin. Under these circumstances, simulated GPP can not explain the variability in observed ANPP. In this case, the lack of spatial variation in GPP favours the homogeneous parameterisations used in global land surface schemes, in which parameters such as V_{max} are considered constant across plant functional types.

How sensitive is simulated GPP to environmental variables?

In the first Chapter GPP was found to be highly sensitive to solar radiation, especially to the diffuse radiation. This is because of the canopy structure of these forests which is formed by the high stature trees with dense canopies and leaf area indexes ranging from 4-6 m^2 leaves m^{-2} ground. Under such conditions a high proportion of leaves are in the shade, and because of their quantity their photosynthesis becomes relevant. Since shaded leaves receive only diffuse radiation, the sensitivity of modelled photosynthesis to the diffuse radiation is also very relevant. Additionally, in a sensitivity analysis of simulated monthly GPP to meteorology, CO_2 and LAI (Chapter 4), solar diffuse irradiance was found to have the highest contribution to the variance in simulated GPP. This emphasizes the importance of solar diffuse irradiance to the total uncertainty in the simulated GPP.

What uncertainties are associated with up scaling relationships based on leaf N and leaf P?

There are three major constraints on the exercise to scale simulations of GPP to the regional level:

1) Simulations were made with a model parameter, V_{max} (used as proxy for photosynthetic capacity) specified at each site. V_{max} was estimated at each site using a linear relationship between V_{max} (obtained in Chapter 3 from the model evaluation against eddy correlation data at 5 sites) against measured foliar N and foliar P. The main constraint in this part of the study relates to the fact that these relationships of V_{max} *vs* leaf N and V_{max} *vs* leaf P were created with only 5 and 4 data points, respectively, all coming from forests in the Brazilian Amazon. Forest dynamics, biomass and soils are different in this region to the conditions in West Amazonia (Baker et al. 2004; Lewis, Phillips et al. 2004; Malhi et al. 2004; Phillips et al. 2004). Hence the scaling up function was built with data from Brazilian sites and used to extrapolate to all regions.

2) As mentioned earlier, our results suggest that if leaf P constrains photosynthesis in the Amazon region,

GPP of the western sites, which have higher leaf P, would be higher than GPP in central and eastern sites, which have lower leaf P. However, it is important to mention that this spatial variation in GPP is based on a relationship of V_{max} *vs* leaf P used for scaling up V_{max} to the whole region. However this was created with only four data points, one of which determined the slope of the regression, which generated the high V_{max} and therefore high GPP at sites with high leaf P.

3) The implementation of P limitation in the model used in this study is very simplistic. It assumes that despite a large amount of leaf N in rubisco, a key enzyme in photosynthesis, leaf P could still be a proxy for photosynthetic capacity and therefore leaf P was related to the V_{max} parameter. However, it is worth mentioning that the mechanism by which P constrains photosynthesis in plants under limited P availability still needs to be better understood (Campbell and Sage 2006).

Recommendations for future work

Field observations and experiments

To test the hypothesis that Amazon forests with high leaf foliar P (western sites) have higher GPP than forests with lower foliar P (central and eastern sites), it would be necessary to compare GPP derived from leaf gas exchange measurements of photosynthesis, and/or an eddy correlation system accompanied by measurements of ecosystem respiration, at any of the western sites with high leaf P against those from a central or eastern site with low foliar P content.

If such an experiment is carried out at contrasting leaf P sites, at the leaf level, it would be useful to investigate the relationship between photosynthesis and foliar N and leaf P. When fitting the leaf gas exchange measurements to a photosynthesis model, inhibition of leaf respiration by light should be taken into account (Atkin et al. 2000; Brooks et al. 1996; Hoefnagel et al. 1998). From the fitting exercise, the difference between fitted V_{max} or J_{max} / V_{max} ratios at contrasting leaf P forest sites can give insights into the extent to which photosynthesis in these rainforest leaves are co-limited by rubisco and light. Measurement of the quantum efficiency of photosynthesis at the leaf level would reveal whether or not these leaves operate at their theoretical optimum quantum efficiency for CO_2 fixation (Farquhar et al. 1980), or whether they operate under sub-optimal conditions, as has been measured by Ehleringer and Bjorkman (1977) for C_3 and C_4 leaves. These measurements could be carried out at sites that differ in dry season length, in order to capture any possible differences caused by drought stress.

To explore the effect of nutrient limitation in these forests, a relevant field manipulation experiment would be to measure the response of forests (at contrasting P sites) to separate N and P fertilization (Bucci et al. 2006; Chapin et al. 1986).

At high CO_2 atmospheric content photosynthesis is often limited by the regeneration of inorganic phosphate, also called triose phosphate utlilization (TPU) limitation (Harley and Sharkey 1991; Harley et al. 1992). However, the response of leaves may differ in high and low P conditions because P deficiency is thought to inhibit the rate of CO_2 fixation (Brooks 1986; Brooks et al. 1988; Campbell and Sage 2006). For instance, some experimental studies have found that photosynthesis in plants grown under P deficiency are not TPU limited (Brooks 1986; Brooks et al. 1988). Therefore a relevant experiment would be to evaluate the

photosynthetic response of leaves to increasing atmospheric CO_2 at contrasting rainforest foliar P sites. With such an experiment it is possible to explore the nature of photosynthetic limitations, i.e. electron transport limitation, Rubisco capacity limitations or by the regeneration of inorganic phosphate, or TPU limitation.

Eddy correlation studies

An eddy correlation system to measure carbon and energy fluxes above the rainforest at any of the western sites where leaf P is higher than in central and eastern Amazonia could give insights into the possible differences in measured (NEE) with the already installed eddy correlation systems in central and eastern Brazil. It would also be useful if such a study is accompanied by ecosystem respiration measurements, to provide an ecosystem GPP for western sites. From parallel measurements of diffuse irradiance, we can gain understanding on the effect of increasing diffuse fraction on GPP in these forest (Gu et al. 2002; Niyogi et al. 2004; Yamasoe et al. 2006). This type of data is of great value for model calibration and evaluation.

A relevant issue related to the use of eddy correlation flux measurements to calibrate and/or validate models is the non closure of the energy balance and also to the possibility of a missing signal in the carbon measurements. In order to use eddy correlation flux data for model calibration and evaluation, some modelling studies (Anderson et al. 2000; Aranibar et al. 2006) have overcome this problem. They use an adjustment factor for carbon and energy fluxes, in such a way that the measured sensible and latent heat fluxes close the net radiation measurements, retaining the measured Bowen ratio. The eddy correlation community could provide similar or more robust methods to help address this issue and thus facilitate modelling activities.

Modelling carbon and energy exchange of the Amazon tropical rainforest

To accurately simulate carbon and energy exchange in Amazon forest, models are recommended here that separate diffuse and direct radiation and include the diurnal dynamics between sunlit and shaded leaves (de Pury and Farquhar 1997). For this rainforest ecosystem, the photosynthesis model should be linked to a stomatal conductance formulation that not only takes into account the demand but also the supply of water (Tyree 2003). The use of measurements of carbon isotopic discrimination within the modelling community is increasing due to their usefulness for model validation, but also to constrain the ranges of certain model parameters (Aranibar et al. 2006; Katul et al. 2000; Ometto et al. 2006). Specifically the use of measured $\delta^{13}C$ was a useful diagnostic in this study to constrain the parameterisation of the stomatal conductance model. Modellers are encouraged here to use this type of data and also data on the isotopic composition of the respired CO_2 fluxes (Aranibar et al. 2006).

It is important to be aware of the limitations/uncertainties in the data used for model parameterisation and evaluation, as it places major constraints on model evaluation. Furthermore, there is a pressing need to deal with the problem of non closure of energy balance from eddy correlation measurements and its possible effects on the measured fluxes of CO_2, which are crucial for model validation.

Results from this study suggest that to simulate GPP in this forest, with Leaf area index ranging between 4 and 6 m^{-2} leaves m^{-2} ground, a very precise prescription of LAI or vertical distribution of leaf N through the canopy is not crucial. Additionally, due to the high sensitivity of simulated GPP to diffuse irradiance,

validation of simulated diffuse irradiance is crucial. Also it is important to understand the nature of the relationship between diffuse irradiance and GPP. Specifically, efforts should focus on getting good estimates of maximum carboxylation capacity (the V_{max} parameter) and canopy quantum efficiency of CO_2 fixation, and also modelling and validating diffuse irradiance and stomata conductance.

Finally, if these rainforests are limited by P, or at least forests in central and eastern Amazon where leaf P is lowest, inclusion of P limitations to photosynthesis into models is necessary for realistic simulations of the regional and global carbon cycle.

5.1 Concluding remarks

The Amazon rainforest is a key contributor to the global carbon budget, due to the amount of carbon that is fixed by vegetation in Amazonia and also due to its high productivity (Dixon et al. 1994; Grace et al. 2001). Understanding its behaviour is therefore of paramount importance, especially in a changing climate (Malhi and Phillips 2004). This study serves to inform the modelling community about major issues and uncertainties in modelling Amazon basin rainforest GPP and the use of eddy correlation measurements to validate models. Also, based on simple representations of N and P limitations to photosynthesis within a model, results from a scaling up exercise of parameters from single stands to regional level suggest that if P constrains photosynthesis in this forest, there should be a gradient of GPP across the study transect, from west to east Amazonia, including Ecuador, North and South Peru, Bolivia and Brazil. Under these conditions, our results indicate a contribution of the spatial variability in GPP, soil properties and plant hydraulic traits to patterns of plant growth across the Amazon basin. The implications of P constraining photosynthesis in these forests include the possibility of forests failing to respond to rising CO_2 content, which may have consequences for expected atmospheric CO_2 concentrations predicted by global climate-carbon cycle models, leading to greater warming than hitherto anticipated. On the other hand, results from this study also suggest that if N constrains photosynthesis in these forests, GPP will not vary across the basin, favouring the homogeneous parameterisations used in global vegetation models. Finally, this study should be considered a sensitivity exercise based on simple assumptions and limited amount of data. Nevertheless, these results are valuable since they point to the need for a greater understanding into the nature of nutrient limitation in forests across the Amazon Basin and its link to photosynthesis in contrasting P conditions.

6 Samenvatting

Het doel van dit proefschrift is de ontwikkeling van een model dat de bruto primaire productiviteit (BPP) van het regenwoud langs een oost-west transect door het stroomgebied van de Amazone simuleert. Resultaten van deze studie kunnen gebruikt worden om tot nauwkeuriger schattingen van de opname van koolstof in de regenwouden te komen. Deze verbetering is gewenst omdat het Amazone regenwoud een belangrijk onderdeel vormt van de mondiale koolstof kringloop. De studie kan in het bijzonder onze kennis van het modelleren van koolstof en water fluxen verbeteren, omdat:

-BPP over het stroomgebied van de Amazone tot nu toe experimenteel slecht bepaald was. De BPP werd tot nu toe afgeleid van eddy-correlatie metingen, die slechts op een paar specifieke meetlocaties in het Braziliaanse gedeelte van de Amazone gedaan zijn.

-De meeste mondiale en regionale modellen BPP voor de Amazone dezelfde set fotosynthese parameters voor het hele gebied gebruiken.

-Er recent bewijs is van de effecten van veranderingen in de CO_2 concentratie in de atmosfeer en klimaat op de groei van het tropisch regenwoud (Lewis et al. 2004; Malhi et al. 2004; Malhi en Philillips 2004). Betere modellen voor de uitwisseling van gassen met het bladerdak, zoals ontwikkeld in deze studie, zijn nodig om de toekomstige reactie van het Amazone regenwoud op verwachte veranderingen in het milieu beter te kunnen te voorspellen.

Om de BPP over de Amazone te modelleren zijn de volgende stappen genomen: in eerste instantie zijn twee methodes om de fotosynthese van het bladerdak te simuleren getest en geëvalueerd voor een enkele meetlocatie in het regenwoud. Deze “grote blad” (“big leaf”) en zon/schaduwmodellen zijn gekalibreerd en geëvalueerd met behulp van eddy-correlatie fluxen en de daarbij horende micrometeorologische metingen (Hoofdstuk 1 en Hoofdstuk 2). Het zon/schaduwmodel komt naar voren als het beste van de twee modellen. Daarom werd dit model verder geëvalueerd voor vijf andere regenwoud locaties waarvoor ook eddy-correlatie fluxen beschikbaar waren. Schaalfuncties zijn afgeleid tussen de maximale carboxylatie snelheid van Rubisco, een maat voor de fotosynthese capaciteit, en nutriënten concentraties in de bladeren (d.w.z. V_{max} tegen N in het blad en relaties tussen V_{max} en P in het blad). Deze zijn vervolgens gebruikt om een schatting te maken van fotosynthese parameters van het bladerdak voor een reeks verschillende bossen over de Amazone regio (Hoofdstuk 3). In eerste instantie is de BPP gesimuleerd op 35 locaties, waarbij gebruik werd gemaakt van de V_{max} in die afgeleid werd van de N en P in het blad. Overeenkomstige BPP schattingen zijn vervolgens beoordeeld op termen van hun gevoeligheid voor klimaat en op hun vermogen om variaties in bovengrondse Netto Primaire Productie (BNPP) over het stroomgebied te verklaren.

Dit proefschrift behandelt in detail de navolgende vragen onder twee algemene hoofdthema’s:

Modellering van fotosynthese en energie-uitwisseling met behulp van eddy-correlatie data op specifieke locaties.

Kunnen de gemeten BPP en energie fluxen afgeleid van eddy-correlatie correct gemodelleerd worden op verschillende locaties in het Amazone regenwoud?

Om deze vraag te beantwoorden moet men de onzekerheden in gedachten houden die verband houden met de data die gebruikt worden voor zowel de evaluatie van het model (zie vragen over onzekerheden) als voor de relaties die gebruikt worden voor de modelparameterisatie. Na herkalibratie was het model in staat de BPP op de 5 geëvalueerde locaties nauwkeurig te simuleren.

Wat zijn de voor- en nadelen van de gebruikte aanpak van modellering?

Van de twee geëvalueerde methodes om fotosynthese te modelleren (zon en schaduw en het “big leaf”), is het zon- en schaduwmodel kwalitatief en kwantitatief superieur, in termen van modelfit voor het modelleren van koolstof opname (Hoofdstuk 1). Dit is gerelateerd aan het vermogen van het model om veranderingen in diffuse straling en veranderingen in bladeren in de zon en in de schaduw goed te verklaren. Er werden vergelijkbare resultaten verkregen voor de koolstof opname en oppervlakte-energiebalans als gebruik gemaakt werd van twee verschillende methoden om de huidmondjesweerstand te modelleren (Lambda en Ball Berry) (Hoofdstuk 1 en 2).

Het model van onze uiteindelijke keuze, de zon en schaduw aanpak met de lambda formule voor huidmondjesweerstand, had de neiging om de gemeten BPP tijdens middagcondities op 3 van de 5 locaties te overschatten. Dit gebuerde vooral bij een hoog dampspanningtekort (VPD) en hoge luchttemperaturen, in zowel het natte als droge seizoen. Dit resultaat onstaat doordat de simpele formule voor huidmondjesweerstand gebaseerd is op enkele de atmosferische vraag om de opening van de huidmondjes te reguleren. Daarnaast had het model de neiging om de gemeten verdampingsfractie (het quotiënt van verdamping en netto beschikbare straling) op 4 van de 5 locaties tijdens zowel natte als droge seizoenen te overschatten. Dit komt ook door de te simpele formule voor de huidmondjesweerstand. Dit probleem komt echter vaker voor bij biosfeer modellen, die óf de gemeten koolstof opname goed kunnen reproduceren, óf de energie balans, maar helaas zelden beide tegelijkertijd (Morales et al. 2005).

Samengevat, lijkt het erop dat het zon en schaduw model voor fotosynthese een geschikte methode is om de koolstof fluxen van het Amazone regenwoud te simuleren, wanneer er een geschikte parameterisatie beschikbaar is. We stellen echter wel dat dit model gekoppeld moet worden aan een huidmondjesweerstand parameterisatie die niet alleen de atmosfersiche vraag bevat, maar ook de toevoer van water van de bodem (Fisher et al. 2006).

Wat beperkt een modelevaluatie die gebruik maakt van eddy-correlatie flux data voor locaties in de Amazone?

De belangrijkste beperkingen van dit type modelevaluatie zijn de onzekerheden, die verbonden zijn aan de

data die gebruikt wordt voor de evaluatie, vooral de netto ecosysteemuitwisseling (Net Ecosystem Exchange NEE), respiratie van het ecosysteem, de energiefluxen van de eddy-correlatie metingen en de relaties tussen de N in het blad en V_{max} (gebaseerd op metingen) die gebruikt zijn voor de parameterisatie van het model. Een beknopte samenvatting van deze beperkingen volgt:

Schattingen van de NEE van eddy-correlatie metingen en schattingen van de respiratiesnelheid van het ecosysteem bepalen de maximale assimilatiesnelheid die gebruikt wordt om de modelvoorspellingen te evalueren. Echter, voor twee locaties in de Amazone, zijn de totale onzekerheden die verbonden zijn met de eddy-correlatie metingen geschat in de orde van 12 tot 32% (Kruijt et al. 2004).

Er zijn grote problemen met het schatten van de ecosysteemrespiratie in deze bossen. Als deze term geschat wordt met behulp van de NEE metingen van eddy-correlatie tijdens de nacht, dan zijn de onzekerheden gerelateerd aan slechte menging en de mogelijke afvoer van CO_2 middels laterale fluxen (Aubinet et al. 2002; Massman en Lee 2002; Pattey et al. 2002; Saleska et al. 2003). Als ecosysteemrespiratie geschat wordt met behulp van individuele respiratie componenten, dan zijn er ook problemen, voornamelijk bij het bepalen van de bodemrespiratie, die zowel temporeel (per seizoen) als in de ruimte varieert. Voor de meeste locaties die in deze studie zijn gebruikt zijn, waren geen parallelle metingen van NEE en bodemrespiratie beschikbaar. Daarom hebben we bodemrespiratie gebruikt van andere jaren dan de meetperioden van de eddy-correlatie data. Vanwege verschillen in neerslag van jaar tot jaar, is het waarschijnlijk dat er fouten zitten in de schattingen van de bodemrespiratie. Verder zijn er ook onzekerheden in de schatting van de respiratie van het grove strooisel, omdat de hoeveelheid van grof strooisel varieert op de verschillende locaties. De Tapajos locatie heeft, bijvoorbeeld, minstens dubbel de hoeveelheid grof strooisel dan de Manaus locatie. Dit kan gemakkelijk leiden tot hogere respiratie van grof strooisel bij Tapajos (Keller et al. 2004). We hebben echter geen vergelijkbare informatie over Caxiuana en Jaru, de andere locaties die in deze studie zijn gebruikt. Een andere belangrijke factor die bijdraagt aan ecosysteemrespiratie is de respiratie van het blad. In deze studie hebben we geen rekening gehouden met de remming van bladrespiratie door licht in simulaties met het zon en schaduw model (alleen bij de “big leaf” aanpak in Hoofdstuk 1). Er is echter groeiend bewijs dat dit effect belangrijk is, ook al is het onzeker in hoeverre bladrespiratie precies door licht wordt afgeremd (Atkin et al. 2000a; Atkin et al 2000b; Brooks en Farquhar 1985; Hoefnagel et al. 1998). Dat de energie balans van eddy-correlatie metingen niet sluitend is (Araújo et al. 2002; Kruijt et al. 2004; von Randow et al. 2004) zorgt ervoor dat modelevaluatie bemoeilijkt wordt en kan ook een onderschatting van de CO_2 flux leiden.

Een andere belangrijke beperking van de huidige modelevaluatie is de betrouwbaarheid van de relaties die gebruikt zijn om V_{max}, een sleutelparameter in het model die de maximale assimilatiesnelheid bepaalt, te parameteriseren. De relaties tussen V_{max} en N in het blad, die geschat zijn met behulp van metingen en hier gebruikt zijn voor modelparameterisatie, leverden erg lage waarden van V_{max} op, vergeleken met recente relaties verkregen van metingen in de Amazone (Domingues et al. 2005; Vale et al. 2003).

Schalen van locatie naar gebied

Wat kan van dit opschalingexperiment worden geleerd over de BPP in het stroomgebied van de Amazone?

Simulaties die een P limitatie voor fotosynthetische opname aannemen

-Ruimtelijke variatie van BPP

Resultaten van deze gevoeligheidsstudie suggereren dat als fotosynthese in het Amazonegebied beperkt wordt door P in het blad, de BPP van de locaties in het westen hoger zal zijn dan de BPP van de locaties in het centrum en oosten omdat op de locaties in het westen meer P in het blad zit dan in het centrum en oosten. Dit duidt op een ruimtelijke variatie in BPP met een factor 1.8 over de Amazone. Onder deze omstandigheden zou een homogene parameterisatie van de fotosynthese parameters, zoals gebruikt in mondiale landoppervlakteschema's niet op zijn plaats zijn.

-Relatie tussen BPP en bovengrondse netto primaire productie (BNPP)

Onder de aanname dat P fotosynthese in deze bossen limiteert, suggereren de resultaten dat niet alleen de ruimtelijke variatie in BPP maar ook de ruimtelijke variabiliteit in de hydraulische eigenschappen van bodem en planten bijdraagt aan het verklaren van patronen in de plantengroei over het stroomgebied van de Amazone. Ook al zijn deze parameterisaties maar gebaseerd op 4 punten, met één enkel punt dat een hoge BPP heeft bij hoge P in het blad, de gemeten gradiënt in de P van het blad over het Amazone stroomgebied suggereert hetzelfde resultaat in P gelimiteerde condities.

Eén van de gevolgen van een P-gelimiteerd Amazone regenwoud, of althans die gebieden waar de P in het blad het laagst is (d.w.z. het centrale en oostelijke Amazone regio's), is dat in een atmosfeer met een hoge CO_2 concentratie, een gebrek aan reactie van de plant op de toenemende CO_2 kan onstaan die het tegenovergestelde kan zijn van de tot nu toe aangenomen reactie. Dit zou kunnen leiden tot een mogelijke reductie in de toekomstige koolstofopname van het landoppervlak in de Amazone en daardoor uiteindelijk tot nog hogere mondiale CO_2 concentraties in de atmosfeer. Dit kan weer een sterkere klimaatverandering tot gevolg hebben dan tot nog toe verwacht werd.

Simulaties die N limitatie voor fotosynthetische opname aannemen

Aan de andere kant suggereren de resultaten van deze gevoeligheidsstudie dat, als fotosynthese gelimiteerd is door N, de BPP waarschijnlijk niet veel zal variëren over het stroomgebied. Onder deze omstandigheden kan gesimuleerde BPP de variabiliteit in gemeten BNPP echter niet verklaren. In dit geval ondersteunt het gebrek aan ruimtelijke variatie in BPP wel de homogene parameterisaties die gebruikt worden in de mondiale landoppervlakteschema's, waarin parameters zoals V_{max} constant worden gehouden voor verschillende plant functionele types.

Hoe gevoelig is de gesimuleerde BPP voor variabelen van het milieu?

In het eerste hoofdstuk was gevonden dat de BPP erg gevoelig is voor zonnestraling, in het bijzonder voor diffuse straling. Dit komt omdat de structuur van het bladerdak van deze bossen wordt gevormd door de hoge bomen met een dicht bladerdek en Leaf Area Indices (LAIs) die variëren van 4-6 m^2 bladeren per m^2 grond. Onder zulke condities bevindt een groot gedeelte van de bladeren zich in de schaduw maar door hun aantal wordt hun fotosynthese wel degelijk relevant. Omdat bladeren in de schaduw alleen diffuse straling ontvangen, is de gevoeligheid van gemodelleerde fotosynthese voor de diffuse straling dus ook zeer relevant.

Bovendien is in een gevoeligheidsanalyse van gesimuleerde maandelijkse BPP voor meteorologie, CO_2 en LAI (Hoofdstuk 4) gevonden dat diffuse zonnestraling de hoogste bijdrage levert aan de variantie in gesimuleerde BPP. Dit benadrukt het belang van diffuse zonnestraling voor de totale onzekerheid in de gesimuleerde BPP.

Welke onzekerheden zijn verbonden aan het opschalen van relaties die gebaseerd zijn op N en P in het blad?

Er zijn drie belangrijke beperkingen voor het opschalen van de simulaties van BPP naar het regionale/continentale niveau:

1) Simulaties zijn gemaakt met de modelparameter V_{max} (gebruikt als maat voor fotosynthetische capaciteit), die gespecificeerd is op elke locatie. V_{max} was op elke locatie geschat met behulp van een lineaire relatie tussen V_{max} (verkregen in Hoofdstuk 3 van modelevaluatie tegen eddy-correlatie data op 5 locaties) en gemeten N en P in het bladerdak. De belangrijkste beperking van dit gedeelte van de studie is dat deze relaties van V_{max} tegenover N in het blad en V_{max} tegenover P in het blad geschat zijn met behulp van respectievelijk 5 en 4 data punten, die allemaal van bossen in het Braziliaanse deel van de Amazone komen. De dynamica, biomassa en bodems van het bos zijn in deze regio's anders dan de condities in het westen van de Amazone (Baker et al. 2004; Lewis, Phillips et al. 2004; Malhi et al. 2004; Phillips et al. 2004).

2) Zoals eerder vermeld, suggereren onze resultaten dat, als P in het blad de fotosynthese in de Amazone regio beperkt, de BPP van de westelijke locaties, die een hogere P in het blad hebben, hoger zou moeten zijn dan de BPP op centrale en oostelijke locaties, die een lagere P in het blad hebben. Het is echter belangrijk om te vermelden dat de ruimtelijke variatie in BPP gebaseerd is op de relatie van V_{max} met P in het blad, die gebruikt is voor opschaling van V_{max} naar de gehele regio. Deze werd bepaald met maar vier datapunten, waarvan één de helling van de regressie bepaalde, die de hoge V_{max} en daaraan gerelateerde hoge BPP op locaties met hoge P in het blad voortbracht.

3) De implementatie van P-limitatie in het model dat voor deze studie is gebruikt, is erg simplistisch. Het neemt aan dat de P in het blad nog steeds een maat kan zijn voor de fotosynthetische capaciteit, ondanks een grote hoeveelheid van N in Rubisco, een sleutelenzym in fotosynthese, in het blad. Om deze reden is P in het blad gerelateerd aan de V_{max} parameter. Het is echter vermeldenswaardig dat het mechanisme waarbij P de fotosynthese in planten onder gelimiteerde P beschikbaarheid beperkt, nog grotendeels onduidelijk is (Campbell en Sage 2006).

Aanbevelingen voor toekomstig onderzoek

Veldwaarnemingen en experimenten

Om de hypothese te testen dat Amazone bossen met hoog P in het blad (westelijke locaties) een hogere BPP hebben dan bossen met lager P in het blad (centrale en oostelijke locaties), is het nodig om de BPP te vergelijken van één van de westelijke locaties met hoog P in het blad, met die van een centrale of oostelijke locatie met een laag P gehalte in het blad. Hiervoor zijn, naast BPP metingen, metingen van gas uitwisseling van fotosynthese van het blad en/of een eddy-correlatie metingen met onafhankelijke ecosysteem respiratie

nodig op beide locaties.
Als een dergelijk experiment wordt uitgevoerd op locaties met contrasterende P in het blad, dan zou het nuttig zijn om de relatie tussen fotosynthese en N en P in het blad nader te onderzoeken. Wanneer een fotosynthese model wordt gekalibreerd met behulp van gasuitwisselingsmetingen van het blad, moet er rekening gehouden worden met afname van respiratie in het blad door licht (Atkin et al. 2000; Brooks et al. 1996; Hoefnagel et al. 1998). Het verschil tussen gekalibreerde V_{max} of J_{max} / V_{max} verhoudingen kan, bij boslocaties met contrasterende P in het blad, inzicht geven in de mate waarin fotosynthese in deze regenwoudbladeren gelimiteerd wordt door een combinatie van Rubisco en licht. Metingen van de kwantumefficiëntie van fotosynthese op het blad niveau zal bovendien kunnen laten zien of deze bladeren op hun theoretische optimum kwantumefficiëntie voor CO_2 fixatie opereren (Farquhar et al. 1980), of dat zij onder sub-optimale condities opereren, zoals dat is gemeten door Ehleringer en Bjorkman (1977) voor C_3 en C_4 bladeren. Deze metingen kunnen worden uitgevoerd op locaties die verschillen in de lengte van het droge seizoen, om de verschillen weer te geven die veroorzaakt kunnen worden door droogtestress.

Het meten van de respons van bossen (op contrasterende P locaties) op gescheiden N en P bemesting, zou een relevant veldmanipulatie-experiment zijn om het effect van limitatie van deze nutriënten in deze bossen te onderzoeken (Bucci et al. 2006; Chapin et al. 1986).

Bij een hoog atmosferisch CO_2-gehalte is fotosynthese vaak gelimiteerd door de regeneratie van anorganisch fosfaat, ook wel “triose phosphate utilization” (TPU) limitatie genoemd (Harley en Sharkey 1991; Harley et al. 1992). De respons van bladeren kan echter verschillen in hoge en lage P-condities, omdat men denkt dat een P-tekort de snelheid van CO_2-fixatie belemmert (Brookes 1986; Brooks et al. 1988; Campbell en Sage 2006). Het evalueren van de fotosyntheserespons van bladeren op toenemende atmosferische CO_2 op regenwoud locaties met contrasterende P in de bladeren, zou daarom een zinnig experiment zijn. Met een dergelijk experiment is het mogelijk om de aard van fotosynthese limitaties, d.w.z. elektron transport limitatie, Rubisco capaciteit limitatie, of limitatie door de regeneratie van anorganisch fosfaat, of TPU limitatie, meer in detail te onderzoeken.

Eddy-correlatie studies
Een eddy-correlatie systeem om de koolstof- en energiefluxen boven een regenwoud te meten op één van de westelijke locaties, waar P in het blad hoger is dan in de centrale en oostelijke Amazone, zou inzicht kunnen geven in de mogelijke verschillen in NEE, die gemeten zijn met de reeds geïnstalleerde eddy-correlatie systemen in centraal en oostelijk Brazilië. Het zou ook nuttig zijn om in een dergelijke studie metingen uit te voeren van de ecosysteemrespiratie, om de ecosysteem-BPP voor westelijke locaties te bepalen. Door parallelle metingen van diffuse straling kunnen we de effecten van een toenemende diffuse fractie op BPP in deze bossen beter leren begrijpen (Gu et al. 2002; Niyogi et al. 2004; Yamasoe et al. 2006). Dit type data is van groot belang voor de modelkalibratie en evaluatie.

Een ander relevant punt, gerelateerd aan het gebruik van de eddy-correlatie fluxmetingen die gebruikt zijn voor het kalibreren en/of valideren van modellen, is het feit dat de energiebalans zelden geheel sluitend is. Dit suggereert ook dat de gemeten CO2 flux te laag kan zijn . Teneinde de eddy-correlatie flux data voor modelkalibratie en evaluatie te kunnen gebruiken, hebben een aantal modelleringstudies (Anderson et al.

2000, Aranibar et al. 2006) dit probleem overwonnen. Zij gebruiken een correctiefactor voor koolstof- en energiefluxen op een dusdanige manier dat de som van de gemeten voelbare en latente warmteflux gelijk wordt gesteld aan de netto stralingsmetingen, met behoud van de gemeten Bowen verhouding. De eddy-correlatie onderzoeksgroepen zouden vergelijkbare of wellicht meer robuuste methoden kunnen ontwikkelen om dit probleem te helpen aanpakken en modelleringsactiviteiten te vergemakkelijken.

Modellering van koolstof- en energieuitwisseling van het Amazone tropisch regenwoud
Om de koolstof- en energieuitwisseling in het Amazonebos nauwkeurig te simuleren, worden hier modellen aangeraden die onderscheid maken tussen directe en diffuse straling en die ook de dagelijkse dynamica tussen bladeren in de zon en die in de schaduw bevatten (de Pury en Farquhar 1997). Voor dit regenwoudecosysteem zou het fotosynthesemodel verbonden moeten worden aan een formule van huidmondjesweerstand, die niet alleen de vraag naar, maar ook de levering van water meeneemt (Tyree 2003). Het gebruik van metingen van de isotopensamenstelling van koolstof neemt binnen de modelleringgroepen toe, dankzij hun bruikbaarheid voor validatie van de modellen, maar beperkt ook het bereik van bepaalde modelparameters (Aranibar et al. 2006; Katul et al. 2000; Ometto et al. 2006). Een specifiek voorbeeld is het gebruik van de gemeten $\delta\,^{13}C$, dat een nuttig hulpmiddel was in deze studie voor de parameterisatie van het model van de huidmondjesweerstand. Modelleurs kunnen dit type data vaker gebruiken en ook data van de isotopensamenstelling van gerespireerde CO_2-fluxen (Aranibar et al. 2006).

Het is belangrijk om zich bewust te zijn van de beperkingen en onzekerheden in de data, die gebruikt zijn voor modelparameterisatie en evaluatie, omdat dit belangrijke beperkingen oplegt voor modelevaluatie. Verder is er een dringende noodzaak om betr om te gaan met het probleem van de niet sluitende energie balans van eddy-correlatie metingen en de mogelijke effecten op de gemeten CO_2 fluxen, die cruciaal zijn voor modelvalidatie.

Resultaten van deze studie suggereren dat een precieze beschrijving van LAI of verticale distributie van N in het blad over het bladerdak niet cruciaal is voor de simulatie van BPP in regenwoud met een LAI ussen 4 en 6 per m^2 blad per m^2 grond. Wel is validatie van gesimuleerde diffuse straling cruciaal, vanwege de hoge gevoeligheid van gesimuleerde BPP voor diffuse straling. Het is ook belangrijk om de aard van de relatie tussen diffuse straling en BPP te begrijpen. Inspanningen zouden zich specifiek moeten richten op het verkrijgen van goede schattingen van de maximale carboxilatiecapaciteit (de V_{max} parameter) en bladerdak kwantumefficiëntie van CO_2-fixatie en ook modellering en validatie van huidmondjesweerstand bij diffuse straling.

Ten slotte, als deze regenwouden door P zijn gelimiteerd, of op zijn minst bossen in de centrale en oostelijke Amazone waar de P in het blad het laagste is, dan is de opname van P limitaties voor fotosynthese in modellen noodzakelijk voor realistische simulaties van de regionale en mondiale koolstof kringloop.

6.1 Concluderende opmerkingen

Het Amazone regenwoud is een sleutelfactor in het mondiale koolstofbudget, vanwege de hoeveelheid koolstof die vastgelegd is door de vegetatie in de Amazone en ook vanwege de hoge productiviteit van het

bos (Dixon et al. 1994; Grace et al. 2001). Het is daarom van het grootste elang om het gedrag van het woud beter te begrijpen, in het bijzonder in een veranderend klimaat (Malhi en Phillips 2004). Deze studie had als doel meer inzicht te krijgen in de belangrijkste problemen en onzekerheden in de modellering van de BPP in het Amazone regenwoud en het gebruik van eddy-correlatie methoden om modellen te valideren. Gebaseerd op simpele representaties van N- en P-limitatie voor fotosynthese in een model, suggereren resultaten van een opschalingoefening van parameters van afzonderlijke locaties tot regionaal niveau, dat als fotosynthese in dit bos beperkt wordt door P, er een gradiënt van BPP over het transect van het studiegebied zou moeten zijn van de westelijke naar de oostelijke Amazone, inclusief Ecuador, Noord en Zuid Peru, Bolivia en Brazilië. Onder deze omstandigheden wijzen onze resultaten op een bijdrage van de ruimtelijke variabiliteit in BPP, bodemeigenschappen en hydraulische kenmerken van de plant aan de patronen van plantengroei in het stroomgebied van de Amazone. De implicaties van de fotosynthesebeperking door P in deze bossen impliceren de mogelijkheid dat bossen niet adequaat kunnen reageren op een toenemend CO_2-gehalte zoals voorspeld door mondiale klimaat – koolstofkringloopmodellen. Dit kan leiden tot nog grotere opwarming dan tot nog toe is voorzien. Aan de andere kant suggereren resultaten van deze studie ook dat als de N de fotosynthese in deze bossen beperkt, de BPP niet zal variëren over het stroomgebied. Dit ondersteunt de homogene parameterisatie die gebruikt wordt in mondiale vegetatiemodellen. Ten slotte zou deze studie het best beschouwd kunnen worden als een gevoeligheidstudie, gebaseerd op relatief simpele aannames en een beperkte hoeveelheid data. Desondanks zijn de resultaten waardevol, omdat ze duiden op een noodzaak voor beter begrip van de aard van nutriëntlimitatie in bossen over het stroomgebied van de Amazone.

7 References

Alados, I., and L. Alados-Arboledas. 1999. Direct and diffuse photosynthetically active radiation: measurements and modelling. Agricultural and Forest Meteorology 93 (1):27-38.

Anderson, M. C., J. M. Norman, T. P. Meyers, and G. R. Diak. 2000. An analytical model for estimating canopy transpiration and carbon assimilation fluxes based on canopy light-use efficiency. Agricultural and Forest Meteorology 101 (4):265-289

Aragao, L.E.O. 2004. Modelagem dos padrões temporal e espacial da produtividade primária bruta na região do tapajós: uma análise multi-escala. PhD, Instituto Nacional de Pesquisas Espaciais, São José dos Campos.

Aranibar, J. N., J. A. Berry, W. J. Riley, D. E. Pataki, B. E. Law, and J. R. Ehleringer. 2006. Combining meteorology, eddy fluxes, isotope measurements, and modeling to understand environmental controls of carbon isotope discrimination at the canopy scale. Global Change Biology 12 (4):710-730.

Araújo, A. C., A. D. Nobre, B. Kruijt, J. A. Elbers, R. Dallarosa, P. Stefani, C. von Randow, A. O. Manzi, A. D. Culf, J. H. C. Gash, R. Valentini, and P. Kabat. 2002. Comparative measurements of carbon dioxide fluxes from two nearby towers in a central Amazonian rainforest: The Manaus LBA site. Journal of Geophysical Research-Atmospheres 107 (D20):art. no.-8090.

Arneth, A., F. M. Kelliher, S. T. Gower, N. A. Scott, J. N. Byers, and T. M. McSeveny. 1998. Environmental variables regulating soil carbon dioxide efflux following clear-cutting of a Pinus radiata D. Don plantation. Journal of Geophysical Research-Atmospheres 103 (D5):5695-5705.

Asner, G. P., M. Keller, R. Pereira, J. C. Zweede, and J. N. M. Silva. 2004. Canopy damage and recovery after selective logging in Amazonia: Field and satellite studies. Ecological Applications 14 (4):S280-S298.

Atkin, O. K., J. R. Evans, and K. Siebke. 1998. Relationship between the inhibition of leaf respiration by light and enhancement of leaf dark respiration following light treatment. Australian Journal of Plant Physiology 25 (4):437-443.

Atkin, O. K., J. R. Evans, M. C. Ball, H. Lambers, and T. L. Pons. 2000. Leaf respiration of snow gum in the light and dark. interactions between temperature and irradiance. Plant Physiology 122 (3):915-923.

Atkin, O. K., Q. S. Zhang, and J. T. Wiskich. 2002. Effect of temperature on rates of alternative and cytochrome pathway respiration and their relationship with the redox poise of the quinone pool. Plant Physiology 128 (1):212-222.

Aubinet, M., B. Heinesch, and B. Longdoz. 2002. Estimation of the carbon sequestration by a heterogeneous forest: night flux corrections, heterogeneity of the site and inter-annual variability. Global Change Biology 8 (11):1053-1071.

Baker, T. R., O. L. Phillips, Y. Malhi, S. Almeida, L. Arroyo, A. Di Fiore, T. Erwin, N. Higuchi, T. J. Killeen, S. G. Laurance, W. F. Laurance, S. L. Lewis, A. Monteagudo, D. A. Neill, P. N. Vargas, N. C. A. Pitman, J. N. M. Silva, and R. V. Martinez. 2004. Increasing biomass in Amazonian forest plots. Philosophical Transactions of the Royal Society of London Series B-Biological Sciences 359 (1443):353-365.

Baker, T. R., O. L. Phillips, Y. Malhi, S. Almeida, L. Arroyo, A. Di Fiore, T. Erwin, T. J. Killeen, S. G.

Laurance, W. F. Laurance, S. L. Lewis, J. Lloyd, A. Monteagudo, D. A. Neill, S. Patiño, N. C. A. Pitman, J. N. M. Silva, and R. V. Martinez. 2004. Variation in wood density determines spatial patterns in Amazonian forest biomass. Global Change Biology 10 (5):545-562.

Baldocchi, D., B.H Bruce, and P.M Tilden. 1988. Measuring Biosphere-Atmosphere Exchanges of Biologically Related Gases with Micrometeorological Methods. Ecology 69 (5):1331-1340.

Baldocchi, D. D., and P. C. Harley. 1995. Scaling Carbon-Dioxide and Water-Vapor Exchange from Leaf to Canopy in a Deciduous Forest .2. Model Testing and Application. Plant Cell and Environment 18 (10):1157-1173.

Baldocchi, D., and T. Meyers. 1998. On using eco-physiological, micrometeorological and biogeochemical theory to evaluate carbon dioxide, water vapor and trace gas fluxes over vegetation: a perspective. Agricultural and Forest Meteorology 90 (1-2):1-25.

Baldocchi, D., E. Falge, L. H. Gu, R. Olson, D. Hollinger, S. Running, P. Anthoni, C. Bernhofer, K. Davis, R. Evans, J. Fuentes, A. Goldstein, G. Katul, B. Law, X. H. Lee, Y. Malhi, T. Meyers, W. Munger, W. Oechel, K. T. P. U, K. Pilegaard, H. P. Schmid, R. Valentini, S. Verma, T. Vesala, K. Wilson, and S. Wofsy. 2001. FLUXNET: A new tool to study the temporal and spatial variability of ecosystem-scale carbon dioxide, water vapor, and energy flux densities. Bulletin of the American Meteorological Society 82 (11):2415-2434.

Baldocchi, D. D. 2003. Assessing the eddy covariance technique for evaluating carbon dioxide exchange rates of ecosystems: past, present and future. Global Change Biology 9 (4):479-492.

Ball, J. T., I.E Woodrow, and J. A. Berry. 1987. A model predicting stomatal conductance and its contribution to the control of photosynthesis under different environmental conditions. In Progress in Photosynthesis Research, edited by J. B. M. Dordrecht: Martinus Nijhoff.

Betts, A. K., and P. Viterbo. 2005. Land-surface, boundary layer, and cloud-field coupling over the southwestern Amazon in ERA-40. Journal of Geophysical Research-Atmospheres 110 (D14):art. no.-D14108.

Bravard, S., and D. Righi. 1989. Geochemical Differences in an Oxisol Spodosol Toposequence of Amazonia, Brazil. Geoderma 44 (1):29-42.

Brooks, A., and G. D. Farquhar. 1985. Effect of temperature on the CO2/O2 specificity of ribulose 1,5-bisphosphate carboxylase oxygenase and the rate of respiration in the light: estimates from gas exchange measurements on spinach. Planta 165 (3):397-406.

Brooks, A. 1986. Effects of Phosphorus-Nutrition on Ribulose-1,5-Bisphosphate Carboxylase Activation, Photosynthetic Quantum Yield and Amounts of Some Calvin-Cycle Metabolites in Spinach Leaves. Australian Journal of Plant Physiology 13 (2):221-237.

Brooks, A., K. C. Woo, and S. C. Wong. 1988. Effects of Phosphorus-Nutrition on the Response of Photosynthesis to Co2 and O-2, Activation of Ribulose Bisphosphate Carboxylase and Amounts of Ribulose Bisphosphate and 3-Phosphoglycerate in Spinach Leaves. Photosynthesis Research 15 (2):133-141.

Brooks, J. R., D. G. Sprugel, and T. M. Hinckley. 1996. The effects of light acclimation during and after foliage expansion on photosynthesis of abies amabilis foliage within the canopy. Oecologia 107 (1):21-32.

Bucci, S.J, F.G Scholz, G. Goldstein, F. C. Meinzer, A.C. Franco, P.I Campanello, V.R Villalobos, M. Bustamante, and W.F. Miralles. 2006. Nutrient availability constrains the hydraulic architecture and

water relations of savannah trees Plant, Cell and Environment 29 (12):2153-2167.

Caemmerer, S., and G. D. Farquhar. 1981. Some relationships between the biochemistry of photosynthesis and the gas exchange of leaves. Planta 153 (4):376-387.

Campbell, C. D., and R. F. Sage. 2002. Interactions between atmospheric CO2 concentration and phosphorus nutrition on the formation of proteoid roots in white lupin (Lupinus albus L.). Plant, Cell and Environment 25 (8):1051-1059.

Campbell, C.D., and R F. Sage. 2006. Interactions between the effects of atmospheric CO2 content and P nutrition on photosynthesis in white lupin (Lupinus albus L.). Plant, Cell and Environment 29 (5):844-853.

Carmo, J.B., M. Keller, J.D. Dias, P. B. de Camargo, and P. Crill. 2006. A source of methane from upland forests in the Brazilian Amazon. Geophysical Research letters 33 (L04809):.

Carswell, F. E., P. Meir, E. V. Wandel M. Bonates, B. Kruijt, E. M. Barbosa, A. D. Nobre, J. Grace, and P. G. Jarvis. 2000. Photosynthetic capacity in a central Amazonian rain forest. Tree Physiology 20 (3):179-186.

Carswell, F. E., A. L. Costa, M. Palheta, Y. Malhi, P. Meir, J. D. R. Costa, M. D. Ruivo, L. D. M. Leal, J. M. N. Costa, R. J. Clement, and J. Grace. 2002. Seasonality in CO2 and H2O flux at an eastern Amazonian rain forest. Journal of Geophysical Research-Atmospheres 107 (D20):art. no.-8076.

Chambers, J. Q., N. Higuchi, J. P. Schimel, L. V. Ferreira, and J. M. Melack. 2000. Decomposition and carbon cycling of dead trees in tropical forests of the central Amazon. Oecologia 122 (3):380-388.

Chambers, J. Q., J. dos Santos, R. J. Ribeiro, and N. Higuchi. 2001. Tree damage, allometric relationships, and above-ground net primary production in central Amazon forest. Forest Ecology and Management 152 (1-3):73-84.

Chambers, J. Q., E. S. Tribuzy, L. C. Toledo, B. F. Crispim, N. Higuchi, J. dos Santos, A. C. Araujo, B. Kruijt, A. D. Nobre, and S. E. Trumbore. 2004. Respiration from a tropical forest ecosystem: Partitioning of sources and low carbon use efficiency. Ecological Applications 14 (4):S72-S88.

Chapin, F. S., P. M. Vitousek, and K. Vancleve. 1986. The Nature of Nutrient Limitation in Plant-Communities. American Naturalist 127 (1):48-58.

Collatz, G. J., J. A. Berry, G. D. Farquhar, and J. Pierce. 1990. The Relationship between the Rubisco Reaction-Mechanism and Models of Photosynthesis. Plant Cell and Environment 13 (3):219-225.

Collatz, G. J., J. T. Ball, C. Grivet, and J. A. Berry. 1991. Physiological and environmental regulation of stomatal conductance, photosynthesis and transpiration: a model that includes a laminar boundary layer. Agricultural and Forest Meteorology 54 (2-4):107-136.

Coutinho, L.M, and A. Lamberti. 1971. Respiracao Edafica e Produtividade Primaria numa Comunidade Amazonica de Mata de Terra-firme. Ciencia e Cultura 23:411-419.

Cowan, I. R. 1977. Stomatal behaviour and environment. Advances in Botanical Research 4:117-121.

Cowan, I.R., and G.D. Farquhar. 1977. Stomatal function in relation to leaf metabolism and environment. Symposium of the Society for Experimental Biology (31):471-505.

Cox, P. M., C. Huntingford, and R. J. Harding. 1998. A canopy conductance and photosynthesis model for use in a GCM land surface scheme. Journal of Hydrology 213 (1-4):79-94.

Cox, P. M., R. A. Betts, C. D. Jones, S. A. Spall, and I. J. Totterdell. 2000. Acceleration of global warming due to carbon-cycle feedbacks in a coupled climate model (vol 408, pg 184, 2000). Nature 408 (6813):750-750.

Cromer, R. N., P. E. Kriedemann, P. J. Sands, and L. G. Stewart. 1993. Leaf Growth and Photosynthetic Response to Nitrogen and Phosphorus in Seedling Trees of Gmelina-Arborea. Australian Journal of Plant Physiology 20 (1):83-98.

da Rocha, H. R., M. L. Goulden, S. D. Miller, M. C. Menton, Ldvo Pinto, H. C. de Freitas, and Ames Figueira. 2004. Seasonality of water and heat fluxes over a tropical forest in eastern Amazonia. Ecological Applications 14 (4):S22-S32.

Davidson, E. A., L. V. Verchot, J. H. Cattanio, I. L. Ackerman, and J. E. M. Carvalho. 2000. Effects of soil water content on soil respiration in forests and cattle pastures of eastern Amazonia. Biogeochemistry 48 (1):53-69.

Davidson, E. A., F. Y. Ishida, and D. C. Nepstad. 2004. Effects of an experimental drought on soil emissions of carbon dioxide, methane, nitrous oxide, and nitric oxide in a moist tropical forest. Global Change Biology 10 (5):718-730.

de Oliveira, A. A., and D. C. Daly. 1999. Geographic distribution of tree species occurring in the region of Manaus, Brazil: implications for regional diversity and conservation. Biodiversity and Conservation 8 (9):1245-1259.

de Pury, D. G. G., and G. D. Farquhar. 1997. Simple scaling of photosynthesis from leaves to canopies without the errors of big-leaf models. Plant Cell and Environment 20 (5):537-557.

Dewar, R. C. 1995. Interpretation of an Empirical-Model for Stomatal Conductance in Terms of Guard-Cell Function. Plant Cell and Environment 18 (4):365-372.

Dixon, R. K., S. Brown, R. A. Houghton, A. M. Solomon, M. C. Trexler, and J. Wisniewski. 1994. Carbon pools and flux of global forest ecosystems. Science 263 (5144):185-190.

Dolman, A.J., A.Verhagen and C.A. Rovers. 2003. Global environmental change and land use. Dordrecht ; Boston : Kluwer Academic Publishers.

Domingues, Tomas F. , Joseph A. Berry, Luiz A. Martinelli, Jean P. H. B. Ometto, and James R. Ehleringer. 2005. Parameterization of Canopy Structure and Leaf-Level Gas Exchange for an Eastern Amazonian Tropical Rain Forest (Tapajos National Forest, Para, Brazil). Earth Interactions 9 (17):1-23.

Ehleringer, James, and Olle Bjorkman. 1977. Quantum Yields for CO2 Uptake in C3 and C4 Plants: Dependence on Temperature, CO2, and O2 Concentration Plant Physiol. 59 (1):86-90.

Ehleringer, James, and Robert W. Pearcy. 1983. Variation in Quantum Yield for CO2 Uptake among C3 and C4 Plants Plant Physiol. 73 (3):555-559.

Ehleringer, J. R., Z. F. Lin, C. B. Field, G. C. Sun, and C. Y. Kuo. 1987. Leaf carbon isotope ratios of plants from a subtropical monsoon forest. Oecologia 72 (1):109-114.

Erbs, D. G., S. A. Klein, and J. A. Duffie. 1982. Estimation of the Diffuse-Radiation Fraction for Hourly, Daily and Monthly-Average Global Radiation. Solar Energy 28 (4):293-302.

Evans, J. R. 1989. Partitioning of Nitrogen between and within Leaves Grown under Different Irradiances. Australian Journal of Plant Physiology 16 (6):533-548.

———. 1989b. Photosynthesis and Nitrogen Relationships in Leaves of C-3 Plants. Oecologia 78 (1):9-19.

———. 1993. Photosynthetic Acclimation and Nitrogen Partitioning within a Lucerne Canopy .1. Canopy Characteristics. Australian Journal of Plant Physiology 20 (1):55-67.

Fan, S. M., P. Wofsy, P. Bakwin, and D. Jacob. 1990. Atmospheric-biosphere exchange of CO2 and O3 in the central Amazon Forest. Journal of Geophysical Research-Atmospheres 95:16,851-16,864.

Farquhar, G. D., S. V. Caemmerer, and J. A. Berry. 1980. A Biochemical-Model of Photosynthetic Co2 Assimilation in Leaves of C-3 Species. Planta 149 (1):78-90.

Farquhar, G. D., M. H. Oleary, and J. A. Berry. 1982. On the Relationship between Carbon Isotope Discrimination and the Inter-Cellular Carbon-Dioxide Concentration in Leaves. Australian Journal of Plant Physiology 9 (2):121-137.

Farquhar, G.D., and S. von Caemmerer. 1982. Modelling of photosynthetic response to environmental conditions. In Enciclopedia of Plant physiology, edited by O. L. Lange, P. S. Nobel, C. B. Osmond and H. Ziegler. Berlin: Springer-Verlag.

Farquhar, G. D., J. R. Ehleringer, and K. T. Hubick. 1989. Carbon Isotope Discrimination and Photosynthesis. Annual Review of Plant Physiology and Plant Molecular Biology 40:503-537.

Farquhar, G. D., J. Lloyd, J. A. Taylor, L. B. Flanagan, J. P. Syvertsen, K. T. Hubick, S. C. Wong, and J. R. Ehleringer. 1993. Vegetation Effects on the Isotope Composition of Oxygen in Atmospheric CO2 (Vol 363, Pg 439, 1993). *Nature* 365 (6444):368-368.

Field, C., and H. A. Mooney. 1986. The photosynthesis-nitrogen relationship in wild plants. In On the Economy of Plant Form and Function. Cambridge: Cambridge University Press.

Field, C. B., M. J. Behrenfeld, J. T. Randerson, and P. Falkowski. 1998. Primary production of the biosphere: Integrating terrestrial and oceanic components. Science 281 (5374):237-240.

Finnigan, J. J., R. Clement, Y. Malhi, R. Leuning, and H. A. Cleugh. 2003. A re-evaluation of long-term flux measurement techniques - Part I: Averaging and coordinate rotation. Boundary-Layer Meteorology 107 (1):1-48.

Fisher, R.A., M. Williams, R L do Vale, A. L. da Costa, and P. Meir. 2006. Evidence from Amazonian forests is consistent with isohydric control of leaf water potential. Plant, Cell and Environment 29 (2):151-165.

Gash, J. H. C., and A. J. Dolman. 2003. Sonic anemometer (co)sine response and flux measurement I. The potential for (co)sine error to affect sonic anemometer-based flux measurements. Agricultural and Forest Meteorology 119 (3-4):195-207.

Goudriaan, J. 1977. Crop micrometeorology: A simulation study. Wageningen, The Netherlands: Centre for Agricultural Publishing and Documentation.

Goulden, M. L., J. W. Munger, S. M. Fan, B. C. Daube, and S. C. Wofsy. 1996. Measurements of carbon sequestration by long-term eddy covariance: Methods and a critical evaluation of accuracy. Global Change Biology 2 (3):169-182.

Goulden, M. L., S. D. Miller, H. R. da Rocha, M. C. Menton, H. C. de Freitas, Ames Figueira, and C. A. D. de Sousa. 2004. Diel and seasonal patterns of tropical forest CO2 exchange. Ecological Applications 14 (4):S42-S54.

Grace, J., J. Lloyd, J. McIntyre, A. Miranda, P. Meir, H. Miranda, J. Moncrieff, J. Massheder, I. Wright, and J. Gash. 1995. Fluxes of Carbon-Dioxide and Water-Vapor over an Undisturbed Tropical Forest in South-West Amazonia. Global Change Biology 1 (1):1-12.

Grace, J., Y. Mahli, N. Higuchi, and P. Meir. 2001. Productivity and carbon fluxes of tropical rain forest. In Global Terrestrial Productivity, edited by H. A. M. J.Roy. San Diego: Academic Press.

Gu, L. H., D. Baldocchi, S. B. Verma, T. A. Black, T. Vesala, E. M. Falge, and P. R. Dowty. 2002. Advantages of diffuse radiation for terrestrial ecosystem productivity. Journal of Geophysical Research-Atmospheres 107 (D5-D6):art. no.-4050.

Harley, P. C., and T. D. Sharkey. 1991. An Improved Model of C3 Photosynthesis at High Co2 - Reversed O-2 Sensitivity Explained by Lack of Glycerate Reentry into the Chloroplast. Photosynthesis Research 27 (3):169-178.

Harley, P. C., R. B. Thomas, J. F. Reynolds, and B. R. Strain. 1992. Modeling Photosynthesis of Cotton Grown in Elevated Co2. Plant Cell and Environment 15 (3):271-282.

Harris, P. P., C. Huntingford, P. M. Cox, J. H. C. Gash, and Y. Malhi. 2004a. Effect of soil moisture on canopy conductance of Amazonian rainforest. Agricultural and Forest Meteorology 122 (3-4):215-227.

Harris, P. P., C. Huntingford, J. H. C. Gash, M. G. Hodnett, P. M. Cox, Y. Malhi, and A. C. Araujo. 2004b. Calibration of a land-surface model using data from primary forest sites in Amazonia. Theoretical and Applied Climatology 78 (1-3):27-45.

Hikosaka, K., and I. Terashima. 1995. A model of the acclimation of photosynthesis in the leaves of C3 plants to sun and shade with respect to nitrogen use. Plant Cell and Environment 18 (6):605-618.

Hirose, T., and M. J. A. Werger. 1987. Maximizing daily canopy photosynthesis with respect to the leaf nitrogen allocation pattern in the canopy. Oecologia 72 (4):520-526.

Hodnett, M. G., L. P. Dasilva, H. R. Darocha, and R. C. Senna. 1995. Seasonal Soil-Water Storage Changes beneath Central Amazonian Rain-Forest and Pasture. Journal of Hydrology 170 (1-4):233-254.

Hodnett, M., J. Oyama, J. Tomasella, and D.O. Marques Filho. 1996. Comparisons of long-term soil water storage behaviour under pasture and forest in three areas of amazonia. In Amazon Deforestation and Climate, edited by J. H. C. Gash, C. A. Nobre, J. M. Roberts and R. L. Victoria. Chichester,UK: John Wiley & Sons.

Hodnett, M.G., J. Tomasella, D.O. Marques Filho, and M.D Oyama. 1996. Deep soil water uptake by forest and pasture in central amazonia: predictions from long-term daily rainfall data using a simple water balance model. In Amazon Deforestation and Climate, edited by J. H. C. Gash, C. A. Nobre, J. M. Roberts and R. L. Victoria. Chichester,UK: John Wiley & Sons.

Hoefnagel, M. H. N., O. K. Atkin, and J. T. Wiskich. 1998. Interdependence between chloroplasts and mitochondria in the light and the dark. Biochimica Et Biophysica Acta-Bioenergetics 1366 (3):235-255.

Iwata, H., Y. Malhi, and C. von Randow. 2005. Gap-filling measurements of carbon dioxide storage in tropical rainforest canopy airspace. Agricultural and Forest Meteorology 132 (3-4):305-314.

Jacob, James, and David W. Lawlor. 1992. Dependence of Photosynthesis of Sunflower and Maize Leaves on Phosphate Supply, Ribulose-1,5-Bisphosphate Carboxylase/Oxygenase Activity, and Ribulose-1,5-Bisphosphate Pool Size. Plant Physiology. 98 (3):801-807.

Janssens, I. A., H. Lankreijer, G. Matteucci, A. S. Kowalski, N. Buchmann, D. Epron, K. Pilegaard, W. Kutsch, B. Longdoz, T. Grunwald, L. Montagnani, S. Dore, C. Rebmann, E. J. Moors, A. Grelle, U. Rannik, K. Morgenstern, S. Oltchev, R. Clement, J. Gudmundsson, S. Minerbi, P. Berbigier, A. Ibrom, J. Moncrieff, M. Aubinet, C. Bernhofer, N. O. Jensen, T. Vesala, A. Granier, E. -D. Schulze, A. Lindroth, A. J. Dolman, P. G. Jarvis, R. Ceulemans, and R. Valentini. 2001. Productivity overshadows temperature in determining soil and ecosystem respiration across European forests. Global Change Biology 7 (3):269-278.

Jones, H.G. 1992. Plants and Microclimate. 2nd edn. ed. Cambridge: Cambridge University Press.

Kallberg, P., A. Simmons, S. Uppala, and M. Fuentes. 2004. The era-40 archive. ECMWF Tech Rep.:

European Centre for Medium Range Weather Forecasts.

Katul, G. G., D. S. Ellsworth, and C.-T. Lai. 2000. Modelling assimilation and intercellular CO2 from measured conductance: a synthesis of approaches. Plant, Cell and Environment 23 (12):1313-1328.

Keeling, C. D., and T. P. Whorf. 2002. Comments on "Millennial climate variability: Is there a tidal connection?". Journal of Climate 15 (4):446-446.

Keller, M., M. Palace, G. P. Asner, R. Pereira, and J. N. M. Silva. 2004. Coarse woody debris in undisturbed and logged forests in the eastern Brazilian Amazon. Global Change Biology 10 (5):784-795.

Keller, M., A. Alencar, G. P. Asner, B. Braswell, M. Bustamante, E. Davidson, T. Feldpausch, E. Fernandes, M. Goulden, P. Kabat, B. Kruijt, F. Luizao, S. Miller, D. Markewitz, A. D. Nobre, C. A. Nobre, N. Priante, H. da Rocha, P. S. Dias, C. von Randow, and G. L. Vourlitis. 2004. Ecological research in the large-scale biosphere-atmosphere experiment in Amazonia: Early results. Ecological Applications 14 (4):S3-S16.

King, David A., Stuart J. Davies, Sylvester Tan, and Nur Supardi MD. Noor. 2006. The role of wood density and stem support costs in the growth and mortality of tropical trees. Journal of Ecology 94 (3):670-680.

Kirschbaum, M. U. F., G. Simioni, B. E. Medlyn, and R. E. McMurtrie. 2003. On the importance of including soil nutrient feedback effects for predicting ecosystem carbon exchange. Functional Plant Biology 30 (2):223-237.

Klinge, H. 1968. Litter Production in an Area of Amazonian Terra Firme Forest. Part I. Litter-fall, Organic carbon and total Nitrogen contents of litter. Amazoniana 1 (4):287-302.

Kruijt, B., J. A. Elbers, C. von Randow, A. C. Araujo, P. J. Oliveira, A. Culf, A. O. Manzi, A. D. Nobre, P. Kabat, and E. J. Moors. 2004. The robustness of eddy correlation fluxes for Amazon rain forest conditions. Ecological Applications 14 (4):S101-S113.

Lambers, H., F.C Stuart , and T.L Pons. 1998. Plant Physiological Ecology. New York: Springer-Verlag.

Law, B. E., E. Falge, L. Gu, D. D. Baldocchi, P. Bakwin, P. Berbigier, K. Davis, A. J. Dolman, M. Falk, J. D. Fuentes, A. Goldstein, A. Granier, A. Grelle, D. Hollinger, I. A. Janssens, P. Jarvis, N. O. Jensen, G. Katul, Y. Mahli, G. Matteucci, T. Meyers, R. Monson, W. Munger, W. Oechel, R. Olson, K. Pilegaard, K. T. Paw, H. Thorgeirsson, R. Valentini, S. Verma, T. Vesala, K. Wilson, and S. Wofsy. 2002. Environmental controls over carbon dioxide and water vapor exchange of terrestrial vegetation. Agricultural and Forest Meteorology 113 (1-4):97-120.

Leopoldo, P. R., W. Franken, E. Salati, and M. N. Ribeiro. 1987. Towards a Water-Balance in the Central Amazonian Region. Experientia 43 (3):222-233.

Leuning, R. 1990. Modeling stomatal behavior and photosynthesis of Eucalyptus grandis. Australian Journal of Plant Physiology 17 (2):159-175.

———. 1995. A Critical-Appraisal of a Combined Stomatal-Photosynthesis Model for C-3 Plants. Plant Cell and Environment 18 (4):339-355.

Leuning, R., F. M. Kelliher, D. G. G. Depury, and E. D. Schulze. 1995. Leaf nitrogen, photosynthesis, conductance and transpiration: scaling from leaves to canopies. Plant Cell and Environment 18 (10):1183-1200.

Lewis, J. D., K. L. Griffin, R. B. Thomas, and B. R. Strain. 1994. Phosphorus Supply Affects the Photosynthetic Capacity of Loblolly-Pine Grown in Elevated Carbon-Dioxide. Tree Physiology 14 (11):1229-1244.

Lewis, S. L., O. L. Phillips, T. R. Baker, J. Lloyd, Y. Malhi, S. Almeida, N. Higuchi, W. F. Laurance, D. A. Neill, J. N. M. Silva, J. Terborgh, A. T. Lezama, R. V. Martinez, S. Brown, J. Chave, C. Kuebler, P. N. Vargas, and B. Vinceti. 2004. Concerted changes in tropical forest structure and dynamics: evidence from 50 South American long-term plots. Philosophical Transactions of the Royal Society of London Series B-Biological Sciences 359 (1443):421-436.

Lloyd, J., and G. D. Farquhar. 1994. 13C discrimination during CO2 assimilation by the terrestrial biosphere. Oecologia 99 (3-4):201-215.

Lloyd, J., J. Grace, A. C. Miranda, P. Meir, S. C. Wong, B. S. Miranda, I. R. Wright, J. H. C. Gash, and J. McIntyre. 1995. A Simple Calibrated Model of Amazon Rain-Forest Productivity Based on Leaf Biochemical-Properties. Plant Cell and Environment 18 (10):1129-1145.

Lloyd, J., S. C. Wong, J. M. Styles, D. Batten, R. Priddle, C. Turnbull, and C. A. McConchie. 1995. Measuring and modelling whole-tree gas exchange. Australian Journal of Plant Physiology 22 (6):987-1000.

Lloyd, J., B. Kruijt, D. Y. Hollinger, J. Grace, R. J. Francey, S. C. Wong, F. M. Kelliher, A. C. Miranda, G. D. Farquhar, J. H. C. Gash, N. N. Vygodskaya, I. R. Wright, H. S. Miranda, and E. D. Schulze. 1996. Vegetation effects on the isotopic composition of atmospheric CO2 at local and regional scales: Theoretical aspects and a comparison between rain forest in amazonia and a boreal forest in Siberia. Australian Journal of Plant Physiology 23 (3):371-399.

Lloyd, J., and G. D. Farquhar. 1996. The CO2 dependence of photosynthesis, plant growth responses to elevated atmospheric CO2 concentrations and their interaction with soil nutrient status .1. General principles and forest ecosystems. Functional Ecology 10 (1):4-32.

Lloyd, J. , M. I. Bird, E.M Veenendaal, and B. Kruijt. 2001. Should Phosphorous Availability be Constraining Moist Tropical Forest responses to incrasing CO2 concentrations? In Global biogeochemical cycles in the climate system, edited by E. D. Schulze, D. S. Schimel, M. Heimann, S. P. Harrison, E. A. Holland, J. Lloyd and I. C. Prentice. San Diego: Academic Press.

Long, S. P., W. F. Postl, and H. R. Bolharnordenkampf. 1993. Quantum Yields for Uptake of Carbon-Dioxide in C-3 Vascular Plants of Contrasting Habitats and Taxonomic Groupings. Planta 189 (2):226-234.

Long, S. P., X. Zhu, S Naidu, and D.R Ort. 2006. Can improvement in photosynthesis increase crop yields?. Plant, Cell and Environment 29 (3):315-330.

Lovelock, C. E., D. Kyllo, M. Popp, H. Isopp, A. Virgo, and K. Winter. 1997. Symbiotic vesicular-arbuscular mycorrhizae influence maximum rates of photosynthesis in tropical tree seedlings grown under elevated CO2. Australian Journal of Plant Physiology 24 (2):185-194.

Luizao, FJ, and H.O.R Schubart. 1987. Litter production and decomposition in a terra-firme forest of Central Amazonia. Experientia (43):259-265.

Luizao, R. C. C., F. J. Luizao, R. Q. Paiva, T. F. Monteiro, L. S. Sousa, and B. Kruijt. 2004. Variation of carbon and nitrogen cycling processes along a topographic gradient in a central Amazonian forest. Global Change Biology 10 (5):592-600.

Malhi, Y., A. D. Nobre, J. Grace, B. Kruijt, M. G. P. Pereira, A. Culf, and S. Scott. 1998. Carbon dioxide transfer over a Central Amazonian rain forest. Journal of Geophysical Research-Atmospheres 103 (D24):31593-31612.

Malhi, Y., D. D. Baldocchi, and P. G. Jarvis. 1999. The carbon balance of tropical, temperate and boreal

forests. Plant Cell and Environment 22 (6):715-740.

Malhi, Y., E. Pegoraro, A. D. Nobre, M. G. P. Pereira, J. Grace, A. D. Culf, and R. Clement. 2002. Energy and water dynamics of a central Amazonian rain forest. Journal of Geophysical Research-Atmospheres 107 (D20):art. no.-8061.

Malhi, Y., and J. Wright. 2004. Spatial patterns and recent trends in the climate of tropical rainforest regions. Philosophical Transactions of the Royal Society of London Series B-Biological Sciences 359 (1443):311-329.

Malhi, Y., and Phillips O. 2005. Tropical Forests & Global Atmoshpheric Change. Oxford: Oxford University Press.

Malhi, Y., T. R. Baker, O. L. Phillips, S. Almeida, E. Alvarez, L. Arroyo, J. Chave, C. I. Czimczik, A. Di Fiore, N. Higuchi, T. J. Killeen, S. G. Laurance, W. F. Laurance, S. L. Lewis, L. M. M. Montoya, A. Monteagudo, D. A. Neill, P. N. Vargas, S. Patiño, N. C. A. Pitman, C. A. Quesada, R. Salomao, J. N. M. Silva, A. T. Lezama, R. V. Martinez, J. Terborgh, B. Vinceti, and J. Lloyd. 2004. The above-ground coarse wood productivity of 104 Neotropical forest plots. Global Change Biology 10 (5):563-591.

Martens, C. S., T. J. Shay, H. P. Mendlovitz, D. M. Matross, S. R. Saleska, S. C. Wofsy, W. S. Woodward, M. C. Menton, J. M. S. De Moura, P. M. Crill, O. L. L. De Moraes, and R. L. Lima. 2004. Radon fluxes in tropical forest ecosystems of Brazilian Amazonia: night-time CO2 net ecosystem exchange derived from radon and eddy covariance methods. Global Change Biology 10 (5):618-629.

Martinelli, L. A., A. H. Devol, R. L. Victoria, and J. E. Richey. 1991. Stable Carbon Isotope Variation in C3 and C4 Plants Along the Amazon River. Nature 353 (6339):57-59.

Martinelli, L. A., R. L. Victoria, L. S. L. Sternberg, A. Ribeiro, and M. Z. Moreira. 1996. Using stable isotopes to determine sources of evaporated water to the atmosphere in the Amazon basin. Journal of Hydrology 183 (3-4):191-204.

Martins, F.R., and L.A.F. Matthes. 1978. Respiracao edafica e nutrientes na Amazonia (Regiao de Manaus):floresta arenicola, campinarana e campina. Acta Amazonica (8):233-244.

Massman, W. J., and X. Lee. 2002. Eddy covariance flux corrections and uncertainties in long-term studies of carbon and energy exchanges. Agricultural and Forest Meteorology 113 (1-4):121-144.

McNaughton, K. G., and P.G Jarvis. 1983. Predicting effects of vegetation changes on transpiration and evaporation. In Water Defficits and Plant Growth, edited by T. T. Kozlowski. New York: Academic Press.

Medina, E., H. Klinge, C. Jordan, and R. Herrera. 1980. Soil Respiration in Amazonian Rain Forests in the Rio-Negro- Basin. Flora 170 (3):240-250.

Medlyn, B. E., R. E. McMurtrie, R. C. Dewar, and M. P. Jeffreys. 2000. Soil processes dominate the long-term response of forest net primary productivity to increased temperature and atmospheric CO2 concentration. Canadian Journal of Forest Research-Revue Canadienne De Recherche Forestiere 30 (6):873-888.

Medlyn, B., D. Barrett, J. Landsberg, P. Sands, and R. Clement. 2003. Conversion of canopy intercepted radiation to photosynthate: review of modelling approaches for regional scales. Functional Plant Biology 30 (2):153-169.

Meir, P. 1996. The exchange of carbon dioxide in tropical rainforest. Doctor of Philosophy, Institute of Ecology and Resource Management, The University of Edinburgh, Edinburgh.

Meir, P., J. Grace, A.C miranda, and J.. Lloyd. 1996. Soil Respiration in a rainforest in Amazonia and in cerrado in central Brazil. In Amazon Deforestation and Climate, edited by J. H. C. Gash, C. A. Nobre, J. Roberts and R. L. Victoria. Chichester,UK: John Wiley & Sons.

Meir, P., J. Grace, and A. C. Miranda. 2000. Photographic method to measure the vertical distribution of leaf area density in forests. Agricultural and Forest Meteorology 102 (2-3):105-111.

Meir, P., J. Grace, and A. C. Miranda. 2001. Leaf respiration in two tropical rainforests: constraints on physiology by phosphorus, nitrogen and temperature. Functional Ecology 15 (3):378-387.

Meir, P., and J. Grace. 2002. Scaling relationships for woody tissue respiration in two tropical rain forests. Plant Cell and Environment 25 (8):963-973.

Melillo, J. M., A. D. McGuire, D. W. Kicklighter, B. Moore, C. J. Vorosmarty, and A. L. Schloss. 1993. Global climate change and terrestrial net primary production. Nature 363 (6426):234-240.

Mercado, L.M, J. Lloyd, F. Carswell, Y. Malhi, P. Meir, A.D. Nobre. 2006. Modelling Amazonian forest eddy covariance data: a comparison of big leaf versus sun/shade models for the C-14 tower at Manaus I. Canopy photosynthesis. Acta Amazonica 36(1):69-82.

Mercado, L.M., C. Huntingford, J.H.C. Gash, P. M. Cox, and V. Jogireedy. 2007. Improving the representation of radiation interception and photosynhtesis for climate model applications. Tellus B (OnlineEarly articles) doi:10.1111/j.1600-0889.2007.00256.x.

Miller, G. T. 1997. Living in the Environment. Wadsworth: Belmont,CA.

Miller, S. D., M. L. Goulden, M. C. Menton, H. R. da Rocha, H. C. de Freitas, Ames Figueira, and C. A. D. de Sousa. 2004. Biometric and micrometeorological measurements of tropical forest carbon balance. Ecological Applications 14 (4):S114-S126.

Moncrieff, J. B., J. M. Massheder, H. deBruin, J. Elbers, T. Friborg, B. Heusinkveld, P. Kabat, S. Scott, H. Soegaard, and A. Verhoef. 1997. A system to measure surface fluxes of momentum, sensible heat, water vapour and carbon dioxide. Journal of Hydrology 189 (1-4):589-611.

Morales, P., M. T. Sykes, I. C. Prentice, P. Smith, B. Smith, H. Bugmann, B. Zierl, P. Friedlingstein, N. Viovy, S. Sabate, A. Sanchez, E. Pla, C. A. Gracia, S. Sitch, A. Arneth, and J. Ogee. 2005. Comparing and evaluating process-based ecosystem model predictions of carbon and water fluxes in major European forest biomes. Global Change Biology 11 (12):2211-2233.

Nascimento, H. E. M., and W. F. Laurance. 2002. Total aboveground biomass in central Amazonian rainforests: a landscape-scale study. Forest Ecology and Management 168 (1-3):311-321.

Nelder, J. A., and R. Mead. 1965. A Simplex-Method for Function Minimization. Computer Journal 7 (4):308-313.

Nemani, R. R., C. D. Keeling, H. Hashimoto, W. M. Jolly, S. C. Piper, C. J. Tucker, R. B. Myneni, and S. W. Running. 2003. Climate-driven increases in global terrestrial net primary production from 1982 to 1999. Science 300 (5625):1560-1563.

Nepstad, D. C., C. R. Decarvalho, E. A. Davidson, P. H. Jipp, P. A. Lefebvre, G. H. Negreiros, E. D. Dasilva, T. A. Stone, S. E. Trumbore, and S. Vieira. 1994. The Role of Deep Roots in the Hydrological and Carbon Cycles of Amazonian Forests and Pastures. Nature 372 (6507):666-669.

Nepstad, D. C., P. Moutinho, M. B. Dias, E. Davidson, G. Cardinot, D. Markewitz, R. Figueiredo, N. Vianna, J. Chambers, D. Ray, J. B. Guerreiros, P. Lefebvre, L. Sternberg, M. Moreira, L. Barros, F. Y. Ishida, I. Tohlver, E. Belk, K. Kalif, and K. Schwalbe. 2002. The effects of partial throughfall exclusion on canopy processes, aboveground production, and biogeochemistry of an Amazon forest.

Journal of Geophysical Research-Atmospheres 107 (D20):art. no.-8085.

Niyogi, D., H. I. Chang, V. K. Saxena, T. Holt, K. Alapaty, F. Booker, F. Chen, K. J. Davis, B. Holben, T. Matsui, T. Meyers, W. C. Oechel, R. A. Pielke, R. Wells, K. Wilson, and Y. K. Xue. 2004. Direct observations of the effects of aerosol loading on net ecosystem CO2 exchanges over different landscapes. Geophysical Research Letters 31 (20).

Norman, J. M. 1980. Interfacing leaf and canopy light interception models. In Predicting photosynthesis for ecosystem models, edited by J. H. a. J. Jones. Boca Raton, Fl: CRC Press.

Ometto, J.P.H.B., J.H. Ehleringer, T.F. Domingues, F. Y. Ishida, J. A. Berry, N. Higuchi, L. Flanagan, G.B. Nardoto, and L. A. Martinelli. submitted. The stable carbon and nitrogen isotopic composition of vegetation in tropical forests of the Amazon region,Brazil.

Orr, J. C., V. J. Fabry, O. Aumont, L. Bopp, S. C. Doney, R. A. Feely, A. Gnanadesikan, N. Gruber, A. Ishida, F. Joos, R. M. Key, K. Lindsay, E. Maier-Reimer, R. Matear, P. Monfray, A. Mouchet, R. G. Najjar, G. K. Plattner, K. B. Rodgers, C. L. Sabine, J. L. Sarmiento, R. Schlitzer, R. D. Slater, I. J. Totterdell, M. F. Weirig, Y. Yamanaka, and A. Yool. 2005. Anthropogenic ocean acidification over the twenty-first century and its impact on calcifying organisms. Nature 437 (7059):681-686.

Öquist, G., J. M. Anderson, S. McCaffery, and W. S. Chow. 1992. Mechanistic Differences in Photoinhibition of Sun and Shade Plants. Planta 188 (3):422-431.

Patiño, S. Describing the patterns of wood density across the Amazon basin: implications for species distribution. In preparation.

Pattey, E., I. B. Strachan, R. L. Desjardins, and J. Massheder. 2002. Measuring nighttime CO2 flux over terrestrial ecosystems using eddy covariance and nocturnal boundary layer methods. Agricultural and Forest Meteorology 113 (1-4):145-158.

Paul, M. J., and C. H. Foyer. 2001. Sink regulation of photosynthesis. Journal of Experimental Botany 52 (360):1383-1400.

Pettersson, R., and A. J. S. McDonald. 1994. Effects of Nitrogen Supply on the Acclimation of Photosynthesis to Elevated CO2. Photosynthesis Research 39 (3):389-400.

Philip, J.R. 1966. Plant water relations: some physical aspects. Annual Review of Plant Physiology (25):245-268.

Phillips, O. L., Y. Malhi, N. Higuchi, W. F. Laurance, P. V. Nunez, R. M. Vasquez, S. G. Laurance, L. V. Ferreira, M. Stern, S. Brown, and J. Grace. 1998. Changes in the carbon balance of tropical forests: Evidence from long-term plots. Science 282 (5388):439-442.

Phillips, O. L., T. R. Baker, L. Arroyo, N. Higuchi, T. J. Killeen, W. F. Laurance, S. L. Lewis, J. Lloyd, Y. Malhi, A. Monteagudo, D. A. Neill, P. N. Vargas, J. N. M. Silva, J. Terborgh, R. V. Martinez, M. Alexiades, S. Almeida, S. Brown, J. Chave, J. A. Comiskey, C. I. Czimczik, A. Di Fiore, T. Erwin, C. Kuebler, S. G. Laurance, H. E. M. Nascimento, J. Olivier, W. Palacios, S. Patiño, N. C. A. Pitman, C. A. Quesada, M. Salidas, A. T. Lezama, and B. Vinceti. 2004. Pattern and process in Amazon tree turnover, 1976-2001. Philosophical Transactions of the Royal Society of London Series B-Biological Sciences 359 (1443):381-407.

Poorter, L., S. F. Oberbauer, and D. B. Clark. 1995. Leaf Optical-Properties Along a Vertical Gradient in a Tropical Rain-Forest Canopy in Costa-Rica. American Journal of Botany 82 (10):1257-1263.

Prentice, I. C., and J. Lloyd. 1998. C-quest in the Amazon Basin. Nature 396 (6712):619-620.

Prentice, I. C., G.D. Farquhar, M.J.R Fasham, M.L Goulden, M. Heimann, V.J Jaramillo, H.S Kheshgi, C.

Le Quere, R.J Schloes, and D. W.R Wallace. 2001. THe carbon cycle and atmospheric carbon dioxide. In Climate Change 2001: The Scientific Basis. Contribution of Working group I to the Third Assesment Report of the Intergovernmental Panel on Climate Change., edited by J. T. Houghton, Y. Ding, D. J. Griggs, M. Noguer, P. J. v. d. Linden, X. Dai, K. Maskell and C. A. Johnson. Cambridge, UK and New York, N.Y, USA: Cambridge University Press.

Raaimakers, D., R. G. A. Boot, P. Dijkstra, S. Pot, and T. Pons. 1995. Photosynthetic Rates in Relation to Leaf Phosphorus-Content in Pioneer Versus Climax Tropical Rain-Forest Trees. Oecologia 102 (1):120-125.

RAINFOR Consortium (www.geog.leeds.ac.uk/projects/rainfor).

Ranquin de Merona, J.M., G.T. Prance, R.W. Hutchings, M. Freitas da Silva, W.A. Rodriguez, and M.E Uehling. 1992. Preliminary results of a large scale tree inventory of upland rain forest in the central amazon. Acta Amazonica 22 (4):494-534.

Reindl, D. T., W. A. Beckman, and J. A. Duffie. 1990. Diffuse Fraction Correlations. Solar Energy 45 (1):1-7.

Rice, A. H., E. H. Pyle, S. R. Saleska, L. Hutyra, M. Palace, M. Keller, P. B. de Camargo, K. Portilho, D. F. Marques, and S. C. Wofsy. 2004. Carbon balance and vegetation dynamics in an old-growth Amazonian forest. Ecological Applications 14 (4):S55-S71.

Roderick, M. L. 2000. On the measurement of growth with applications to the modelling and analysis of plant growth. Functional Ecology 14 (2):244-251.

Roderick, M. L., G. D. Farquhar, S. L. Berry, and I. R. Noble. 2001. On the direct effect of clouds and atmospheric particles on the productivity and structure of vegetation. Oecologia 129 (1):21-30.

Rödenbeck, C., S. Houweling, M. Gloor, and M. Heimann. 2003. CO2 flux history 1982-2001 inferred from atmospheric data using a global inversion of atmospheric transport. Atmospheric Chemistry and Physics. Discussion 3:1919-1964.

Sage, Rowan F. 1990. A Model Describing the Regulation of Ribulose-1,5-Bisphosphate Carboxylase, Electron Transport, and Triose Phosphate Use in Response to Light Intensity and CO2 in C3 Plants Plant Physiol. 94 (4):1728-1734.

Sakai, R. K., D. R. Fitzjarrald, and K. E. Moore. 2001. Importance of low-frequency contributions to eddy fluxes observed over rough surfaces. Journal of Applied Meteorology 40 (12):2178-2192.

Saleska, S. R., S. D. Miller, D. M. Matross, M. L. Goulden, S. C. Wofsy, H. R. da Rocha, P. B. de Camargo, P. Crill, B. C. Daube, H. C. de Freitas, L. Hutyra, M. Keller, V. Kirchhoff, M. Menton, J. W. Munger, E. H. Pyle, A. H. Rice, and H. Silva. 2003. Carbon in amazon forests: Unexpected seasonal fluxes and disturbance-induced losses. Science 302 (5650):1554-1557.

Salimon, C. I., E. A. Davidson, R. L. Victoria, and A. W. F. Melo. 2004. CO2 flux from soil in pastures and forests in southwestern Amazonia. Global Change Biology 10 (5):833-843.

Salisburry, F.B., and C.W Ross. 1992. Plant Physiology. Fourth edition ed. Belmont, California: Wadsworth.

Santiago, L. S., G. Goldstein, F. C. Meinzer, J. B. Fisher, K. Machado, D. Woodruff, and T. Jones. 2004. Leaf photosynthetic traits scale with hydraulic conductivity and wood density in Panamanian forest canopy trees. Oecologia 140 (4):543-550.

Schuur, E. A. G. 2001. The effect of water on decomposition dynamics in mesic to wet Hawaiian montane forests. Ecosystems 4 (3):259-273.

Sellers, P. J., J. A. Berry, G. J. Collatz, C. B. Field, and F. G. Hall. 1992. Canopy Reflectance,

Photosynthesis, and Transpiration III. A Reanalysis Using Improved Leaf Models and a New Canopy Integration Scheme. Remote Sensing of Environment 42 (3):187-216.

Sharkey, Thomas D. 1985. O2-Insensitive Photosynthesis in C3 Plants: Its Occurrence and a Possible Explanation. Plant Physiol. 78 (1):71-75.

Sharkey, T. D., J. R. Seemann, and J. A. Berry. 1986. Regulation of Ribulose-1,5-Bisphosphate Carboxylase Activity in Response to Changing Partial-Pressure of O-2 and Light in Phaseolus-Vulgaris. Plant Physiology 81 (3):788-791.

Shuttleworth, W. J., and R. E. Dickinson. 1989. Modeling Tropical Deforestation - a Study of Gcm Land-Surface Parametrizations - Comment. Quarterly Journal of the Royal Meteorological Society 115 (489):1177-1179

Shuttleworth, W. J. 1989. Micrometeorology of Temperate and Tropical Forest. Philosophical Transactions of the Royal Society of London Series B-Biological Sciences 324 (1223):299-334.

———. 1998. Evaporation from Amazonian rainforest. Philosophical Transactions of the Royal Society of London Series B-Biological Sciences 233:321-346.

Silva de Souza, J. 2004. Dinamica espacial e temporal do fluxo de CO2 do solo em floresta de terra firme na amazonia central. Master Thesis. Mestre em Ciencias Agrarias, Area de concentracao em ciencias de Florestas Tropicais, Universidad Federal do Amazonas, Manaus.

Silva Dias, P.L., J.P. Bonatti, and V.E. Kousky. 1987. Diurnally forced tropical trophospheric circulation over South America. Monthly Weather Review (115):1465-1478.

Simon, E., F. X. Meixner, U. Rummel, L. Ganzeveld, C. Ammann, and Kesselmeier. 2005. Coupled carbon-water exchange of the Amazon rain forest, II. Comparison of predicted and observed seasonal exchange of energy, CO2, isoprene and ozone at a remote site in Rondônia. Biogeosciences 2:231-253.

Sitch, S., B. Smith, I. C. Prentice, A. Arneth, A. Bondeau, W. Cramer, J. O. Kaplan, S. Levis, W. Lucht, M. T. Sykes, K. Thonicke, and S. Venevsky. 2003. Evaluation of ecosystem dynamics, plant geography and terrestrial carbon cycling in the LPJ dynamic global vegetation model. Global Change Biology 9 (2):161-185.

Sotta, E. D., E. Veldkamp, B. R. Guimaraes, R. K. Paixao, M. L. P. Ruivo, and S. S. Almeida. 2006. Landscape and climatic controls on spatial and temporal variation in soil CO2 efflux in an Eastern Amazonian Rainforest, Caxiuana, Brazil. *Forest Ecology and Management* 237 (1-3):57-64.

Sotta, E. D., P. Meir, Y. Malhi, A. D. Nobre, M. Hodnett, and J. Grace. 2004. Soil CO2 efflux in a tropical forest in the central Amazon. Global Change Biology 10 (5):601-617.

Sperry, J. S., F. R. Adler, G. S. Campbell, and J. P. Comstock. 1998. Limitation of plant water use by rhizosphere and xylem conductance: results from a model. Plant Cell and Environment 21 (4):347-359.

Spitters, C. J. T., Hajm Toussaint, and J. Goudriaan. 1986. Separating the Diffuse and Direct Component of Global Radiation and Its Implications for Modeling Canopy Photosynthesis .1. Components of Incoming Radiation. Agricultural and Forest Meteorology 38 (1-3):217-229.

Tanner, C.B. 1963. Energy Relations in Plant Comunities. In Environmental Control of Plant Growth, edited by L. T. Evans. New York: Academic Press.

Taylor, J. A., and J. Lloyd. 1992. Sources and sinks of atmospheric CO2. Australian Journal of Botany 40 (4-5):407-418.

Terry, Norman, and Albert Ulrich. 1973. Effects of Phosphorus Deficiency on the Photosynthesis and Respiration of Leaves of Sugar Beet Plant Physiol. 51 (1):43-47.

Thornley, J. H. M. 2002. Instantaneous canopy photosynthesis: Analytical expressions for sun and shade leaves based on exponential light decay down the canopy and an acclimated non-rectangular hyperbola for leaf photosynthesis. Annals of Botany 89 (4):451-458.

Tian, H. Q., J. M. Melillo, D. W. Kicklighter, A. D. McGuire, J. V. K. Helfrich, III, B. Moore, III, and C. J. Vörösmarty. 1998. Effect of interannual climate variability on carbon storage in Amazonian ecosystems. Nature 396 (6712):664-667.

Trumbore, S. E., E. A. Davidson, P. B. Decamargo, D. C. Nepstad, and L. A. Martinelli. 1995. Belowground Cycling of Carbon in Forests and Pastures of Eastern Amazonia. Global Biogeochemical Cycles 9 (4):515-528.

Tuzet, A., A. Perrier, and R. Leuning. 2003. A coupled model of stomatal conductance, photosynthesis and transpiration. Plant, Cell and Environment 26 (7):1097-1116.

Tyree, M. T. 2003. Hydraulic limits on tree performance: transpiration, carbon gain and growth of trees. Trees-Structure and Function 17 (2):95-100.

Uppala, S. M., P. W. Kallberg, A. J. Simmons, U. Andrae, V. D. Bechtold, M. Fiorino, J. K. Gibson, J. Haseler, A. Hernandez, G. A. Kelly, X. Li, K. Onogi, S. Saarinen, N. Sokka, R. P. Allan, E. Andersson, K. Arpe, M. A. Balmaseda, A. C. M. Beljaars, L. Van De Berg, J. Bidlot, N. Bormann, S. Caires, F. Chevallier, A. Dethof, M. Dragosavac, M. Fisher, M. Fuentes, S. Hagemann, E. Holm, B. J. Hoskins, L. Isaksen, Paem Janssen, R. Jenne, A. P. McNally, J. F. Mahfouf, J. J. Morcrette, N. A. Rayner, R. W. Saunders, P. Simon, A. Sterl, K. E. Trenberth, A. Untch, D. Vasiljevic, P. Viterbo, and J. Woollen. 2005. The ERA-40 re-analysis. Quarterly Journal of the Royal Meteorological Society 131 (612):2961-3012.

Vale, R.L., J.P Maroco, C. R. J. Carvalho, S. Almeida, P. Meir, J. Grace, J.S Pereira, and M. M. Chaves. 2003. Carbon assimilation in an amazonian rainforest: a rain exclusion experiment. Paper read at Abstracts of the Annual Main Meeting of the Society for Experimental Biology, 31st March-4th April, at Southampton, UK.

Valentini, R., G. Matteucci, A. J. Dolman, E. D. Schulze, C. Rebmann, E. J. Moors, A. Granier, P. Gross, N. O. Jensen, K. Pilegaard, A. Lindroth, A. Grelle, C. Bernhofer, T. Grunwald, M. Aubinet, R. Ceulemans, A. S. Kowalski, T. Vesala, U. Rannik, P. Berbigier, D. Loustau, J. Guomundsson, H. Thorgeirsson, A. Ibrom, K. Morgenstern, R. Clement, J. Moncrieff, L. Montagnani, S. Minerbi, and P. G. Jarvis. 2000. Respiration as the main determinant of carbon balance in European forests. Nature 404 (6780):861-865.

van der Molen, M. K., J. H. C. Gash, and J. A. Elbers. 2004. Sonic anemometer (co)sine response and flux measurement - II. The effect of introducing an angle of attack dependent calibration. Agricultural and Forest Meteorology 122 (1-2):95-109.

Vance, Carroll P. 2001. Symbiotic Nitrogen Fixation and Phosphorus Acquisition. Plant Nutrition in a World of Declining Renewable Resources. 10.1104/pp.010331. Plant Physiology. 127 (2):390-397.

Vitousek, P. M. 1984. Litterfall, Nutrient Cycling, and Nutrient Limitation in Tropical Forests. Ecology 65 (1):285-298.

Vitousek, P. M., and R. L. Sanford. 1986. Nutrient Cycling in Moist Tropical Forest. Annual Review of Ecology and Systematics 17:137-167.

von Randow, C., A. O. Manzi, B. Kruijt, P. J. de Oliveira, F. B. Zanchi, R. L. Silva, M. G. Hodnett, J. H. C. Gash, J. A. Elbers, M. J. Waterloo, F. L. Cardoso, and P. Kabat. 2004. Comparative measurements and seasonal variations in energy and carbon exchange over forest and pasture in South West Amazonia. Theoretical and Applied Climatology 78 (1-3):5-26.

Wang, Y. P., and R. Leuning. 1998. A two-leaf model for canopy conductance, photosynthesis and partitioning of available energy I: Model description and comparison with a multi-layered model. Agricultural and Forest Meteorology 91 (1-2):89-111.

Wang, Y. P. 2003. A comparison of three different canopy radiation models commonly used in plant modelling. Functional Plant Biology 30 (2):143-152.

Weiss, A., and J. M. Norman. 1985. Partitioning solar radiation into direct and diffuse, visible and near-infrared components. Agricultural and Forest Meteorology 34 (2-3):205-213.

Werth, D., and R. Avissar. 2002. The local and global effects of Amazon deforestation. Journal of Geophysical Research-Atmospheres 107 (D20).

Wielicki, B. A., A. D. Del Genio, T. M. Wong, J. Y. Chen, B. E. Carlson, R. P. Allan, F. Robertson, H. Jacobowitz, A. Slingo, D. A. Randall, J. T. Kiehl, B. J. Soden, C. T. Gordon, A. J. Miller, S. K. Yang, and J. Susskind. 2002. Changes in tropical clouds and radiation - Response. Science 296 (5576):U2-U3.

Williams, M., Y. Malhi, A. D. Nobre, E. B. Rastetter, J. Grace, and M. G. P. Pereira. 1998. Seasonal variation in net carbon exchange and evapotranspiration in a Brazilian rain forest: a modelling analysis. Plant Cell and Environment 21 (10):953-968.

Wilson, K., A. Goldstein, E. Falge, M. Aubinet, D. Baldocchi, P. Berbigier, C. Bernhofer, R. Ceulemans, H. Dolman, C. Field, A. Grelle, A. Ibrom, B. E. Law, A. Kowalski, T. Meyers, J. Moncrieff, R. Monson, W. Oechel, J. Tenhunen, R. Valentini, and S. Verma. 2002. Energy balance closure at FLUXNET sites. Agricultural and Forest Meteorology 113 (1-4):223-243.

Wofsy, S. C., R. C. Harriss, and W. A. Kaplan. 1988. Carbon-Dioxide in the Atmosphere over the Amazon Basin. Journal of Geophysical Research-Atmospheres 93 (D2):1377-1387.

Wohlfahrt, G., M. Bahn, A. Haslwanter, C. Newesely, and A. Cernusca. 2005. Estimation of daytime ecosystem respiration to determine gross primary production of a mountain meadow. Agricultural and Forest Meteorology 130 (1-2):13-25.

Wright, J.S, L.H.C Muller, R. Condit, and S.P Hubbell. 2003. Gap-Dependent Recruitment, Realized Vital Rates, And Size Distributions Of Tropical Trees. Ecology 84 (12):3174-3185.

Yamasoe, M. A., C. von Randow, A. O. Manzi, J. S. Schafer, T. F. Eck, and B. N. Holben. 2006. Effect of smoke and clouds on the transmissivity of photosynthetically active radiation inside the canopy. Atmospheric Chemistry and Physics 6:1645-1656.

Zhan, X. W., Y. K. Xue, and G. J. Collatz. 2003. An analytical approach for estimating CO2 and heat fluxes over the Amazonian region. Ecological Modelling 162 (1-2):97-117.

Zhang, H., K. McGuffie, and A. Henderson Sellers. 1996. Impacts of tropical deforestation .2. The role of large-scale dynamics. Journal of Climate 9 (10):2498-2521.

8 Appendixes

8.1 Appendix 3A

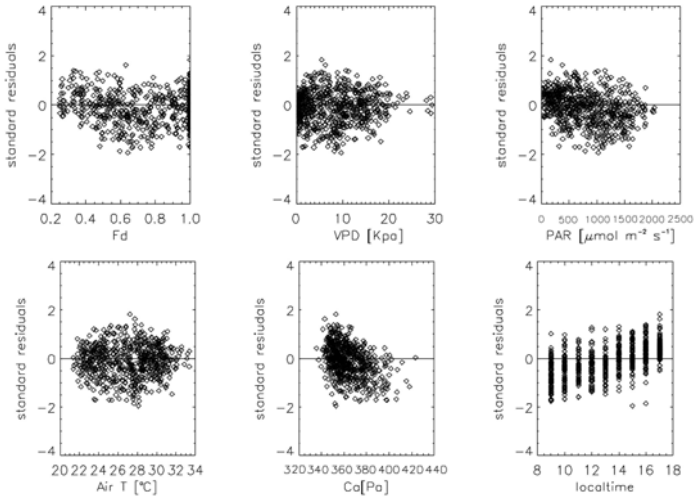

Figure 3A-1. Man C14. End of dry season 1995. Residual responses to different variables. A positive residual means underestimation, negative means overestimation of model over observations**.**

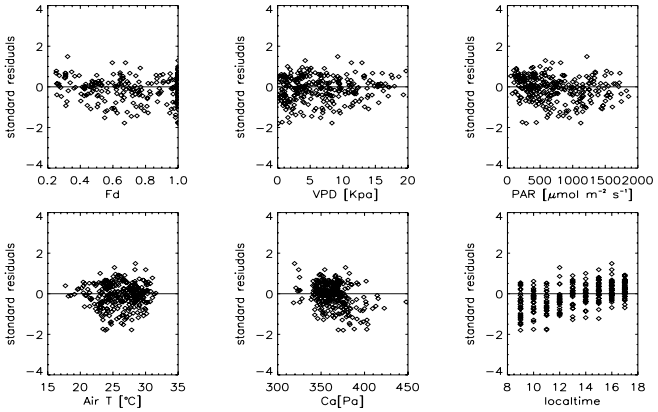

Figure 3A-2. Man C14. Rainy season 1996. Residual responses to different variables. A positive residual means underestimation, negative means overestimation of model over observations.

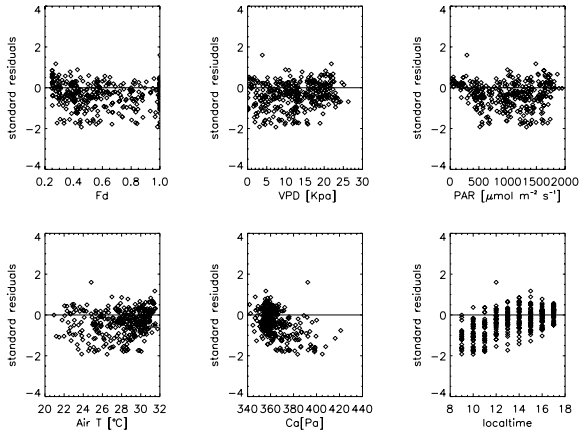

Figure 3A-3. Man C14. Dry season 1996. Residual responses to different variables. A positive residual means underestimation, negative means overestimation of model over observations.

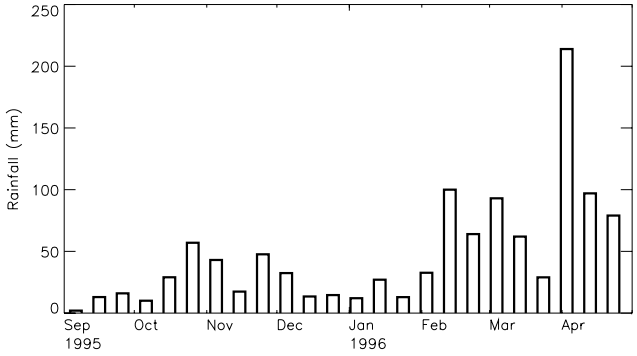

Figure 3A-4. Precipitation at Man C14 (from Harris et al. (2004)).

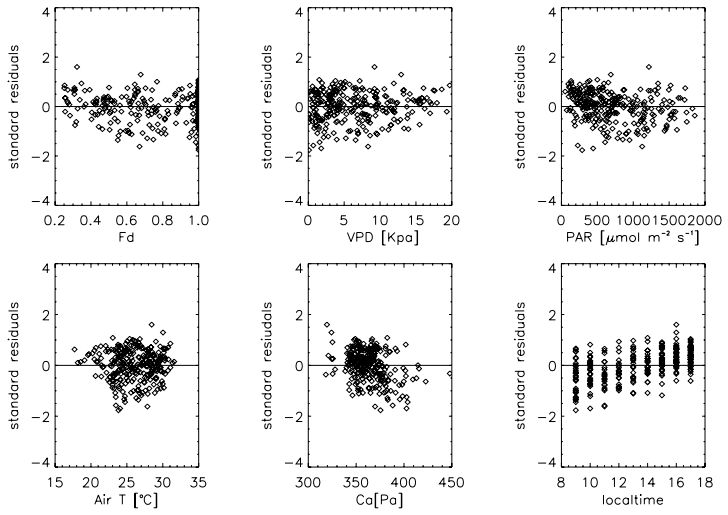

Figure 3A-5. Man C14. Rainy season 1996 using higher respiration. Residual responses to different variables. A positive residual means underestimation, negative means overestimation of model observations.

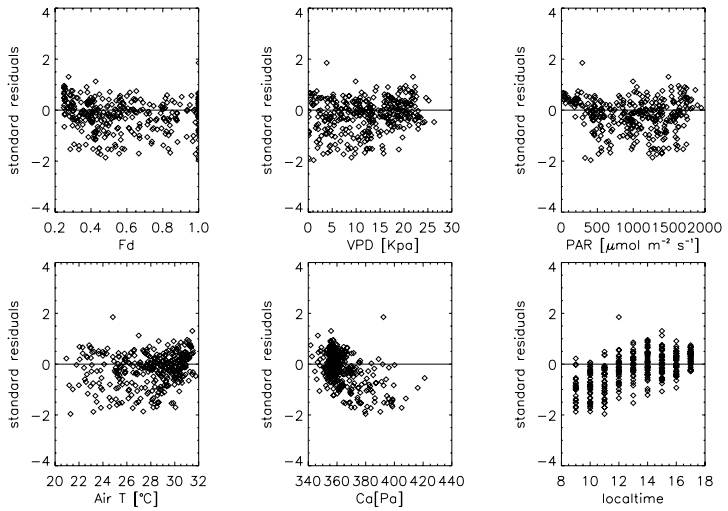

Figure 3A-6. Man C14. Dry season 1996 using higher soil respiration values that provide an improved model fit. Residual responses to different variables. A positive residual means underestimation, negative means overestimation of model over observations.

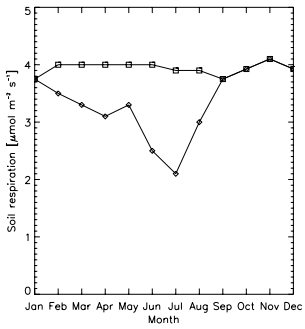

Figure 3A-7. Soil respiration measurements from Chambers et al. (2004) (◊) and the new respiration values used to provide an improved model fit (□).

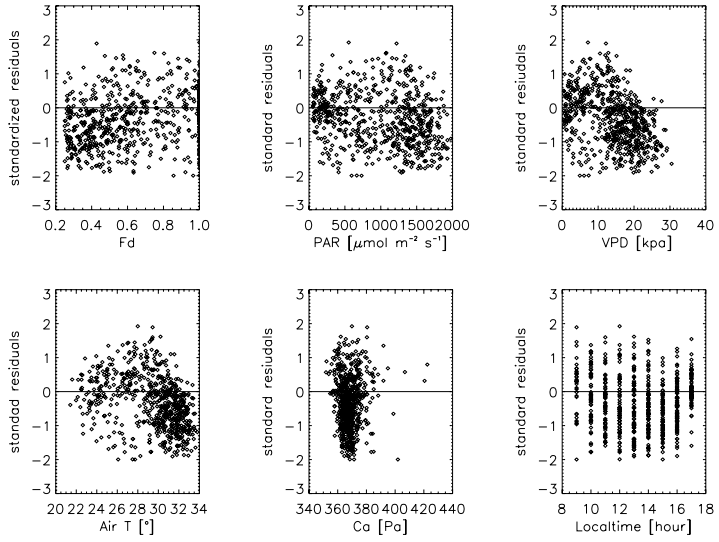

Figure 3A-8. Man K34. End of dry season 1999. Residual responses to different variables. A positive residual means underestimation, negative means overestimation of model over observations.

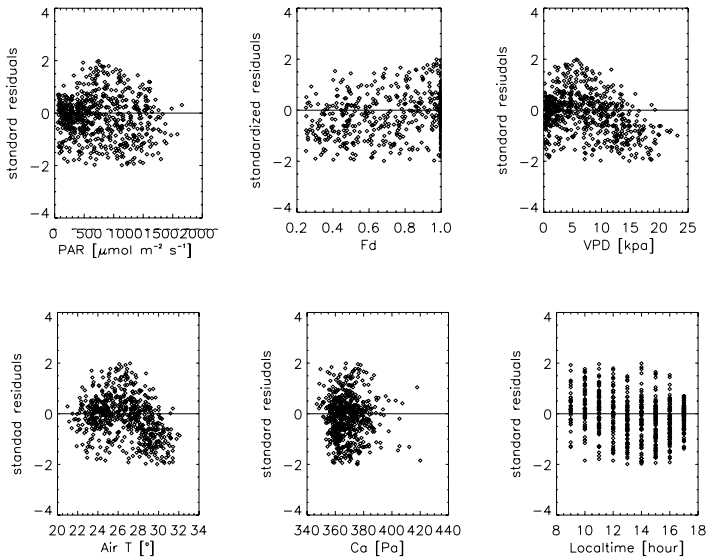

Figure 3A-9. Man K34. Rainy season 2000. Residual responses to different variables. A positive residual means underestimation, negative means overestimation of model over observations.

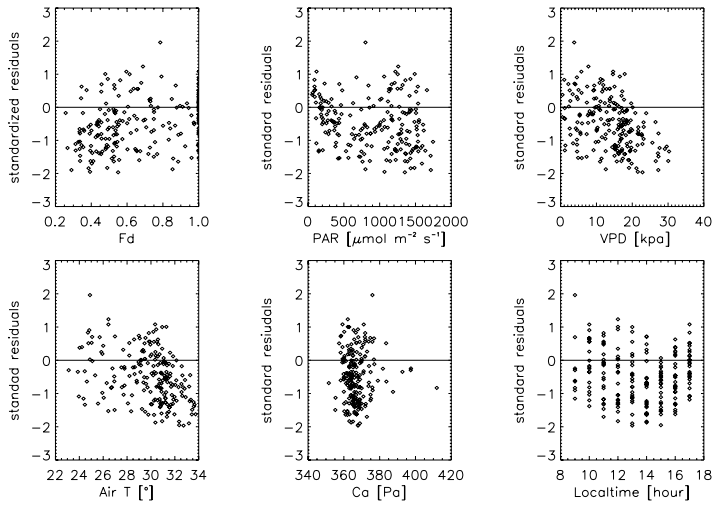

Figure 3A-10. Man K34. End of dry season 2000. Residual responses to different variables. A positive residual means underestimation, negative means overestimation of model over observations.

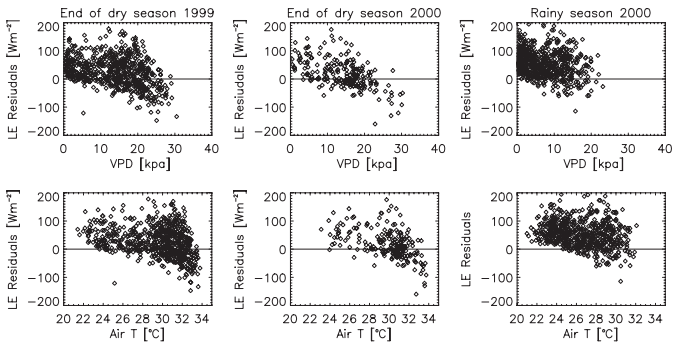

Figure 3A-11. Man K34. Residual of 'observed' latent heat flux (calculated as measured net radiation minus measured sensible heat) minus simulated latent heat flux by sun/shade responses to different variables. A positive residual means underestimation, negative means overestimation of model over observations.

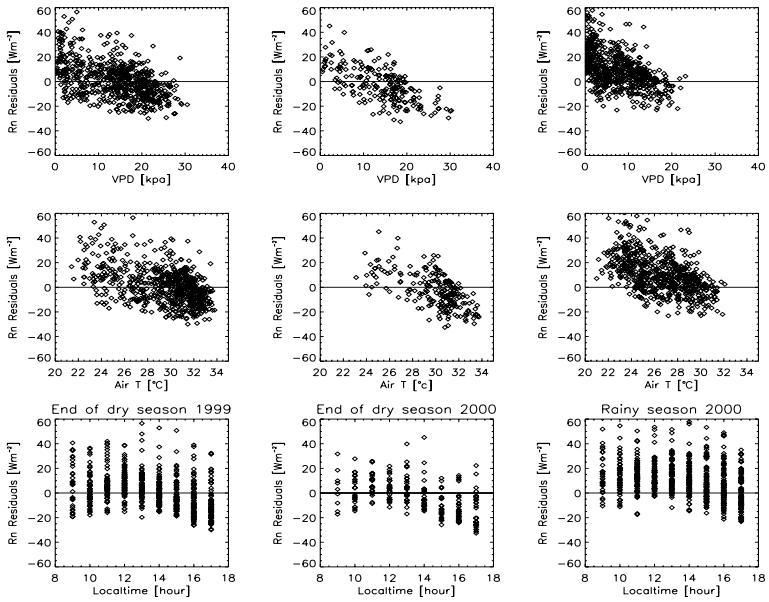

Figure 3A-12. Man K34. Residual responses of measured minus simulated net radiation to different variables. A positive residual means underestimation, negative means overestimation of model over observations.

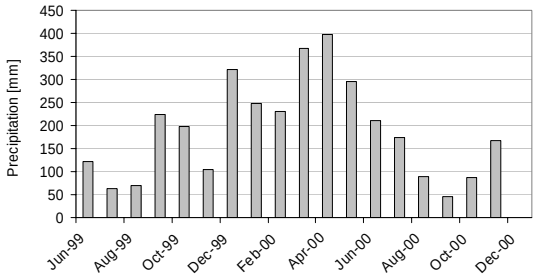

Figure 3A-13. Monthly precipitation at Manaus K34.

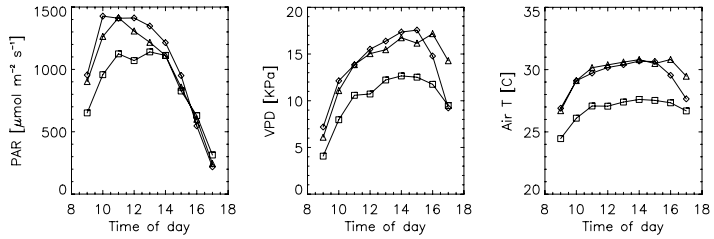

Figure 3A-14. Mean diurnal cycle of PAR, VPD and air temperature at Man K34. End of dry season 2000 (Δ) end of dry season 1999 (◊) and rainy season 2000 (□).

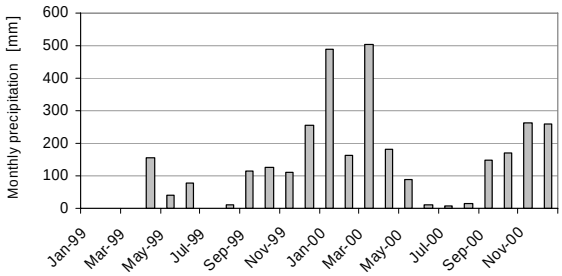

Figure 3A-15. Monthly precipitation at Jaru.

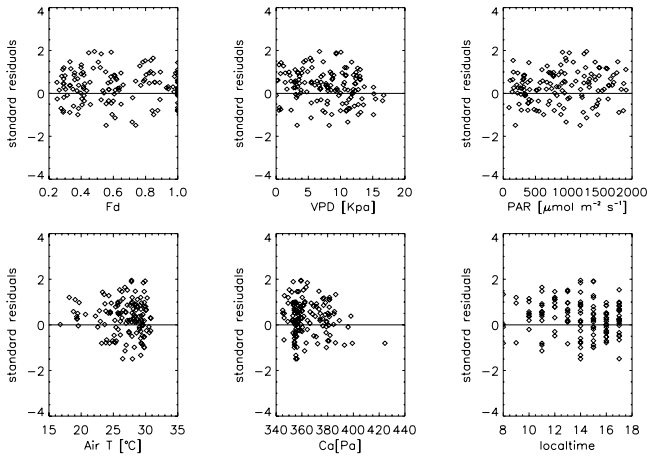

Figure 3A-16. Jaru. Rainy season 1999. Residual responses to different variables. A positive residual means underestimation, negative means overestimation of model over observations.

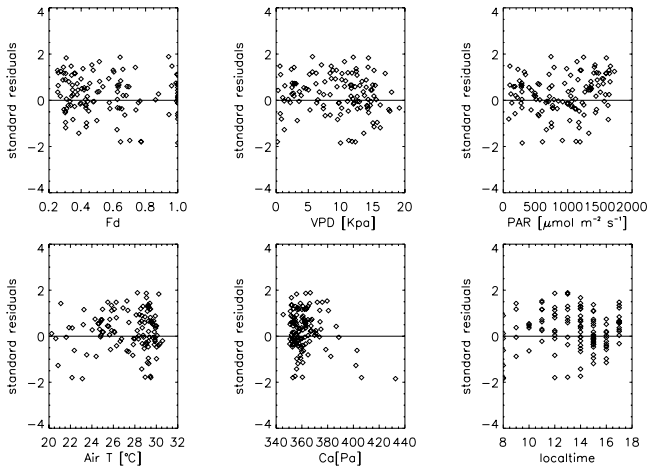

Figure 3A-17. Jaru. Dry season 1999. Residual responses to different variables. A positive residual means underestimation, negative means overestimation of model over observations.

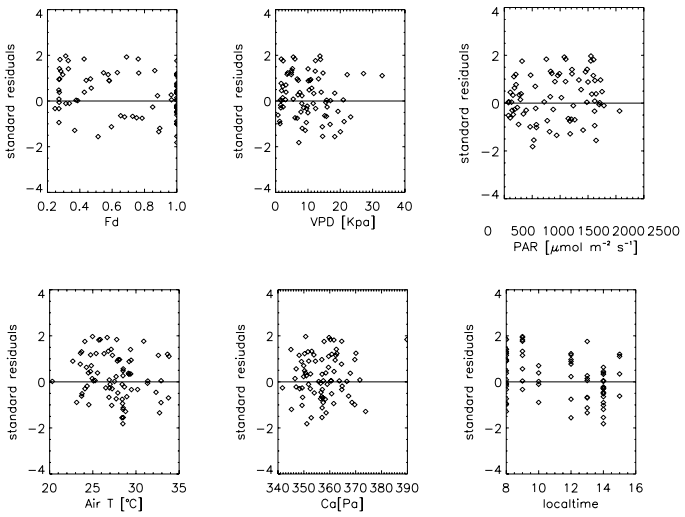

Figure 3A-18. Jaru. End of dry season 1999. Residual responses to different variables. A positive residual means underestimation, negative means overestimation of model over observations.

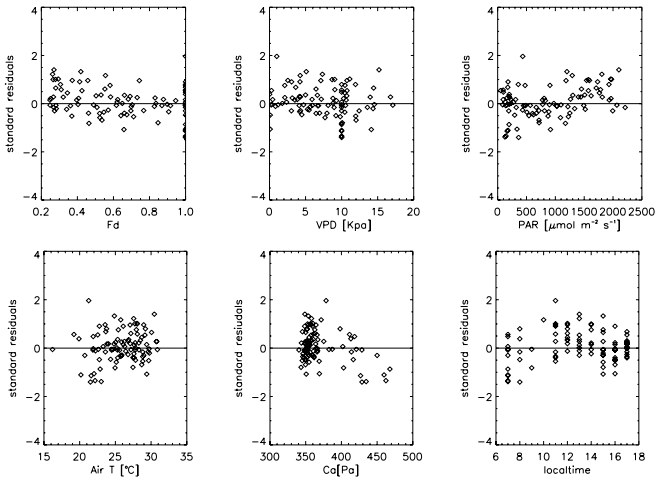

Figure 3A-19. Jaru. Rainy season 2000. Residual responses to different variables. A positive residual means underestimation, negative means overestimation of model over observations.

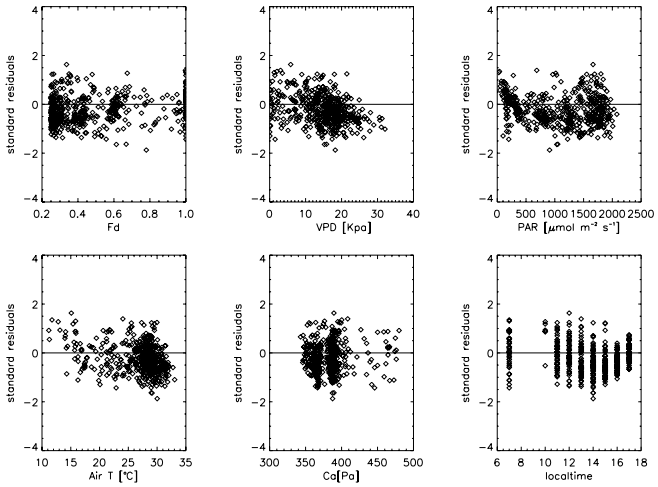

Figure 3A-20. Jaru. Dry season 2000. Residual responses to different variables. A positive residual means underestimation, negative means overestimation of model over observations.

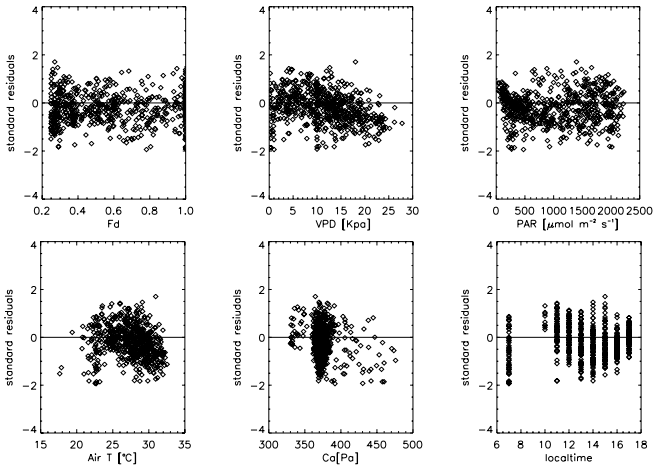

Figure 3A-21. Jaru. End of dry season 2000. Residual responses to different variables. A positive residual means underestimation, negative means overestimation of model over observations.

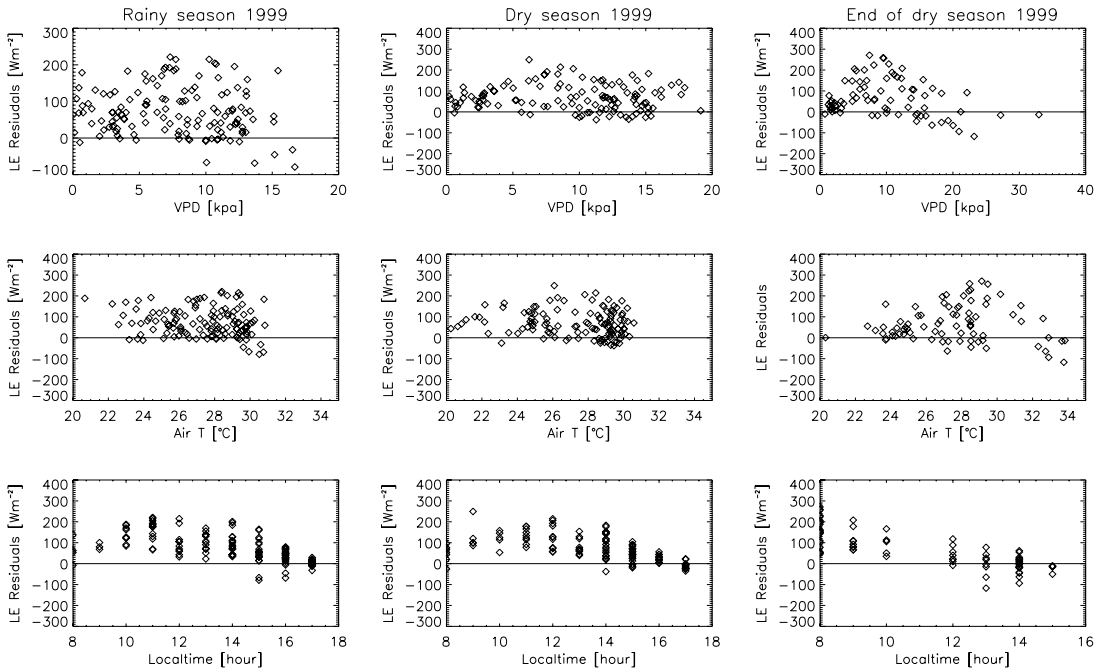

Figure 3A-22. Jaru 1999. Residual of 'observed' latent heat flux (calculated as measured net radiation minus measured sensible heat) minus simulated latent heat flux by sun/shade responses to different variables. A positive residual means underestimation, negative means overestimation of model over observations.

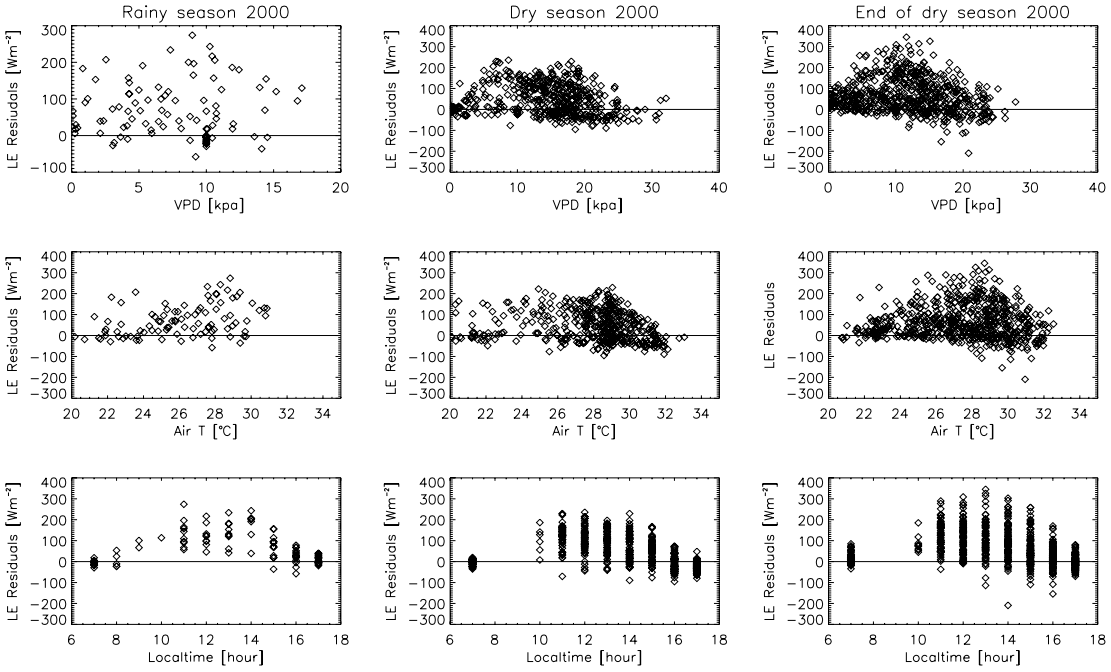

Figure 3A-23. Jaru 2000. Residual of 'observed' latent heat flux (calculated as measured net radiation minus measured sensible heat) minus simulated latent heat flux by sun/shade responses to different variables. A positive residual means underestimation, negative means overestimation of model over observations.

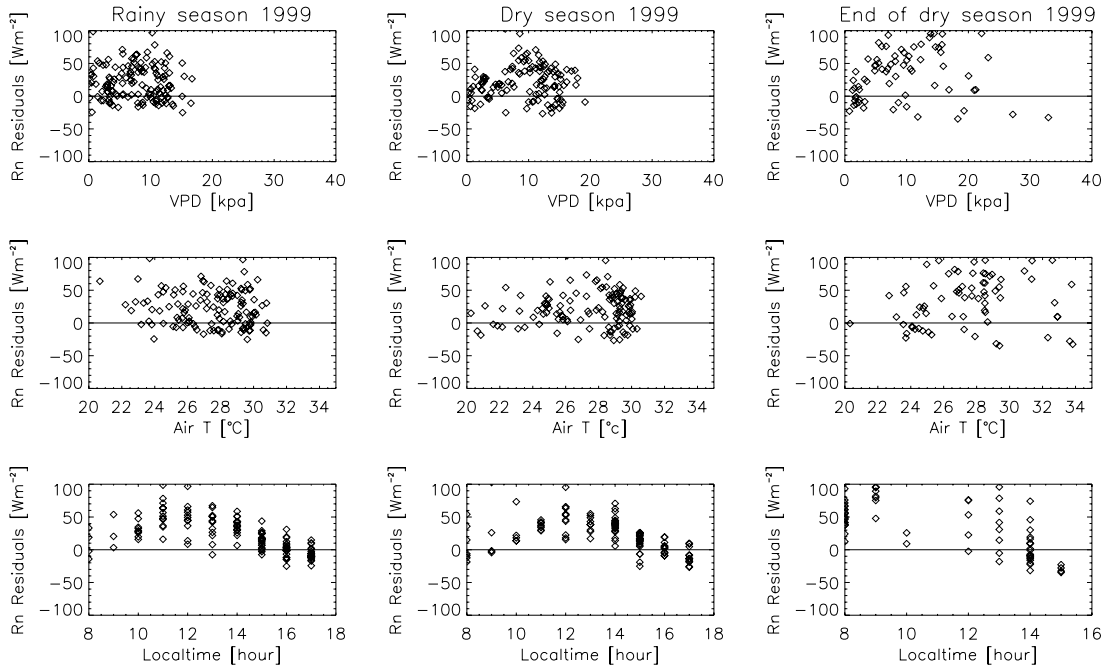

Figure 3A-24. Jaru 1999. Residual responses of measured minus simulated net radiation to different variables. A positive residual means underestimation, negative means overestimation of model over observations.

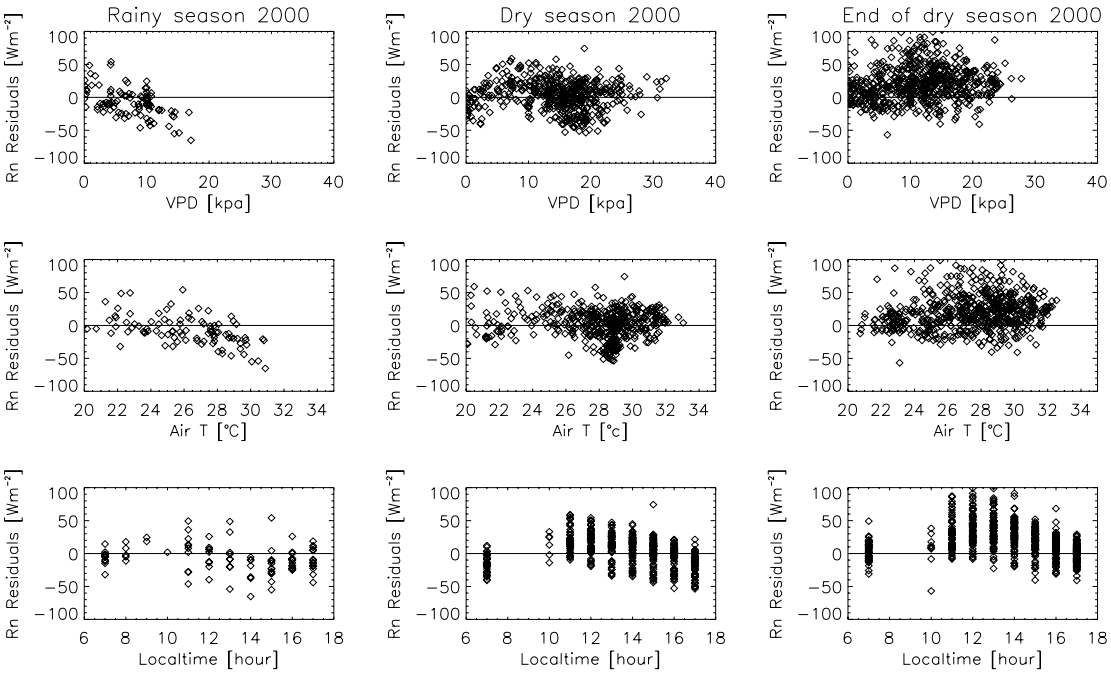

Figure 3A-25. Jaru 2000. Residual responses of measured minus simulated net radiation to different variables. A positive residual means underestimation, negative means overestimation of model over observations.

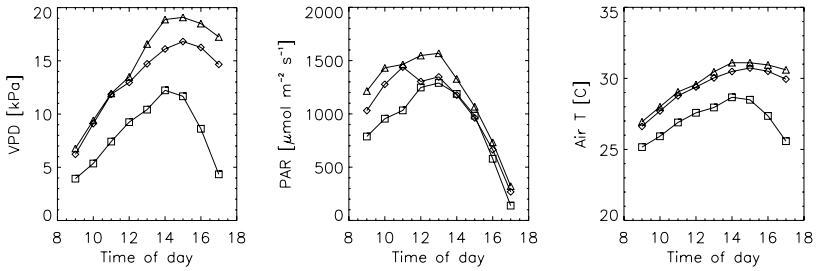

Figure 3A-26. Mean diurnal cycle of PAR, VPD and air temperature at Caxiuana. Dry season 1999 (Δ), end of dry season 1999 (◊) and rainy season 1999 (□).

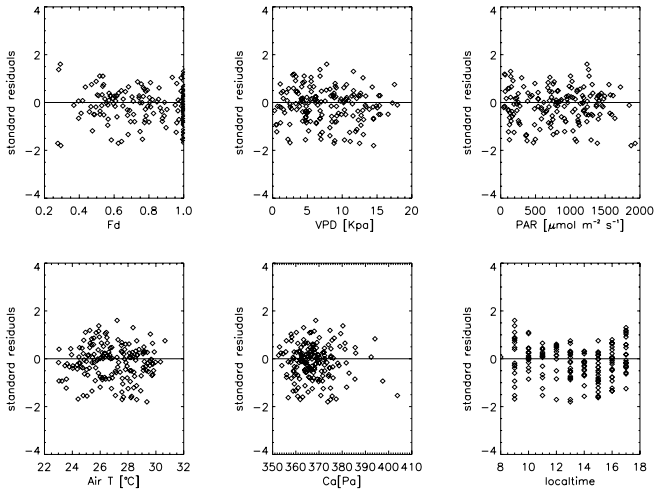

Figure 3A-27. Caxiuana. Rainy season 1999. Residual responses to different variables. A positive residual means underestimation, negative means overestimation of model over observations.

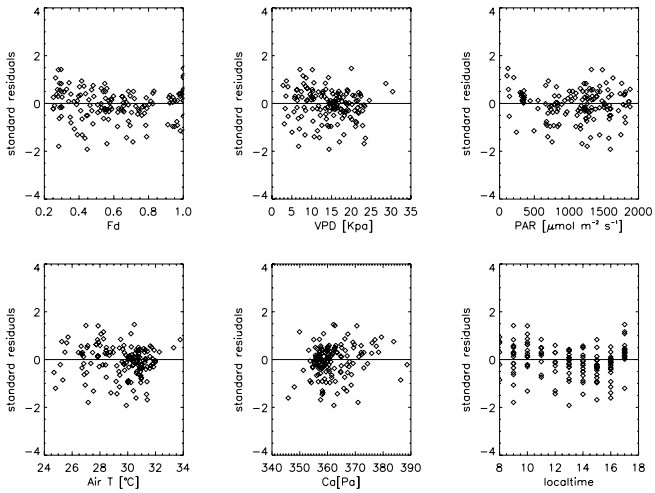

Figure 3A-28. Caxiuana. Dry season 1999. Residual responses to different variables. A positive residual means underestimation, negative means overestimation of model over observations.

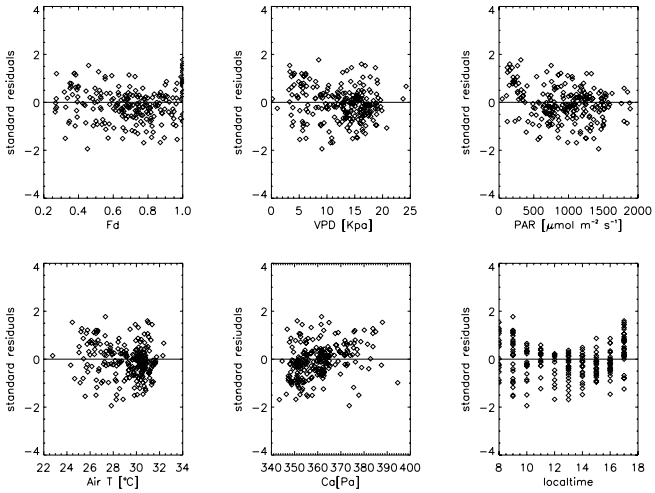

Figure 3A-29. Caxiuana. End of dry season 1999. Residual responses to different variables. A positive residual means underestimation, negative means overestimation of model over observations.

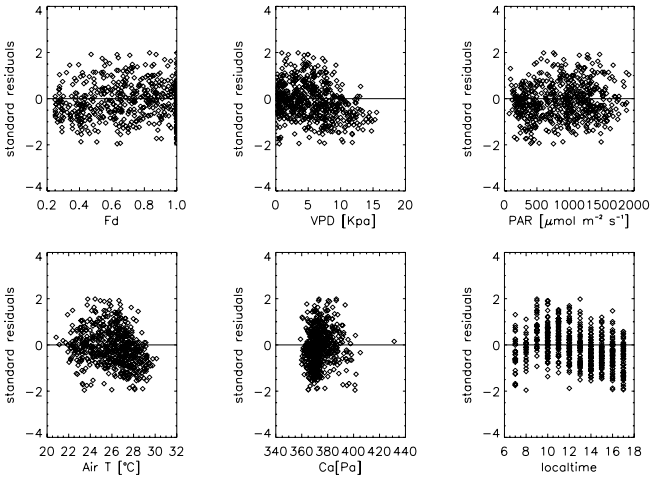

Figure 3A-30. Tapajos. Wet season 2001. Residual responses to different variables. A positive residual means underestimation, negative means overestimation of model over observations.

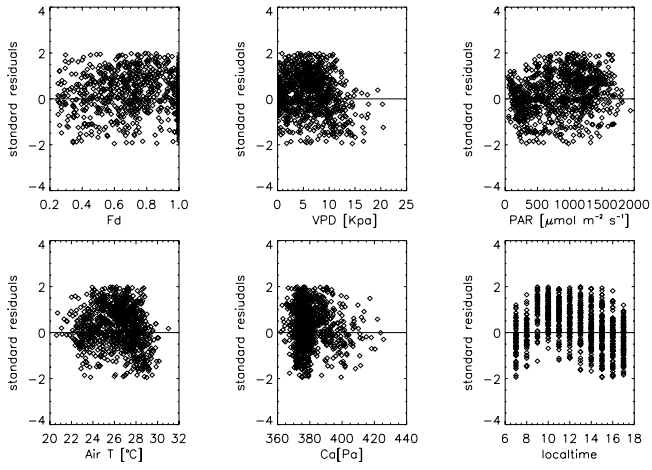

Figure 3A-31. Tapajos. Wet season 2002. Residual responses to different variables. A positive residual means underestimation, negative means overestimation of model over observations.

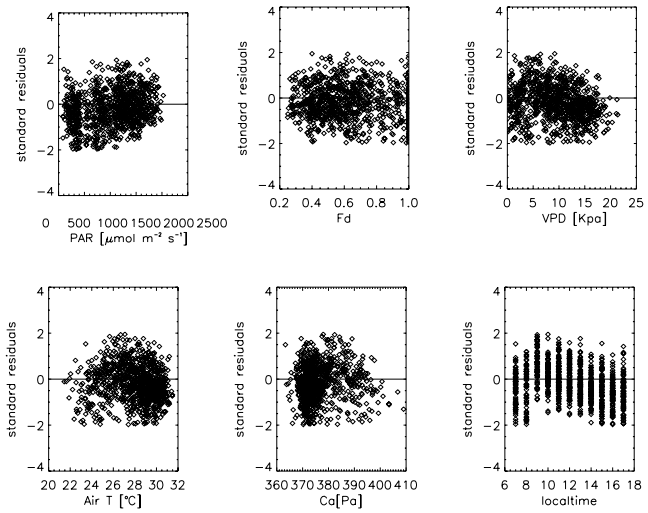

Figure 3A-32. Tapajos. Dry season 2001. Residual responses to different variables. A positive residual means underestimation, negative means overestimation of model over observations.

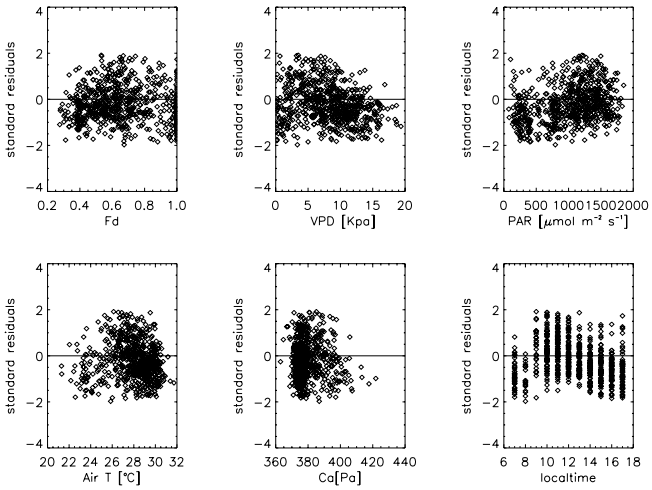

Figure 3A-33. Tapajos. Dry season 2002. Residual responses to different variables. A positive residual means underestimation, negative means overestimation of model over observations.

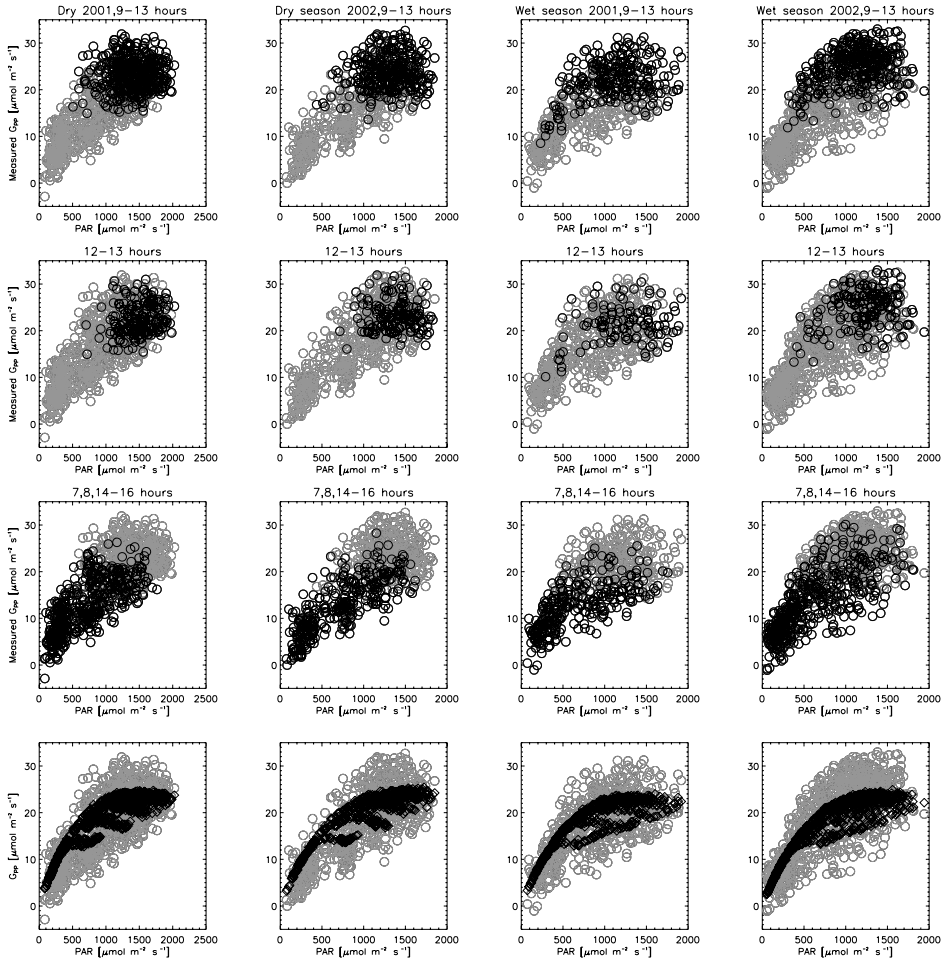

Figure 3A-34. Light response of observed G_{PP} from the eddy correlation ($-N_E$ $+R_E$) (rows 1-3). Data in black correspond to the time of day indicated in the legend from each plot. Row 4 includes simulated gross uptake (black diamonds).

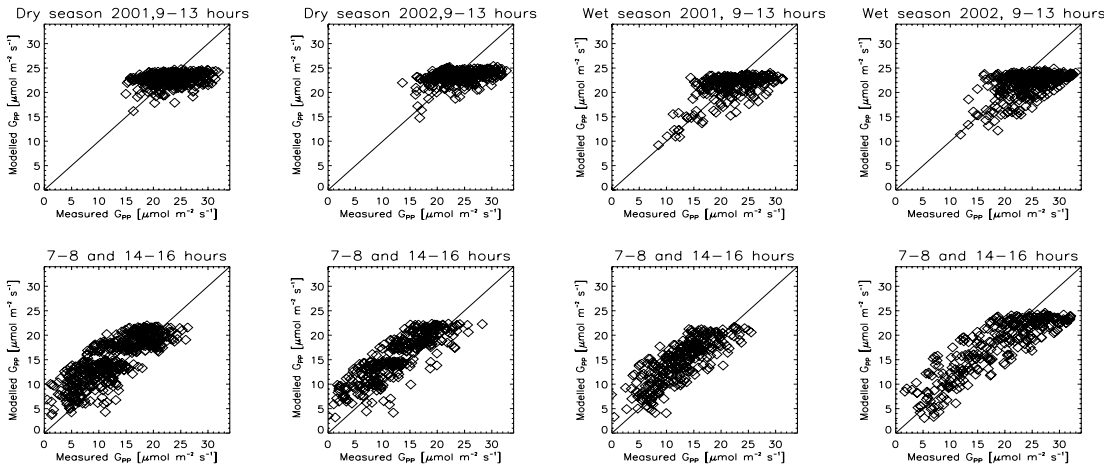

Figure 3A-35. Tapajos 2001-2002. 1:1 line of simulated versus observed gross uptake. Upper rows correspond to time of day 0900-1300 and lower rows correspond to time of day 0700-0800 and 1400-1600.

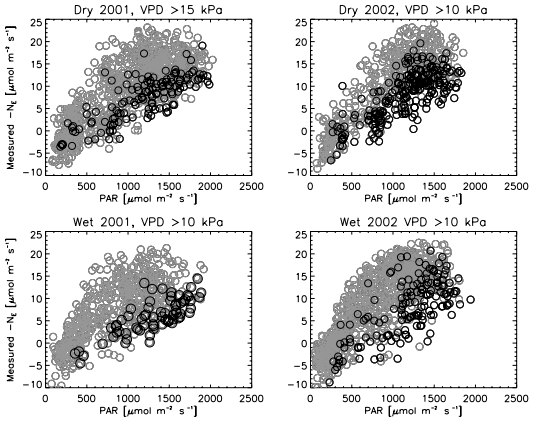

Figure 3A-36. Tapajos wet and dry season 2001 and 2002. Light response of $-N_E$ from eddy correlation. Black points correspond to high VPD values during each season.

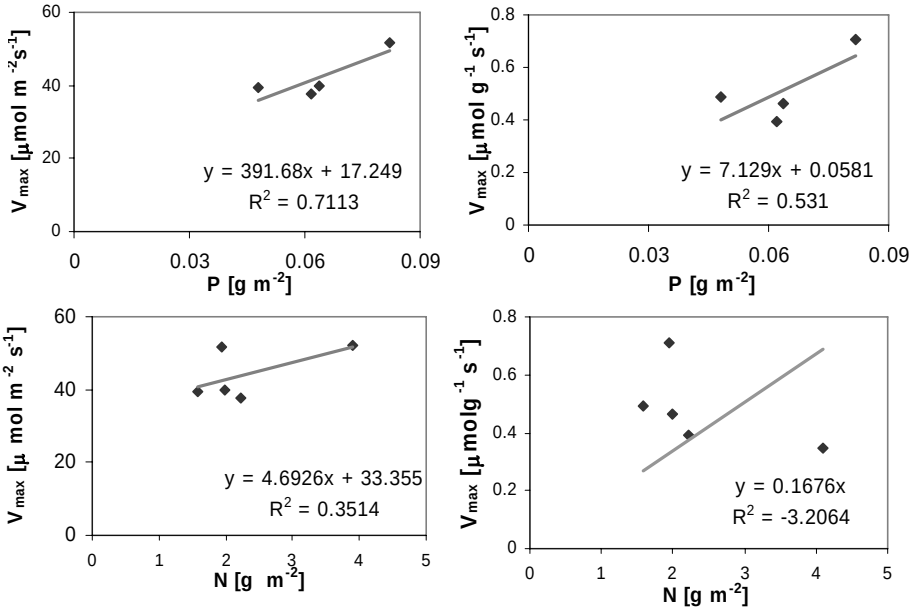

Figure 3A-37. Linear regressions obtained from best fitted V_{max} in DW and in area basis against foliar N and foliar P in area basis (with Φ=0.4).

8.2 Appendix 4A: Data used to force the model

8.2.1 Meteorology

The ECMWF model produces output based on the average altitude of any given grid cell which may differ significantly from the altitude of any site within that cell. Site specific altitudinal corrections for temperature and specific humidity were therefore undertaken using elevation data for each site from local measurements where possible or else estimated from the US Geological Service 1km Digital Elevation Model, as reported by Malhi et al. (2004, Table 4.1). This correction was important, especially for some of the southern Peruvian (TAM) and Ecuadorian (JAS) sites due to the significantly higher altitudes assumed in the ECMWF model. Figures 4A-1A and 4A-1B show the altitude of each site from the ECMWF model and from Malhi et al. (2004), and air temperatures at each site from ECMWF, and site-specific altitude corrected air temperatures.

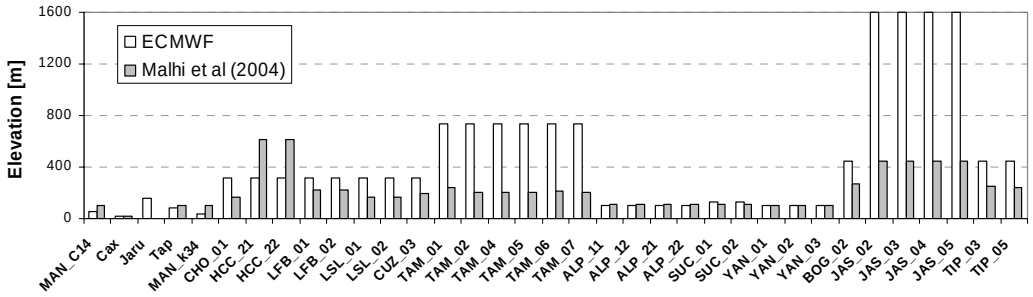

Figure 4A-1A. Elevation simulated by the ECMWF model and reported by Malhi et al (2004).

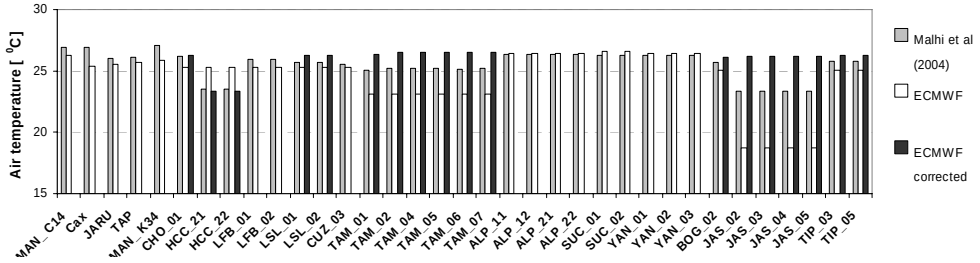

Figure 4A-1B. Mean annual temperature from the ECMWF model, from Malhi et al. (2004) and altitude corrected air temperatures from the ECMWF model.

Spatial patterns in the distribution of mean annual solar radiation, air temperature, and precipitation for the period 1982-2001 are shown in Figure 4A-2. Mean annual temperatures do not vary greatly across sites whereas solar radiation varies markedly. After making the altitude corrections for air temperatures, lowest temperatures are found in Bolivia at HCC-21 and HCC-22, the sites with the highest elevation (See Figure 4A-1A). Sites in southern Peru have the lowest solar incoming radiation from the studied sites. This could be a model artefact or it could be caused by real variations in cloud cover. A comparison of mean annual solar radiation, precipitation and latitude (See Table 4.2 in Chapter 4 for latitude) at the southern Peruvian and Bolivian sites, shows that the Bolivian sites, although located further south (by about 1.6 decimal degrees) receive higher incoming solar radiation than those in southern Peru. This is probably due to a longer dry season and associated lower levels of cloudiness (See Figure 4A-5). Note that southern Peru has

higher precipitation. However, despite a significant difference in mean annual precipitation at the Ecuadorian sites, which are all located at similar latitudes (precipitation at Jatun Sacha, JAS, higher than Bogi, BOG, and Tiputini,TIP) the difference in mean annual solar radiation is not as high as between the Bolivian and the South Peruvian sites. All Ecuadorian sites with the exception of TIP-03, TIP-05 and BOG-02 have greater precipitation than sites in northern Peru and lower incoming solar radiation, consistent within the ECMWF meteorology. According to the mean annual precipitation reported by Malhi et al. (2004, Table 1), estimated using the 0.5 degree resolution Climate Research Unit, University of East Anglia, Observational climatology and /or local field site rainfall data, most of the sites have similar annual precipitation to that simulated by the ECMWF model (See Figure 4A-3). However this is not the case for the northern Peruvian sites, Cuzco (CUZ), BOG-02 and for both of the TIP sites in Ecuador. Implications of differences in precipitation for the model simulations are discussed below.

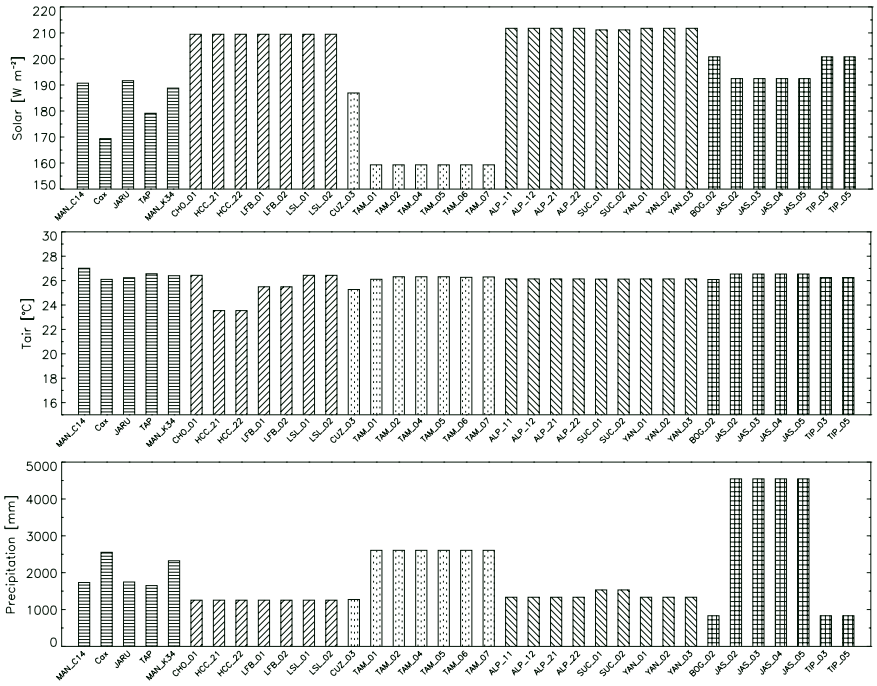

Figure 4A-2. Spatial distribution of mean annual solar radiation, air temperature, and precipitation for the period 1982-2001. Each pattern represents a different region, from left to right, Brazil, Bolivia, south Peru, north Peru and Ecuador.

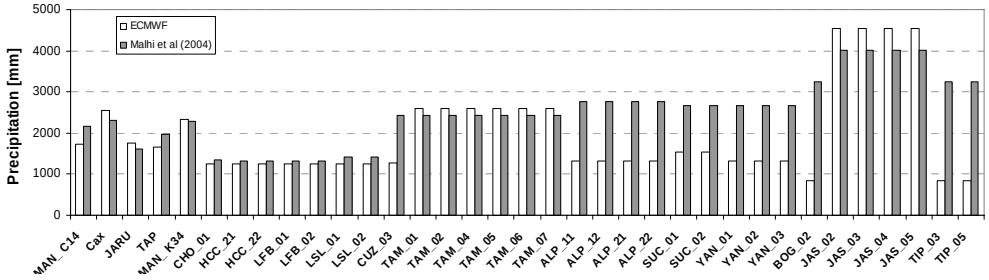

Figure 4A-3. Mean annual precipitation simulated by the ECMWF model and reported by Malhi et al. (2004).

The meteorology (mean diurnal and seasonal cycles and interannual variation) used are first illustrated for the 12 grid cells of the ECMWF model associated with the 35 sites. Figure 4A-4 shows the mean diurnal cycles of solar radiation, air temperatures, wind speed and relative humidity for selected sites during wet and

dry seasons of different years. Dots in Figure 4A-4 correspond to mean hourly values at each 3 hour time step as provided by the ECMWF model.

The mean annual cycles of incoming solar radiation, air temperature, precipitation and relative humidity are shown in Figure 4A-5. As expected, solar radiation and air temperature have similar patterns. Also the seasonal variations in precipitation and relative humidity are similar. Solar radiation and precipitation have opposite seasonality. Of note is the lower solar incoming radiation and higher precipitation in southern Peru (TAM-05) compared to sites in Bolivia (LFB-01 and HCC-22). There seems to be a problem with a severe underestimation in precipitation at North Peru and Ecuador by the ECMWF model. Model estimates are more than 1000 mm lower than estimates from Malhi et al. (2004). According to the ECMWF model the JAS sites in Ecuador have a strong dry season during June, July and August. However, according to data from a weather station at JAS (Neil D., not published), monthly precipitation is seldom below 100 mm with a monthly average of 300 mm calculated for the period 1992-2001. Due to the geographical location of sites near the Andes, and lack of validation data, the ECMWF model is not able to reliably reproduce the rainfall patterns in these areas.

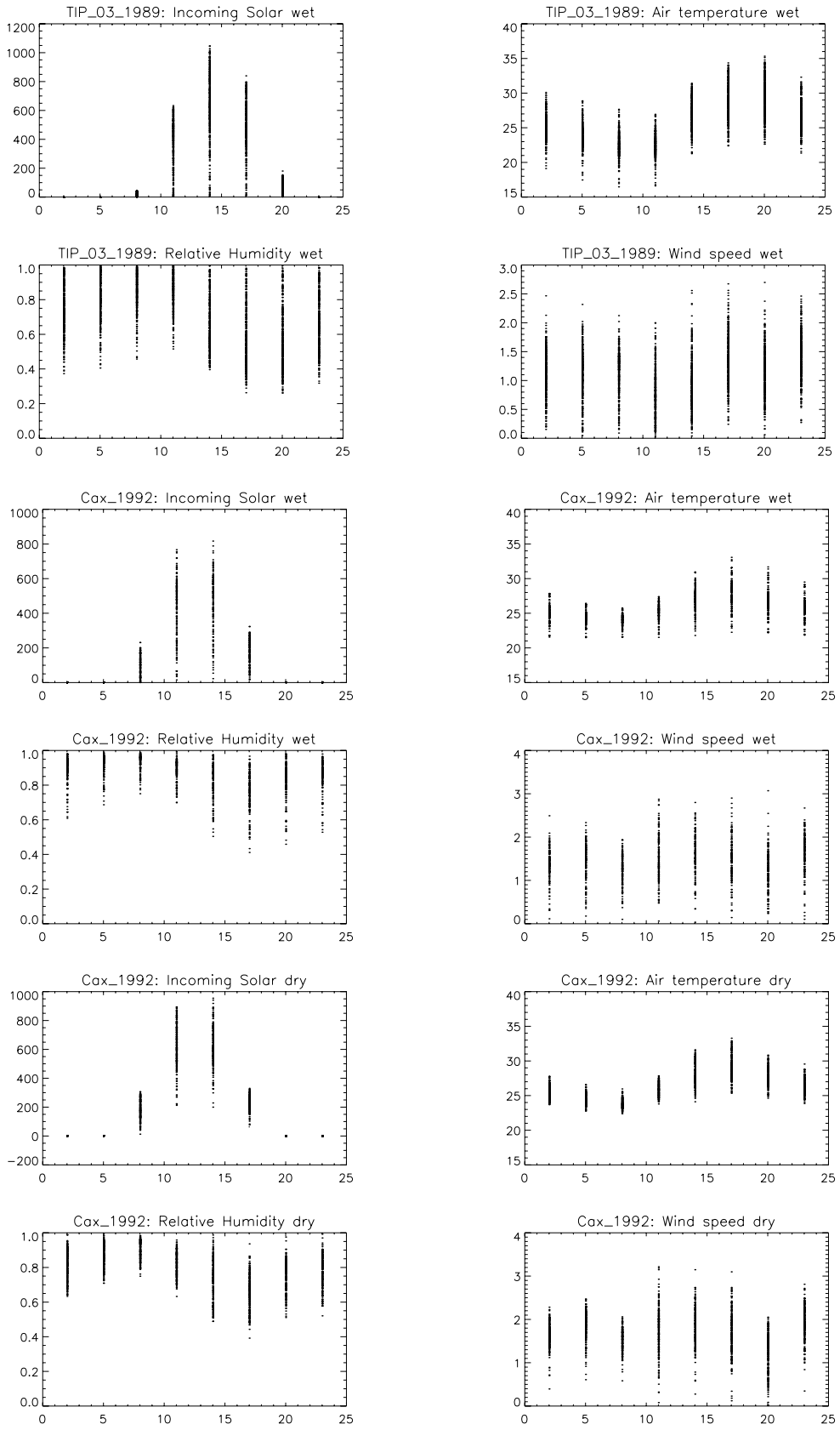

Figure 4A-4-I. Diurnal cycle of solar radiation [W m^{-2}], air temperature [°C], wind speed [m s^{-1}] and relative humidity at TIP-03 and Caxiuana in Ecuador and Brazil, respectively. Dots correspond to mean hourly values at each 3 hour time step as provided by the ECMWF model.

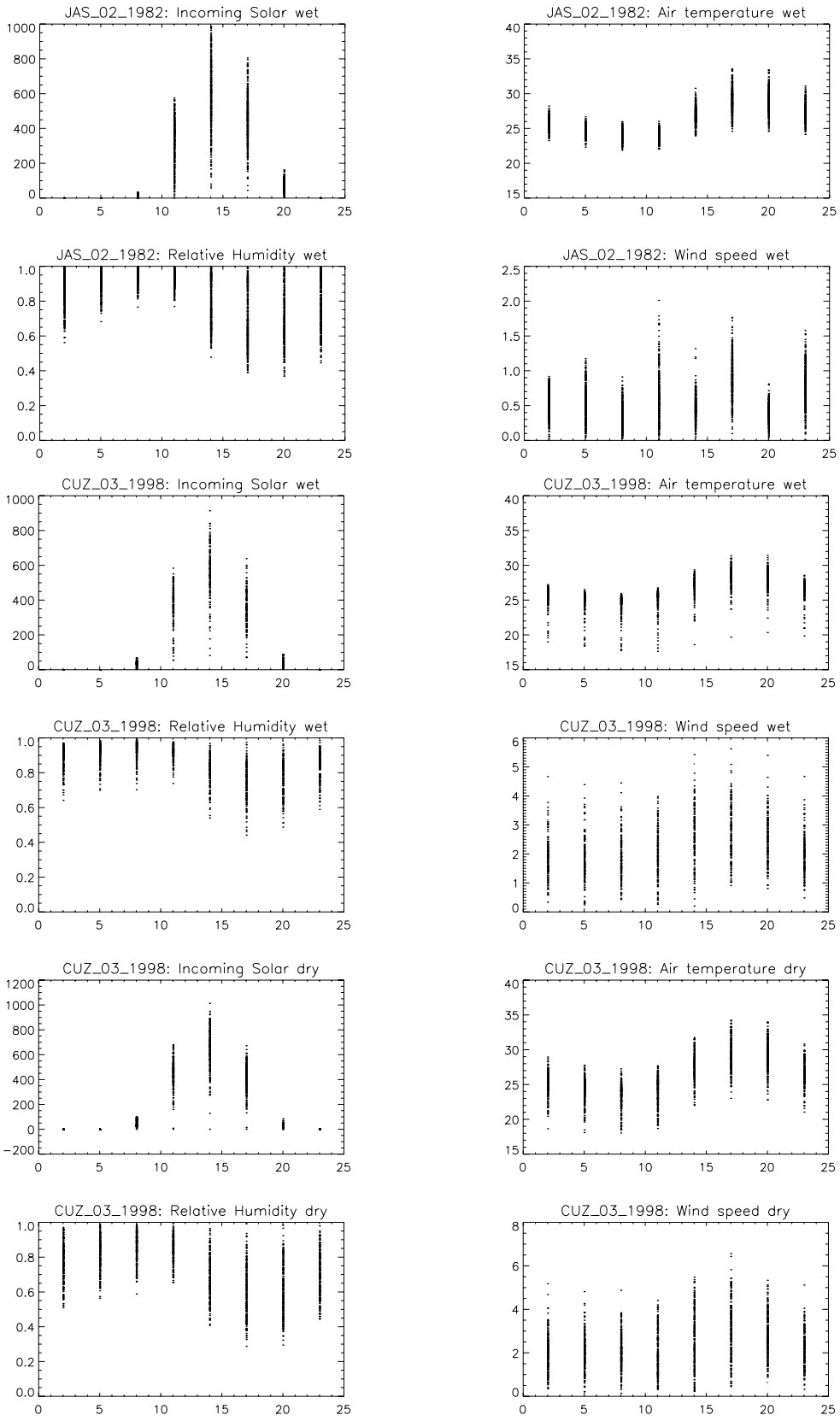

Figure 4A-4-II. Diurnal cycle of solar radiation [W m^{-2}], air temperature [°C], wind speed [m s^{-1}] and relative humidity at JAS-02 and CUZ-03 in Ecuador and southern Peru, respectively. Dots correspond to mean hourly values at each 3 hour time step as provided by the ECMWF model.

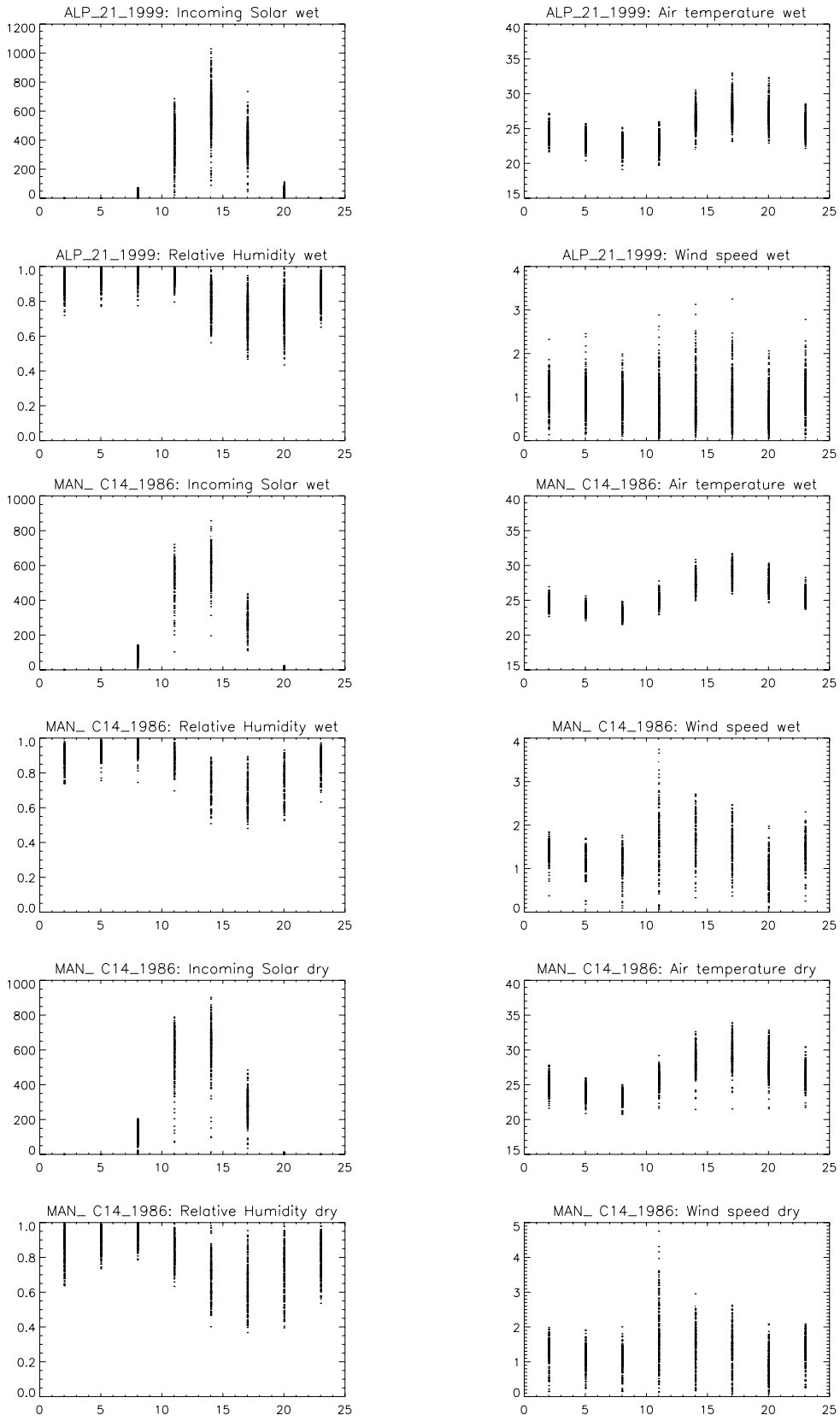

Figure 4A-4-III. Diurnal cycle of solar radiation [W m^{-2}], air temperature [°C], wind speed [m s^{-1}] and relative humidity at ALP-21 and MAN-C14 in northern Peru and Brazil, respectively. Dots correspond to mean hourly values at each 3 hour time step as provided by the ECMWF model.

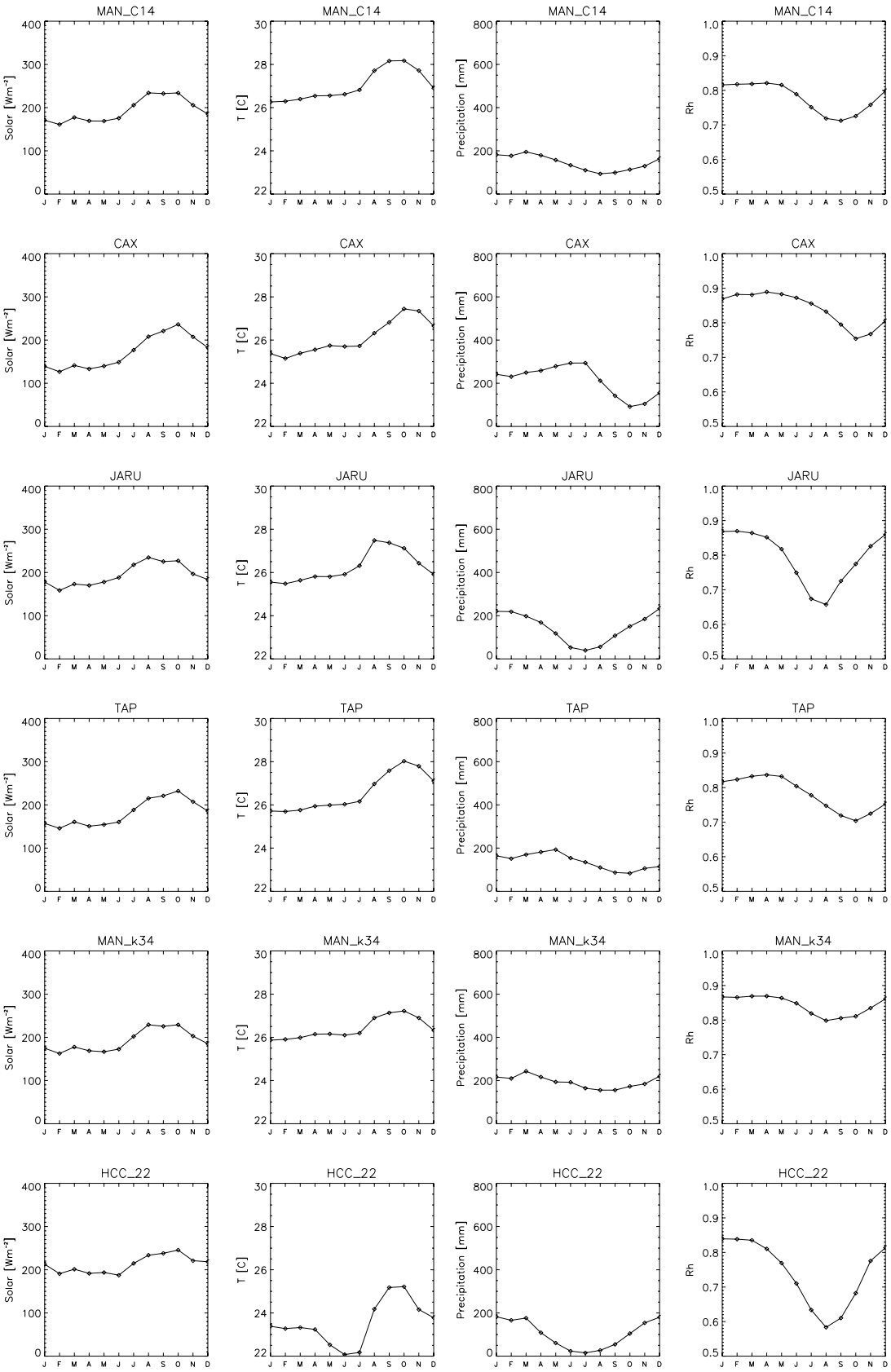

Figure 4A-5-I. Mean monthly values of incoming solar radiation, air temperature, wind speed, precipitation and specific humidity over the period 1982-2001 at MAN-C14, CAX, JARU, TAP and MAN-K34 in Brazil and HCC-22 in Bolivia.

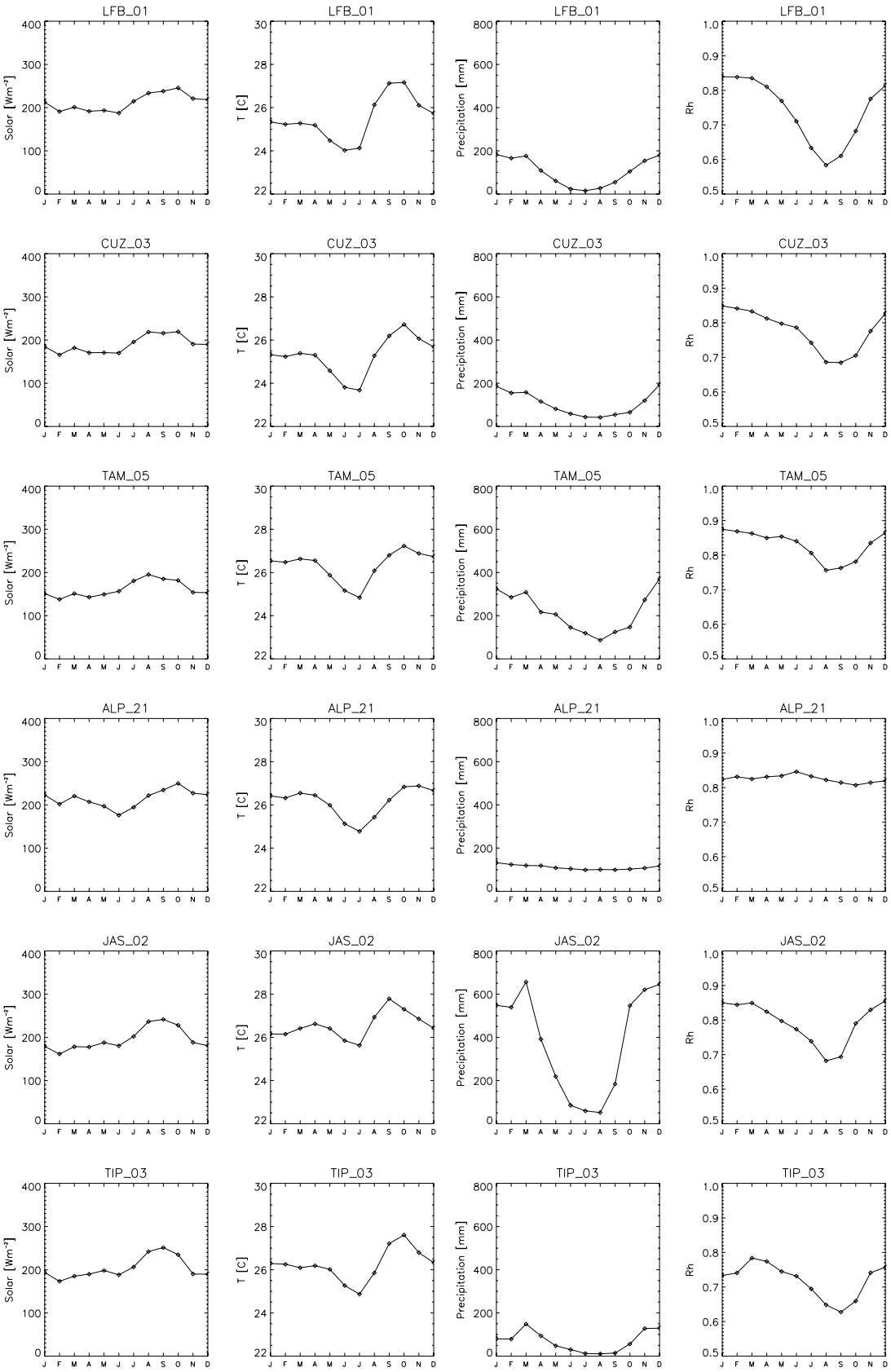

Figure 4A-5-II. Mean monthly values of incoming solar radiation, air temperature, wind speed, precipitation and specific humidity over the period 1982-2001 at LFB-01 in Bolivia, CUZ-03 ant TAM-05 in southern Peru, ALP-21 in northern Peru, and JAS-02 and TIP-03 in Ecuador.

Interannual variations in the ECMWF meteorology for the period 1982-2001 are shown in Figure 4A-6 for the selected sites. Again, a consistency between solar radiation and air temperature, between precipitation and relative humidity and between solar radiation and precipitation can be seen.

There is a general consistency in the ECMWF meteorology from year-to-year across sites. However, it is well established that Central and eastern Amazonia are affected by negative precipitation anomalies caused during the warm ENSO phase (*El Niño*) with concurrent increases in precipitation in the most western parts of Ecuador and North Peru (Peixoto and Oort 1982). The opposite occurs during the cold phase of ENSO (*La Niña*). To check the ability of the ECMWF model to simulate these patterns *El Niño* (red dots) and *La Niña* (blue dots) episodes are indicated in Figure 4A-6 (column 3). Only at some sites such as Man C14 and Man K34 (sites at Manaus where there is availability of precipitation records), the ECMWF model has a coherent response to *El Niño* and *La Niña* with increases and decreases in precipitation according to expectation. However in general the ECMWF interannual variability did not look realistic and the accuracy of the simulations is difficult to assess without available rainfall data at each location. The potential effects of interannual variability caused by ENSO events were not considered as part this study.

In order to assess longer-term climatic trends as simulated by the ECMWF model, recent observational changes in solar radiation, temperature and precipitation in the Amazon region reported in the literature are briefly described. According to Malhi and Wright (2004) and Victoria et al. (1998), the Amazon region has shown a warming tendency since mid-1970s. In association with this warming trend, increases in solar radiation over the tropics have been reported as a result of decreases in tropical cloudiness during the last two decades, as deduced from satellite images (Wielicki et al. 2002). Using the same satellite data as used in Wielicki et al. (2002) study, Nemani et al. (2003) reported increases in solar radiation over Amazonia for the period 1982-1999. Malhi and Wright (2004) found no significant trend in precipitation over the Amazon region for the period 1960-1998.

From the simulated annual solar incoming radiation in Figure 4A-6, column 1, there is, however, no significant trend at the central and eastern Brazilian sites or at the southern Peruvian sites. Nevertheless, solar radiation is modelled to have increased by about 30 to 40 W m^{-2} during the period 1982-1993 at the Bolivian sites (LFB-01 in Figure 4A-6-II) and during 1982-1995 at Jaru, followed by a decrease of 30 W m^{-2} by 2001. Simulations at the northern Peru and Ecuadorian sites (ALP-21, JAS-02 and TIP-03 in Figure 4A-6-II) indicate a decrease of approximately 30 to 40 W m^{-2} during the period 1982-2001. Simulated trends in temperature generally seem to follow the same trends as simulated for solar radiation. There is no clear trend in precipitation at most sites, except in the north Peru and Manaus grid-cells (ALP-21, MAN-C14 and MAN-K34 in Figure 4A-6) where there is a trend of increasing rainfall over the last two decades for the ECMWF simulations.

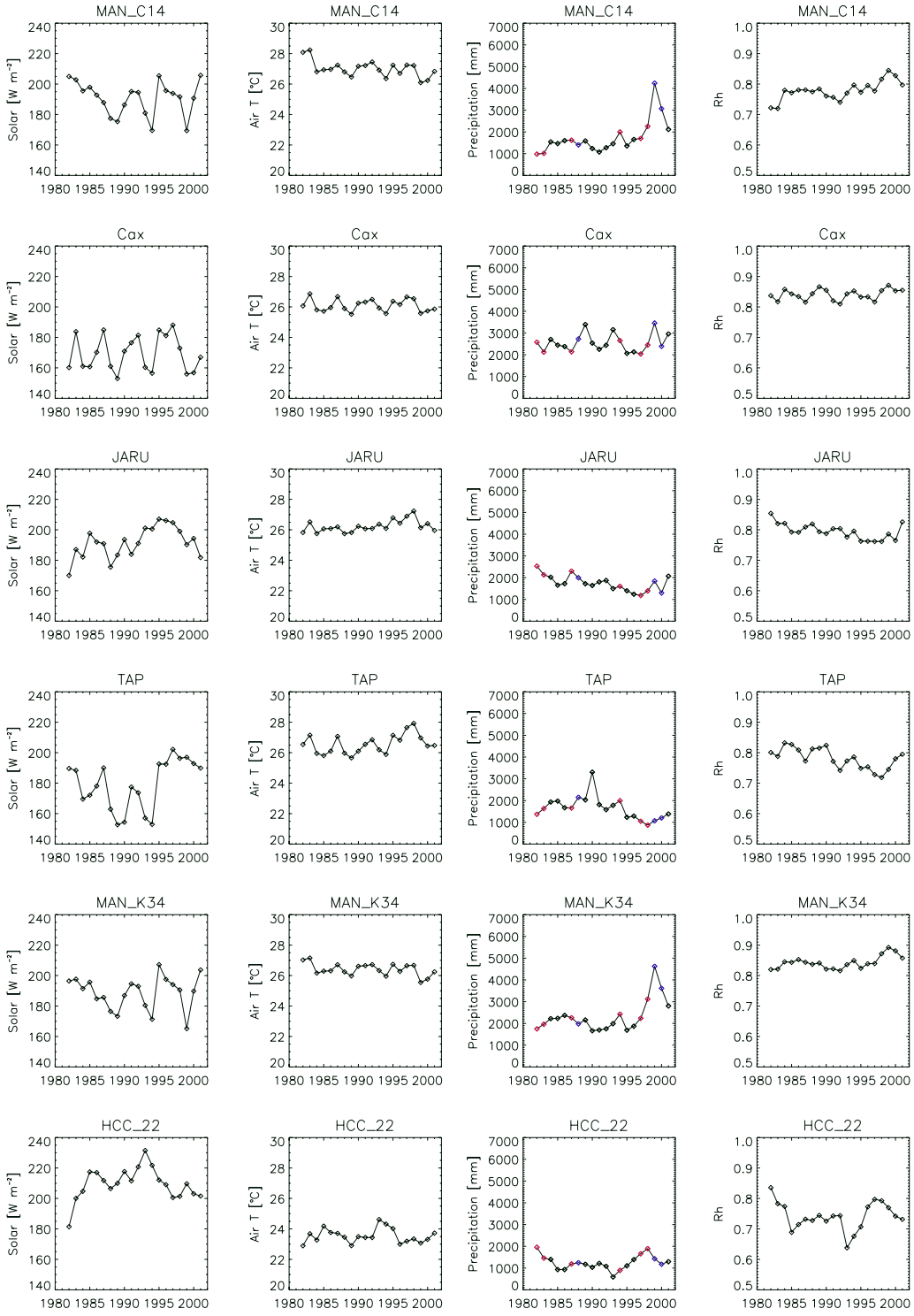

Figure 4A-6-I. Annual trends in the simulated ERA40-ECMWF meteorology. Annual total solar radiation and precipitation (red dots and blue dots correspond to *El Niño* and *La Niña* years, respectively) and mean annual air temperature and relative humidity are shown for MAN-C14, CAX, JARU, TAP and MAN-K34 in Brazil and HCC-22 in Bolivia.

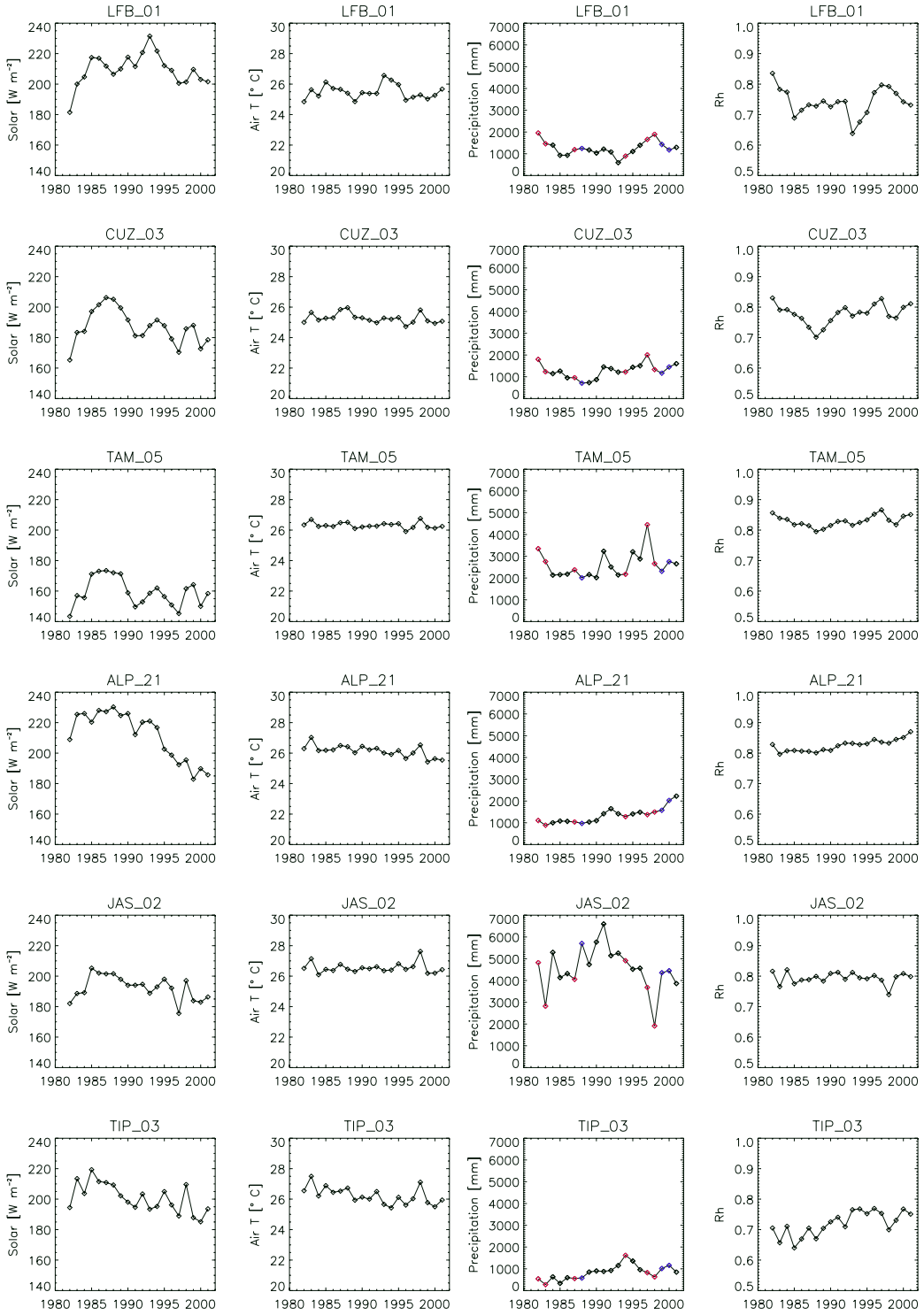

Figure 4A-6-II. Annual trends in the simulated ERA40-ECMWF meteorology. Annual total solar radiation and precipitation (red and blue dots correspond to *El Niño* and *La Niña* years, respectively) and mean annual air temperature and relative humidity are shown for LFB-01 in Bolivia, CUZ-03 ant TAM-05 in south Peru, ALP-21 in north Peru, and, JAS-02 and TIP-03 in Ecuador.

8.2.2 LAI data

Two sources of LAI data were used for the G_P simulations. Firstly, estimates of LAI derived from hemispherical photographs for each site using a fish eye type of lens (RAINFOR Consortium, unpublished data) were used. According to the protocols from the RAINFOR Consortium, approximately 20 hemispherical photographs were taken at each site to determine the average LAI of the forest.

LAI was also derived from remotely sensed normalized difference vegetation index and a biome map. The data set used is from the Global Inventories Monitoring and Modelling Studies, GIMMS, project (Nemani et al. 2003). This consists of 20 years of monthly LAI derived from satellite observations with a spatial resolution of a quarter of a degree. Figure 4A-7 shows some typical LAI patterns for selected sites. For some sites, at least during some years, the change of LAI from month to month is not very smooth and that as a consequence of these abrupt changes it is difficult to identify any seasonality in LAI. There are also months where there were no data available or where LAI was unreasonably high or low relative to the minimum and maximum values inferred from the RAINFOR Consortium data set. In an attempt to correct for such values, LAI was modified as follows:

If LAI < 3.5 LAI = LAI /10 + 3.5 A1)
If LAI > 7.0 LAI = LAI/10 - 7.0 A2)

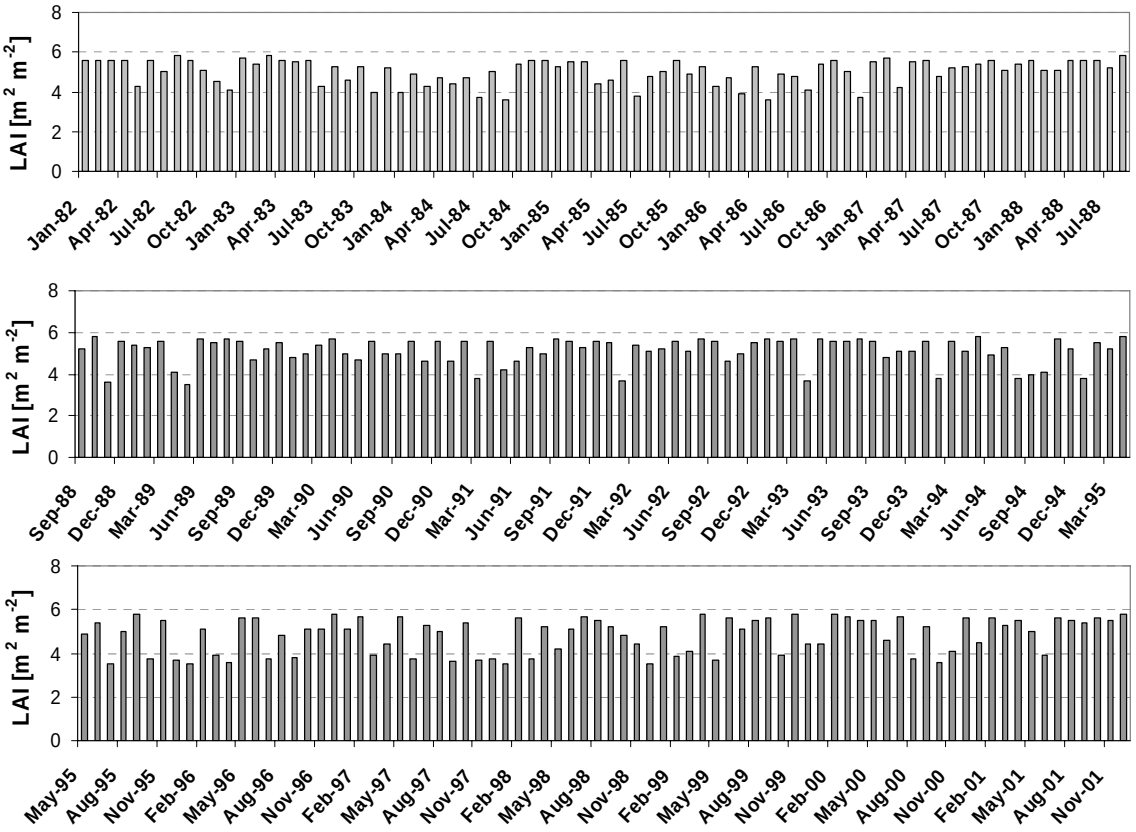

Figure 4A-7-I. Monthly LAI from GIMMS at TIP-03 in Ecuador.

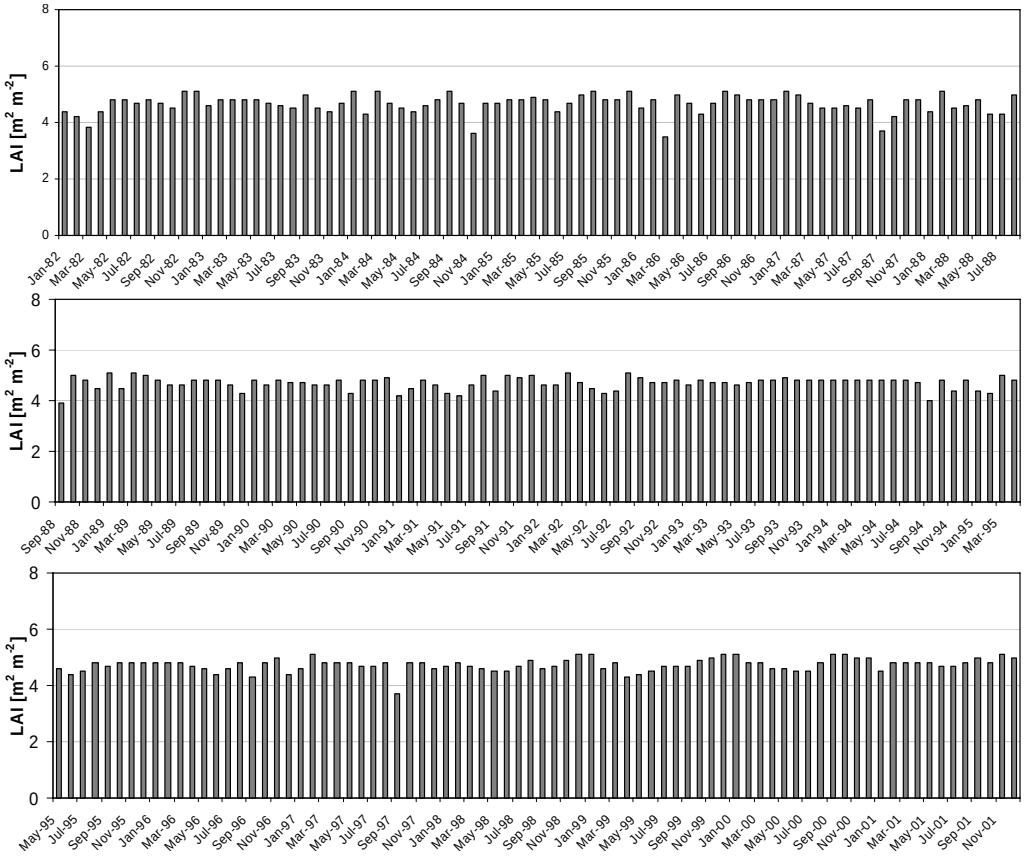

Figure 4A-7-II. Monthly LAI from GIMMS at HCC-21 in Bolivia.

8.3 Appendix 4B. Sensitivity tests

Sensitivity of simulated V_{max} at the top of the canopy to the regressions of V_{max} against foliar N given in Table 4.1 was tested for all sites as shown in Figure 4B-1. Here, foliar N at all sites usually ranged from 1 to 3 g m $^{-2}$ with one outlier at 4.1 [g m^{-2}] that corresponds to Man C14 which had the highest estimated V_{max} using all regressions. Estimated V_{max} was usually lowest using the regression obtained from data at Manaus and Caxiuana. There is more variability in estimated V_{max} when regressions obtained from data at Tapajos, Caxiuana, or pooled data from Manaus and Caxiuana are used than regressions derived from the best fitted V_{max} from the tower sites in Chapter 3.

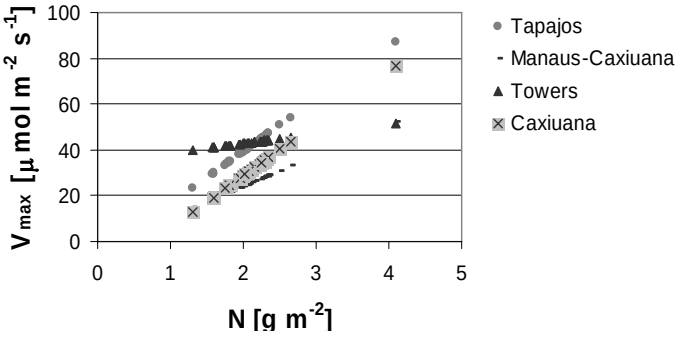

Figure 4B-1. Sensitivity of canopy top V_{max} to the V_{max} against foliar N regression from Table 4.1 using foliar N from all 35 sites. Regressions included in Table 4.1 are: 1) original regression used for parameterisation of tower sites in Chapter 3, i.e. obtained from Manaus and Caxiuana data sets (Carswell et al. (2000) and Vale et al. (2003) respectively), 2) regression obtained only using Caxiuana data, 3) Domingues et al. (2005) regression using Tapajos data set and 4) regression obtained in Chapter 3 from fitted top of the canopy V_{max} and foliar N for the tower sites.

8.3.1 Sensitivity of $G_{P(N)}$ to variations in the vertical distribution of N within the canopy

The control simulation assumes for all sites an exponential decrease of leaf N content per leaf area with increasing cumulative LAI using the same measured N and leaf density distribution as measured at Manaus C14 (Carswell et al. 2000; Meir et al. 2000). Under this assumption, estimated N allocation coefficients vary between 0.15 and 0.28 for all sites. This variation is due to variations in site LAI from the RAINFOR Consortium data set (unpublished data). To consider other possible N allocations, the sun/shade model was therefore run at five sites using different N allocation coefficients (k_n =0.5, 0.8 and 1, i.e. steeper vertical foliar N distributions than the control distribution, but also k_n = 0 the uniform distribution was considered) keeping constant the total canopy N (i.e. canopy V_{max}) and leaf area index used for calculations in the control simulation. Figure 4B-2 illustrates the effect of changing k_n on the vertical distribution of V_{max} at Caxiuana. By increasing k_n (and keeping constant LAI and total canopy N), the vertical distribution of foliar N and V_{max} gets steeper i.e. higher values of V_{max} at the top of the canopy and lower at the bottom when compared to the control simulation. For a constant canopy N content, using k_n = 0 implies an invariable leaf N and therefore invariable V_{max} through the canopy. Hence V_{max} for this N allocation is much lower for top canopy leaves and higher at the bottom of the canopy when compared to the control allocation.

Calculated V_{max} at the top of the canopy using k_n=0, 0.5, 0.8, 1.0 and k_n from the control N allocation and the corresponding $G_{P(N)}$ for five selected sites are given in Table 4B-1. For k_n = 0.5, 0.8 and 1.0, V_{max} at the top

of the canopy increased by more than 50, 100 and 150 %, respectively, compared to the control N allocation case (Scenario 1), whereas the corresponding $G_{P(N)}$ values did not vary to such an extent. From the five sites tested, when k_n was taken as 0.5 and 0.8, $G_{P(N)}$ decreased on average by only 4% and 1%, respectively, compared with simulated $G_{P(N)}$ for the control N allocation. On the other hand, when k_n was taken as 0 or 1.0, $G_{P(N)}$ increased on average by 7 and 0.3 %, respectively. From these results, it can be concluded that for the same total canopy nitrogen and LAI as in the control simulation, the use of different nitrogen allocation coefficients did not change to a large extent simulated mean annual $G_{P(N)}$. For subsequent analyses, the leaf N allocation from Manaus C14 was taken as in the control scenario.

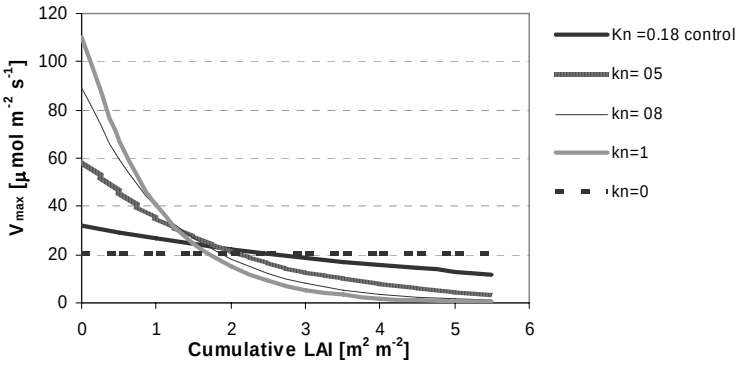

Figure 4B-2. Vertical profile of V_{max} under different N allocations (k_n=0.5, 0.8 and 1.0 for control run k_n =0.18) at Caxiuana.

Table 4B-1. Scenarios of vertical distribution of N within the canopy. V_{max} at the top of the canopy in μmol m^{-2} s^{-1} calculated using k_n=0, 0.5, 0.8, 1.0 and *k*n from the control run. The percentage of the simulated $G_{P(N)}$ in each case relative to the control run is also presented

	$k_{n\_control}$	k_n=0	k_n=05	k_n=08	k_n=1
CAX					
V_{max} ($k_{n\_control}$=0.18)	32	21	59	89	110
% of $G_{P(N)}$ control		**104**	**95**	**99**	**101**
ALP-21					
V_{max} ($k_{n\_control}$=0.22	32	21	51	75	92
% of $G_{(P)N}$ control		**107**	**96**	**98**	**100**
LS-02					
V_{max} ($k_{n\_control}$=0.22		9	24	36	44
% of $G_{(P)N}$ control	15	**112**	**99**	**98**	**100**
JAS-03					
V_{max} ($k_{n\_control}$= 0.23)		17	42	62	76
% of $G_{(P)N}$ control	27	**108**	**98**	**100**	**100**
TAM-02					
V_{max} ($k_{n\_control}$= 0.2)		17	49	73	90
% of $G_{(P)N}$ control	28	**104**	**95**	**99**	**101**

8.3.2 Scenarios of LAI

Modelled mean annual $G_{P(N)}$ using the "control" N distribution for four scenarios of LAI across the 35 sites for the period 1983-2001 are presented in Figure 4B-3. Bars correspond to simulated $G_{P(N)}$ under different LAI scenarios: -LAI derived from satellite images, -smoothed LAI satellite derived, - LAI derived from

hemispherical pictures taken at each site (and assumed to be constant throughout the year) and -LAI derived from hemispherical pictures but assuming a 20% decrease in LAI during the dry season for sites. Dry season months are considered as months when precipitation is less than 100 mm.

Mean annual modelled $G_{P(N)}$ was highest at 23, 4 and 8 of the 35 sites using LAI derived from hemispherical photographs, from satellite images and smoothed satellite images, respectively. Comparing all simulations, the difference between highest and lowest simulated $G_{P(N)}$ was on average 5% and varied between 0.6 and 10%. The largest difference was found at the Bolivian site (LSL-02) where differences in $G_{P(N)}$ were only 10% and the smallest difference was simulated at a site in central Brazil (Man C14) where the minimum modelled $G_{P(N)}$ was 0.6% of the maximum. Comparison of $G_{P(N)}$ using both scenarios with hemispherical photos, showed that on average simulated $G_{P(N)}$ differed by only 2.2 % (range of variation 0.3- 4.9 %), being larger for the scenario which considered a constant LAI. Correlations of $G_{P(N)}$ among the different scenarios are shown in Table 4B-2. From this table, it can be seen that correlations between $G_{P(N)}$ for different scenarios of LAI were relatively high (greater than 0.95). From this sensitivity analysis it is concluded that at the stand scale mean annual $G_{P(N)}$ for the period 1983-2001 was relatively insensitive to the method of LAI calculations at all sites. Therefore, for the subsequent analyses, modelled $G_{P(N)}$ and $G_{P(P)}$ uses LAI derived from GIMMS (Nemani et al. 2003) across the basin corrected for low and high values as described in the methods section of Chapter 4.

Table 4B-3. Matrix of correlations for $G_{P(N)}$ simulated under different scenarios of LAI.

	LAI satellite	LAI smooth	LAI (HP)	LAI (HP 20%)
LAI satellite	1.000	0.998	0.963	0.960
LAI smooth	0.998	1.000	0.960	0.956
LAI H pictures	0.963	0.960	1.000	0.996
LAI H pictures 20	0.960	0.956	0.996	1.000

Smooth: Smoothed satellite derived LAI.
HP: Hemispherical pictures.
HP 20%: LAI decreased by 20% during dry season months.

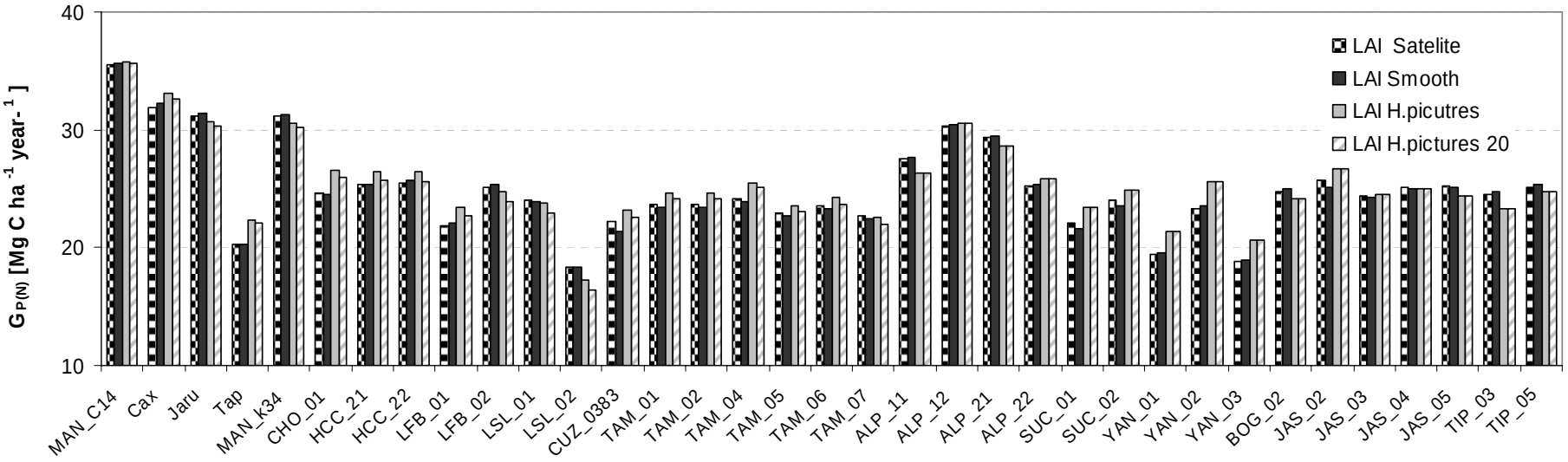

Figure 4B-3. Simulated $G_{P(N)}$ using four scenarios of LAI: LAI satellite - satellite derived LAI; LAI smooth - smoothed satellite derived LAI; LAI H. pictures - LAI estimated from hemispherical pictures and considered constant during the whole study period, and LAI H. pictures 20 - same as previous but includes a 20% decrease in LAI during dry periods.

8.4 Appendix 4C

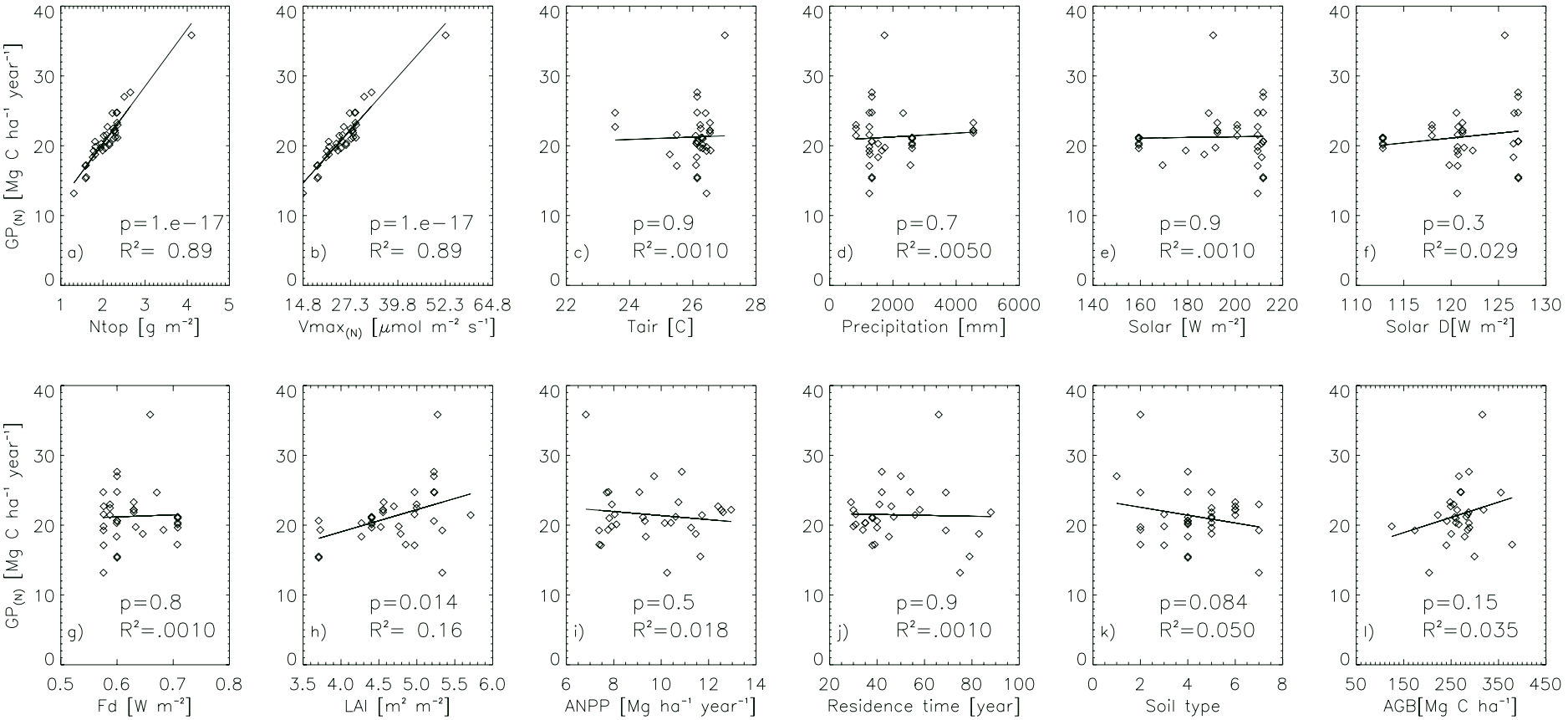

Figure 4C-1. $G_{P(N)}$ parameterised using regression of V_{max} against foliar N obtained from data from Manaus–C14 (Carswell et al. 2000) and Caxiuana (Vale et al. 2003). Relationships between simulated mean annual $G_{P(N)}$ averaged over the period 1982-2001 with a) N content from top canopy leaves, b) $V_{max(N)}$ at the top of the canopy, c) mean annual air temperature, d) mean annual precipitation, e) mean annual solar incoming radiation, f) mean annual solar incoming diffuse radiation, g) fraction of diffuse irradiance h) mean annual LAI, i) above ground NPP, j) mean residence time, k) soil type, l) above ground biomass. i), j), and k) are taken from Malhi et al. (2004) and l) is taken from Baker et al. (2004).

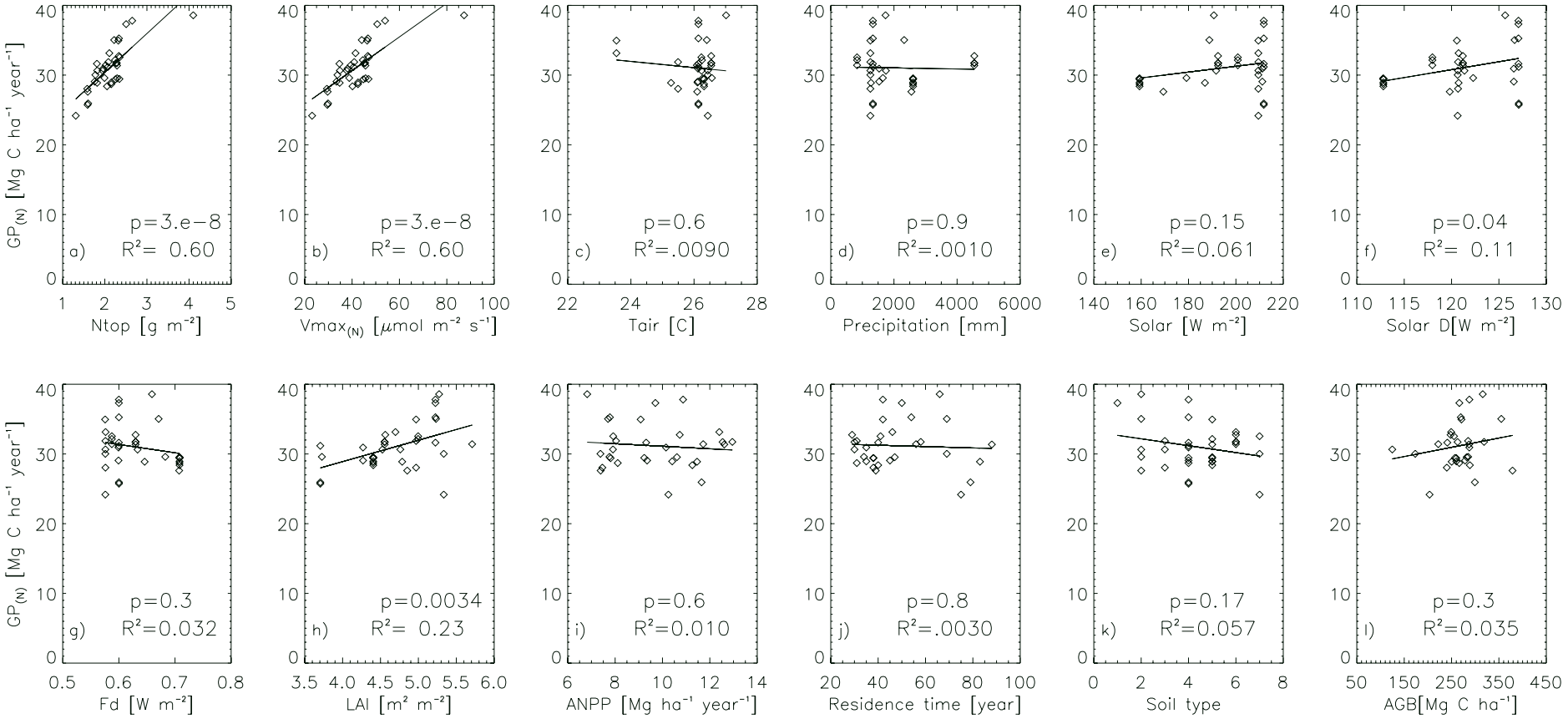

Figure 4C-2. $G_{P(N)}$ parameterised using regression of V_{max} against foliar N obtained from data from Tapajos (Domingues et al. 2005). Relationships between simulated mean annual $G_{P(N)}$ averaged over the period 1982-2001 with a) N content from top canopy leaves ,b) $V_{max(N)}$ at the top of the canopy, c) mean annual air temperature, d) mean annual precipitation, e) mean annual solar incoming radiation, f) mean annual solar incoming diffuse radiation, g) fraction of diffuse irradiance h) mean annual LAI, i) above ground NPP, j) mean residence time, k) soil type, l) above ground biomass. i), j), and k), are taken from Malhi et al. (2004) and l) is taken from Baker et al. (2004).

Acknowledgments

Financial support for this thesis was provided by the EU Project “Carbonsink–LBA Proposal No. EVK-1999-00191” and by the Max Planck Institute for Biogeochemistry, Jena-Germany.

Special thanks for support and recommendations to my PhD promoters Han Dolman in the Free University of Amsterdam and Jon Lloyd in Leeds University. I am grateful to Patrick Meir and Bart Kruijt for very detailed and useful feedback on this work. Thanks to all members of the PhD committee, Bart Kruijt, John Grace, Yadvinder Malhi, Patrick Meir, and Maarten Waterloo for their time and willingness to read this thesis.

This thesis would have not been possible without the help, support and patience of many colleagues and friends from home, Jena, Wallingford, Leeds, Brazil and from other places.

At the Max Planck Institute I give special thanks to Annett Börner, Leticia Cotrim da Cunha, Ingo Ensminger, Holger Fritsch, Martin Heimann, Martin Jung, Jens Kattge, Peer Koch, Stefen Körner, Olaf Kolle, Corinne Le Quéré, Andrew Manning, Martina Mund, Corinna Rebmann, Ernst-Detlef Schulze, Jens Schumacher, Marcus Schumacher, Kristina Trusilova and Ulrike Seibt.

At the University of Leeds, thanks a lot to Tim Baker, Sandra Patiño, Oliver Philips and Pia Wohland.

In Wallingford, I am very grateful to my friends and colleagues: Richard Ellis, John Gash, Anna Maria Giacomello, Atul Haria, Phil Harris, Monika Jürgens, Tim Jupp, Thomas Kjeldsen, Colin Lloyd, Dermot O'Regan, Caroline Sullivan, Christopher Taylor and Rita Yam.

In Medellín, thanks to Carolina Mercado, Orlando Mercado, José Manuel Mercado, Gloria Montoya, Germán Poveda and special thanks to Andrés Ochoa.

Thanks to friends and colleagues from other places and institutions: Alessandro Araújo, Jan Elbers, Fiona Carswell, Martin Hodnett, Raquel Lobo do Vale, Ranga Myneni, David Neil, Antonio Nobre, Romilda Pavia, Carlos Alberto Quesada, Scott Saleska, Celso von Randow and Alexandre Santos.

I had a wonderful experience in the field in the Amazon rainforest in Ecuador and Peru. Thanks to the RAINFOR team that worked during the field campaigns I was part of. I had the chance to meet a part of the scientific community by attending to various interesting and motivating scientific meetings. Special thanks for sponsorship to the Max Planck Institute from Biogeochemistry.

Finally, I have to say that I would not have finished this work without huge support and help from Stephen Sitch who corrected my awful and sloppy English but also gave me a lot of ideas to improve the structure of the whole document. Without this help, I would not have managed to come to the end of this challenging and some times really hard experience.